THE UNIVERSITY *of* EDINBURGH

Synthesis and *In Vitro* Applications of Fluorescent Imaging Agents

Aurélie Brunet

Doctor of Philosophy

The University of Edinburgh

2014

Abstract

Fluorescent imaging technologies that offer new ways to visualise and quantify fluorescently labelled molecules are increasing, necessitating the development of fluorescent molecules that can efficiently and specifically label targets *in vitro* and *in vivo*.

The first aim of this thesis was the study of human neutrophil elastase. Human neutrophil elastase is an important enzyme in the regulation of inflammation but if over expressed can become part of the cause of inflammation itself. To elucidate this dual function and have a greater understanding of this enzyme, an imaging probe for neutrophil elastase was designed. Firstly, the syntheses of fluorescently labelled three branched dendron core structures were optimised, and studied in neutrophils. The selected core structure was functionalised with an elastase specific peptide sequence and fluorescently labelled. The probe was specifically cleaved by neutrophil elastase in an enzymatic assay and in the presence of activated neutrophils (Chapter 1).

Fluorescein and rhodamine are dyes that are readily available, are affordable and have convenient wavelengths for microscopy and flow cytometry. Carboxyfluorescein diacetate *N*-succinimidyl ester (CFDA-SE) is a commonly used fluorescein derivative, widely used in cell proliferation assay. It is mainly used as a mixture of isomers and its synthesis is not reported. Herein a short and simple synthesis of the two individual isomers of carboxyfluorescein diacetate *N*-succinimidyl ester as well as the equivalent rhodamine variation (carboxytetraethylrhodamine *N*-succinimidyl ester) is reported (Chapter 2). The labelling properties of these probes were studied in proliferation assays on mouse and human T lymphocytes.

Finally, the nuclear penetration of the dendron structure combined with nuclear localisation sequences (NLS) was investigated. Attachment of nuclear localisation sequences to the probe in the presence of fluorescein demonstrated successful entry into the nucleus in human alveolar adenocarcinoma cell line (A549) (Chapter 3).

Lay summary

The world of medicine was truly revolutionised by the discovery of medical imaging techniques. Scientists gave doctors the tools to be able to see within the human body. Modalities such as X-rays and ultrasound have been used for many years and remain major tools for many forms of analysis from broken bones to pregnancy. The development of new imaging techniques that are safer, quicker, cheaper and enable better visualisation of organs or individual cells are much sought after.

Fluorescent molecular imaging is an emerging technique involving fluorescently labelled molecules that can facilitate the detection and recognition of particular cells (e.g. cancer cells).

In this thesis, the synthesis and study of fluorescent compounds that only emit strong fluorescence light in the presence of human neutrophil elastase, an enzyme involved in lung inflammation are targeted, as is the synthesis of widely used cell labelling fluorophore. New simple synthetic routes leading to purer fluorophores of two different colours were developed, and their cell labelling properties investigated. Finally the synthesis and study of fluorescent compounds with the ability to penetrate cell membranes as well as the nucleus of cancer cells are presented.

Highly specific fluorescent molecules used in conjunction with imaging techniques will in the future, help doctors make more accurate diagnoses of disease as well as facilitating and directing surgical procedures.

Declaration

I, Aurélie Brunet, declare that this thesis entitled "Synthesis and *in vitro* applications of fluorescent imaging agents" and the work presented in it are my own.

I confirm that the research described in this thesis was carried out under the supervision of Professor Mark Bradley at the University of Edinburgh (September 2009 – July 2013). Where work was performed either jointly or wholly by others, this is clearly attributed. Where I have consulted the published work of others, this is clearly attributed; where I have quoted the work of others, the source is always given. No part of this thesis has been previously submitted for any other degree or professional qualification.

Signed: Date:

Acknowledgements

First of all, I would like to thank Prof. Mark Bradley, for giving me the opportunity to carry out my PhD in his research group, but also for his support and understanding.

On the chemistry side, I would like to thank Dr Tashfeen Walton, for her help and patience in the lab but also for her moral support. Tashfeen is the light of the lab and she carries hope and happiness around. A big thank you to Martha MacKay who became a sister to me and Dr Claudia Cavalluzzo with whom I connected from day one and has been a fantastic friend since. To the lunch team for brightening my days: Andrew, Holly, Martin, Martha, Neil. A big thank you in no special order to: Thingsoon, Matt, Frank, Cairnan, Liz, Iain, Melissa, Nanna and Jeff. Thank you to all the Bradley group members (past and present), there would be so many names to write here, I really thank you all.

On the biology side, I would like to thank Dr Chesney Michels, Dr Neil McDonald, Miss Emma Scholefield, Prof. Haslett and Dr Kev Dhaliwal and their group for their help and guidance with the cell work. A special thank you to Dr Manuelle Debunne, Dr Christophe Portal and Lily Portal, who became my little French family, and a great support in my life and my work.

On the personal side, I would like to thanks my parents and especially my mum who really is everything to me, my sister Cristelle and my new brother Maxime, who have always been there, helping me in every way they could. To my close friends, Amandine, Emilie, Helen and Julie, who have believed in me since day one (literately). A special thank you to Emilie for convincing me to go into the science section in high school, if it was not for you I would not be writing this. Also a big thank you for great times to James, Natasha, Matt W, Claire, Eileen, Amber and Mary.

Finally, I would like to thank Neil, for absolutely everything, he has been my best friend, my rock in all situations, he made precious corrections to this manuscript, brought peace and happiness to my heart, and I have learnt to be a better stronger person from him.

Abbreviations

δ:	Chemical shift in ppm
A549:	Human adenocarcinomic alveolar basal epithelial cells
Boc:	*tert*-Butoxycarbony
CFDA:	Carboxyfluorescein diacetate
CFDA-SE:	Carboxyfluorescein diacetate *N*-succinimidyl ester
CFSE :	Carboxyfluorescein *N*-succinimidyl ester
Cy:	Cyanine
DCC:	Dicyclohexyl carbodiimide
DCM:	Dichloromethane
dd:	Doublet of doublets
Dde:	1-(4,4-Dimethyl-2,6-dioxacyclohexylidene)ethyl
DdeOH:	2-(1-Hydroxyethylidene)-5,5-dimethylcyclohexane-1,3-dione
DIC:	*N*,*N'*-Diisopropylcarbodiimide
DIPEA:	*N*,*N*-Diisopropylethylamine
DMAP:	4-Dimethylaminopyridine
DMEM:	Dulbecco's modified eagle medium
DMF:	*N*,*N*-Dimethylformamide
DMSO:	Dimethyl sulfoxide
DSC:	*N*,*N'*-Disuccinimidyl carbonate
EDC.HCl:	*N*-(3-Dimethylaminopropyl)-*N'*-ethylcarbodiimide hydrochloride
EDTA:	Ethylenediaminetetraacetic acid
EEDQ:	*N*-Ethoxycarbonyl-2-ethoxy-1,2-dihydroquinoline
ELSD:	Evaporative light scattering detector
eq:	Equivalent(s)
ES:	Electrospray
ESI:	Electrospray ionisation
FACS:	Fluorescence-activated cell sorting
FAM:	5(6)-Carboxyfluorescein
FITC:	Fluorescein isothiocyanate

Fmoc:	Fluorenylmethoxycarbonyl
FRET:	Fluorescence (Förster) resonance energy transfer
FTIR:	Fourier transform infrared spectroscopy
HBTU:	*O*-Benzotriazole-*N*,*N*,*N*',*N*'-tetramethyl-uronium-hexafluoro-phosphate
HEPES:	2-[4-92-Hydroxyethyl)piperazin-1-yl]ethanesulfonic acid
HFIP:	Hexafluoroisopropanol
HMPA:	4-Hydroxymethylphenoxyacetic acid
HNE:	Human neutrophil elastase
HOBt:	Hydroxybenzotriazole
HPLC:	High-performance liquid chromatography
HR:	High resolution
HRMS:	High resolution mass spectra
IMDM:	Iscove's modified dulbecco's medium
IR:	Infrared
J:	Coupling constant
m/z:	Mass to charge ratio
m:	Multiplet
MALDI-TOF:	Matrix-assisted laser desorption/ionization – time of flight
Mp:	Melting point
MS:	Mass spectrometry
mw:	Microwave
NE:	Neutrophil elastase
NHS:	*N*-Hydroxysuccinimide
Ninhyrdrin:	2,2-Dihydroxy-l,3,-indandione
NIR:	Near infrared
NLS:	Nuclear localisation sequence
NMP:	*N*-Methyl-2-pyrrolidone
NMR:	Nuclear magnetic resonance
Oxyma:	Ethyl 2-cyano-2-(hydroxyimino)acetate
Pbf:	2,2,4,6,7-Pentamethyldihydrobenzofuran-5-sulfonyl
PBS:	Phosphate-buffered saline

PE:	Phycoerythrin
PEG:	Polyethyleneglycol
PeT:	Photo-induced electron transfer
pH:	Potentiahydrogenii
ppm:	Parts *per* million
PS:	Polystyrene resin
Pyr:	Pyridine
q:	Quartet
quint:	Quintet
Rho:	Tetraethylrhodamine
Rhodamine B:	Tetraethylrhodamine
Rho-SE:	Carboxytetraethylrhodamine *N*-succinimidyl ester
ROS:	Reactive oxygen species
RP-HPLC:	Reverse-phase high-performance liquid chromatography
rpm:	Revolutions *per* minute
RPMI:	Roswell park memorial institute
s:	Singlet
t:	Triplet
TAMRA:	Tetramethylrhodamine
TBTU:	*O*-(Benzotriazol-1-yl)-*N*,*N*,*N*',*N*'-tetramethyluroniumtetrafluoroborate
TEA:	Triethylamine
TFA:	Trifluoroacetic acid
TFE:	Trifluoroethanol
THF:	Tetrahydrofuran
TLC:	Thin-layer chromatography
Trityl:	Triphenylmethyl chloride
UV:	Ultraviolet
λ:	Wavelength
λ_{em}:	Emission wavelength
λ_{ex}:	Excitation wavelength
Φ:	Quantum yield

Table of Contents

Chapter 1:

Fluorescence imaging in the life sciences

1.1 Fluorescence overview

Fluorescence and its applications can be seen as a great advancement, if not a revolution, in the world of microscopy and cell biology. New technologies which utilise fluorescence, united with microscopy have shown how cells are structured. Using fluorescence microscopy, scientists have been able to investigate the localisation of molecules within the cell including specific genes within a chromosome.[6] The fluorescence revolution has also allowed quantification of specific molecules within a cell,[7] changes in the concentration of ions within organelles and cells,[8, 9] sort cells,[10] assess cell viability,[11] study enzyme activities[12] and investigate biologically relevant species or parameters such as reactive oxygen species,[13] hydrogen peroxide,[14] metals,[3,15] or pH.[14, 16] Such discoveries have not been contained within the world of fundamental research, and fluorescence technologies have now entered the world of medicine at many levels. The work of van Dam (2011) illustrates perfectly the possibilities that fluorescence imaging offers in medicine (Figure 1).[17] With the knowledge that ovarian cancer cells overexpress folate receptors, an inexpensive fluorescein labelled folate agent was introduced, resulting in ovarian cancer cells appearing green while healthy cells remain

uncoloured, assisting the surgeon in the complete removal of the tumours (Figure 1). The procedure itself was quick and yet the application is remarkable.

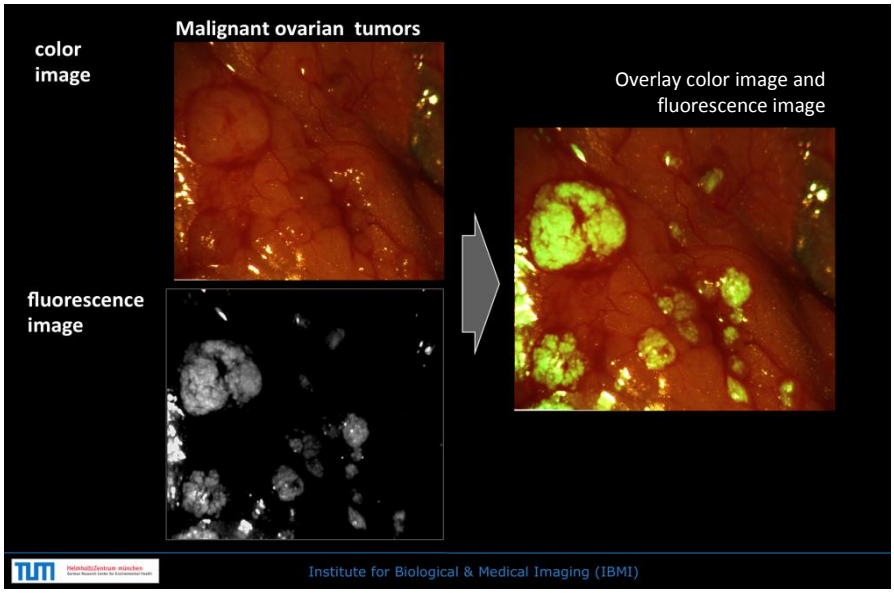

Figure 1: View of the localised region in the peritoneal cavity of an ovarian cancer patient as seen with the naked eye (colour image, top left) with the aid of fluorescent agent (fluorescence image, bottom left) and the overlay (right). Reprinted with permission from Technische Universitaet Muenchen, Institute for Biological and Medical Imaging, Faculty of civil engineering and surveying medicine.

1.2 Fluorescence principle

Fluorescence is an emission of light from a substance that is in an electronically excited state on relaxation to its ground state.[18] These states, more commonly known as the ground, first, and second electronic states are represented by the terms S_0, S_1 and S_2 (see Figure 2). At each of these excited states the fluorophore can exist in a number of vibrational energy levels. When an electron in a molecular orbital belonging to a molecule in its electronic ground state (S_0) absorbs energy from a suitable light wave, the electron will be promoted to a higher molecular orbital. The

molecule absorbs energy from light and will be raised from the ground state to an electronically excited state at various vibrational levels (**1**), which quickly relaxes to the lowest vibrational level of the electronically excited state (S_1) (**2**). It loses this excitation energy by transitioning to a lower electronic level through photon emission (i.e. fluorescence) (**3**) or in *via* a nonradiative decay (quenching) (**4**).

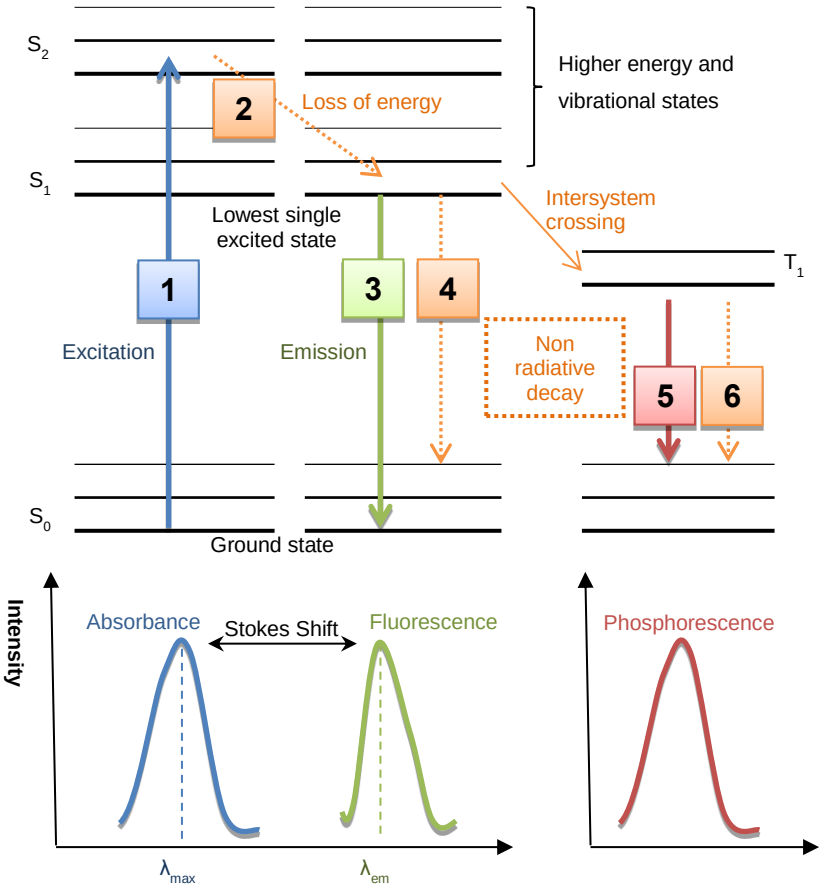

Figure 2: Energy diagram suggested by Jablonski.[19] **1** Excitation of the fluorophore through photon absorption, **2** relaxation to lowest vibrational state with small loss of energy, **3,5** transition to ground state with emission of visible light, **4, 6** transition to ground state without emission of light.

The excited state can also undergo forbidden inter-system crossing to the triplet excited state where the excitation energy is lost by either photon emission (i.e. phosphorescence) (**5**) or quenching (**6**).[20]

There are a variety of processes responsible for quenching, among them are energy transfer where the excitation energy is transferred to another molecule, static quenching which occurs when there is a stacking interaction resulting in the fluorophore forming a non-fluorescent complex,[21] dynamic and collisional quenching which can occur when an excited fluorophore makes contact with a molecule that can facilitate non radiative transition to the ground state,[22] photo-induced electron transfer (PeT) (see later),[23] and finally molecular rearrangement.[18]

1.3 History of fluorescence techniques

The earliest description of fluorescence is often associated with the studies of wood by Monárdes in the sixteenth century. In 1852 Stokes introduced the word 'fluorescence' describing the light emission induced during excitation and the study of numerous fluorescent substances in a one hundred page publication.[24, 25] It was in 1871 that the first fluorescent dye, fluorescein, was synthesised by von Bayer.[26]

Fluorescence was for the first time combined with a microscope in 1911 by the physicist Heimstädt.[27] In 1914, based on this new discovery, von Provazek used a fluorescent dye as a stain to enhance the visibility of cells and tissues.[28] In 1929, Ellinger, designed the first epi-fluorescence microscope,[29] with the light source lying on the same side of the sample as the objective, to allow efficient sample excitation, and a filter barrier absorbing incident light reflected from the surface of the

specimen.[28] Various improvements[30] were made during the following years but it was the original confocal microscope, developed and patented by Minsky that had the greatest impact.[31] Its invention introduced a point source of light focused upon a specimen. The specimen could move across the focal point of illumination so that a selected area of the specimen traverses, and is examined by the point of light. This new discovery offered several advantages over standard optical microscopes such as reduced blurring of the image from light scattering, improved signal-to-noise ratio, increased resolution, clear examination of thick or scattering specimens and x, y and z scanning became possible. Although the discovery was at the time astonishing, the need for this instrument only came in the late eighties, with the development of fluorescently labelled biomolecules.

In 1941, Coons attached a fluorescent dye (fluoresceinisothiocyanate) to an antibody,[32] to localise its respective antigen in a tissue section. His later studies[33] greatly contributed to the use of fluorescent antibodies in research. In 1961, Coons wrote "I suggest lightly that this is the hour of the fluorescent antibody",[34] without knowing that nearly 50 years after its original discovery,[32] immunofluorescence remains a cornerstone of histochemistry, a powerful tool in nearly every field of biomedical research.[35]

In the mid-eighties the limitations of the optical microscope were obvious, specimen thickness being the major inconvenience, it was becoming obsolete.[36] In 1987 White, after reconsideration of the Minsky work, presented the first prototype of a commercial laser scanning confocal microscope.[37] New research could be carried out, thicker samples could be analysed as well as three dimensional studies. In 1990

O'Rourke published the full three dimensional mapping of a specific neuron labelled with a fluorescent lipid in the cortex of a tadpole. The study was carried out over several days, during which the branching pattern of cell growth could be seen.[38]

The literature then began to bloom with confocal studies on all sorts of models, with investigation of the dynamics and localisation of cytoplasmic proteins,[39-42] nuclear and chromosomal behaviours,[43, 44] or intracellular localisation of specific nucleic acids.[45, 46] Fluorescent confocal microscopy was widely used for human and rodent studies, such as measurements of Ca^{2+} ions in various cell organelles (ER,[47] mitochondria,[48-50] nucleus[51]), and the analysis of other chemical sensors to detect biologically relevant species or parameters such as reactive oxygen species,[13] hydrogen peroxide,[14] nitric oxide,[52] metals[3,15] or pH.[14, 16] Figure 3 shows a transgenic root to illustrate the use of confocal microscopy in a thick sample. Figure 4 shows multi stained cancer cells and highlights the ability of the microscope to look at a single cell from different angles.

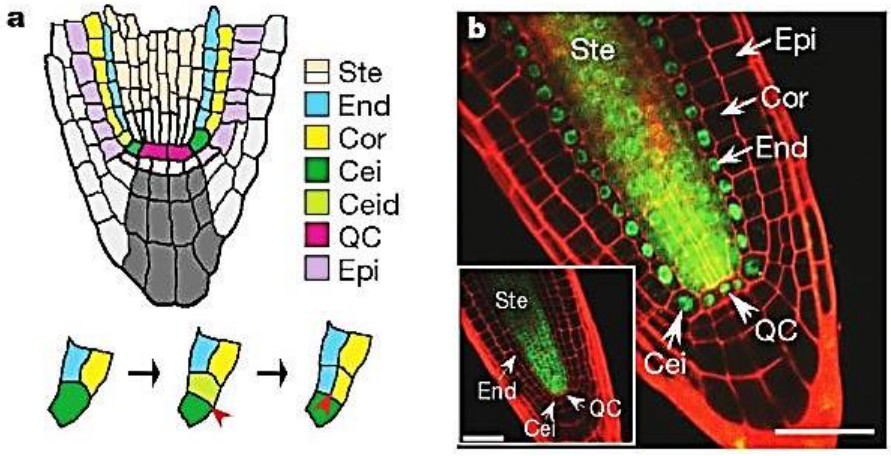

Figure 3: Diagram and confocal image of root tip. **a** Diagram of Arabidopsis root tip and cell divisions (red arrowheads). **b** Confocal images of the SHR:GFP transgenic roots. Scale bars 50 µm. Reprinted with permission from Nakajima.[53] Copyright 2001 Macmillan Publishers Ltd.

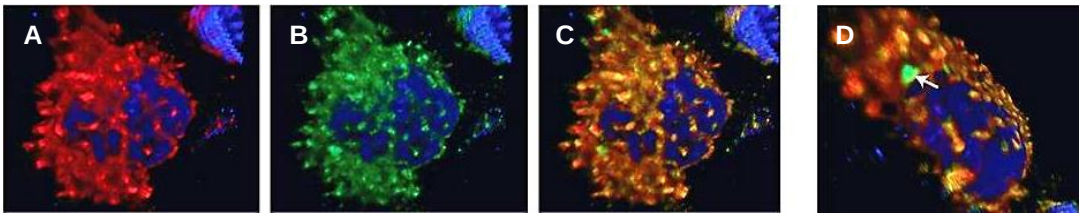

Figure 4: Confocal pictures of cancer cells (HeLa), **A.** stained cell nucleus (blue) and stained mitochondria (red), **B.** stained cell nucleus (blue) and mitochondria-localised fluorescent compound (green), **C.** merged image (orange indicates co-localization), **D.** merged image of the same cell observed from a different angle. Reprinted with permission from Yusop.[54] Copyright 2011 Macmillan Publishers Ltd.

It has now been over twenty five years since the first commercial laser scanning confocal microscope and its use in science has not lessened. The field of microscopy highlights the uses of fluorescence, but many different techniques have also been developed for cellular studies such as fluorescence-activated cell sorting (FACS), a machine which allows counting, separation and sorting of cell populations using different fluorescent markers;[55] or the fluorescent microplate reader, an automated instrument that can perform complex cell-based assays, reading absorbance or fluorescence of up to 1536 samples in parallel. There have been major developments in the imaging of whole animals with fluorescence molecular tomography (FMT). FMT allows three dimensional imaging of fluorescent markers in whole animal.[56] Finally, great improvements in fluorescent imaging agents have been made to develop probes with high target specificity, high fluorescence intensity and low background fluorescence.

1.4 Fluorescent imaging agents

The design of fluorescent imaging agents is complex requiring many parameters to be thought through before any synthesis is carried out. The fluorophore must be compatible with the targeted technique and the nature of the biological system, for example, excitation in the ultraviolet can cause direct tissue damage,[57] therefore parameters such as wavelength, brightness, stability, target delivery, multiphase imaging, and perhaps FDA approval must be considered. The probe itself must be planned with the biological target in mind considering parameters such as solubility, target specificity and low background fluorescence.

1.4.1 General requirements of the fluorophore

Wavelength

A fluorophore must undergo excitation (to reach an excited state), followed by emission. Excitation within the blue, green or yellow regions (< 650 nm) have poor tissue penetration. Near infrared (NIR) dyes overcome this issue,[58-60] however, commercial NIR dyes often have lower quantum yields than green and yellow dyes and have the tendency to aggregate in solution due to hydrophobicity.[61, 62]

Brightness

Brightness of the fluorophore is another important feature. The brighter the dye, the less excitation is required, resulting in better signal to noise ratios. The most common way to compare fluorophores is to look at their quantum yields Φ, the number of

photons emitted over the number of photon absorbed with the ideal fluorophore coming close to 1.

Stability

Another essential property of the dye is its stability *in vitro* and *in vivo*. The dye must be soluble and stable in aqueous media and not precipitate, aggregate or degrade in biological systems. For intracellular studies, photobleaching and dye degradation must be considered. Although the dye should be stable long enough for the study to be carried out, it must also be degradable to allow excretion, particularly if the study aims to be translated to human imaging.

Target delivery

The influence of the dye over the targeting moiety is another important consideration, even more so when more than one fluorophore per targeting moiety is used. Dyes can increase the efficiency of a targeting moiety, for example fluorescein has been shown to drive metal complexes into the nucleus,[63] or on the contrary negate a targeting moiety, for example, Cy5.5 dyes (Figure 5) conjugated to a protein molecule lead to rapid liver accumulation before successful targeting.[64]

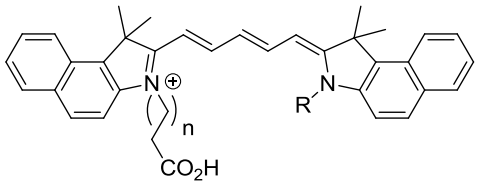

Figure 5: Generic structure of Cy5.5.

Multicolour imaging

Using multiple fluorophores that have distinct emission wavelengths is an attractive option that fluorescence molecular imaging offers. Multiple targets can be identified and followed simultaneously, using different filters to excite and detect the emission of each fluorophore. These methods are routinely used in laboratories using confocal microscopy or flow cytometry.[65] Kobayashi (2007) simultaneously imaged five separate lymphatic flows in living mice using five different emission wavelengths.[65] Multicolour imaging is a fast growing approach with future applications in the field of medicine, as it could allow imaging of more than one physiological condition and evaluate the pharmacokinetics and interactions of multiple drugs, an asset for drug development.[66, 67] The study of multiple receptors expressed on target cells especially for cancer diagnosis,[68, 69] may increase the understanding of a living tumour or assist the surgeon in multi-coloured fluorescence-guided surgery.[70]

1.4.2 Targeted fluorescent probes

Targeted fluorescent probes consist of a fluorophore combined to a targeting moiety. Fluorescent labels are powerful tools with broad applications from cellular component labelling to biomolecule imaging. All fluorescent targeting probes must be non-toxic and able to reach and specifically and efficiently label their target.

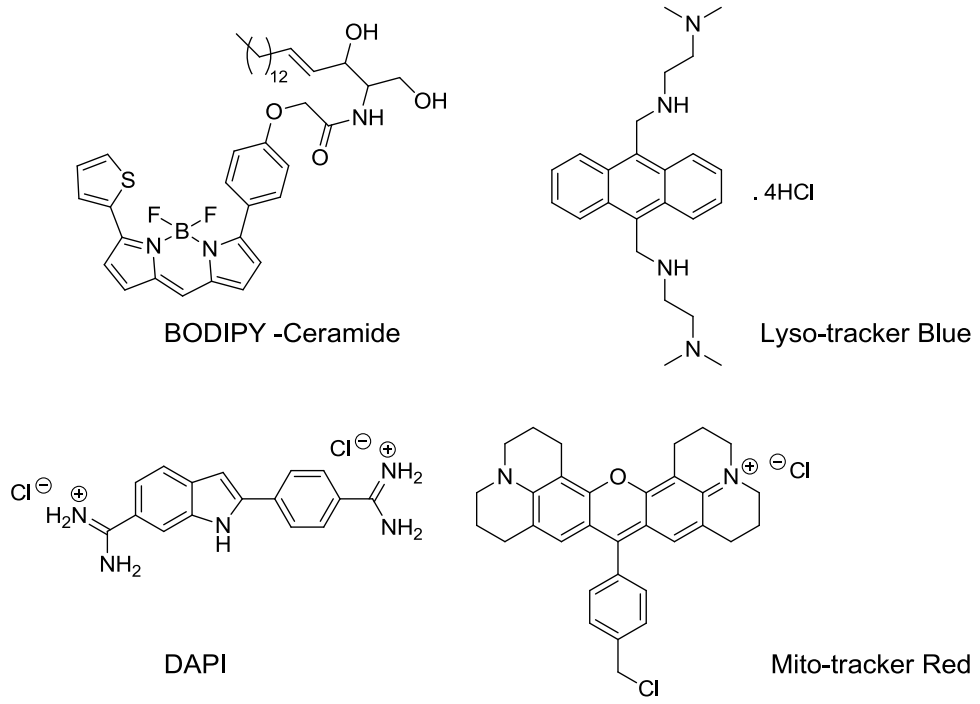

Figure 6: Structures of common organelle stains

Some fluorescent labels have been developed to increase the visibility of particular organelles such as BODIPY-Ceramide for Golgi apparatus, lyso-trackers for lysosomes, DAPI or Hoechst for DNA/nuclei (Figure 7), or mito-trackers for mitochondria (Figure 6).[71, 72] Other well-known dye includes propidium iodide, a DNA stain that selectively labels dead cells, a useful tool for cell viability assays.[11, 73] Antibodies are common targeting moieties,[74-76] Figure 7 illustrates this methodology, where human epithelial cancer cells were labelled with two fluorescent antibodies and a nucleus stain, the extracellular domain and intracellular domain can be easily visualised as well as the nuclei. Other biomolecules are also commonly used as targeting moieties such as peptides,[77-79] protein,[80, 81] or DNA.[82]

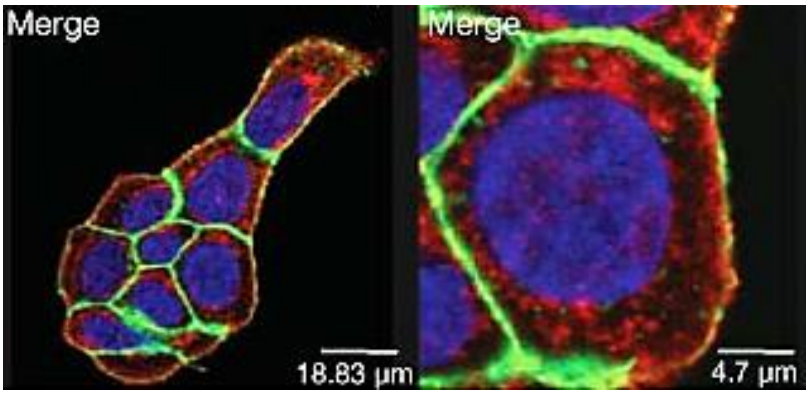

Figure 7: Human epithelial cancer cells (FaDu) were labelled with two specific primary antibodies in combination with fluorescently labelled secondary antibodies (green and red). Nuclei were counterstained with Hoechst 33342 (blue).The location of the extracellular domain (green) and the intracellular domain (red) was revealed using laser scanning microscopy. Reprinted with permission from Maetzel.[83] Copyright 2009 Macmillan Publishers Ltd.

1.4.3 Smart probes

Smart probes, are molecules that will emit fluorescence after interaction with the subject of interest. They can be classified into three categories: *small smart molecules* that have a particular structure, allowing them to fluoresce or be quenched, *self-quenching molecules* where, for example, close proximity of multiple dyes result in quenching with disaggregation restoring the fluorescence; and finally *quenched molecules* where a dark quencher moiety is attached to a dye to absorb its fluorescence and detachment of the two results in restored fluorescence.

Small smart probes

Small smart probes are varied in term of structure, mode of action and targets. They are often target-specific and rarely translatable to a different target. To illustrate the principle, a few representative examples will be presented.

Aminomethylcoumarin (AMC) is a common dye that is fluorescent and contains a primary amine group. When this primary amine is coupled to an acid the resulting amide modifies the electronic structure of the coumarin molecule which renders it non-fluorescent. This quenched probe can then be used to monitor enzyme activity, that can cleave the peptide bond and restore the fluorescence (Scheme 1).[84]

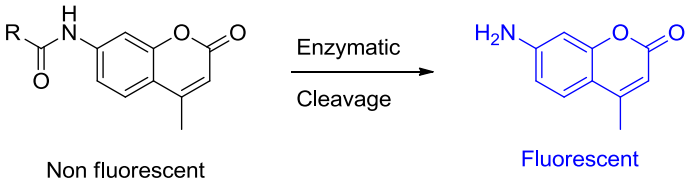

Scheme 1: Aminomethylcoumarin based probe for enzyme detection. Amide bond of the non-fluorescent amidomethylcoumarin can be enzymatically cleaved to free fluorescent aminomethylcoumarine.

Diacetylated fluorescein has no fluorescence until an esterase cleaves the acetyl groups to restore fluorescein.[85] Carboxyfluorescein diacetate *N*-succinimidyl ester (CFDA-SE) is used to label proteins within the cytoplasm and is widely used for cell division studies.[1]

Environmental indicators or chemical sensors are typically small activatable molecules that detect biologically relevant species or parameters. For example, in 1997 Crow synthesised a reduced fluorescein derivative that in the presence of reactive oxygen species (ROS) is oxidised to fluorescein, restoring its fluorescence.[86] Similarly Seo developed silica nanoparticles functionalised with a fluorescein derivative that binds reversibly to copper. When the metal complex is formed the fluorescence is altered, allowing imaging of Cu^{2+} in living cells.[15] Environmental

indicators allow real-time studies of intracellular events, for the understanding of fundamental aspects of cells.[87]

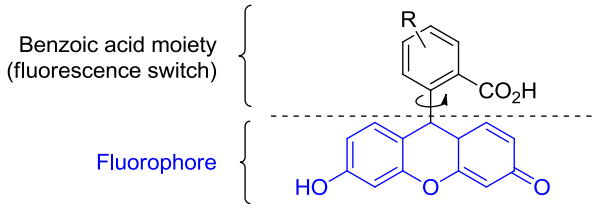

Figure 8: Fluorescein structure divided into two parts, the benzoic acid moiety (fluorescence switch) and the xanthene moiety (fluorophore), angle between the moieties varies depending on the R group switching the fluorescence on or off.

Another type of activatable molecule is based on photo-induced electron transfer (PeT). In this case, when the fluorophore is excited, an electron is excited to a higher energy orbital. This excited state leaves a vacancy in a ground state orbital that can be filled by an electron donor, turning off the fluorescence. In the case of fluorescein, the xanthene moiety and the benzoic acid moiety sit at a 90° angle (Figure 8).[88] Miura showed that when the angle is modified the resulting molecule can be non-fluorescent or highly fluorescent.[89] Ueno have used this knowledge and developed BODIPY derivatives with a benzene moiety that can selectively monitor nitrative stress (Figure 9).[4] Compound NiSPY-1 undergoes nitration in the presence of peroxynitrite ($ONOO^-$) resulting in the formation of the fluorescent NiSPY-1 N (Figure 9). This new strategy of rational design led to the development of numerous novel fluorescent probes based on various dyes for the detection of ROS, enzymes or pH.[4, 88, 90-96]

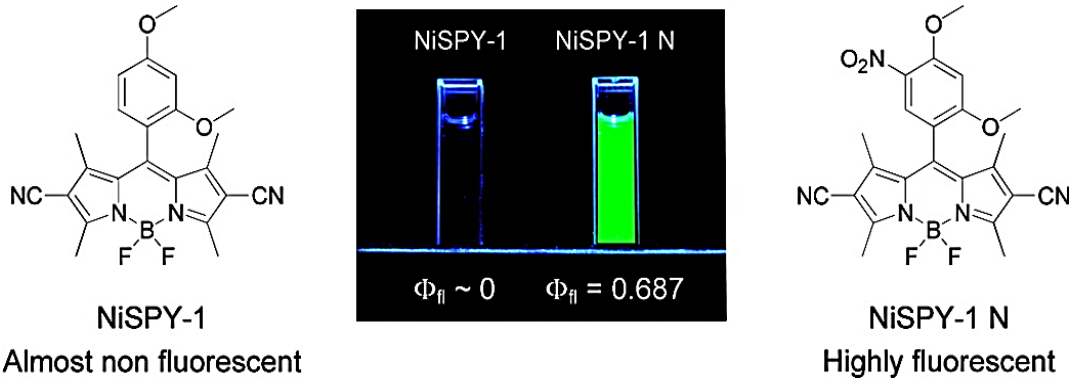

Figure 9: Sensor for imaging nitrative stress. In the presence of $ONOO^-$ non fluorescent NiSPY-1 undergoes aromatic nitration, the resulting compound NiSPY-1 N is highly fluorescent with a quantum yield of 0.687. Reprinted with permission from Ueno.[4] Copyright 2006 American Chemical Society.

Self-quenched molecules

Self-quenched molecules are designed with multiple fluorophores in close proximity resulting in a non-fluorescent probe. The probe can be cleaved by an enzyme, releasing the fluorophores; or they can be cell specific, and once internalised in the cell, the structure is degraded or unfolded allowing the fluorescence emission.

A first method is based on Förster resonance energy transfer (FRET), where two different fluorophores are used. The fluorophores must be carefully selected as the first fluorophore must emit at the wavelength the second fluorophore is excited at. The efficiency of this process is strongly distance dependent. In close proximity, solely the fluorescence of the second fluorophore will be observed and the first fluorophore will be quenched, when separated, both emissions can be detected (Figure 10A). This principle has been used in various ways; Yang (2006) investigated disulfide bond-reducing activity in endosomal compartments and for that purpose built a FRET probe where two fluorophores were linked by a disulphide

bond. When cleaved the fluorophores were separated and emission of both dyes could be detected.[97]

FRET probes for enzymatic assays are molecules where the two fluorophores are attached at the *N*- and *C*-terminus of a specific peptide (or on opposite end of the cleavage point) that once recognised by the targeted enzyme is cleaved, freeing the two fluorophores from each other (Figure 10A).[98]

FRET probes have also been designed without a need of cleavage between the two fluorophores, solely sufficient distance (Figure 10B). Sato (2002) developed a probe where the linker between the fluorophores separates them enough to prevent energy transfer and quenching. This link is composed of two domains which, upon phosphorylation by a kinase brings the two fluorophores in close proximity allowing them to FRET.[99]

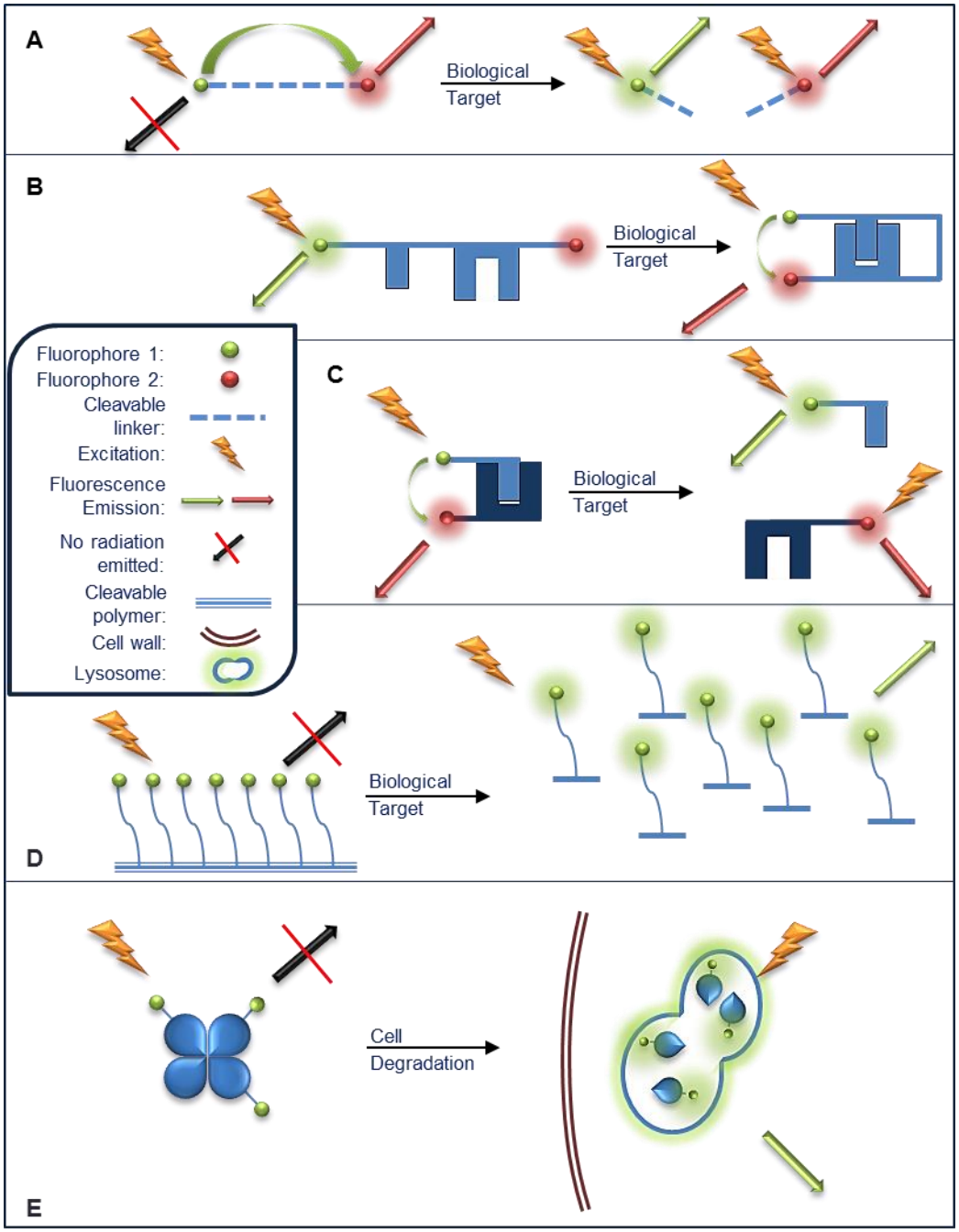

Figure 10: Representation of self-quenching approaches: **A.** FRET probe with a cleavable linker, **B.** Intramolecular FRET probe with two complementing domains, **C.** intermolecular FRET probe, **D.** self-quenched polylysine polymer, **E.** self-quenched tetrameric glycoprotein.

FRET can also be observed intermolecularly, this approach has been particularly used to study protein interactions, for example, Azpiazu (2004) studied the

association of G-protein coupled receptors (GPCRs) (Figure 10C).[100] Their probes consisted of two fluorescently labelled G-proteins. Before activation by GPCRs, the two studied proteins bind together, causing the fluorophores to FRET. After activation, receptor mediated dissociation of the proteins, results in the loss of FRET.[100]

Another type of self-quenched molecule is based on a mechanism where excited fluorophores of the same type absorb the energy emitted from each other that would otherwise have led to an emitted photon. The self-quenching properties of several xanthene based fluorophores has been investigated, Valdes-Aguilera (1989) have shown that homodimer formation induces shifts in absorbance spectra, resulting in the complete quenching of the emission fluorescence signal.[101-104] The first type of construct was developed by Weissleder (1999) and is based on multiple fluorophores on a synthetic polymer.[105] The polymer consists of a poly-L-lysine chain that is cleaved by proteases resulting in fluorophore separation and thus dequenching (Figure 10D). This polymer has been used with trypsin,[106] cathepsins[107-111] and matrix metalloproteinase.[112-115] The second type of construct was developed by Bradley (2002) and consisted of a dendron structure where the branches are built with specific peptide sequences and fluorophores.[116] The resulting probe is non fluorescent or weakly fluorescent due to the close proximity of the multiple dyes but once the targeted enzyme recognises and cleaves the specific peptide sequence, the fluorophores are released resulting in the restored fluorescence. Advantages such as ease of preparation, homogeneity and small size, have allowed the study of proteases such as protease endoproteinase AspN, and neutrophil elastase.[116, 117]

Macromolecules are another approach to self-quenched molecules, as demonstrated by Hama (2007), where multiple copies of carboxy-X-rhodamine (ROX) conjugated to avidin, a non-covalently bound tetrameric glycoprotein resulted in a quenched complex. After internalisation into the cell, the tetramer is broken down into monomer units resulting in fluorescence emission (Figure 10E).[118]

Quenched molecules

An alternative to fluorophore-fluorophore quenching is the combination of fluorophore-dark quencher. Dark quenchers are non-fluorescent molecules that absorb energy from an excited fluorophore and dissipate the absorbed energy as heat without emitting light.[119]

Similarly to self-quenched molecules, the FRET principle has also been used to construct probes using a fluorophore-dark quencher pair. Farber (2001) synthesised a cleavable phospholipid covalently linked to a fluorophore (BODIPY) and a dark quencher (dinitrophenyl).[120] Enzymatic cleavage of the phospholipid successfully resulted in de-quenching and detectable fluorescence emission.[120] Using the same concept, many peptides have been used as cleavable linkers, such as Bullok (2005) who used a caspase specific peptide to detect apoptosis,[121] or Bulm (2007) who synthesised a cathepsin specific peptide to detect tumours in mice.[122]

Similarly to self-quenched molecules, avidin was constructed with a combination of dark quenchers and fluorophores and upon tetramer digestion within lysosomes the fluorescence was restored, resulting in the visualisation of peritoneal cavity.[123] Another example is the design of trastuzumab, a monoclonal antibody synthesised with a fluorophore and a dark quencher. Once the antibody is recognised

and penetrates the cells, its degradation in lysosomes results in fluorescence emission, allowing the visualisation of lung tumours.[123]

Pre-targeting activation is another strategy where two complementary imaging agents are used. For example, Ogawa (2008) used a monoclonal antibody with a fluorophore and a biotin molecule, after sufficient accumulation of the fluorescing antibody to the target, another agent was added.[124] This agent was a combination of a dark quencher and a neutravidin molecule, unbound antibody was then bound to the neutravidin−quencher, reducing the background signal. By using this pre-targeting activation method, they successfully visualized breast cancers with minimal background signals.[124]

1.5 Thesis aim

The aim of this thesis was to contribute to the field of fluorescent imaging agents by developing targeted fluorescent probes and activatable imaging probes, as well as improving the synthesis and purity of well-known dyes such as fluorescein and rhodamine.

Previously, in the Bradley group self-quenched dendrons were developed. To broaden their application and further understand their mode of action, the first aim of this thesis was to synthesise and study a "dual-colour" self-quenched dendron for the detection of neutrophil elastase. The second aim of this thesis was to establish a single isomer synthesis of 5- and 6-carboxyfluoresceindiacetate *N*-succinimidyl ester as well as 5- and 6-carboxytetraethylrhodamine *N*-succinimidyl ester and study their cytoplasm labelling properties. The final aim was to synthesise and investigate the

nuclear labelling property of the dendron structure when conjugated to nuclear localisation sequences.

Chapter 2:

Fluorescent probes for the detection of neutrophil elastase

2.1 Introduction

2.1.1 The immune system

The immune system is a collection of organs, cells, and molecules with the function of protecting the organism against infectious agents. If a microbe enters the body, the immune system will react to destroy or contain this invading organism (as well as any harmful materials it may produce) using white blood cells and defensive peptides.[125] If the first non-specific attempt at defence is unsuccessful, the system will try to adapt and develop a specialised countermeasure. The types of leukocytes that perform the first generic defence attempt are produced in the bone marrow, predominantly from hematopoietic stem cells.[126] Stem cells renew themselves through cell division and they can differentiate to give rise to a diverse range of blood cell types.[125]

One of the major distinguishing features between various types of leukocytes is the presence or absence of granules. Among the so-called granulocytes are neutrophils, eosinophils and basophils. These cells contain distinctive membranes enclosing cytoplasmic granules which contain an armoury of enzymes and proteins.[125] Neutrophils constitute 50 – 75% of circulating leukocytes, while eosinophils represent 1 – 6% and basophils constitute less than 1%.[127] This large number of

neutrophils allows them to respond quickly, being the first cell type to be recruited by the immune system.

2.1.2 Neutrophils

The main function of neutrophils is host defence. To fulfil this role, the cell must respond to chemical signals generated in the affected tissue, migrate to the site of action, recognise and then kill the foreign cells.[128] They primarily engulf pathogens and foreign material by phagocytosis after which bacterial killing is mediated within the phagolysosome. The intracellular killing of microorganisms generally involves a respiratory burst via non-mitochondrial reduction of oxygen to highly reactive oxygen species (ROS). Respiratory burst products and their derivatives include superoxide, singlet oxygen, hydrogen peroxide, hydroxy radicals and chloramines.[129] As well as performing intracellular mediated pathogen killing, neutrophils have also evolved to rapidly degranulate preformed bactericidal products such as ROS and cytokines to the extracellular environment.[130] These released moieties work by withholding essential factors that bacteria require to multiply (e.g. iron *via* the release of iron-binding proteins) or by delivering cytotoxic agents (e.g. hypochlorous acid) to the bacterium.[129, 131] There are distinct sets of granules, the so-called secondary and tertiary granules, which facilitate neutrophil recruitment to the inflammation site and tissue breakdown, and the primary (or azurophilic) granules, which can release antimicrobial agents and bactericides.[130]

Among these antimicrobial agents and bactericides are proteases, the serine protease on which this project is focused on is human neutrophil elastase, an enzyme whose function is the destruction of bacteria.[132]

2.1.3 Neutrophil elastase

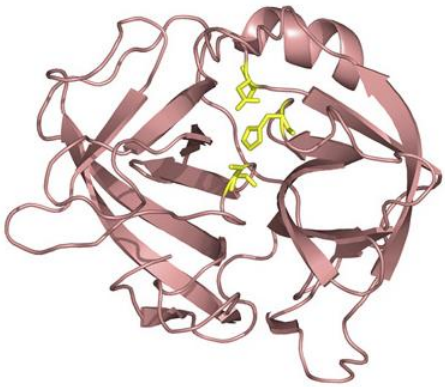

Figure 11: 3D X-ray structure of NE. Reprinted with permission from Korkmaz.[3] Copyright 2008 Elsevier Masson SAS.

Neutrophil Elastase (NE) is a 30 kD serine protease glycoprotein consisting of 218 amino acids. NE has a well-defined catalytic triad of histidine, aspartic acid and serine residues.[3] The X-ray three dimensional structure reported by Korkmaz (2008) highlights the catalytic site (Figure 11 in yellow).[3] Serine proteases bind substrates and their active sites hydrolyse peptide bonds very efficiently (Figure 12).[2] The imidazole moiety of histidine deprotonates the hydroxyl group of serine which attacks the polarised carbonyl group of an amide bond. The negative charge formed on this intermediate is stabilised by hydrogen bond interactions with the protein. Following cleavage of the amide bond, an acyl enzyme intermediate is generated

along with release of the free amine. Finally, hydrolysis of the ester releases a carboxylic acid, regenerating the catalytic active site.[2]

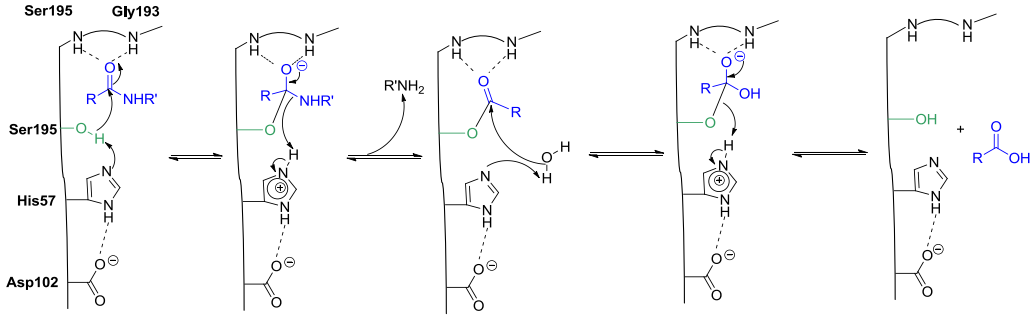

Figure 12: Hydrolysis mechanism in the active site of NE, adapted with permission from Hedstrom.[2] Copyright 2002 American Chemical Society.

NE is stored in the primary granules at concentrations surpassing the millimolar range, making it a major constituent for neutrophils.[133] NE has been shown to contribute significantly to host protection against microbial infections, by extracellular killing of micro-organisms.[134] However, when dysregulated NE can contribute to acute and chronic inflammation diseases.[135]

2.1.4 Dys-function of neutrophil elastase

Acute lung injury and the maladaptive repair process that leads to acute respiratory distress syndrome (ARDS) are inflammatory diseases. ARDS is characterised by a fibroproliferative phase that is phenotypically similar to a condition called idiopathic pulmonary fibrosis (IPF), a term that refers to the unknown cause of the disease, hence difficulties in diagnosis and treatment, but which can be seen as a dysregulated inflammatory and repair response.

Different mechanisms, by which neutrophil elastase might contribute to the inflammation and maladaptive repair seen in ARDS and IPF have been proposed.[136] Kawabata (2002) describes different ways NE can preserve its catalytic activity in the case of acute lung injury (a simplified figure summarises their proposed mechanism (see Figure 13)).[136]

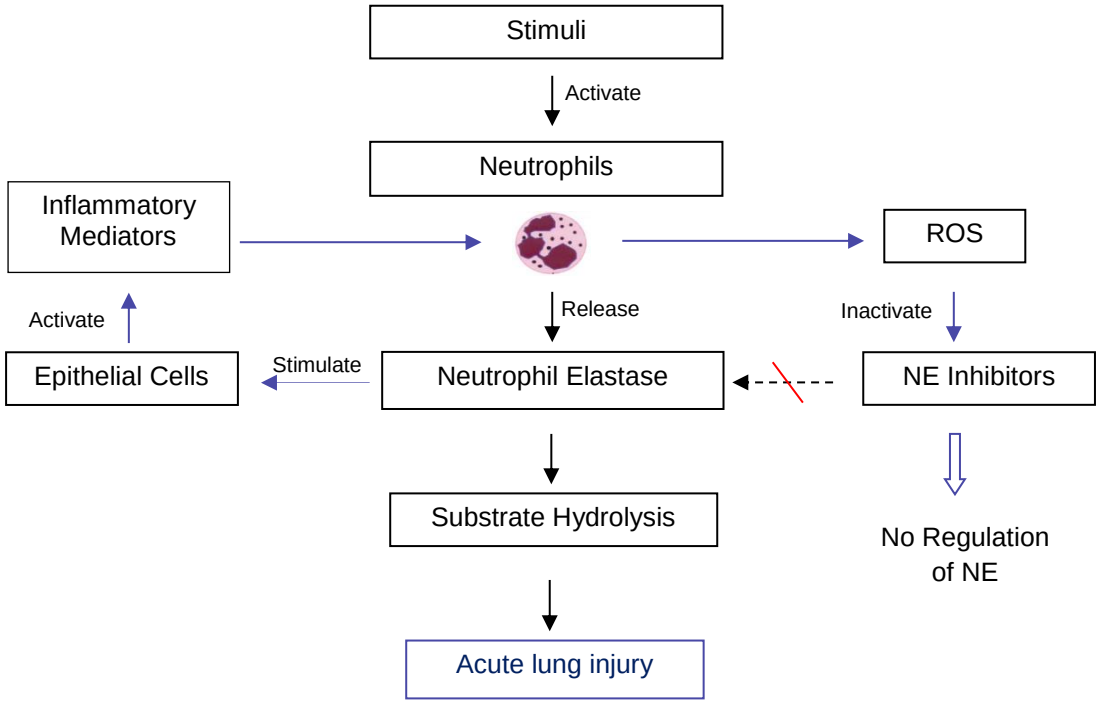

Figure 13: Proposed mechanism of NE dys-function adapted from Kawabata.[136] Copyright 2002 with permission from Elsevier.

Under stimuli, such as acid respiration or pro-inflammatory substances that activate neutrophils, NE is released. NE can interfere with epithelial cells and stimulate their production of pro-inflammatory cytokines which will activate neutrophils. Activated neutrophils will produce NE as well as ROS, which will inactivate the protease inhibitors responsible for the regulation of NE, resulting in the accumulation of excessive NE.[136-138]

To understand more precisely the role of NE in ARDS and/or IPF, there is a need to image neutrophil elastase *in vivo* to be able to measure variation in its activity following administration of therapeutics to direct intervention and develop more efficacious treatments.

2.1.5 Chapter aim

This project has the ambition to develop fluorescent probes for the detection of neutrophil elastase *in vitro*.

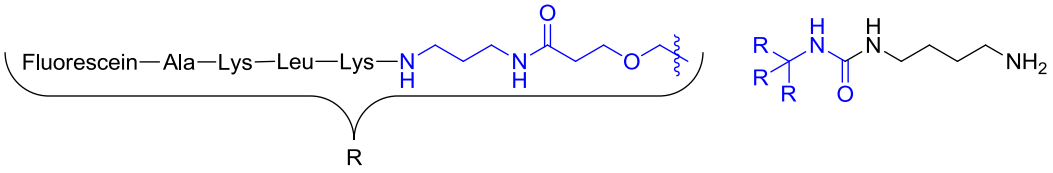

Figure 14: Internally fluorescence quenched dendron structure developed by Bradley.[116]

Bradley has developed an internally fluorescence quenched dendron structure where each branch contains a sequence peptide specific to AspN endoproteinase and a fluorophore (Figure 14).[116] This high local concentration of fluorophores results in a non-fluorescent molecule which, upon protease cleavage detaches the fluorophores from the dendron moiety removing the quenching (Figure 15).

In this project, the aim was to develop the Bradley strategy further. Firstly, the dendron core was to be studied with respect to cell permeability and solubility; secondly, peptide sequences specific to neutrophil elastase (Table 1) were added as well as a second fluorophore (Figure 15).

The targeted peptide sequence was discovered by Korkmaz (2004), it is a nine-mer peptide specifically cleaved by NE over two similar serine proteases namely proteinase 3 and cathepsin G (Table 1).[5]

Entry	Substrate	k_{cat}/K_m ($mM^{-1} . s^{-1}$)		
		Elastase	**Proteinase 3**	**Cathepsin G**
8	APEEIM**D**RQ	683±75	14.6±1.3	n.s.h
9	APEEIM**R**RQ	531±47	<1	n.s.h
10	APEEIM**P**RQ	11.5±1.5	<1	n.s.h.

Table 1: Specific substrate for NE discovered by Korkmaz[5] (n.s.h: no significant hydrolysis). Reprinted with permission from Kormaz.[5] Copyright 2013 American Thoracic Society.

Korkmaz prepared several substrates and monitored their cleavage by the three enzymes using the kinetic parameter k_{cat}/K_m, Table 1 illustrates three relevant entries. The substrate shown in Entry 9 displays rapid cleavage from elastase but remains uncleaved in the presence of proteinase 3 or cathepsin G. A carton of the newly designed probe is shown Figure 15.

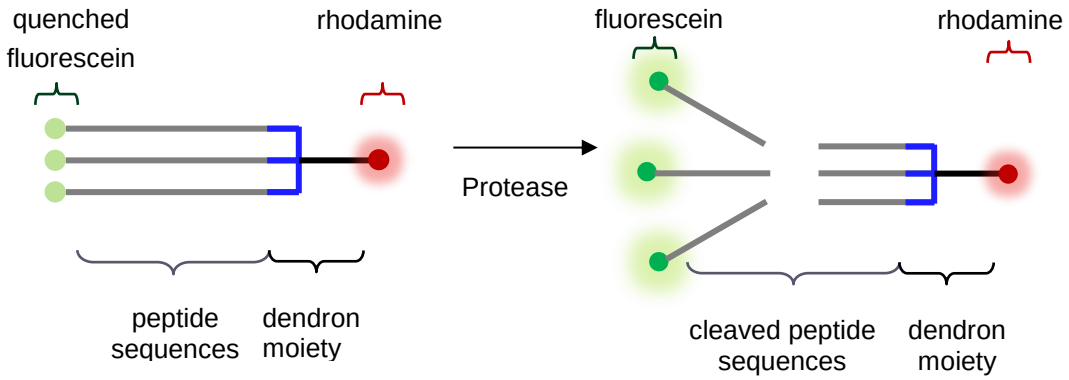

Figure 15: Mechanism of action of targeted probes.

The targeted probe contains peptide sequences specific to neutrophil elastase as well as two distinct fluorophores. Due to the dual labelling envisaged, the molecule will be traceable before and after enzymatic cleavage, while offering an internal standard. Finally it will allow us to follow the dendron moiety once the peptide sequences are cleaved and quantify the fluorescence increase during enzymatic cleavage.

2.2 Synthesis of dual labelled dendrons

2.2.1 Synthesis of the dendron monomer

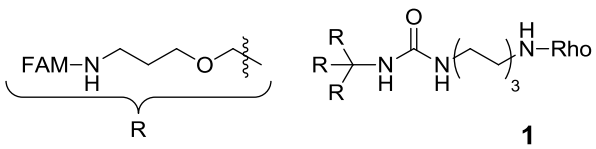

1

Figure 16: First targeted probe – dual labelled dendron.

The first targeted probe was dual labelled dendron consisting of a dendron core moiety, three fluorescein units and a tetraethylrhodamine unit (probe **1** Figure 16).

In Figure 14 the dendron core structure is highlighted in blue, it was planned to use a slightly modified dendron monomer **4** adapted from the dendron moiety **3** published by Trouche (Figure 17).[139]

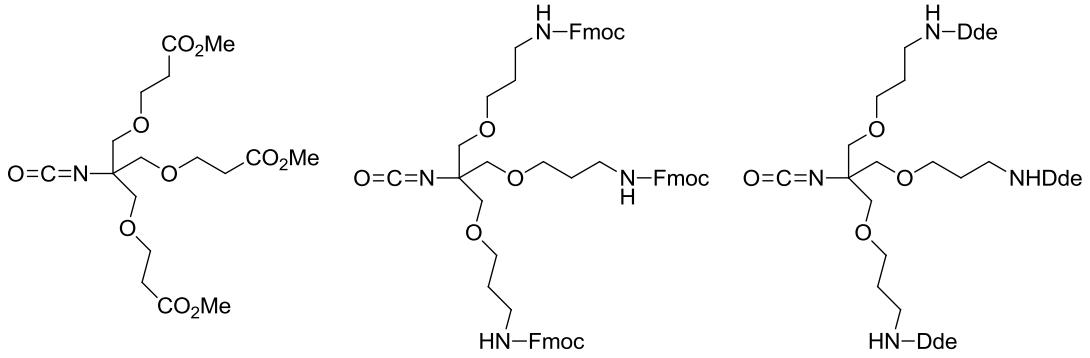

Bradley monomer - 2 **Trouche monomer - 3** **Newly designed monomer - 4**

Figure 17: Dendron moieties developed by Bradley **2**,[116] Trouche **3** [139] and newly designed monomer **4**.

This modification introduces the Dde protecting group, a moiety easy to synthesise and couple in solution with the advantage of being suitable for solid phase synthesis using Fmoc strategy.[140]

The synthesis of **1** started with the construction of the three branched dendron monomer unit (**7**).

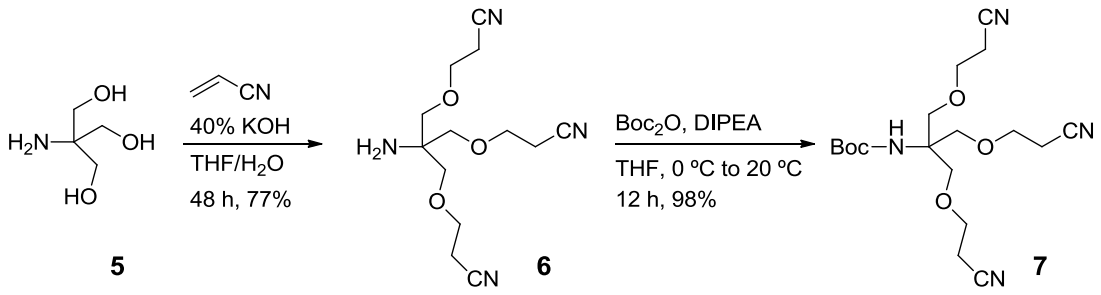

Scheme 2: Michael addition and protection of monomer unit.

The first reaction was a 1,4 addition of the three alcohols of trizma base **5** onto acrylonitrile. The reaction was originally carried out in tetrahydrofuran (THF) following a literature protocol but yielded just 35% of the desired product rather than

the 54% reported.[139] Since the reagents were not fully soluble in THF, the yield was optimised to 77% using a mixture of water and THF as solvent and an increased reaction time of 48 h (Scheme 2). The next step was the protection of the free amine **6** using di-*tert*-butyl dicarbonate. The high yielding reaction gave the nitrile **7** (Scheme 2).

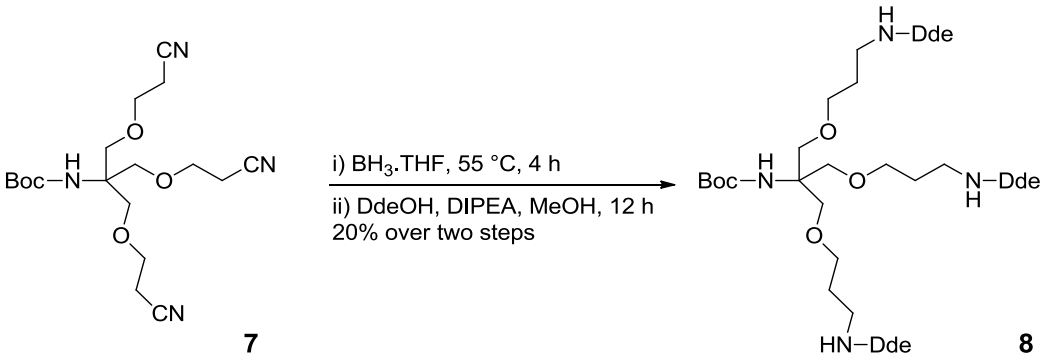

Scheme 3: Reduction and orthogonal protection of the monomer.

The next stage of the monomer unit synthesis was the reduction of the nitrile groups to the free amine using borane, followed by protection of the resulting free amines with 2-(1-Hydroxyethylidene)-5,5-dimethylcyclohexane-1,3-dione (DdeOH) (Scheme 3).[141] The reduction has to be quenched by the sequential addition of acid and base.

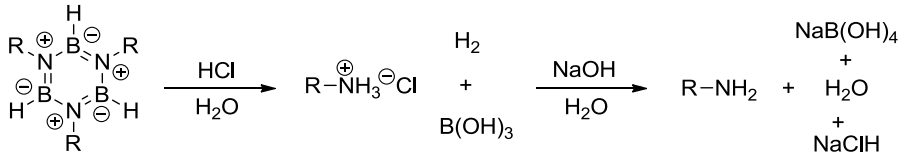

Scheme 4: Hydrolysis of the borazine.

The reason lies in the mechanism explained by Brown.[142] Once the nitrile groups are reduced they form a borazine. The addition of acid hydrolyses the borazine giving the amine salt, with the addition of base freeing the amine (Scheme 4).

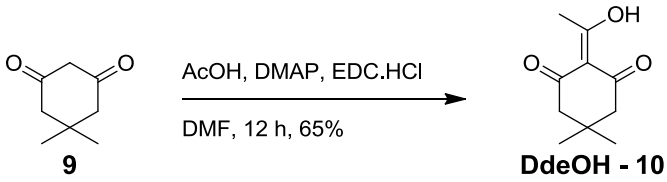

Scheme 5: Synthesis of DdeOH.

The DdeOH protecting group was chosen for various reasons. Firstly, it allows orthogonality as the Boc protecting group is removed under acidic conditions to which Dde is stable. Secondly Dde is suitable for solid phase synthesis as its removal using hydrazine is quick, highly effective, and does not induce cleavage of the linker from the resin.

The synthesis of DdeOH was carried out following a protocol published by Kessler as shown in Scheme 5.[140]

Scheme 6: Boc deprotection under acidic conditions.

Once the three branches were Dde protected, the Boc protecting group was removed using standard conditions (trifluoroacetic acid (TFA) in dichloromethane (DCM)) to give, after a basic wash the free amine product **11** in quantitative yield (Scheme 6).

2.2.2 Linker synthesis

Modified HMPA linker

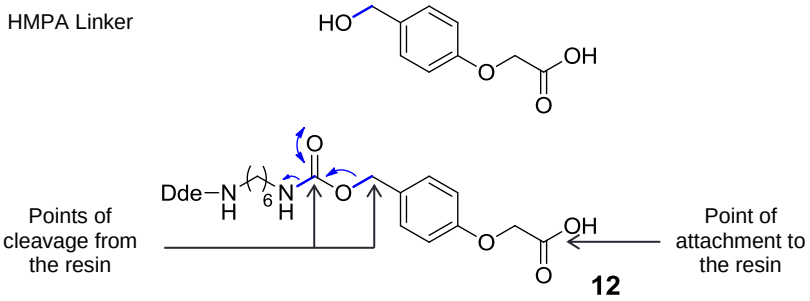

Figure 18: HMPA linker and Modified HMPA linker **12**.

Core resins, such as polystyrene or TentaGel, have by themselves restricted utility for peptide synthesis. Thus conditions to allow peptide cleavage from solid supports are modulated by the use of linkers. By manipulating the structure of the linker, peptides can be cleaved under a variety of conditions ranging from strong to weak acids.[143] The 4-hydroxymethylphenoxyacetic acid (HMPA) linker has good stability to a variety of conditions including basic and nucleophilic medium, but can be readily cleaved by treatment with trifluoroacetic acid.[143] The first linker used was a modified HMPA to give after cleavage, a free amine as a handle for the attachment of a second dye (Figure 18).[144] The synthesis was based on the synthesis by Bradley.[145]

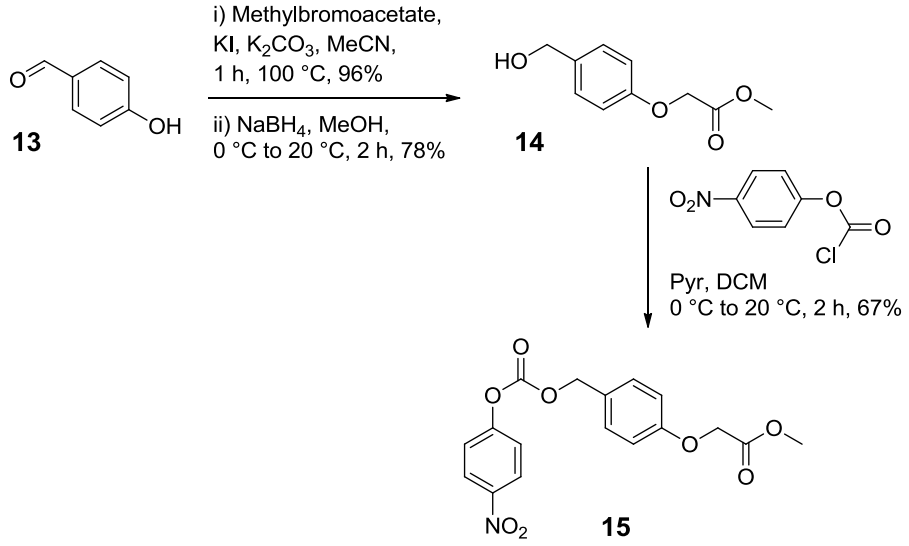

Scheme 7: Synthesis of the carbonate **15.**

Hydroxybenzaldehyde was reacted with methylbromoacetate under basic conditions in the presence of potassium iodide. The reaction was heated at 100 °C and the resulting product obtained in high yields (Scheme 7). The aldehyde moiety was reduced using sodium borohydride in methanol to give the corresponding alcohol **14**. Initially, the conversion of the alcohol to the carbonate **15** proved to be difficult. The reaction is sensitive to water and nucleophilic solvents such as methanol used in the previous step. The compound was obtained by reacting the benzyl alcohol (**14**) with *p*-nitrobenzyl chloroformate in the presence of pyridine under dry conditions. The product could not be purified by extraction but was stable enough to be purified by column chromatography (Scheme 7).

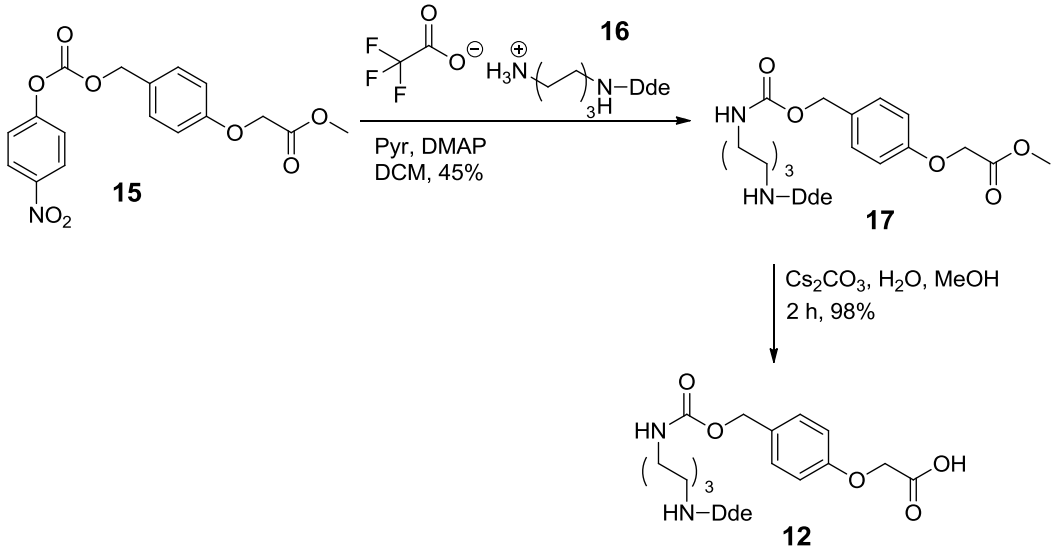

Scheme 8: Linker synthesis.

The mono-protected amine TFA salt **16** was given by Thingsoon Jong. The TFA salt **16** proved to be extremely unstable when neutralised, giving rise to a mixture of diaminohexane and the diprotected diamine. Although the migration of Dde groups in solution was unexpectedly rapid, it was not surprising as it has been reported to occur on solid support.[146, 147] The mono-Dde protected diamine TFA salt **16** was therefore reacted directly with carbonate **15** in the presence of pyridine to obtain the stable carbamate **17** (Scheme 8). The methyl ester was hydrolysed to the desired acid moiety using 2 M cesium carbonate in methanol and water, (the Dde group is stable under these conditions).[148] The stability of the Dde group during saponification was a major advantage over Fmoc protection which often requires re-protection step after ester hydrolysis.[149]

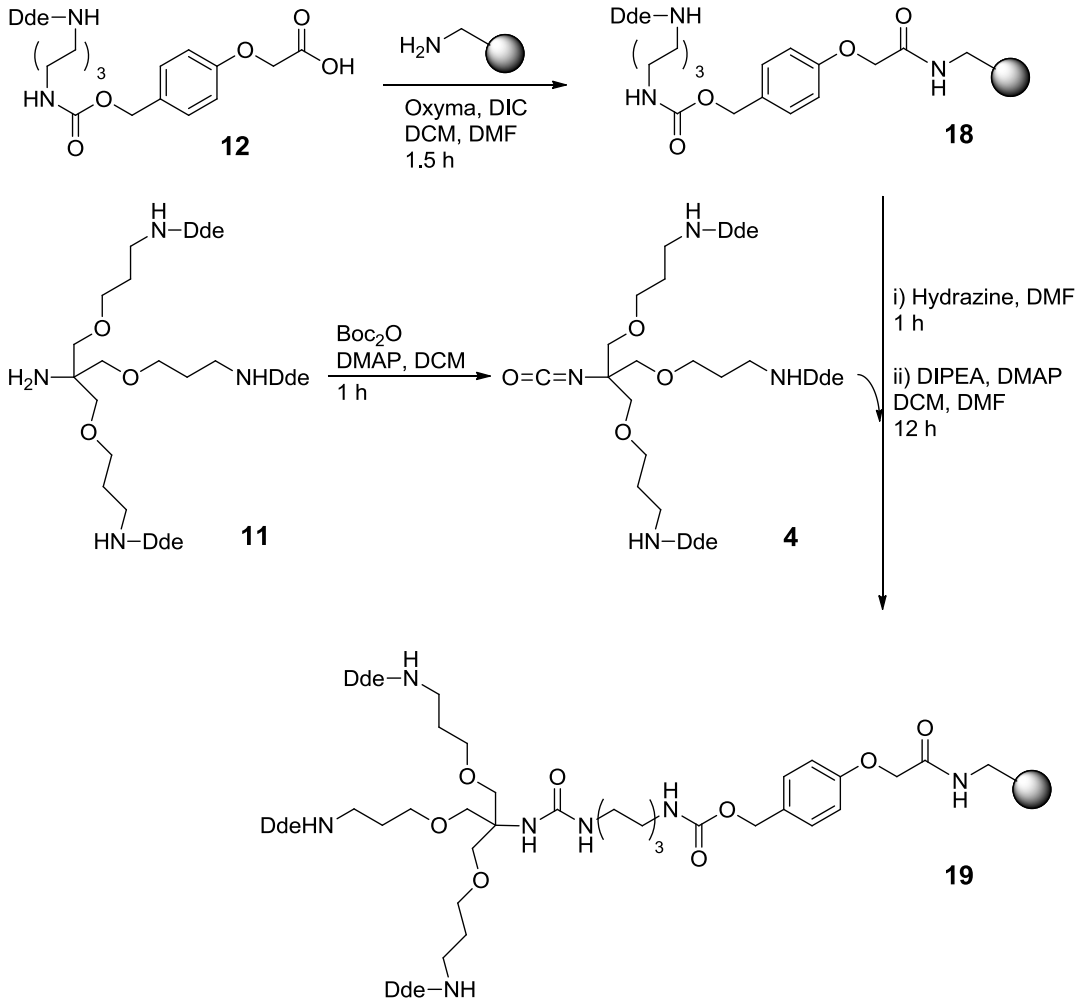

Scheme 9: Attachment of the linker and monomer onto the resin.

The acid moiety of **12** was converted to the active ester using ethyl 2-cyano-2-(hydroxyimino)acetate (Oxyma) and *N*,*N*′-diisopropylcarbodiimide (DIC) and coupled onto amino functionalised TentaGel resin (Scheme 9) with reaction completion monitored by the Kaiser test.[150] A wide variety of coupling reagents have been developed for the synthesis of amide bond,[151] a combination of Oxyma and DIC were used as they are a highly efficient combination and have recently been shown to give better result than 1-hydroxybenzotriazole (HOBt) with DIC in terms of coupling efficiency.[152]

Once the linker was attached onto the resin, Dde protecting groups were removed using a solution of 4% hydrazine in DMF. The monomer unit **11** was converted to isocyanate **4** using Boc anhydride in the presence of DMAP and then attached onto the linker in the presence of a base, with the reaction again monitored by the Kaiser test (Scheme 9).[150]

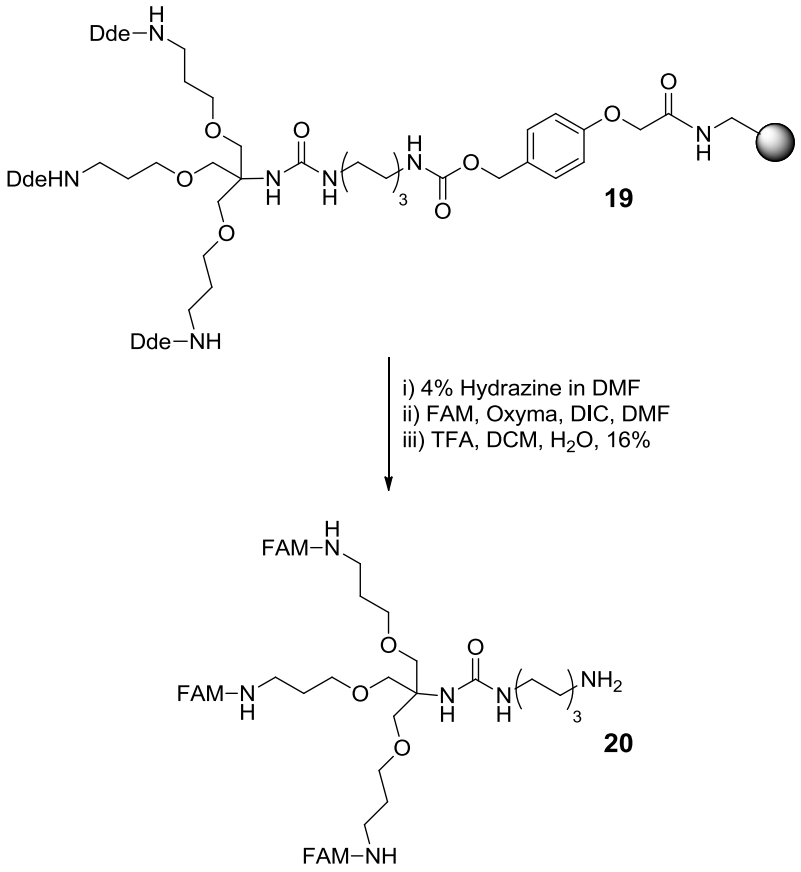

Scheme 10: Dye attachment and cleavage from the resin.

Once the dendron moiety was attached onto the linker and Dde groups were removed using 4% hydrazine in DMF (Scheme 10). 5(6)-Carboxyfluorescein (FAM) was then attached using Oxyma and DIC. Prior to cleavage the construct was washed with 20% piperidine in DMF in order to cleave any undesired fluorescein esters.[153] The

compound **20** was then cleaved from the linker using a trifluoroaceticacid (TFA), (Scheme 10) to give the desired compound in poor yield (16%). Since the synthesis on solid-phase was short, the yield did not meet expectations. An alternative linker that would also allow generation of a primary amine following cleavage was sought. The trityl linker was a logical choice and thus the 2-chlorotrityl linker on polystyrene resin **21** was chosen.

Trityl linker

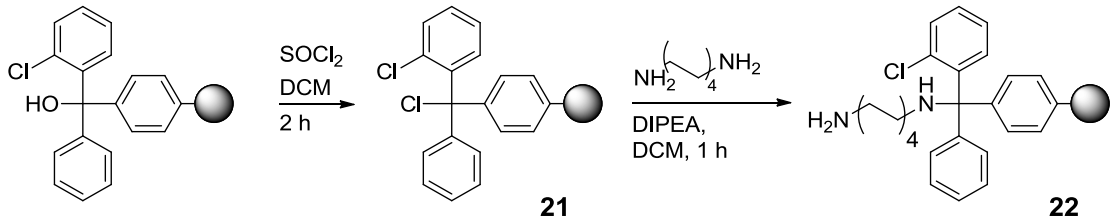

Scheme 11: Spacer attachment.

2-Chlorotrityl linker generates an electrophilic centre when the chlorine leaves. As a result the linker is very reactive to nucleophiles including water. As a precaution, the synthesis started with the re-activation of the linker using thionyl chloride (Scheme 11). The pre-activated linker **21** was then reacted with the desired spacer 1,4-diaminooctane in large excess and at high concentration (5 M). Before each reaction, the resin was pre-swollen in dry DCM to ensure maximum penetration of the reagents within the beads.

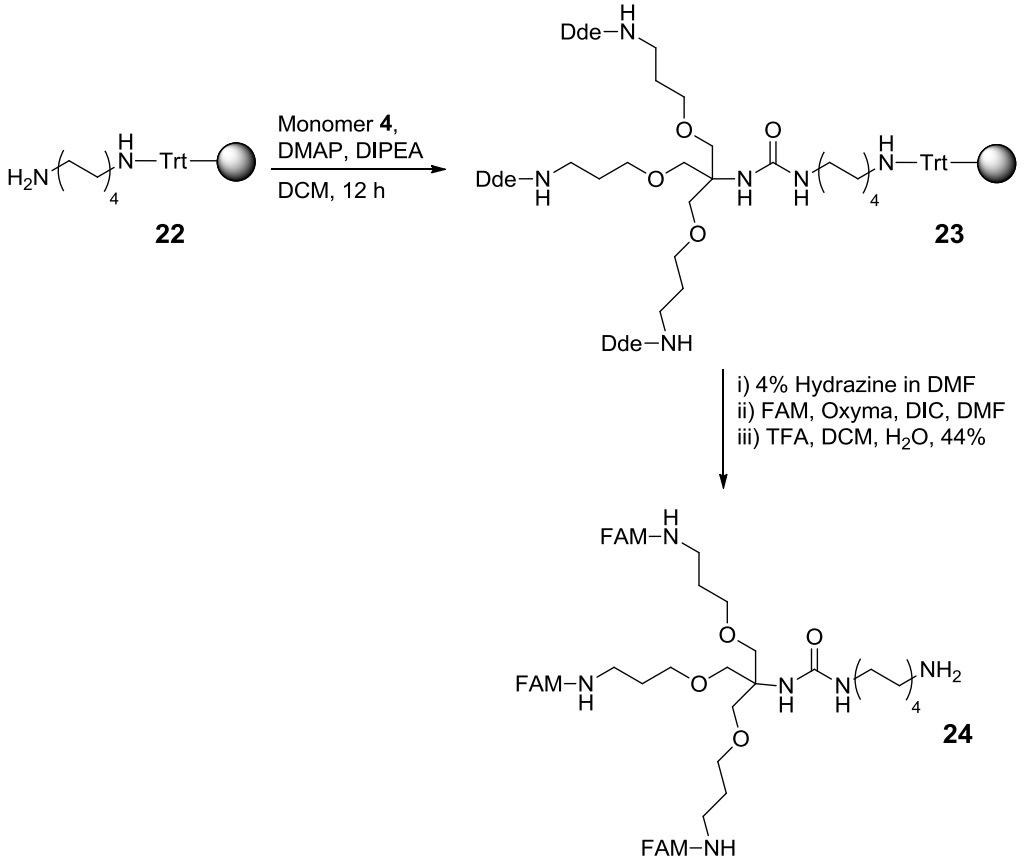

Scheme 12: Dye attachment and cleavage of the probe from the resin.

The freshly prepared isocyanate **4** was then attached onto the spacer. Once again the reaction was monitored with the Kaiser test.[150] Dde protecting groups were removed using standard procedures and 5(6)-carboxyfluorescein coupled using Oxyma and DIC in DMF (Scheme 12). The final product was obtained after TFA cleavage in 44% yield. A third route was attempted in order to reduce further the number of steps - the construction of the probe entirely in solution (Scheme 13).

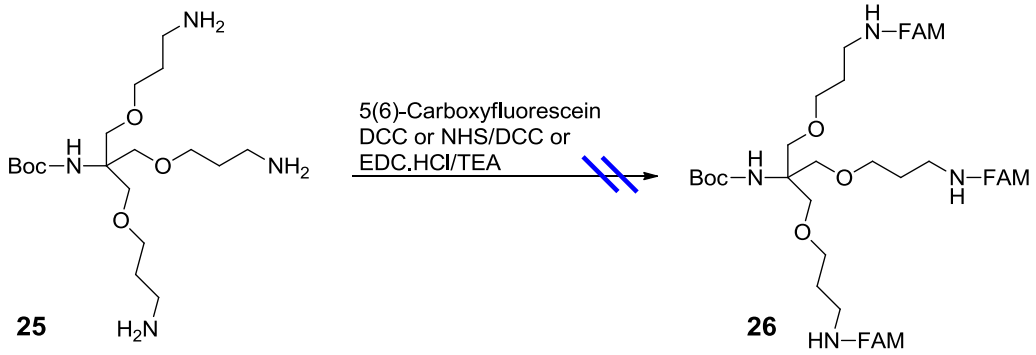

Scheme 13: Coupling in solution of the dye.

Attempts to couple 5(6)-carboxyfluorescein (FAM) to **25** were unsuccessful. Three coupling reagent combinations were tried to preactivate the acid moiety. The first attempt was using 5(6)-carboxyfluorescein and *N*,*N*'-dicyclohexylcarbodiimide (DCC) in DMF for 20 min followed by addition of the solution to **25**. The reaction resulted in a complex mixture with no sign of the target compound. The next approach was to form the *N*-succinimidyl ester of the fluorescein, using *N*-hydroxysuccinimide (NHS), DCC and 5(6)-carboxyfluorescein followed by addition of the monomer **4**. Once again the reaction appeared to be very messy and after extensive purification no product was found. The last and final attempt was stirring 5(6)-carboxyfluorescein with *N*-(3-dimethylaminopropyl)-*N*′-ethyl carbodiimide hydrochloride (EDC.HCl) and triethylamine (TEA) in DMF for 30 min and the resulting bright red solution added to the monomer. Once again, no desired product was found. Different hypothesis as to why the reactions did not work can be made with the coupling in solution of 5(6)-carboxyfluorescein being discussed extensively in chapter 3. The unprotected phenol groups of fluorescein render all couplings in solution difficult. The phenols of fluorescein are known to react with active esters, however, on solid phase, undesired fluorescein esters can be cleaved

using a simple piperidine wash,[153] with all fluorescein ester by-products that have not attached onto the resin being removed by filtration. Further, their formation does not impair the reaction as excess of starting material is often used in solid phase chemistry.

2.2.3 Dye attachment in solution

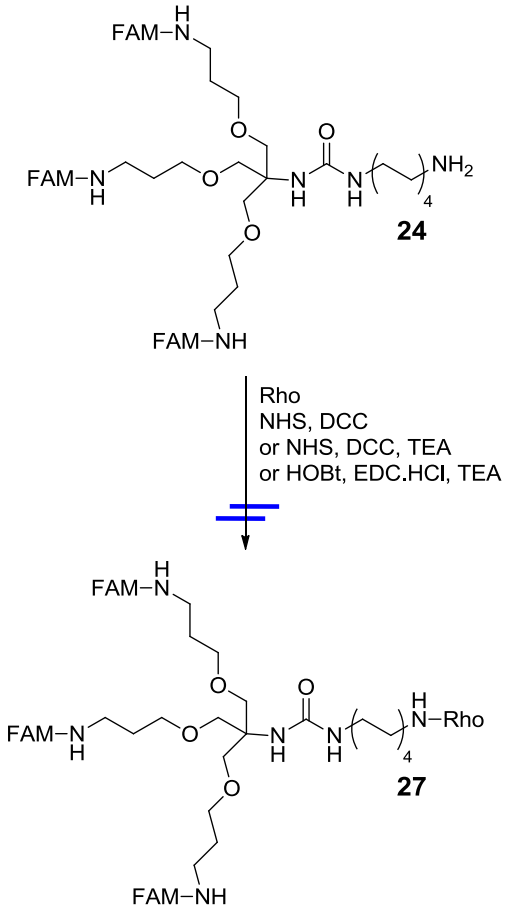

Scheme 14: Rhodamine coupling in solution.

The final step of the probe synthesis was the attachment of a second dye in solution. The second dye chosen was 5(6)-tetraethylcarboxyrhodamine (Rho). Three different

coupling reagents combinations were carried out. First, the procedure of Liu, using NHS and DCC in THF was attempted.[154] Some of the target product was found but only in 8% yield. It was thought that TFA traces from the previous reaction could have prevented some amines to react and so, the reaction was repeated after thorough removal of the TFA using freeze drying techniques. A base was also introduced but in vain. Another procedure from Mukai was attempted.[155] The procedure involved three and a half equivalents of base with HOBt and EDC.HCl. Reaction analyses again showed it was extremely messy and yielded no useful products.

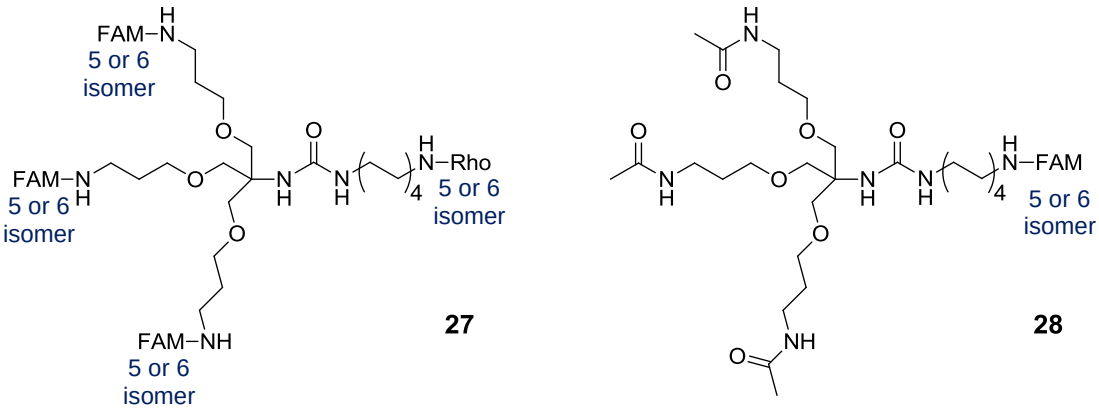

Figure 19: Reduced isomer combination with single fluorescein labelled target probe.

To overcome this problem, two ideas have been combined. First, a model study will be carried out on a commercially available primary amine and 5-(6) carboxyfluorescein to screen the best activating agents (Scheme 15). Second of all, a monomer unit with a single fluorophore will be first synthesised to simplify analysis. Indeed the use of the mixture of isomers 5-(6) carboxyfluorescein on a three branch dendrimer can lead to different isomer combinations that are reacted to a mixture of isomers of 5-(6) carboxytetraethylrhodamine, giving further possible isomer

combinations **27** (Figure 19). The new simplified target dendrimer **28** is shown Figure 19.

Model study

The model study was carried out on benzyl amine and 5(6)-carboxyfluorescein. The different conditions used are summarised in Table 2. Two solvents were chosen, DMF and pyridine. DMF was chosen for its ability to dissolve a wide range of acids, amines and amides. Pyridine was chosen in order to study the efficiency of the coupling reaction under basic conditions.

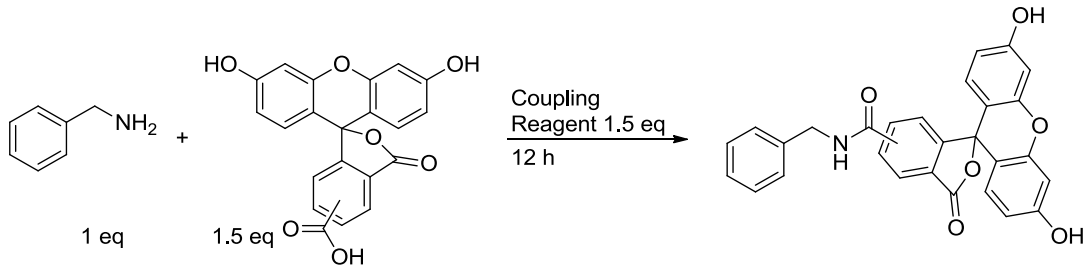

Scheme 15: Screened reaction.

Coupling Reagents	Solvent	Reaction time	Desired product	By-product	Benzyl amine
1. Oxyma / DIC **2.** Oxyma / DIC	DMF	12 h	✓	×	×
	Pyridine	12 h	✓	×	×
3. DIC **4.** DIC	DMF	12 h	✓	×	✓
	Pyridine	12 h	✓	×	✓
5. EDC.HCl **6.** EDC.HCl	DMF	12 h	×	×	✓
	Pyridine	12 h	×	×	✓
7. EDC.HCl/DMAP **8.** EDC.HCl/DMAP	DMF	12 h	✓	✓	×
	Pyridine	12 h	✓	×	✓
9. TBTU **10.** TBTU	DMF	12 h	✓	×	✓
	Pyridine	12 h	✓	×	×
11. NHS/DCC **12.** NHS/DCC	DMF	12 h	✓	×	×
	Pyridine	12 h	✓	×	×

Table 2: Result of screening conditions - reactions monitored by high-performance liquid chromatography (HPLC) and mass spectroscopy (MS).

The combination of Oxyma and DIC showed full conversion to the product in both solvents without any sign of by-products (entries 1 and 2 of Table 2). The third and fourth entries of the table were the use of DIC without Oxyma. Oxyma is traditionally used to prevent racemisation/epimerisation of amino acids, the resulting active ester is more stable resulting in less potential side reactions such as the formation of *N*-acylisoureas.[152, 156] As an achiral acid was used it was natural to try the reaction without Oxyma. In both solvents the reaction did not go to completion. Although benzylamine was the limiting reagent; it was partially recovered, confirming that the reaction did not go to completion.

The fifth and sixth entries were the use of EDC.HCl. The reaction did not give any product and starting materials were recovered.

For the seventh and eighth entries, catalytic amount of DMAP was used in combination of EDC.HCl to facilitate the reaction. The use of the catalyst help the reaction as the product was observed in both solvents, but the reaction did not go to completion in pyridine and produced an unidentified by-product in DMF.

In the ninth and tenth entries, O-(benzotriazol-1-yl)-*N*,*N*,*N*',*N*'-tetramethyluronium tetrafluoroborate (TBTU) was the chosen activating agent. The product was observed in both solvents, but without pyridine the reaction did not go to completion.

The eleventh and twelfth entries were the formation of the NHS activated ester using hydroxysuccinimide NHS and DCC. In both solvents the product was formed in full conversion.

To conclude this model study, five conditions gave the desired compound in full conversion. Those were Oxyma and DIC in DMF or pyridine, TBTU in pyridine and

NHS/DCC in DMF or pyridine. Conditions that were found to work on the model study were then taken forward and attempted on the dendron.

Three non peptidic dendrons were designed and synthesised (Scheme 16). These are different in their spacers: a two carbon spacer an eight carbon chain to decrease steric hindrance between the dendron core and the fluorophore and finally a polyethylene glycol PEG spacer to alter probe solubility.

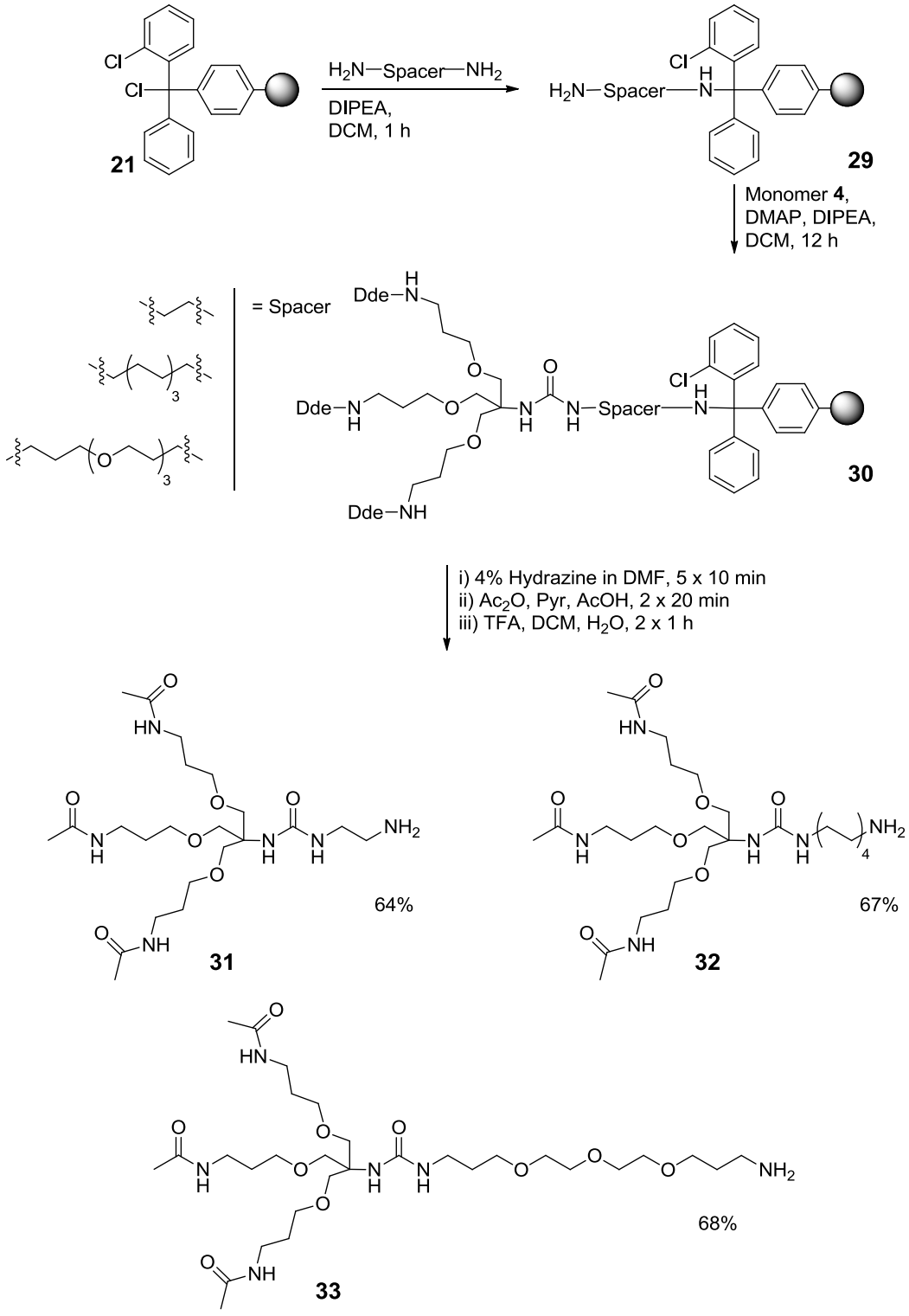

Scheme 16: Non peptidic dendrons.

The synthesis starts with 2-chlorotrityl functionalised polystyrene resin. The spacers were used in large excess at a high concentration of 5 M and hence did not require monoprotection.[157] The isocyanate dendron monomer **4** was freshly prepared and attached (Scheme 16), with the Dde groups being removed using 4% hydrazine in DMF. The resulting free primary amines were acylated using standard conditions, acetic anhydride, pyridine and acetic acid in DMF. The desired compounds were obtained in satisfactory yields following TFA cleavage (Scheme 16).

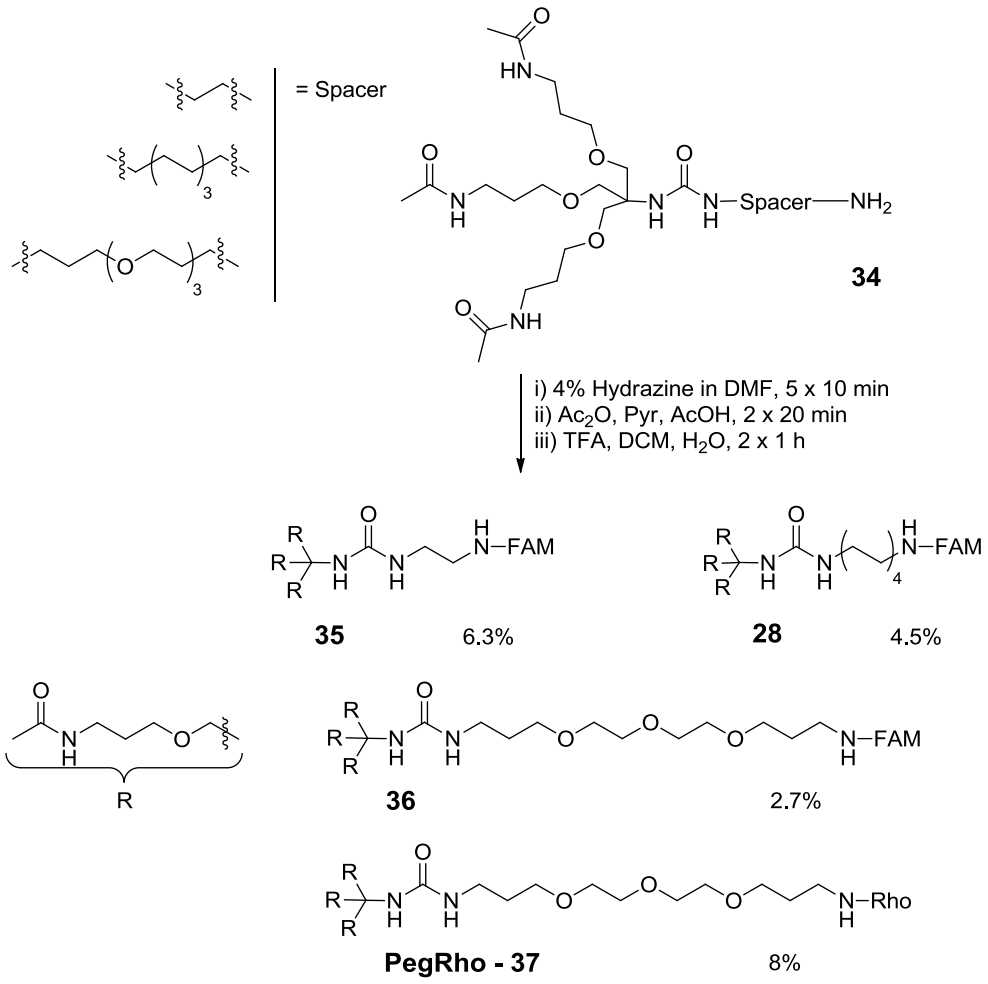

Scheme 17: Coupling in solution of the fluorophore.

The final step was the coupling in solution of the dye (Scheme 17). Among the few successful conditions found with the model study, the combination of Oxyma and DIC was chosen. The reactions were carried out in DMF, although the desired compounds were obtained, ELSD analysis showed a complex reaction profile therefore giving unsatisfactory yields. It was important to obtain a simple reaction profile to be able to later construct a more complex probe with peptide sequences.

For that purpose, the fluorescein activation was investigated as so far it had been assumed to work efficiently and the by-products of the activation to not interfere with the amide formation. As NHS activation had shown good results in the previous model study and the active ester had been reported to be stable under purification,[154] it was chosen for activation studies.

Dye activation study

5(6)-Carboxyfluorecein and NHS were dissolved in dry THF, and DCC added and the reaction stirred for 2 h (Scheme 18). Surprisingly, the reaction did not meet our expectations as a complex reaction profile was observed.

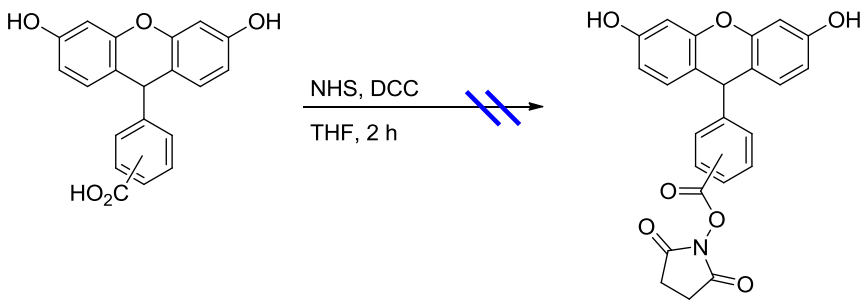

Scheme 18: NHS activation of 5(6)-carboxyfluorescein.

Looking in the literature, the phenol groups of fluorescein are known to be reactive and readily react with active esters.[153] It was therefore decided to protect the phenol groups of carboxyfluorescein before acid activation. The original protecting group chosen was Boc (Scheme 19) Table 3 summarises the reaction conditions that were attempted.

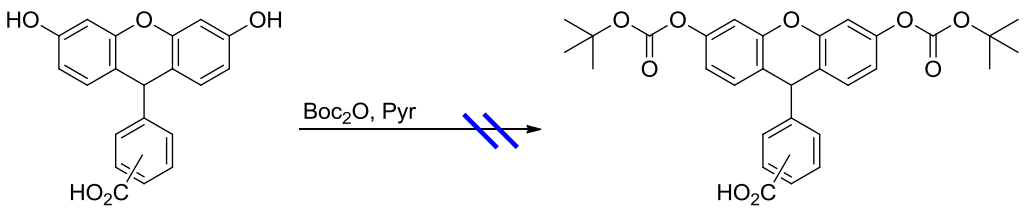

Scheme 19: Boc protection of 5(6)-carboxyfluorescein.

Entry	FAM	Boc_2O	Pyridine	Solvent	Temp.	Microwave	Time
1	1 eq	2.5 eq	3.5 eq	THF	60 °C	No	1 h, 12 h
2	1 eq	4 eq	cat	THF	r.t.	No	1 h, 12 h
3	1 eq	4 eq	cat	MeCN	60 °C	Yes	15 min
4	1 eq	4 eq	cat	MeCN	60 °C	Yes	30 min
5	1 eq	4 eq	cat	MeCN	60 °C	Yes	1 h
6	1 eq	4 eq	10 eq	MeCN	100 °C	Yes	15 min

Table 3: Reaction conditions for the Boc protection of 5(6)-carboxyfluorescein **-** All reactions were carried out under anhydrous conditions, and all reactions monitored by TLC.

In the first entry of Table 3 NMR analysis of the crude product showed the presence of starting material confirmed by MS and TLC, and the presence of various by-products.

In the second entry milder conditions were attempted as it was thought that heat could be responsible for the by-product formation. Pyridine was used in a catalytic

amount, although fewer by-products were formed, NMR spectroscopy showed the reaction did not go to completion as starting material was observed and confirmed by MS. Entries 3, 4 and 5 were microwaved assisted reactions. THF being a non-polar solvent does not respond well to microwave energy and was for that purpose replaced by acetonitrile (MeCN),[158] with the temperature fixed at 60 °C with three reaction times, 15 min, 30 min and 1 h. Once again, none of the reactions went to completion. A final attempt at this protection was to increase the amount of pyridine to ten equivalents, and increase the temperature to 100 °C over a short time of 15 min. Once again some by-products were formed, and the presence of starting material observed.

The Boc-protection was not investigated further and a new protecting group was sought. The acetyl protecting group, is a commonly used protecting group for the protection of the phenol groups of carboxyfluorescein.[159]

Although commercially available the single isomer version of the carboxyfluorescein diacetate *N*-succinimidyl ester (CFDA-SE) has no published synthesis and while a few groups have published different protocols for the single isomer separation of carboxyfluorescein, no efficient methods have been reported. The synthesis of CFDA-SE and single isomer purification was successfully investigated and reported in chapter 3 of this thesis.

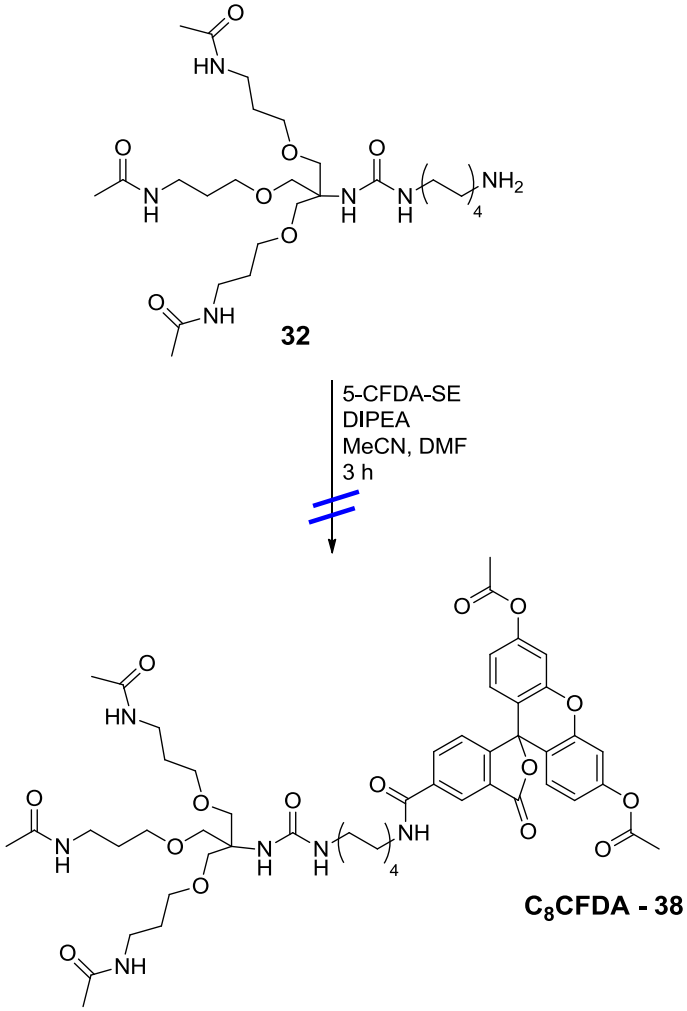

Scheme 20: Solution coupling of 5-CFDA-SE with amine **32.**

Amine **38** was reacted with 5-carboxyfluorescein diacetate *N*-succinimidyl ester (5-CFDA-SE) in the presence of DIPEA in a mixture of MeCN and DMF at a concentration of 0.1 M of 5-CFDA-SE. The crude mixture was unexpectedly complex, while the strong orange colour appeared upon addition of the base suggesting that the protecting groups had been removed. To further investigate the stability of the acetyl groups under basic conditions, 5(6)-carboxyfluorescein diacetate (5(6)-CFDA) was stirred in DMF with DIPEA over 3 h. Two variables

were independently investigated in this study, the equivalents of base and the quantity of DMF (reported in Table 4 as the concentration of 5(6)-CFDA).

Entry	Base	5(6)-CFSE	[5(6)-CFSE]	Deprotection
1	3 eq	1 eq	0.1 M	Yes
2	2 eq	1 eq	0.1 M	Yes
3	1 eq	1 eq	0.1 M	No
4	2 eq	1 eq	0.01 M	No
5	1 eq	1 eq	0.01 M	No

Table 4: Deprotection study conditions of 5(6)-CFDA in DIPEA and DMF, [5(6)-CFSE] represent the concentration of 5(6)-CFSE.

Table 4 shows that 3 equivalents of the base in high concentration deprotects the phenols (entry 1), 2 equivalents of base in concentrated conditions also cause deprotection (entry 2) but lower concentrations preserve the protecting groups (entry 4). Using solely 1 equivalent of base does not deprotect the phenols regardless of the concentration chosen (entry 3 and 5).

Thus, the reaction of coupling in solution of 5-carboxyfluorescein diacetate *N*-succinimidyl ester to the amine **32** was attempted with lower concentration of 5-CFDA-SE-**53** (0.01 M) and two equivalents of base (Scheme 21).

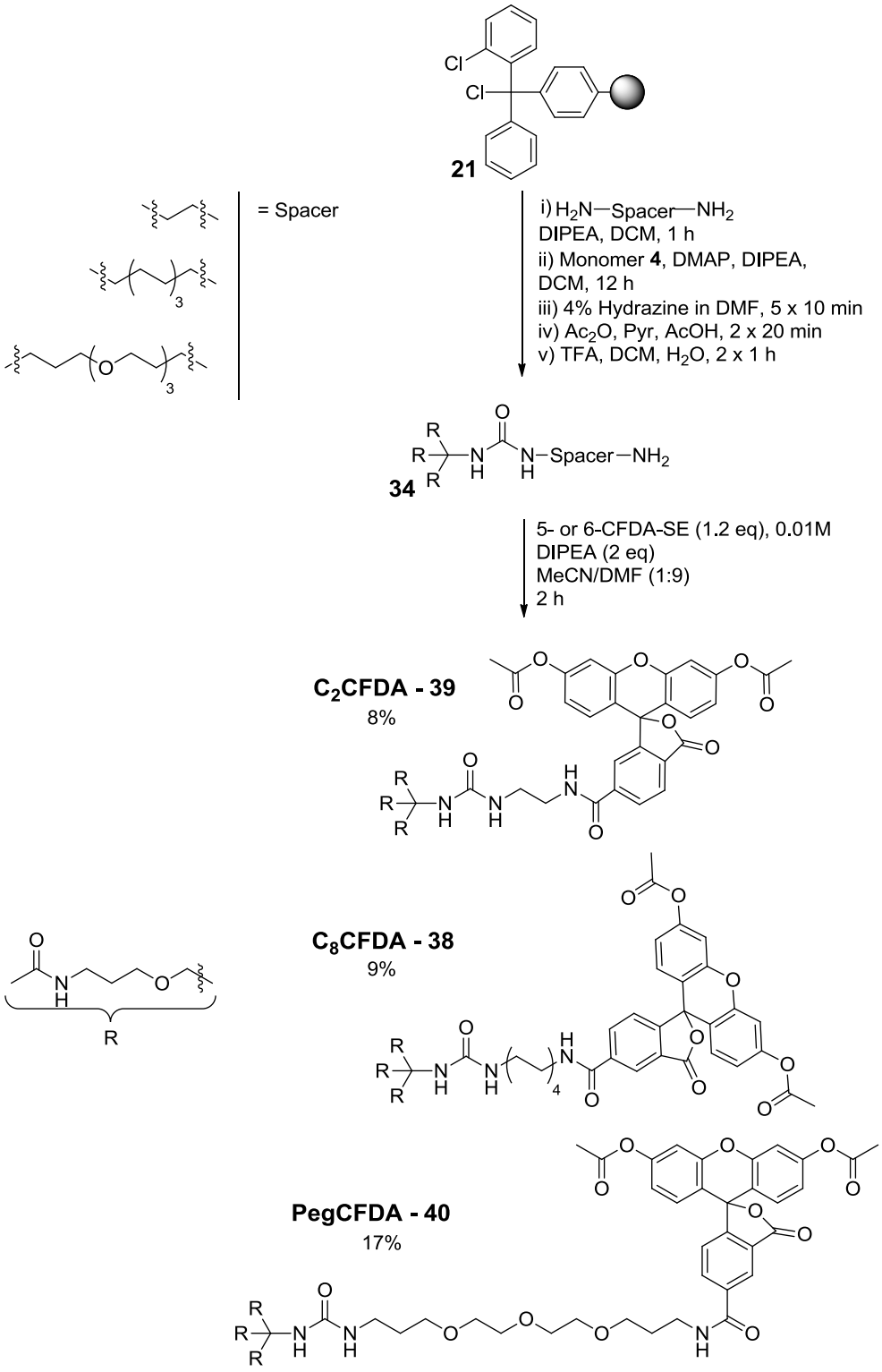

Scheme 21: Solution coupling of 5- or 6-CFDA-SE to **34.**

The reaction was complete after 2 h, and purified using semi-preparative HPLC (Scheme 21). Two other probes were synthesised using these conditions (Figure 19). The reaction of Scheme 21 was repeated on the two other spacer constructs and the protecting groups removed using 20% piperidine in DMF to obtain the three target compounds (Figure 20). They were purified using semi-preparative HPLC.

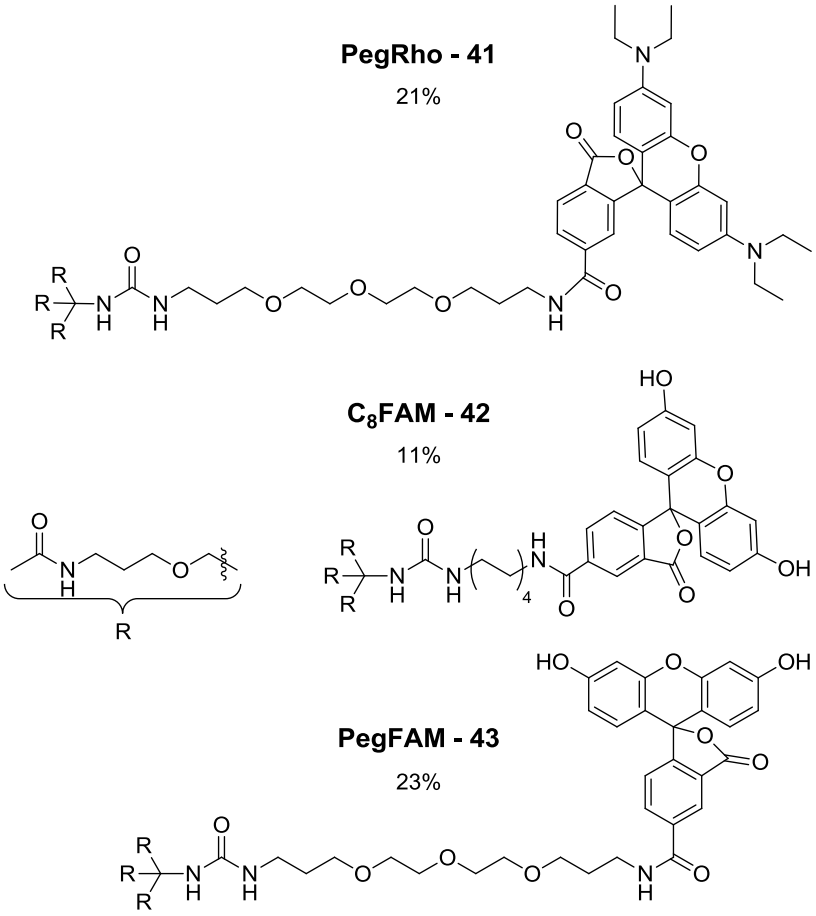

Figure 20: Structures of purified products.

Although the yields were not as high as desired due to difficult purification, reaction monitoring confirmed full conversion to the product.

Human neutrophil elastase specific probe

To develop a human neutrophil elastase specific probe a peptide sequence specific to NE must be introduced. The designed probe **44** is shown in Figure 21.

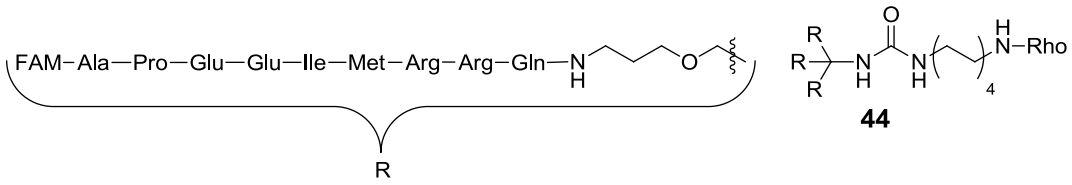

Figure 21: Target compound.

The synthesis started in the same manner as seen previously (Scheme 16) with linker activation and attachment of 1,8-diaminooctane followed by addition of the tribranched monomer unit **4**, and Dde removal. The first method was to synthesise the fully protected peptide as a single a strand followed by attachment onto the dendron. The strategy started with the synthesis of the fully protected peptide shown Figure 22 which was synthesised using an automatic peptide synthesiser, with a polystyrene resin functionalised with a 2-chlorotrityl linker.

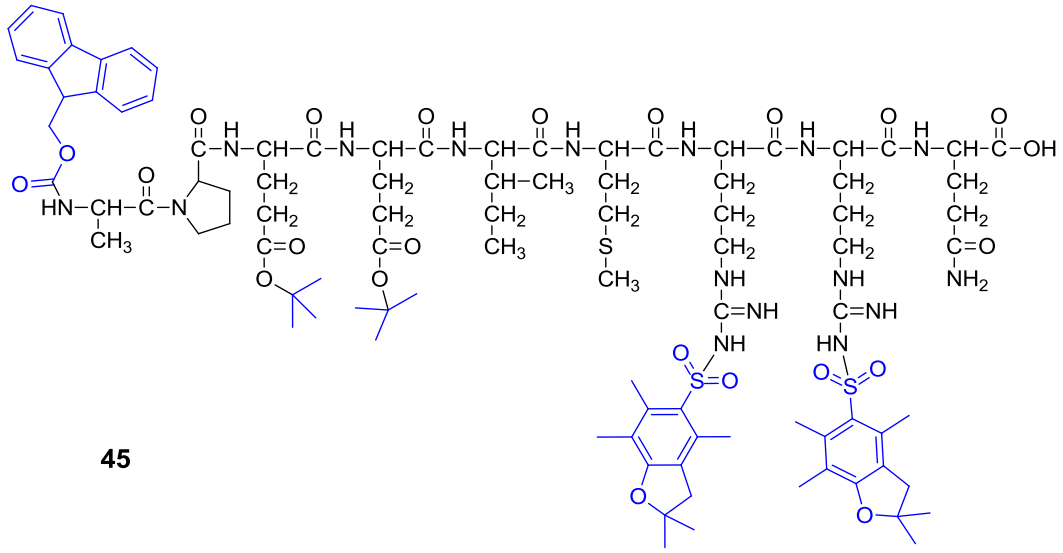

45

Figure 22: Fully protected elastase peptide **45.**

The peptide was cleaved using the cleavage cocktail developed by Barlos,[160] consisting of a mixture of acetic acid and trifluoroethanol (TFE) in DCM.

The next stage was to couple the protected peptide on to the dendron loaded resin. However, when attempting, to activate the protected peptide, solubility issues were encountered. The amount of solvent required for a concentration of 0.1 M or even 0.01 M was not sufficient to dissolve the peptide. Due to solubility issues, only one equivalent of DIC for three equivalents of peptide was used to prevent unwanted side reactions. After 2 h, *N*-ethoxycarbonyl-2-ethoxy-1,2-dihydroquinoline (EEDQ) was added to reactivate the peptide and the reaction left for another 2 h. EEDQ has the advantage of not reacting with amines but rapidly with carboxylic acid.[161]

After the reaction, the resin was filtered and washed, however, the ninhydrin test showed the presence of free amines. Coupling was repeated under the same conditions and reactivated with EEDQ, unsuccessfully. To overcome the solubility issue, a wide variety of solvent and solvent mixtures (DMSO, NMP, DMF, DCM)

were tried in order to find the system that would dissolve the peptide in the smallest volume. The peptide did not seem to fully solubilise in any reasonable concentrations.

The second approach to obtain the target compound was to build the peptide step wise onto the tribranched resin.

The resin used so far was a preloaded 2-chlorotrityl polystyrene resin with a loading value of 1.2-1.6 mmol/g. This rather high loading value was thought to be a disadvantage for the construction of a bulky tribranched dendron. A smaller loading value would lower the amount of compound on the resin in turn reducing the steric hindrance. The next resin chosen was the 2-chlorotrityl functionalised ChemMatrix resin. The loading value being lower (0.65 mmol/g) the performance of this resin was promising. In the meantime a shortened peptide sequence for the detection of neutrophil elastase was discovered in our research group.[117] The new targeted sequence is shown Scheme 22.

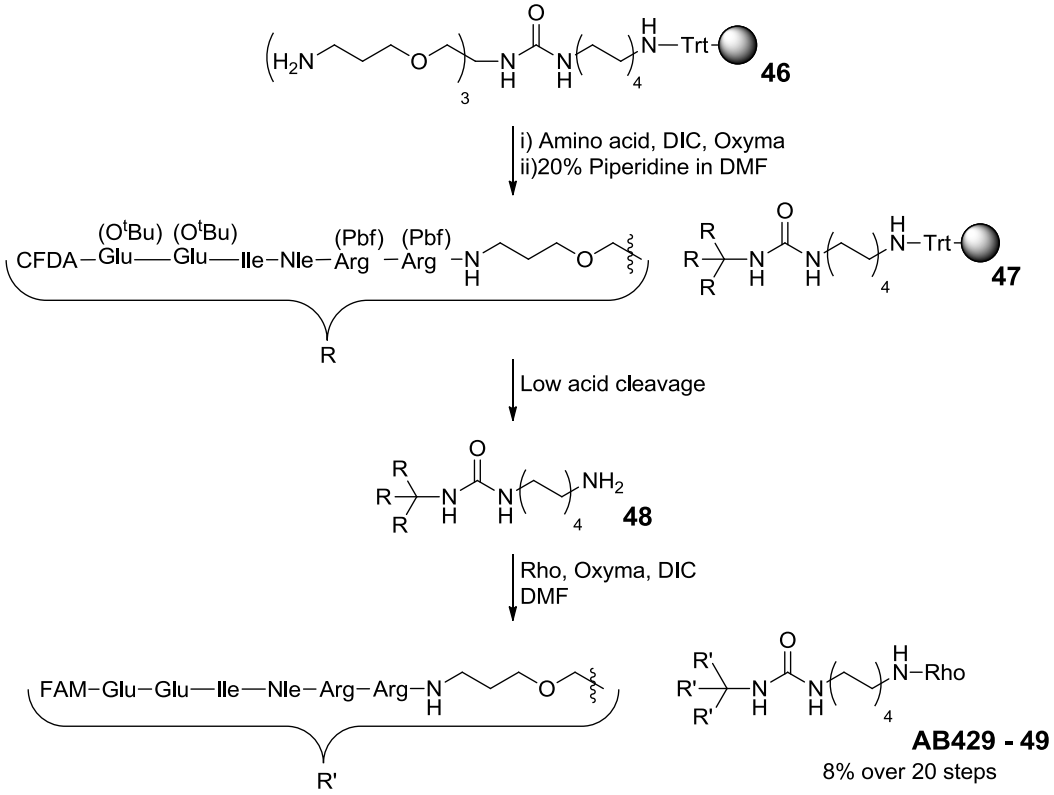

Scheme 22: Synthesis overview.

For the synthesis of **AB429-49**, 1,8-diaminooctane was used at a high concentration (5 M), in the presence of a base. The tribranched monomer unit **4** was loaded onto the resin and the Dde protecting groups were removed using hydrazine (Scheme 16). Then, the peptide was built stepwise using standard Fmoc strategy. The most efficient coupling reagents for Arg(Pbf) were found to be O-benzotriazole-*N*,*N*,*N*',*N*'-tetramethyl-uronium-hexafluoro-phosphate (HBTU) and DIPEA, especially for the addition of Arginine onto Arginine, all other amino acids were coupled using a combination of Oxyma and DIC. CFDA-SE being an active ester did not require any activating reagents and was added onto the peptide in the presence of DIPEA.

Attempted cleavage (with acetic acid and TFE) did not cleave compound **48** from the resin. In the original paper, the compound was attached to the linker through an ester moiety. Due to the delocalisation of the charge over the two oxygen atoms, the acid moiety is a better leaving group than the amine group. Therefore the latter requires stronger conditions to be cleaved (Scheme 23).

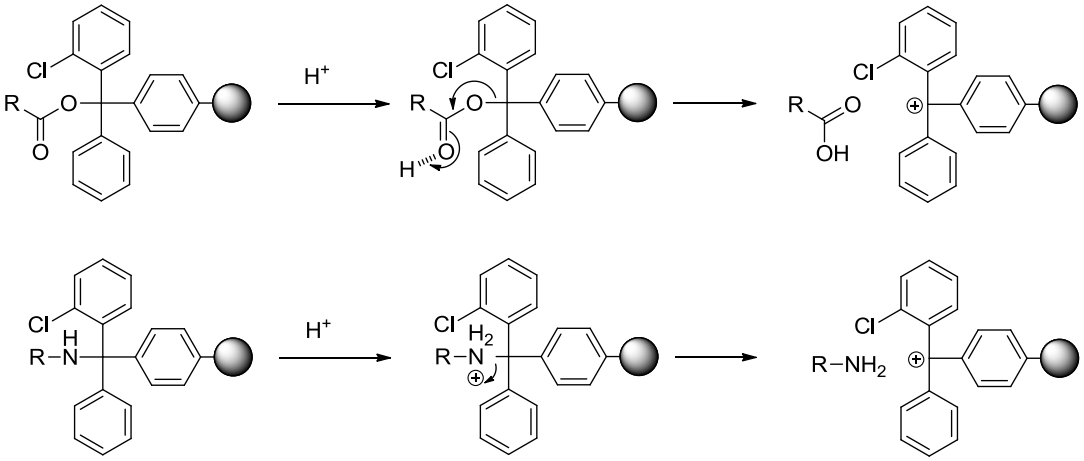

Scheme 23: Cleavage mechanism of the trityl linker.

Bollhagen developed a new cocktail for the cleavage of fully protected peptides from trityl linkers using hexafluoroisopropanol (HFIP) in DCM.[162] Interestingly this cocktail even dissolves hydrophobic peptides unlike the Barlos method, making it a better choice. The new cleavage conditions using 30% HFIP in DCM was successful and **48** was cleaved (Scheme 22).

The final step of the synthesis was the attachment of tetraethylcarboxyrhodamine (Rho) via activation with Oxyma and DIC in DMF and added to the solution of intermediate **48** (Scheme 22).

2.3 *In vitro* studies

Cell line studies

To study the dendron core-structure the six probes (C_2CFDA-**39**, C_8CFDA-**38**, PegCFDA-**40**, C_8FAM-**42**, PegFAM-**43**, PegRho-**41**) were incubated with two cell types, human adenocarcinomic alveolar basal epithelial cells A549 and primary human neutrophils and studied using confocal microscopy. The A549 cell line is derived from human pulmonary adenocarcinoma and it is the most used alveolar epithelial model.[163] Unlike neutrophils, A549 cells are not lymphocytes and do not participate in the ingestion of foreign organisms, making them a control for cellular entry study.

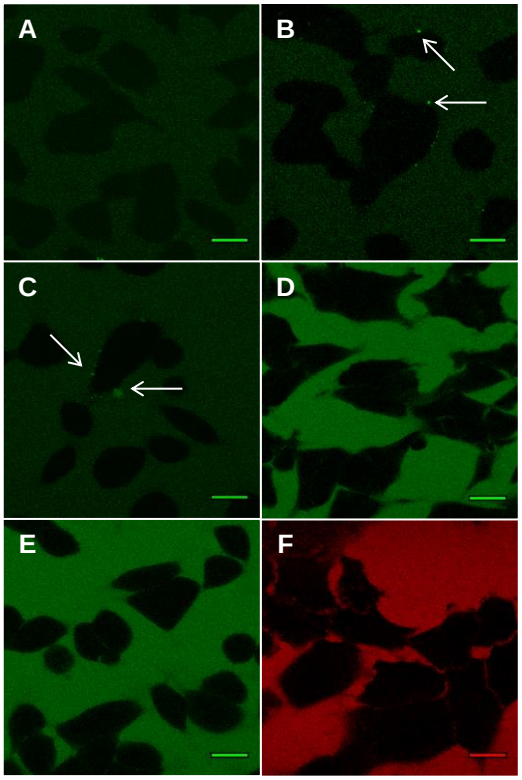

Figure 23: Confocal microscopy images of A549 cells incubated with probes. A549 were fixed on multiwell chambers using poly-D-lysine. Probes were incubated at 10 µM for 16 h at 37 °C. **A.** C_2CFDA-**39**, **B.** C_8CFDA-**38**, **C.** PegCFDA-**40**, **D.** C_8FAM-**42**, **E.** PegFAM-**43**, **F.** PegRho-**41**. **A-E.** Fluorescein emission image (λ_{ex} = 488 nm, λ_{em} = 512 – 565 nm). **F.** Rhodamine emission image (λ_{ex} = 543 nm, λ_{em} = 565 – 608 nm). Arrows show: localised high fluorescence intensities. Scale bars: 20 µm. Images are representative of duplicates experiments carried out on different days.

Confocal microscopy studies show that none of the six probes (C_2CFDA-**39**, C_8CFDA-**28**, PegCFDA-**40**, C_8FAM-**42**, PegFAM-**43**, PegRho-**41**) entered the cells after overnight incubation on A549 cells. Figure 23A, B and C show low fluorescence intensities for acetylated fluorescein compounds; arrows highlight punctual fluorescence signal where fluorescein must have been deacetylated. Figure 23D, E display high fluorescence intensity for non-acetylated fluorescein probes, as

well as Figure 23F where rhodamine probe was incubated. Non cellular penetration of the probes was confirmed by Z-stacking 3D experiments.

Enzyme kinetics studies

The peptide sequence used in probe AB429-**49** was specific to human neutrophil elastase, meaning it is cleaved by this enzyme. However, it must be determined whether the peptide sequences on the three branched dendron construction can enter the active site of the enzyme to be cleaved. Probe AB429-**49** is designed to release an unquenched fluorescein moiety following cleavage by the enzyme (Figure 15), with the resulting fluorescence recorded. Different concentrations of probe were analysed with HNE and the data were processed to obtain the standard Michealis-Menten parameters.

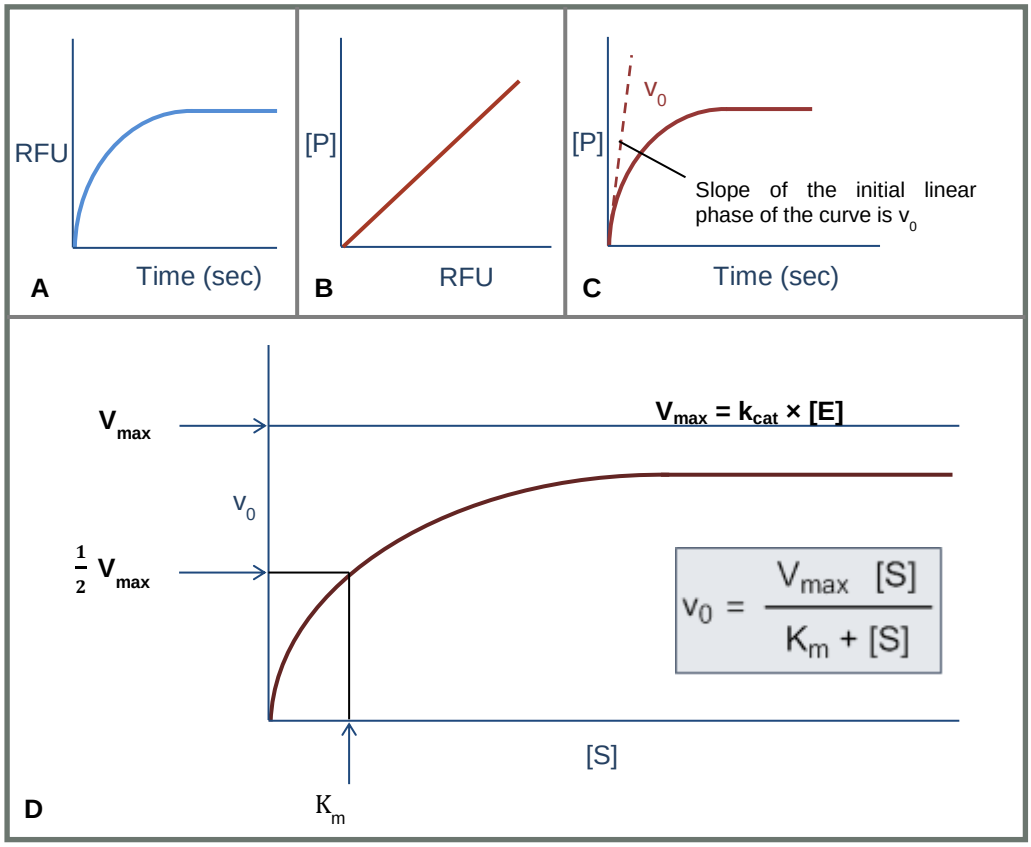

Figure 24: Method used to convert raw data to Michaelis-Menten parameters. **A.** Raw data of fluorescence unit increase over time, **B.** standard curve of concentration of fluorophore per fluorescence unit, **C.** concentration of fluorophore released calculated from fluorescence units over time, **D.** calculated initial rates for substrate concentrations. Michaelis-Menten parameters k_{cat} and K_m calculated from graph D.

By measuring the fluorescence (RFU) of various concentration of fluorescein [P], a standard curve was realised to allow us to convert units of fluorescence into product concentrations (Figure 24) (See appendices section). The Michaelis-Menten graph was obtained by plotting the initial rate against the concentrations of substrate (Figure 24).[164]

From the graph, K_m and V_{max} (the maximum rate achieved by the system), can be determined. The number of molecules of substrate cleaved by each enzyme unit per second is the rate constant (or turn over constant) k_{cat} calculated by dividing the V_{max} by the concentration of the enzyme [E].

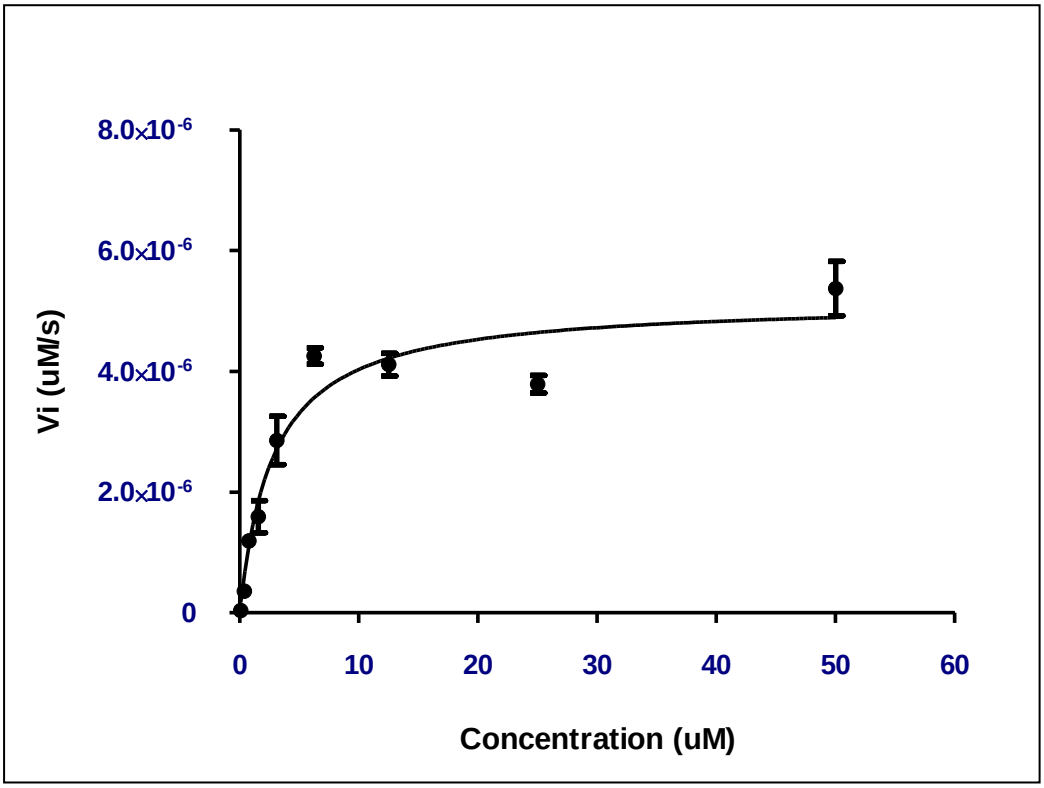

Figure 25: Experimental Michaelis-Menten graph of **AB429** incubated with human sputum elastase (17 nM).

The K_m obtained was: 2.8 ± 0.6 µM, with a k_{cat}: 304 ± 16.1 s^{-1} giving a k_{cat}/K_m value of 10800 $mM^{-1}.s^{-1}$. Although the Michaelis-Menten parameters are not reported for this specific peptide sequence[117] the k_{cat}/K_m value for the original peptide (APEQIMRRQ) sequence is reported to be 531 $mM^{-1}.s^{-1}$.[5]

This study confirms that the probe is a substrate for HNE and therefore could be taken to the next stage, namely the study of human neutrophils.

Primary cell studies

Neutrophils are primary cells and are extracted from human blood. When a blood sample is taken a response called hemostatsis occurs, which is based on clot

formation. The process must be controlled in order to separate the different components of the blood and obtain neutrophils.

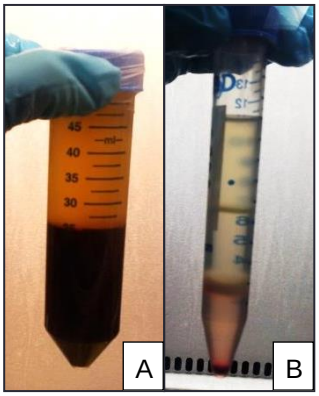

Figure 26: Blood preperation - Courtesy of Neil McDonald. **A.** Separation of serum and platelets (top layer) from red and white blood cells (dark bottom layer). **B.** Percoll^{TM} gradient separation, base of the top layer contains monocytes, base of the middle layer contains neutrophils, and base of the bottom layer contains red cells.

Insoluble fibrin production and platelets activation is initiated by thrombin and is produced by the prothrombinase complex in the presence of calcium ion.[165] By removing the presence of calcium ions, the cascade is stopped and the blood sample is prevented from clotting. Various anticoagulants can be used such as, oxalate $(COO)_2^{2-}$, EDTA, or Sodium citrate.[166] Once the anticoagulant is added, the blood sample can be centrifuged to separate the serum and platelets, and red and white blood cells (Figure 26A). Serum can be extracted from the platelets by addition of calcium chloride, which activates the platelets into a plug, allowing filtration of the serum. Dextran and sodium chloride are added to the bottom layer causing sedimentation which allows for easy separation of the white blood cells from the red blood cells. White blood cells can then be separated using Percoll^{TM}, a non-toxic medium consisting of coated silica particle designed for density gradients.[167] By

carefully superposing layers of different concentrations of Percoll™ in PBS we can allow the white blood cells to separate, and obtain neutrophils (Figure 26 B).

In Figure 27 confocal experiments on activated neutrophils showed cellular entry and de-acetylation of the three acetylated probes (C_2CFDA-**39**, C_8CFDA-**38** and PegCFDA-**40**).

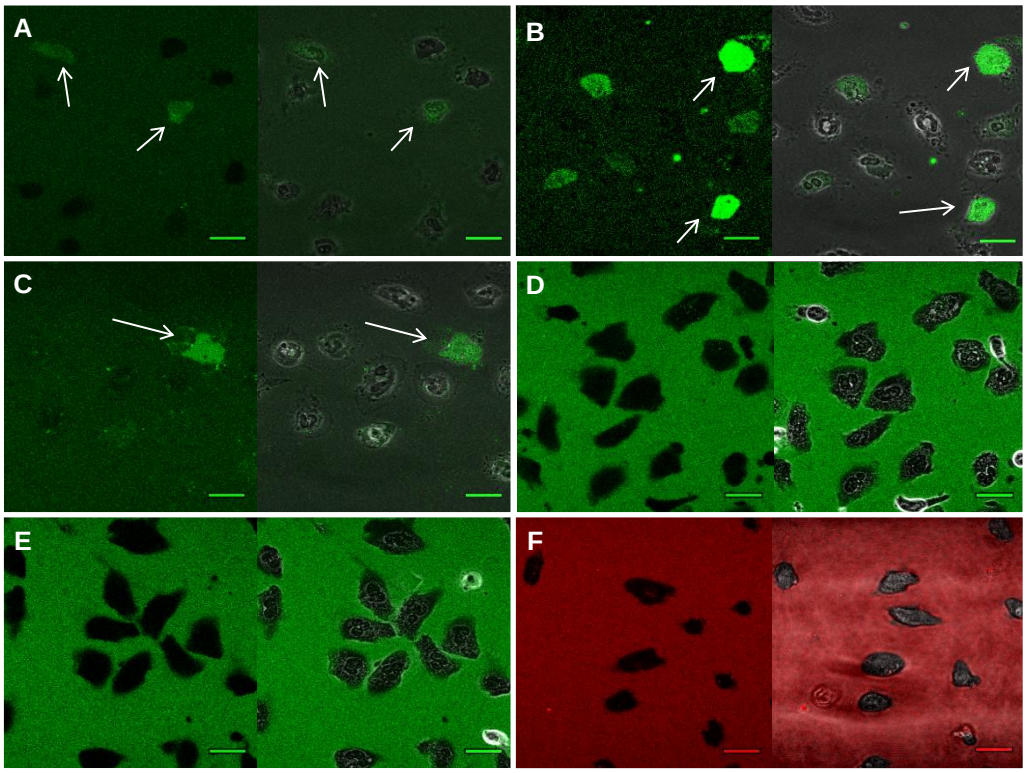

Figure 27: Confocal microscopy images of activated neutrophils incubated with probes. (The neutrophils were purified from human blood sample of healthy volunteers courtesy of Dr. Neil McDonald and Miss Emma Schoefield). Neutrophils were fixed on coverslip using fibronectin. Probes were incubated at 10 µM for 1 h at 37 °C, and neutrophils activated by addition of calcium ionophore A23187.[5] **A.** C_2CFDA-**39**, **B.** C_8CFDA-**38**, **C.** PegCFDA-**40**, **D.** C_8FAM-**42**, **E.** PegFAM-**43**, **F.** PegRho-**41**. **A-E.** Left fluorescein emission image (λ_{ex} = 488 nm, λ_{em} = 512 – 565 nm), right image merge of bright field and fluorescent image. **F.** Left rhodamine emission image (λ_{ex} = 543 nm, λ_{em} = 565 – 608 nm) right image merge of bright field and fluorescent image. Arrows show: localised high fluorescence intensities. Scale bars: 20 µm. Images are representative of duplicates experiments carried out on different days.

C_8CFDA-**38** showed stronger fluorescence intensities than C_2CFDA-**39** and PegCFDA-**40** (Figure 27 A,B and C). The non-acetylated probes and rhodamine

probe did not seem to enter the cells even upon neutrophil activation. To confirm the cellular entry of the acetylated probes, Z-stacking 3D experiments were carried out on all acetylated probes.

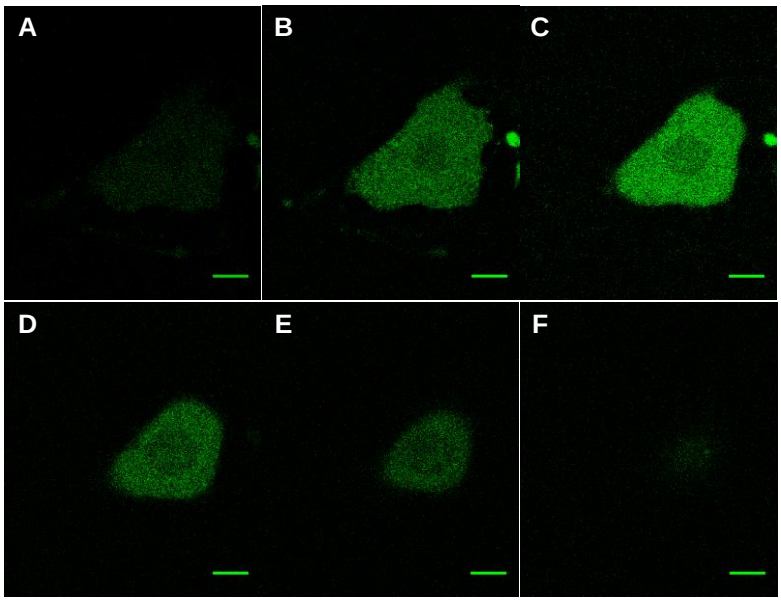

Figure 28: Z-staking confocal microscopy images of activated neutrophils incubated with probes. (The neutrophils were purified from human blood sample of healthy volunteers courtesy of Dr. Neil McDonald and Miss Emma Schoefield.) Neutrophils were fixed on coverslip using fibronectin. C_8CFDA-**38** (10 µM) added, and neutrophils activated by addition of calcium ionophore A23187. **A-F** Show the different planes of a neutrophil cell. Fluorescein emission image (λ_{ex} = 488 nm, λ_{em} = 512 – 565 nm). Slice thickness: 0.44 µm. Scale bars: 5 µm. Images are representative of duplicates experiments carried out on different days.

Z-stack 3D experiments of the acetylated probes show fluorescence intensity within the cell in all planes confirming the cellular penetration of the compounds.

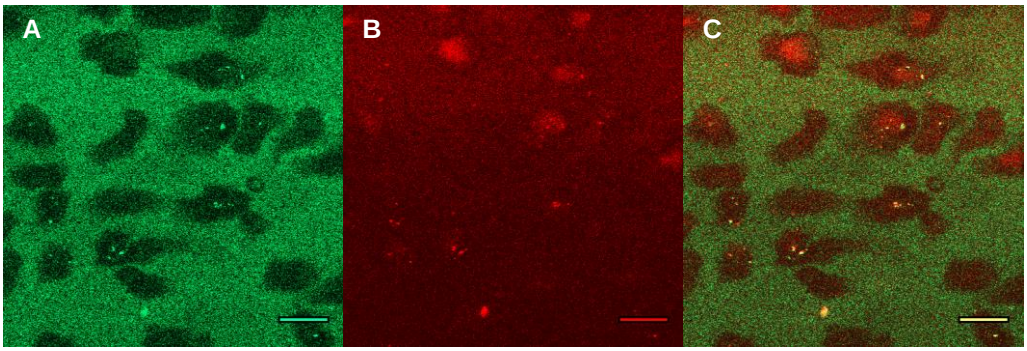

Figure 29: Confocal microscopy images of neutrophils incubated with AB429-49. (The neutrophils were purified from human blood sample of healthy volunteers courtesy of Dr. Neil McDonald and Miss Emma Schoefield). Neutrophils were fixed on coverslip using fibronectin, and AB429-**49** (10 µM) added. **A.** Fluorescein emission image (λ_{ex} = 488 nm, λ_{em} = 512 – 565 nm), **B.** rhodamine emission image (λ_{ex} = 543 nm, λ_{em} = 565 – 608 nm), **C.** merge of fluorescein and rhodamine emission images. Scale bars: 20 µm. Images are representative of duplicates experiments carried out on different days.

In Figure 29 the probe shows some cell penetration and, it remains uncleaved in the presence of non-activated neutrophils. In Figure 30, calcium ionophore A23187 was added and the resulting activation of the neutrophils was recorded. All experiments were carried out in duplicates on different days.

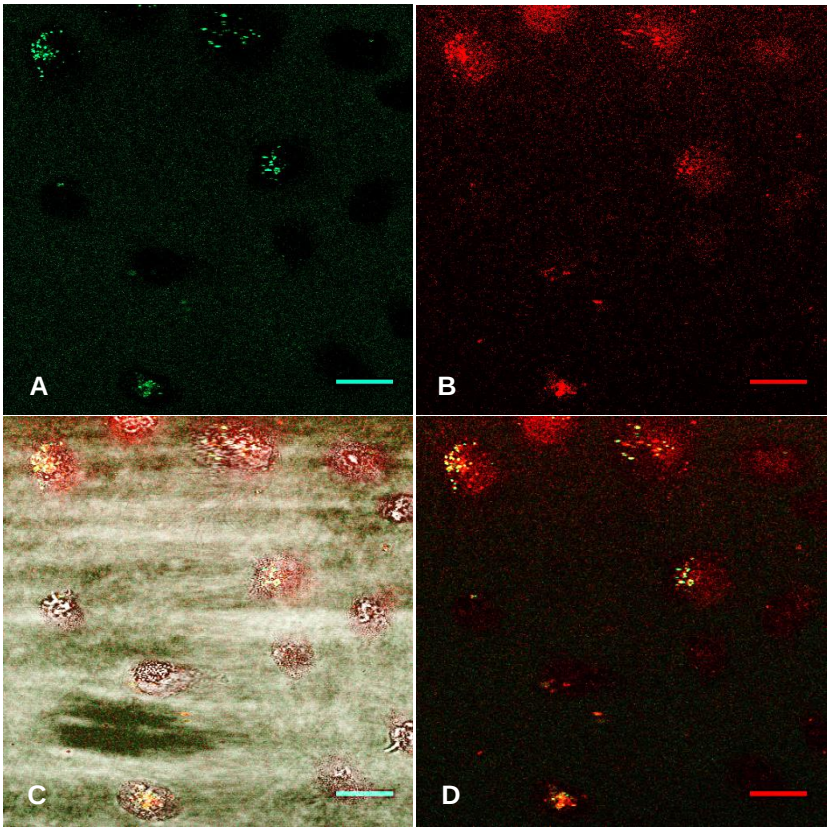

Figure 30: Confocal microscopy images of activated neutrophils incubated with AB429-49. (The neutrophils were purified from human blood sample of healthy volunteers courtesy of Dr. Neil McDonald and Miss Emma Schoefield). Neutrophils were fixed on coverslip using fibronectin, AB429-**49** (10 µM) added, and neutrophils activated by addition of calcium ionophore A23187. **A.** Fluorescein emission image (λ_{ex} = 488 nm, λ_{em} = 512 – 565 nm), **B.** rhodamine emission image (λ_{ex} = 543 nm, λ_{em} = 565 – 608 nm), **C.** merge of fluorescein and rhodamine emission images, **D.** merge of bright field and fluorescein and rhodamine emission images. Arrows show: localised high fluorescence intensities. Scale bars: 20 µm. Images are representative of duplicates experiments carried out on different days.

In Figure 30B clusters of strong fluorescence intensities can be seen inside the cells, the probe has therefore entered the neutrophils. From the fluorescein channel, strong green fluorescent vesicles have appeared resulting from the cleavage of the branches. We can see from the overlay channels that some vesicles are red, indicating that the probe has entered the cells but not green indicating that either all branches have been

cleaved or that none of the branches have been cleaved remaining unquenched. To further investigate dye co-localisation, the microscope was set to analyse individual cell (image range 38 × 38 µm).

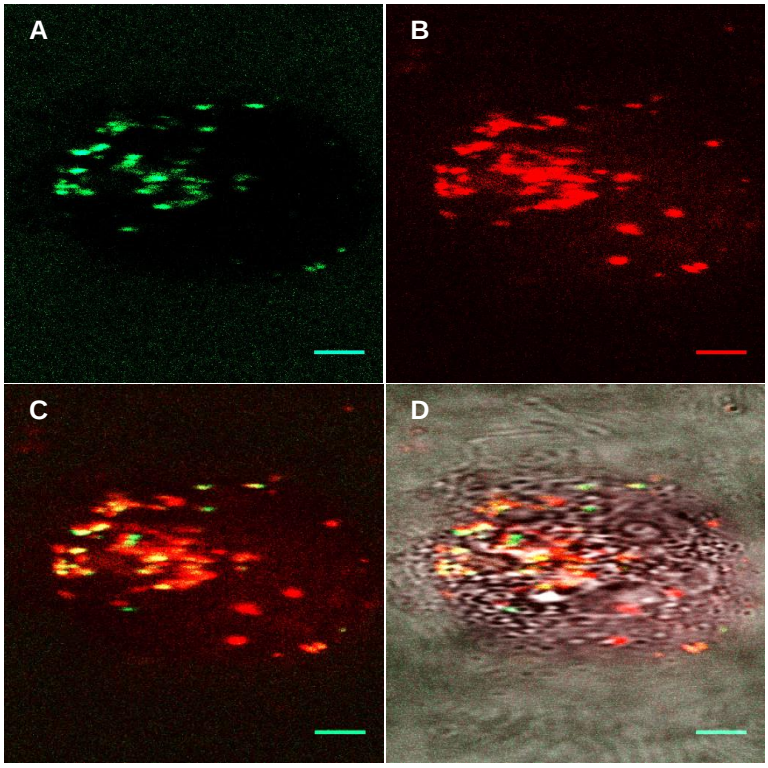

Figure 31: Single cell analysis confocal microscopy images of activated neutrophils incubated with AB429-49. (The neutrophils were purified from human blood sample of healthy volunteers courtesy of Dr. Neil McDonald and Miss Emma Schoefield). Neutrophils were fixed on coverslip using fibronectin, AB429-**49** added to the cells at 10 µM, and neutrophils activated by addition of calcium ionophore A23187. **A.** Fluorescein emission image (λ_{ex} = 488 nm, λ_{em} = 512 – 565 nm), **B.** rhodamine emission image (λ_{ex} = 543 nm, λ_{em} = 565 – 608 nm), **C.** merge of fluorescein and rhodamine emission images, **D.** merge of bright field, fluorescein and rhodamine emission images. Scale bars: 5 µm. Images are representative of duplicates experiments carried out on different days.

Figure 31 displays a close up image of a neutrophil. We can confirm from the fluorescein channel cleavage of the probe. From the rhodamine channel we can

observe the accumulation of the probe in vesicles of the cell. In the overlay channels the superposition of the green signal and red signal appears as orange. We can see red pockets which can result from molecules being fully cleaved with no fluorescein moieties left or molecules that have not been cleaved and fluorescein signal quenched.

To confirm the presence within the cell and rule out the possibility of an artifact due to an accumulation of the probe on the cell membrane, Z-stack 3D experiments were carried out.

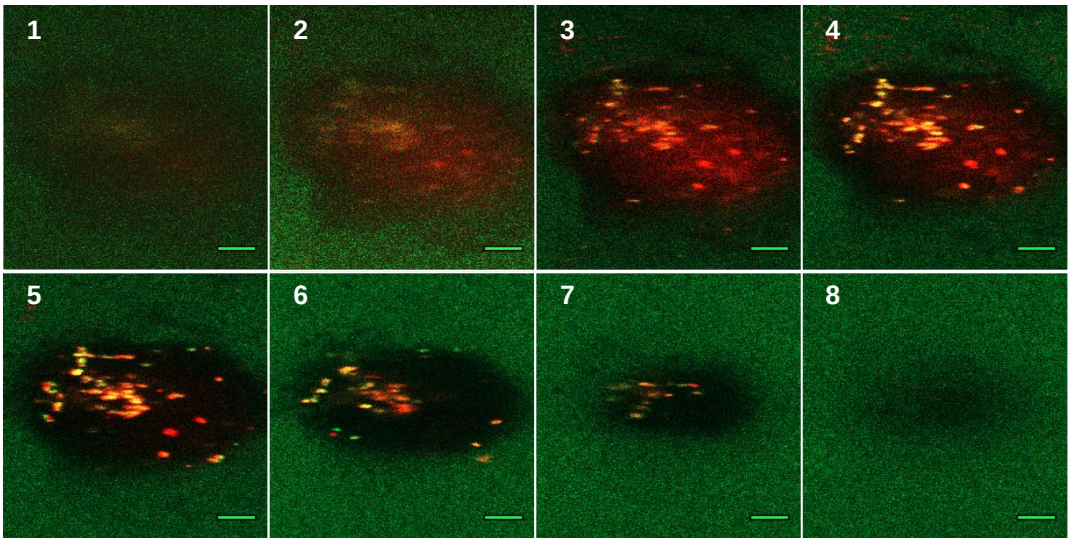

Figure 32: Z-staking confocal microscopy images of activated neutrophils incubated with AB429-49. (The neutrophils were purified from human blood sample of healthy volunteers courtesy of Dr. Neil McDonald and Miss Emma Schoefield). Neutrophils were fixed on coverslip using fibronectin, AB429-**49** (10 µM) added, and neutrophils activated by addition of calcium ionophore A23187. **1-8** Show the different planes of a neutrophil cell. Images show merge of fluorescein emission image (λ_{ex} = 488 nm, λ_{em} = 512 – 565 nm) and rhodamine emission image (λ_{ex} = 543 nm, λ_{em} = 565 – 608 nm). Slice thickness: 0.38 µm. Scale bars: 5 µm. Images are representative of duplicates experiments carried out on different days.

The Z-staking 3D experiments confirmed that the probe does enter activated neutrophils. Picture 1 to 8 are different planes of the cell, the co-localisation of the

rhodamine and the fluorescein signals appear orange, and are clearly present throughout the different planes.

The probe enters activated neutrophil and is cleaved inside the cell. To control whether the cleavage is specific to elastase the following experiments involved the use of sivelestat a well-known elastase inhibitor.[168] The probes were incubated with inhibitor and cells and observed by confocal microscopy. The neutrophils were then activated with calcium ionophore A23187 (Figure 33).

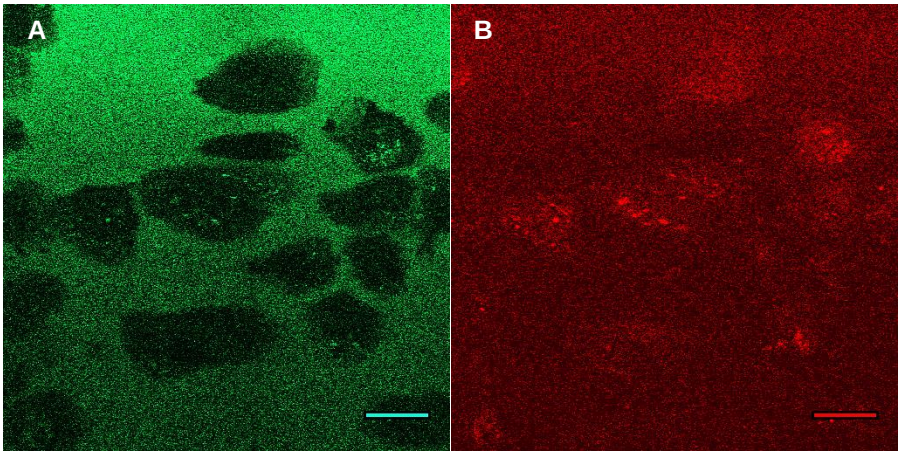

Figure 33: Confocal microscopy images of activated neutrophils in the presence of elastase inhibitor Sevelestat and incubated with probe AB429-49. (The neutrophils were purified from human blood sample of healthy volunteers courtesy of Dr. Neil McDonald and Miss Emma Schoefield). Neutrophils were fixed on coverslip using fibronectin, and incubated with elastase inhibitor Sevelestat at 50 µM for 15 min at 37 °C. AB429-**49** was added to the cells at 10 µM in the presence of Sevelestat, and neutrophils activated by addition of calcium ionophore A23187. **A.** Fluorescein emission image (λ_{ex} = 488 nm, λ_{em} = 512 – 565 nm), **B.** Rhodamine emission image (λ_{ex} = 543 nm, λ_{em} = 565 – 608 nm). Scale bars: 20 µm. Images are representative of duplicates experiments carried out on different days.

The negative control experiment shown Figure 33, indicates that the probe has entered the cells during activation (Figure 33B), and that the probe is not being

cleaved as no fluorescence increase was observed in the fluorescein channel (Figure 23A).

2.4 Conclusions

Six non peptidic probes were synthesised with optimisation of reaction conditions. Studies on A549 cells show that the dendron core does not enable penetration of the cells while acetylation of the fluorescein allows cell penetration of activated neutrophils. A dual labelled dendron-based probe specific to neutrophil elastase was synthesised. Its cleavage by the target enzyme was confirmed by enzyme kinetics studies. This peptidic probe was not cleaved in the presence of non-activated neutrophils while after activation of the neutrophils a strong fluorescence increase resulted. When a neutrophil elastase inhibitor was used in the presence of activated neutrophils the probe was observed to enter the cell but was not cleaved, confirming its specificity to NE.

Chapter 3:

Synthesis and *in vitro* studies of single isomers of fluorescein and rhodamine derivatives

Part of this chapter was published as:

Aurélie Brunet, Tashfeen Aslam and Mark Bradley, Separating the isomers – Efficient synthesis of the *N*-hydroxysuccinimide esters of 5 and 6-carboxyfluorescein diacetate and 5 and 6-carboxyrhodamine B, in Bioorganic & Medicinal Chemistry Letters (2014).

3.1 Introduction

Fluorescent probes combined with imaging techniques are capable of sensing and visualising processes from living cells to pre-clinical and even clinical applications. The development of this area of scientific research requires fluorophores with greater purity, solubility and ease of conjugation. Amongst the abundant classes of fluorophores xanthene derivatives, such as fluorescein and rhodamine dyes, have attracted extensive interest due to features such as commercial availability, low cost, sensitivity, multi-wavelength possibilities and excellent photophysical properties.[169]

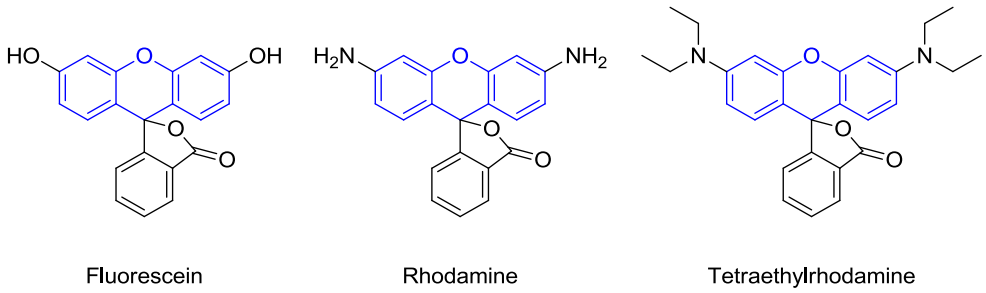

Fluorescein Rhodamine Tetraethylrhodamine

Figure 34: Xanthene based dyes.

3.1.1 Fluorescein and its derivatives

Fluorescein was originally synthesised in 1871 by Adolf von Baeyer.[170] It possesses high fluorescent quantum yield ($\Phi_{Fluorescein}$: 0.91 ± 0.05 in 1 M NaOH)[171] and represents one of the most popular fluorescent labelling agents of biomolecules.[172, 173] Protocols using fluorescein derivatives to label glycoproteins or immunoglobins are well established,[172] and the literature is rich with biomolecules labelled with fluorescein derivatives, including actin,[174-176] myosin,[175, 177] troponin,[178] hemoglobin,[179] histone,[180] proteins,[175, 181-186] DNA,[187] RNA,[188-192] and antibodies[193-197].[172]

Peptides can be easily tagged with carboxyfluorescein as shown by Nguyen (2001) who developed fluorescent probes that label nerves in human tissues, showing a contrast with adjacent tissue up to ten fold, potentially facilitating surgical repair of injured nerves and help prevent accidental transection.[198]

Common methods for DNA sequencing, such as the Sanger method, are using fluorescein.[199] Developed in the mid-1970s, the Sanger method uses chain terminating fluorescent or radiolabelled nucleotides and is to this date still described as the "gold standard of DNA sequencing and mutation identification".[200]

Carboxyfluorescein remains at the forefront of fundamental and applied research in DNA sequencing as recently shown by Xie (2011) and his new method of DNA sequencing using fluorophore releasing nucleotides,[201] or the SMRT technology developed from Pacific biosciences, a technique also based on fluorophore releasing nucleotides in conjunction with powerful light microscopes able to detect volumes of 10^{-21} litres, reaching a read of ten bases per second leading to a chain of thousands of nucleotides to be made within minutes.[202] 5(6)-Carboxyfluorescein is rendered non-fluorescent by phosphorylation and conjugation to the four nucleoside triphosphates. When a DNA polymerase recognises the nucleoside, the carboxyfluorescein moiety is released and the resulting fluorescence detected.

The monitoring of enzymatic activities by fluorescein has also been illustrated by Tanaka (2010), who designed a non-fluorescent phosphate-linked fluorescein polymer that in the presence of alkaline phosphatase, releases fluorescein.[203]

Fluorescein has also been derivatised into various chemical sensors to detect biologically relevant species or parameters such as reactive oxygen species,[13] hydrogen peroxide,[14] nitric oxide,[52] metals[3,15] or pH.[14, 16]

The synthesis of carboxyfluorescein typically results in a mixture of isomers (Figure 35), which complicates the purification and analysis of the final fluorescein probes.[204]

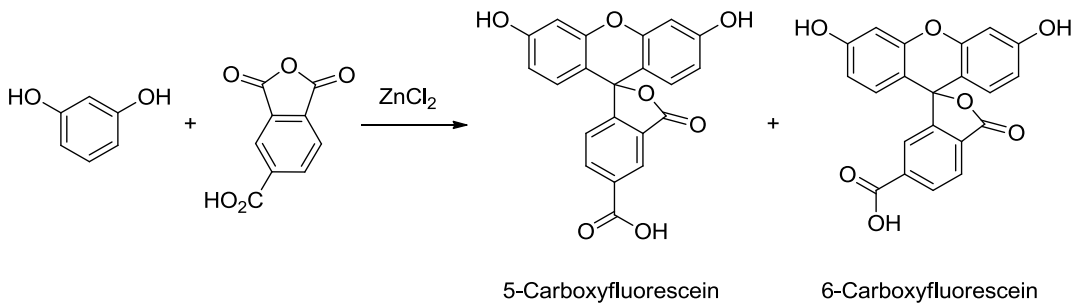

Figure 35: Synthesis of 5(6)-carboxyfluorescein.

Kvach (2007), studied the different properties of 5- and 6-carboxyfluorescein attached to an oligonucleotide and although they have similar absorbance profiles and fluorescence quantum yields the emission band of 6-carboxyfluorescein was substantially sharper making it a better choice than 5-carboxyfluorescein for multiplex detection of fluorochromes.[205]

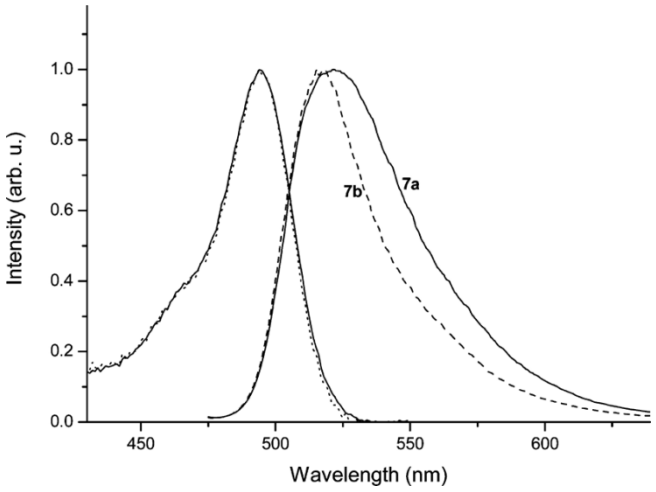

Figure 36: Absorption spectra (left) and fluorescence spectra (right) of 5-carboxyfluorescein labelled oligonucleotide **7a** (straight lines) and 6-carboxyfluorescein labelled oligonucleotide **7b** (doted and dashed lines) in sodium carbonate buffer, pH 8.35, excitation at λ = 470 nm. Reprinted with permission from Kvach.[205] Copyright 2007 American Chemical Society.

3.1.2 Carboxyfluorescein diacetate *N*-succinimidyl ester

The most extensively used derivative of fluorescein is a mixture of 5(6)-carboxyfluorescein, while another widely used derivative is the diacetate *N*-succinimidyl ester commonly referred to as CFSE or CFDA-SE (Figure 37). Confusion over the acronyms is present in the literature when CFSE should only be used for carboxyfluorescein *N*-succinimidyl ester, CFDA for carboxyfluorescein diacetate and CFDA-SE for carboxyfluorescein diacetate *N*-succinimidyl ester. [1]

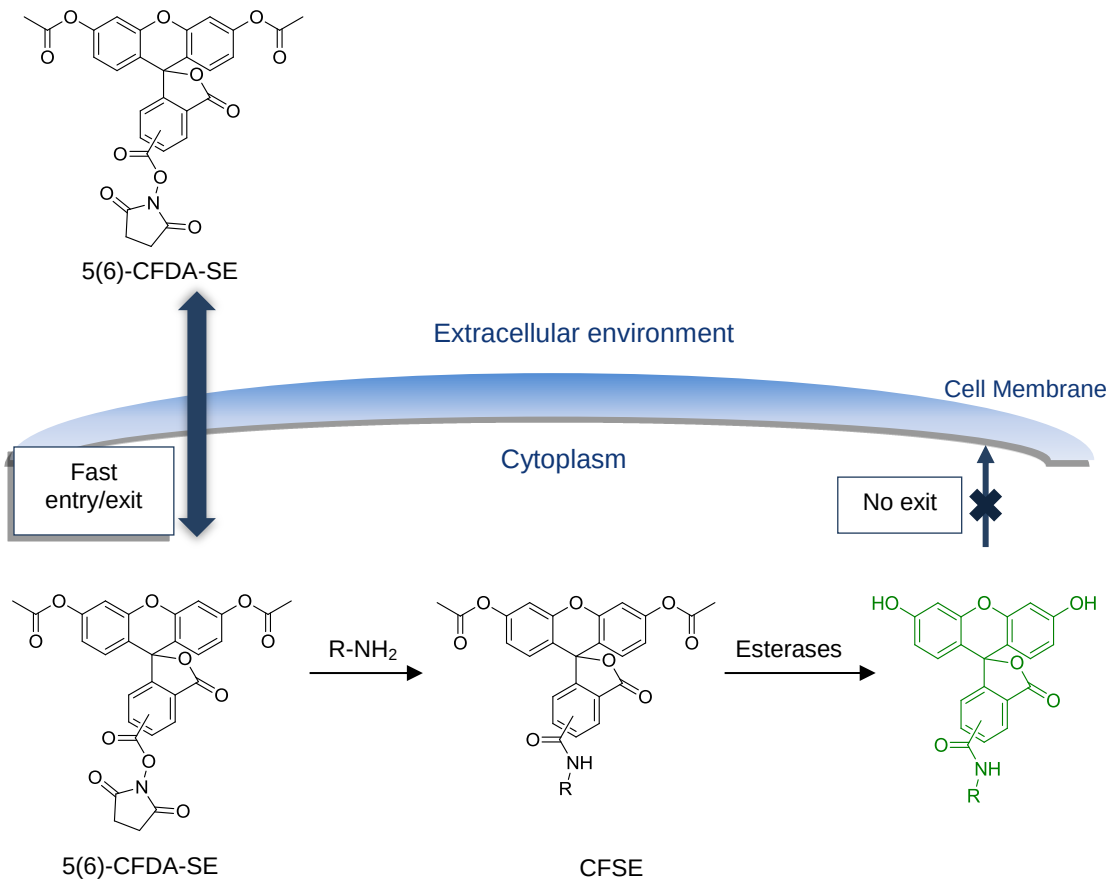

Figure 37: Mechanism of action of cellular labelling of CFDA-SE.[1]

The mode of action of carboxyfluorescein diacetate *N*-succinimidyl ester is hypothesised in Figure 37.[1] The two acetate side chains render the molecule highly

membrane permeable. Once inside cells, the *N*-succinimidyl ester reacts with proteins and the acetate groups are removed by intracellular esterases. The resulting fluorescent proteins cannot exit the cells, allowing thorough washes to remove any unreacted dye that could have led to high background fluorescence, a considerable advantage in flow cytometry and fluorescent microscopy.[1] Due to its effective coupling to intracellular amines and its long-lived fluorescence, it is widely used to track cellular division-dependent processes.[1, 206-210]

To highlight its wide-spread application, 5(6)-carboxyfluorescein diacetate *N*-succinimidyl ester has been reported 160 times in Nature journals and 18 times in Science journals in 2013 alone. However, it is used predominantly as a mixture of isomers and is also very expensive.

3.1.3 Carboxytetraethylrhodamine *N*-succinimidyl ester

Rhodamine and derivatives such a tetraethylrhodamine (Rhodamine B) and tetramethylrhodamine (TAMRA) were discovered by Noelting and Dziewonsky in 1905.[211] They are readily available, inexpensive, nontoxic, are highly water soluble and, have high fluorescent quantum yields ($\Phi_{\text{Rhodamine B}}$: 0.70 ± 0.02 in methanol[212]).[94] The fluorescence of rhodamine is photo and chemically stable[169] and, its excitation and emission wavelengths (500 - 600 nm) are within the range where autofluorescence of the cells is negligible.[94, 213] These points explain why rhodamine dyes remain, over a hundred years later, extensively used for applications such as fluorescence standards for quantum yields,[214] detection of reactive oxygen species,[94] ion sensors in living cells (e.g. chromium (III),[215, 216] copper (II),[217-219]

mercury (II),[220-224] iron (III)[216, 225],[226-229] reversible molecular switches,[230] temperature indicators,[231, 232] DNA [233, 234] and protein labelling.[169, 235-238]

Tetraethylrhodamine, also called rhodamine B, basic violet 10 and is sometimes wrongly referred to as TAMRA.[233] Despite these extended uses, the activation of rhodamine B to the *N*-hydroxysuccinimide (NHS) ester is not well established.

3.1.4 Chapter aim

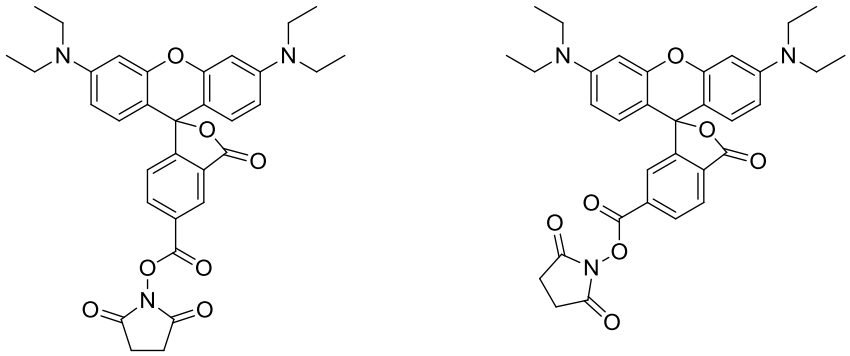

5-Rho-SE - 50 **6-Rho-SE - 51**

Figure 38: *N*-succinimidyl esters of Rhodamine

In this chapter, the separation of isomers of the 5- and 6- carboxyfluorescein diacetate *N*-succinimidyl esters (CFDA-SE) and 5- and 6- carboxytetraethyl rhodamine *N*-succinimidyl esters were investigated. Additionally, a study of 5-Rho-SE and 6-Rho-SE as "red" alternatives of carboxyfluorescein diacetate *N*-succinimidyl ester for proliferation studies of $CD4^+$ T lymphocytes and the cellular labelling differences between the isomers were explored.

3.2 Results and discussion

3.2.1 Synthesis of single isomers

Carboxyfluorescein diaceate N-succinimidyl ester

In this thesis a simple two-step process is reported for the synthesis and subsequent separation of the two isomers of diacetate of 5- and 6- carboxyfluorescein *N*-hydroxysuccinimide esters. The proposed route, unlike previously reported methods,[204] has the advantage to offer easy separation of the two isomers using a small plug of silica.

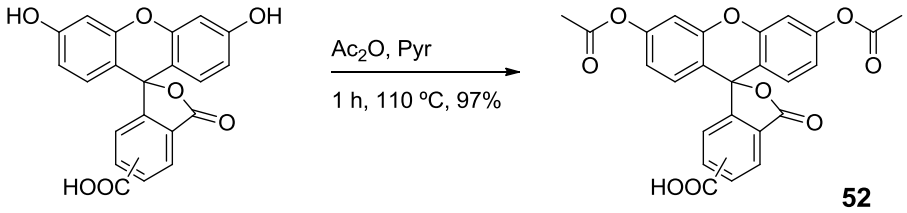

Scheme 24: Acetylation of phenol groups of carboxyfluorescein.

Initially, the procedure reported by Tour (2007) was attempted,[159] stirring 5(6)-carboxyfluorescein in pyridine with acetic anhydride (Ac_2O) and acetic acid for 3 h at 60 °C. The yields were extremely scale dependant and the method was not optimal. Thus the reaction was carried out at 100 °C and the removal of acetic acid as a solvent shortened the reaction time to 30 min, probably due to the increased concentration of acetic anhydride. Pyridine was as expected crucial for the reaction, and its removal prevented the formation of the product.

The purification reported was via trituration,[159] but a mild acid wash proved to be an easier, more reliable method to purify the product. This newly improved procedure

gave consistent yields (over 95%) on scales ranging from 200 milligrams to 15 grams.

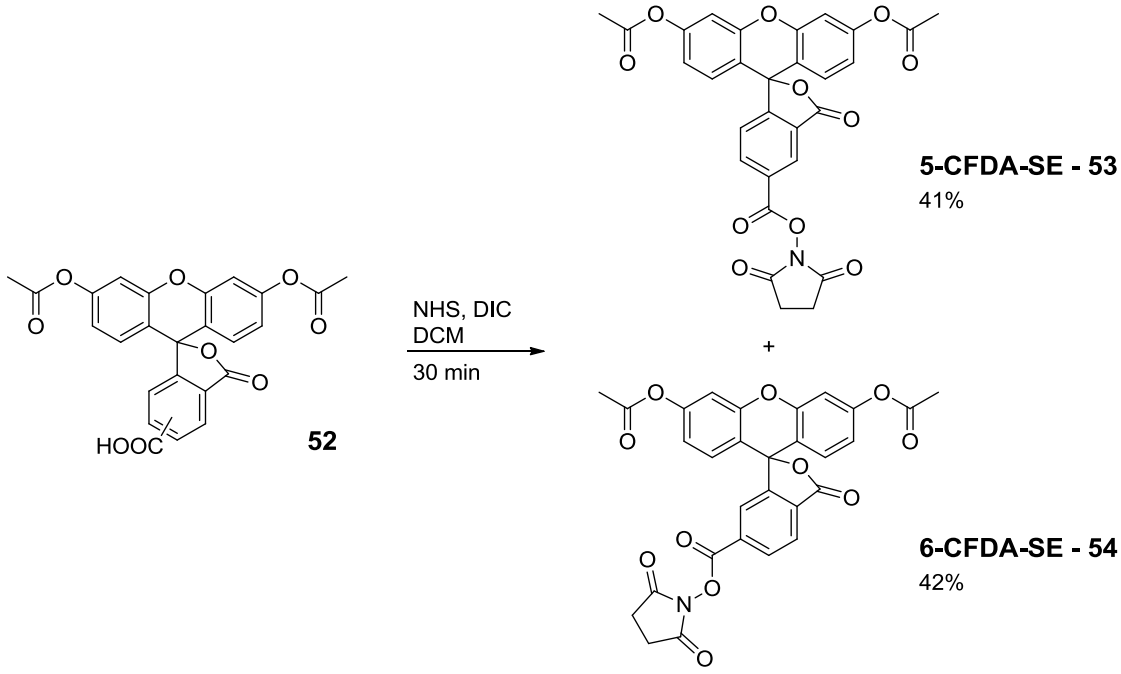

Scheme 25: NHS activation and isomer separation of 5- and 6- CFDA.

In the literature numerous conditions have been reported to give NHS esters.[154, 239] A study was carried out at room temperature to determine optimal conditions (Table 5), with 5(6)-diacetatecarboxyfluorescein the limiting reagent. The desired compound was formed in all cases, but, only a few conditions gave full conversion (Table 5). Entry 1 was carried out under dry conditions to assess whether or not the presence of water affected the reaction. The HPLC profile of reactions 1 and 2 was identical suggesting that the presence of water did not affect the reaction, while also indicating the presence of starting material. In entry 3 DMAP was added along with NHS and DCC, but full conversion was again not obtained. The replacement of THF by DCM in entry 4 allowed the reaction to reach completion in 1 h. Entries 5, 6 and 7 showed

the combination of NHS and EDC.HCl in DCM or DMF did not reach completion. Nevertheless, the use of NHS with DIC (Entry 7) in DCM gave full conversion within 30 min. The reaction was successfully repeated on scale ranging from 100 milligrams to 10 grams.

Entry	Activating Agents	Solvents	Time	Full conversion
1	NHS, DCC	Dry THF	2 h	No
2	NHS, DCC	THF	2 h	No
3	NHS, DCC, DMAP	THF	2 h	No
4	NHS, DCC	DCM	1 h	Yes
5	NHS, EDC.HCl	DCM	2 h	No
6	NHS. EDC.HCl	DMF	2 h	No
7	NHS, DIC	DCM	30 min	Yes

Table 5: Study of NHS activation of 5(6)-diacetatecarboxyfluorescein (1 eq, 0.1 M) with indicated reagents (1.2 eq) at room temperature. Conversion monitored by HPLC, TLC and MS.

Unlike 5(6)-carboxyfluorescein, the isomers of 5(6)-carboxyfluorescein diacetate *N*-succinimidyl ester (CFSE) are easily separable by simple column chromatography. Indeed, the retention factors (R_f) are 0.37 and 0.53 for 5-CFSE-**53** and 6-CFSE-**54** respectively (in 50% ethylacetate in toluene), while the isomers of 5(6)-carboxyfluorescein co-run in all attempted solvent combinations. Using a slow gradient from 100% toluene to 10% EtOAc in toluene using column chromatography, yields as high as 41% and 42% for 5- and 6-CFDA-SE respectively

were obtained. For larger scales, the isomers were separated on a silica plug (15 g scale 35% and 25%, for 5- and 6-CFDA-SE respectively).

The entire two-step procedure takes 1 day, and once purified and dried, CFDA-SE can be kept at room temperature for over 4 months without degradation.

Carboxy tetraethyl rhodamine N-succinimidyl ester

The separation of the isomers of 5(6)-carboxytetraetheylrhodamine and 5(6)-carboxyrhodamine B was straight-forward using a gradient of TEA:DCM:MeOH (5:95:0 to 5:75:20).

To form the *N*-succinimidyl active ester of carboxyrhodamine B, various conditions were attempted and were summarised in Table 6. Initially the combination of NHS and DIC used for the activation of carboxyfluorescein was attempted, however the presence of a by-product was observed (Table 6 – Entry 1). THF was replaced with dry DCM to optimise the solubility of all reagents and although the starting material disappeared, the by-product remained (Entry 2). DIC was replaced with EDC.HCl and the equivalents reduced to 1.05 instead of the previous 1.5 equivalents. The reaction was also attempted in dry THF but after 1 h the by-product was also present. The reagents quantities were increased to 1.5 equivalents and the solvent changed to dry acetonitrile (MeCN). After 2 h the by-product still remained. Mass spectrometry showed the by-product was the di-activated compound **55** (Figure 39), benzylamine was added to the reaction and the di-benzylated compound **56** was isolated (Figure 39).

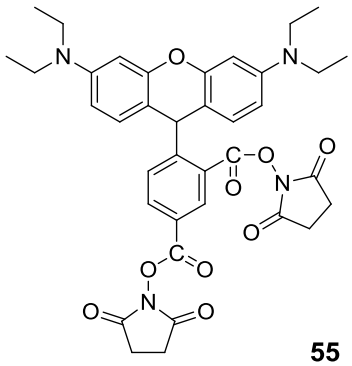

55

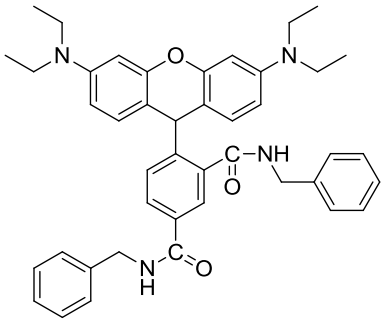

56

Figure 39: Di-activated by-product and the di benzylated product.

To regioselectivity obtain a reaction of the 5- or 6-carboxylic acid over the 3-carboxylic acid, the rhodamine must react in its closed form. Unlike fluorescein, rhodamine B is closed under basic conditions and open under acidic conditions.[240] Caminade showed that when the 3-carboxylic acid was converted to an active ester and reacted with an amine the resulting amide forms the closed form of the rhodamine (spirolactam) rendering the molecule non fluorescent.[219, 221, 222, 224, 226, 241] It was therefore crucial to prevent the 3-carboxylic acid from reacting, by increasing the pH with the addition of a base. Although by-product formation was successfully prevented, very low conversion rates were observed (Entry 5-11). Longer reaction times reaching 12 h and higher temperatures (up to 120 °C) were attempted, but the conversion rate did not improve and extreme conditions yielded the hydrolysis of the product to the original starting material (Entry 5-11). Increasing to 1.5 equivalents NHS and EDC.HCl instead of 1.05 did not improve the reaction (Entry 12). Decreasing the amount of base from 9 equivalents to 2 equivalents and lowering the temperature to 0 °C resulted in the formation of the by-product (Entry 11).

A patent reported the successful synthesis of carboxytetraethylrhodamine *N*-succinimidyl ester using DSC, and DMAP.[242] These reaction conditions were used

but as expected the lack of base gave the formation of the by-product (Entry 21). TEA was therefore introduced into the reaction and quantities of DSC and DMAP were varied (Entry 15-20). To prevent by-product formation 9 equivalents of base were used with 2 equivalents of DSC (Entry 18-20). Full conversion was obtained in 1 h with an increase of DMAP to 5 equivalents (Entry 20).

Although full conversion was obtained the purification proved difficult, as solvent removal caused hydrolysis of the product. To ease purification, the organic base was replaced with sodium carbonate (Entry 22) and potassium carbonate (Entry 23). However, both gave by-products. The conditions yielding to full conversion found in Entry 20 using DMAP, DSC and TEA were used but the solvent replaced by DCM for its low boiling point (Entry 24-26), to obtain the optimum conditions (Entry 26).

	Succinimide	Carbodiimide	Base	Catalyst	Solvent	Time	Temp.	Starting material	55-By product	Product 50
1	NHS - 1.5 eq	DIC - 1.5 eq	-	-	Dry THF	1 h	r.t.	✓	✓	✓
2	NHS - 1.5 eq	DIC - 1.5 eq	-	-	Dry DCM	1 h	r.t.		✓	✓
3	NHS - 1.05 eq	EDC.HCl - 1.05 eq	-	-	Dry THF	2 h	r.t.	✓	✓	✓
4	NHS - 1.15 eq	EDC.HCl - 1.15 eq	-	-	Dry MeCN	2 h	r.t.		✓	✓
5	NHS - 1.05 eq	EDC.HCl - 1.05 eq	TEA - 9 eq	-	Dry DMF	1 h	r.t.	✓		
6	NHS - 1.05 eq	EDC.HCl - 1.05 eq	TEA - 9 eq	-	Dry DMF	3h30	r.t.	✓		
7	NHS - 1.05 eq	EDC.HCl - 1.05 eq	TEA - 9 eq	-	Dry DMF	o/n	r.t.	60%		40%
8	NHS - 1.05 eq	EDC.HCl - 1.05 eq	TEA - 9 eq	-	Dry DMF	20 min	mw 60 °C	60%		40%
9	NHS - 1.05 eq	EDC.HCl - 1.05 eq	TEA - 9 eq	-	Dry DMF	30 min	mw 80 °C	60%		40%
10	NHS - 1.05 eq	EDC.HCl - 1.05 eq	TEA - 9 eq	-	Dry DMF	30 min	mw 120 °C	✓		
11	NHS - 1.05 eq	EDC.HCl - 1.05 eq	TEA - 2 eq	-	Dry DMF	2 h	0 °C	✓	✓	✓
12	NHS - 1.5 eq	EDC.HCl - 1.5 eq	TEA - 9 eq	-	Dry DMF	o/n	40 °C	70%		30%
13	NHS - 1.05 eq	DIC - 1.05 eq	TEA - 9 eq	-	Dry DMF	o/n	r.t.	90%		10%
14	NHS - 2.0 eq	DIC - 2.0 eq	TEA - 9 eq	-	Dry DMF	1 h	r.t.	✓	✓	✓
15	DSC - 1.0 eq	-	TEA - 9 eq	-	Dry DMF	1 h	0 °C	✓		
16	DSC - 1.0 eq	-	TEA - 9 eq	-	Dry DMF	3 h	r.t.	✓		
17	**DSC - 2.5 eq**	-	**TEA - 9 eq**	**DMAP - 2 eq**	**Dry DMF**	**3 h**	**r.t.**			✓
18	DSC - 1.5 eq	-	TEA - 9 eq	DMAP - 2 eq	Dry DMF	3 h	r.t.	✓		✓
19	DSC - 2.0 eq	-	TEA - 9 eq	DMAP - 3 eq	Dry DMF	1 h	r.t.	✓		✓
20	**DSC - 3.0 eq**	-	**TEA - 9 eq**	**DMAP - 5 eq**	**Dry DMF**	**1 h**	**r.t.**			✓
21	DSC - 1.5 eq	-	-	DMAP - 2 eq	Dry DCM	1 h	r.t.	✓	✓	
22	DSC - 2.0 eq	-	Na_2CO_3 - 9 eq	DMAP - 3 eq	Dry MeCN	3 h	r.t.		✓	✓
23	DSC - 2.0 eq	-	K_2CO_3 - 9 eq	DMAP - 5 eq	Dry MeCN	3 h	r.t.	✓	✓	✓
24	DSC - 2.0 eq	-	TEA - 3 eq	DMAP - 5 eq	Dry DCM	1 h	r.t.		✓	✓
25	DSC - 2.0 eq	-	TEA - 3 eq	DMAP - 3 eq	Dry DCM	1 h	r.t.	✓	✓	✓
26	**DSC - 2.0 eq**	-	**TEA - 5 eq**	**DMAP - 5 eq**	**Dry DCM**	**1 h**	**r.t.**			✓

Table 6: Reaction conditions for the *N*-succinimidyl ester formation of carboxy rhodamine B.

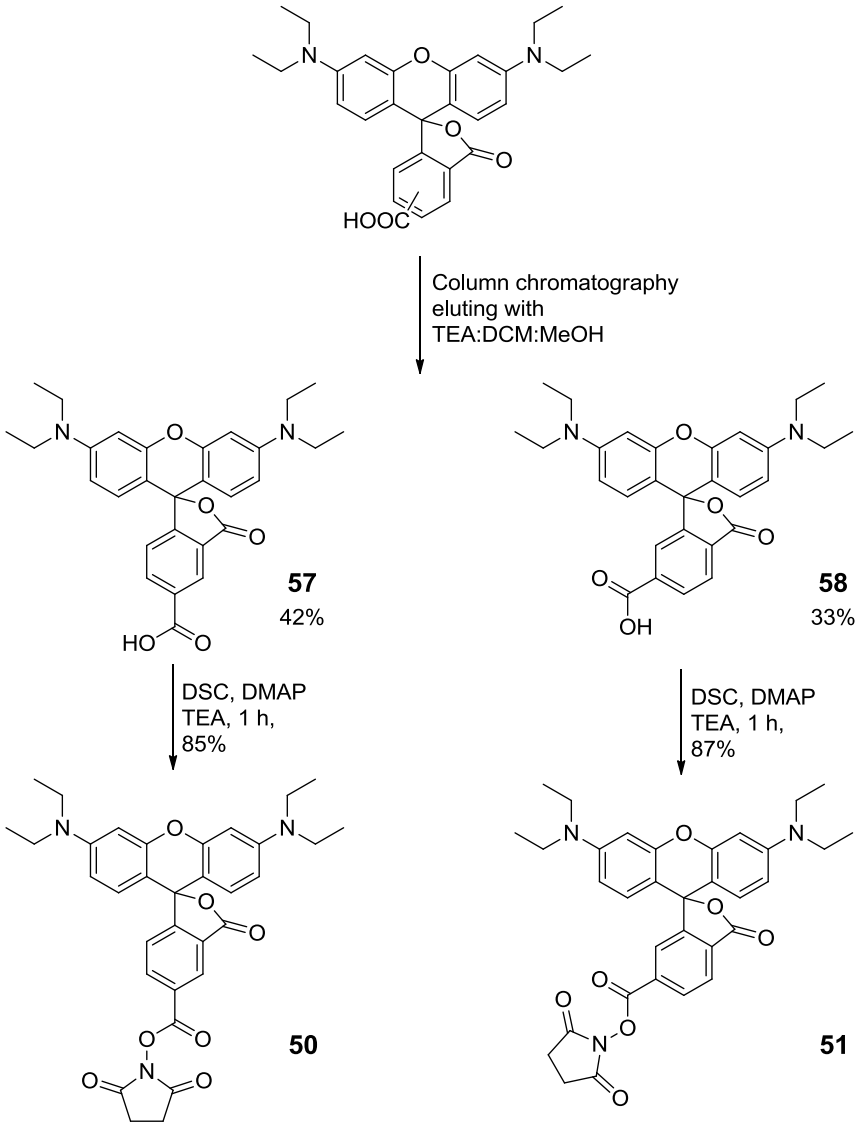

Scheme 26: 5- and 6- carboxyrhodamine B ester synthesis.

The optimal route was therefore to separate the isomers via column chromatography under basic conditions. These were converted to their corresponding *N*-succinimidyl ester using a combination of DSC, DMAP and TEA. The reaction was then quenched with 10 equivalents of acetic acid to prevent rearrangement and decomposition of the

active ester (when concentrated). The mixture was purified using column chromatography eluting with 1% AcOH in acetone.

3.2.2 Cell proliferation assay on primary T cells

Immune system

When a foreign entity succeeds in overcoming the human body's physical barriers (skin, mucous membranes, saliva proteases), an immediate line of defence called the innate immune system is activated. This first, non-specific response will react to destroy or contain this invading organism (as well as any contaminated cells).[125] A broad range of pathogens can be recognised by the innate immune system. However, the diversity of this defence is limited and has no memory of encountered pathogens. Thus, the response remains the same even under repeated exposure to a pathogen. If the spreading of the pathogen persists, a second line of defence called adaptive immune system will develop. This response predominately involves two types of cells called T lymphocytes and B lymphocytes (Figure 40). These cells possess an almost infinite number of extremely diverse and adaptive receptors that will specifically target foreign entities or antigens.[243] Pathogens are remembered by memory cells and the defence will be more vigorous and more finely tuned with repeated exposure.

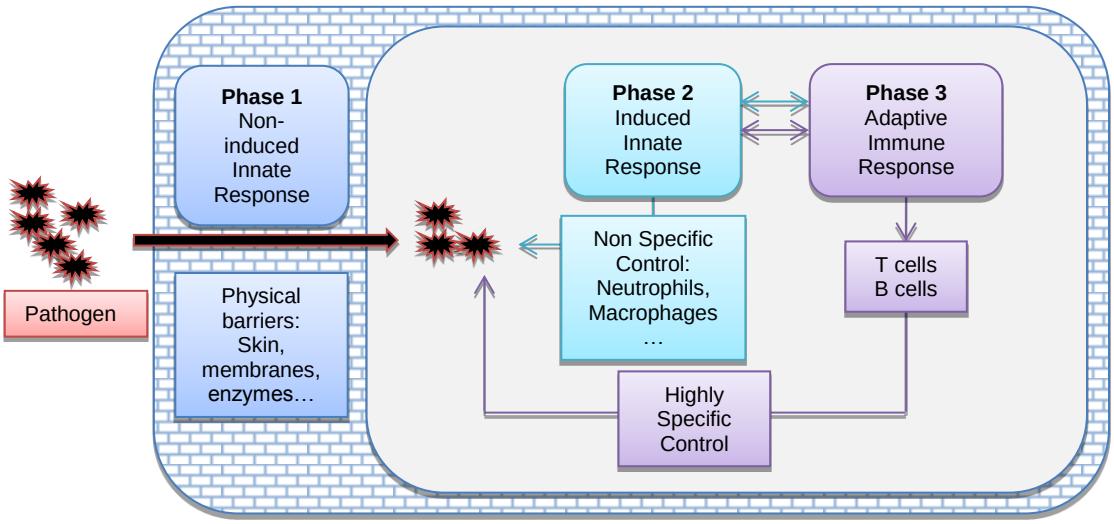

Figure 40: Immune system response mechanism.

T Lymphocyte

Non activated T cells also called naïve T cells, have a long lifespan, they rarely divide, circulate in blood and lymph and populate certain areas of the body such as the spleen.[244] Binding of a target cell by T cells activates them to proliferate rapidly.[245] T cell receptors do not bind to antigens that are soluble or in their native conformation. In order for a T cell to respond to an antigen, a separate host cell must first digest it into peptide fragments, and then attach the individual peptides to specialized cell surface molecules called major histocompatibility complex (MHC) molecules. It is the overall shape of the peptide–MHC complex, presented as a unit by the host cell to the T cell, that is critical for recognition by the T cell receptor.[246]

T cells can be divided into two categories: $CD8^+$ T cells and $CD4^+$ T cells. $CD8^+$ T cells are defined by the presence of CD8 receptors on the cell membrane. They act as killer or cytotoxic cells. They specifically recognise and lyse altered host cells such as virus infected cells or malignant cells.[244] The $CD4^+$ T cells present CD4 receptors

on the cell membrane. They are also called T helper cells as they produce signalling molecules called lymphokines to assist B cells in their antibody production and $CD8^+$ T cells in their destruction of targeted cells.[244] $CD4^+$ T helper cells (T_h) can synthesise a variety of lymphokines immediately after activation but differences in their release pattern can further divide them into subtypes.[247]

T cells extraction from spleen

T cells were chosen as they were the first population studied by Parish *et al.* when they initially identified CFDA-SE as a tracking dye for cell migration.[1, 248] Furthermore, CFDA-SE use for measuring lymphocyte proliferation by flow cytometry has become a widely used and well established assay.[1, 249] Splenocytes from three C57BL/6 mice were used to isolate T lymphocytes. C57BL/6 mice are a wild type mouse strain containing a full complement of murine genes (no genetic modification).

Spleens were extracted from the three mice and T cells separated (in collaboration with Dr. Chesney Michels and Miss Emma Scholefield). The T cell population was purified by magnetic separation using MicroBeads and an autoMACS pro 1400 (Miltenyi Biotec).

The labelling of the cells was carried out according to standard protocol that can be found in commercial CFDA-SE cell proliferation kit such as the CellTrace™ developed by Invitrogen.[250] Probes were individually incubated for 10 min at 37 °C. The reaction was stopped by the addition of cold complete media, which contains proteins[251] that quench unreacted active esters. The cells were thoroughly washed to ensure complete excess probe removal. Each cell experiment was re-suspended in

complete media, halved and plated onto a 96-well plate pre-coated with anti-CD3/28 to activate cell division.[252] The cells were incubated at 37 °C for 48 h and 72 h before flow cytometry experiments and microscopy.

Microscopy studies

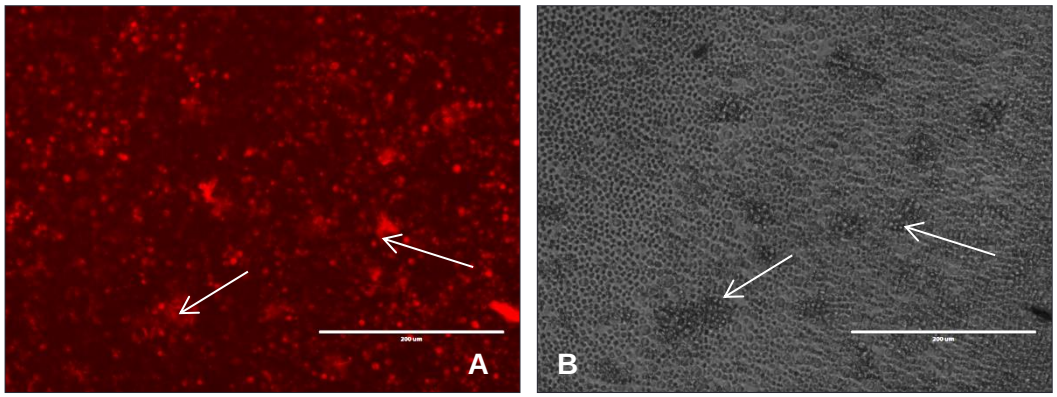

Figure 41: Microscopy images of primary T cell clusters. T cell labelled with 6-Rho-SE-**51** activated with anti-CD3/28 and cultured for 3 days at 37 °C. **A.** Rhodamine emission image (λ_{ex} = 543 nm, λ_{em} = 565 – 608 nm). **B**. Bright field image. Scale bar equals 200 µm. Arrows highlight some cell clusters.

After labelling with probes (5-CFDA-SE-**53**, 6-CFDA-SE-**54**, 5-Rho-SE-**50** and 6-Rho-SE-**51**) the cells were cultured for 72 h and from microscopy studies, cellular division was assessed, with observation of cell clusters. Figure 41A and B show T cells where 6-Rho-SE-**51** has been used and analysed under rhodamine emission chanel and bright field.

Flow cytometry studies

After labeling with probes (commercial 5(6)-CFDA-SE, 5-CFDA-SE-**53**, 6-CFDA-SE-**54**, 5-Rho-SE-**50** and 6-Rho-SE-**51**), the cells were left to divide at 37 °C, and analysed using flow cytometry after 72 h and 96 h. Flow cytometry allows the

measurement of fluorescence intensity in individual cells, cells that have been successfully labelled will be fluorescent.

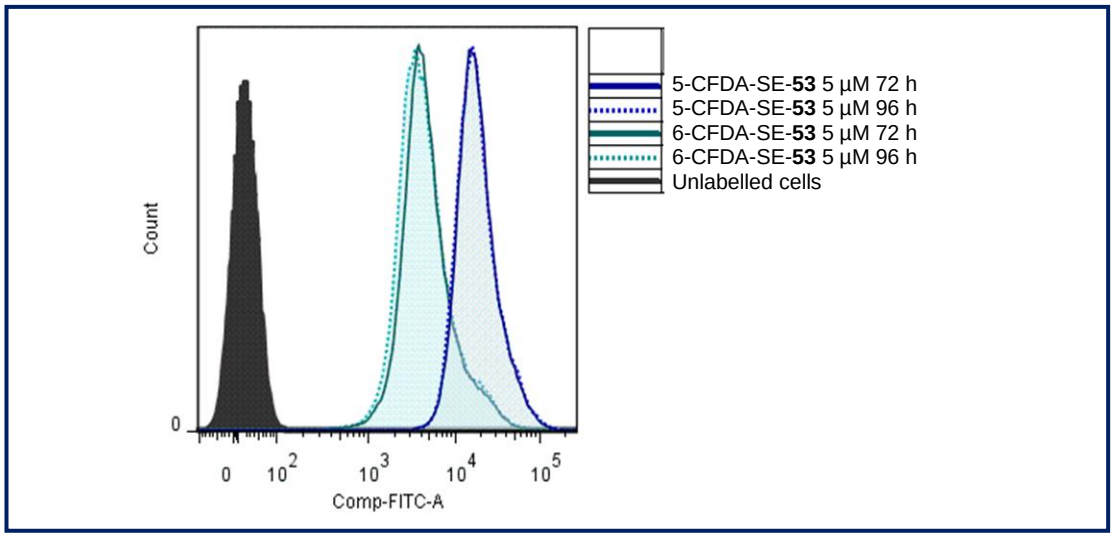

Figure 42: Fluorescence histograms of T cells labelled with 5-CFDA-SE-**53** (5 µM) (dark blue) and 6-CFDA-SE-**54** (5 µM) (turquoise) after 72 h (solid lines) and 96 h (dotted lines). FITC-A channel (λ_{ex} = 488 nm, λ_{em} = 515 – 545 nm). Histograms representative of triplicate experiments.

High fluorescence intensities from the cells incubated with 5-CFDA-SE-**53** and 6-CFDA-SE-**54** confirmed that the cells had been succesfully labelled (Figure 42). Higher fluorescence intensities were seen in cells labelled with 5-CFDA-SE-**53** compared to cells labelled with 6-CFDA-SE-**54**. Decrease in fluorescence intensity over time due to cellular division was expected, however, it was not observed.

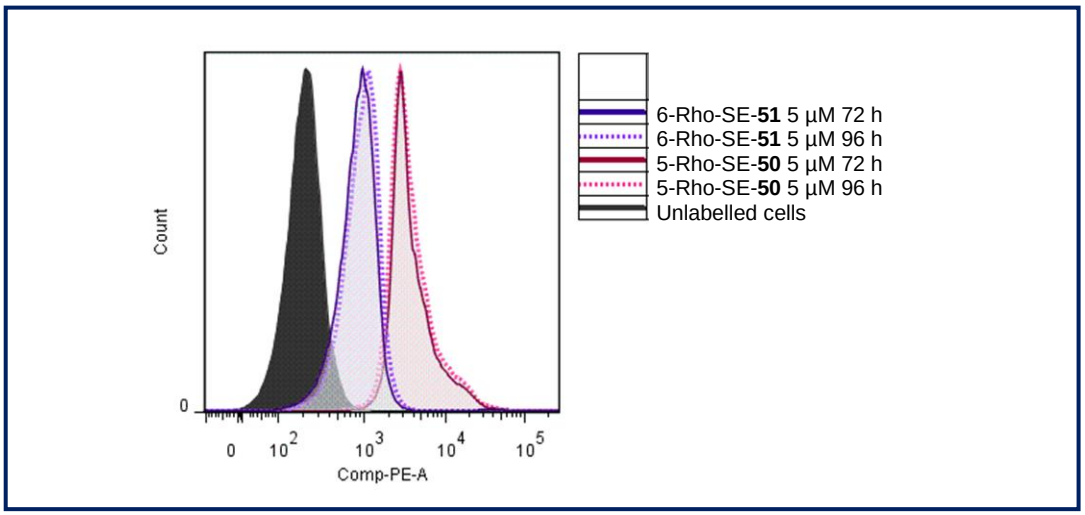

Figure 43: Fluorescence histograms of T cells labelled with 6-Rho-SE-**51** (5 µM) (purple) and 5-Rho-SE-**50** (5 µM) (pink) after 72 h (solid lines) and 96 h (dotted lines). PE-A channel (λ_{ex} = 488 nm, λ_{em} = 515 – 545 nm). Histograms representative of triplicate experiments.

Fluorescence was observed from cells incubated with 5-Rho-SE-**50** and 6-Rho-SE-**51**, confirming successful labeling (Figure 43). Stronger fluorescence intensities were observed for cells labelled with 5-Rho-SE-**50** than with cells labelled with 6-Rho-SE-**51** (Figure 43).

The fluorescence intensity of cells labelled with 5-CFDA-SE-**53** and 6-CFDA-SE-**54** cannot be compared to those labelled with 5-Rho-SE-**50** and 6-Rho-SE-**51**. The BD Canto II FACS machine used has an excitation source with three lasers at the wavelengths of 405 nm, 488 nm and 633 nm. Therefore rhodamine based compounds are excited at 488 nm (Figure 44).

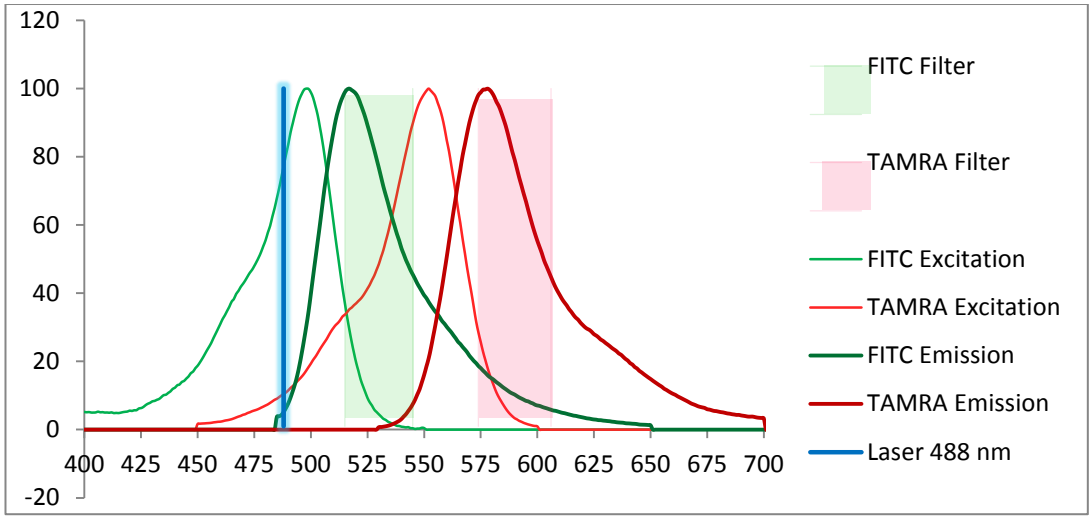

Figure 44: Fluorescence spectra related to BD Canto FACS machine.[253]

The above diagram shows the laser excitation of the machine (488 nm) as well as the two selected emission filters fluorescein (515 - 545 nm) and rhodamine (574 - 606 nm). From the diagram it is clear that the excitation wavelength is ideal for fluorescein but too low for optimum rhodamine excitation.

3.2.3 Cell proliferation assay on jurkat cell line

Flow cytometry studies

To further investigate these compounds, proliferation experiments were repeated on Jurkat cells. Jurkat cells are human leukaemic T cells, developed in the early eighties as a source of human T cells.[254-256] The cells were incubated with five probes: commercial 5(6)-CFDA-SE, and the four synthesised single isomers 5-CFDA-SE-**53**, 6-CFDA-SE-**54**, 5-Rho-SE-**50** and 6-Rho-SE-**51**, at the concentraions of 5 µM and 1 µM for 10 min at 37 °C.[250] The reaction quenched with cold complete media, and

cells washed thoughroughly to ensure excess probe removal. The cells were analysed by flow cytometry over six days.

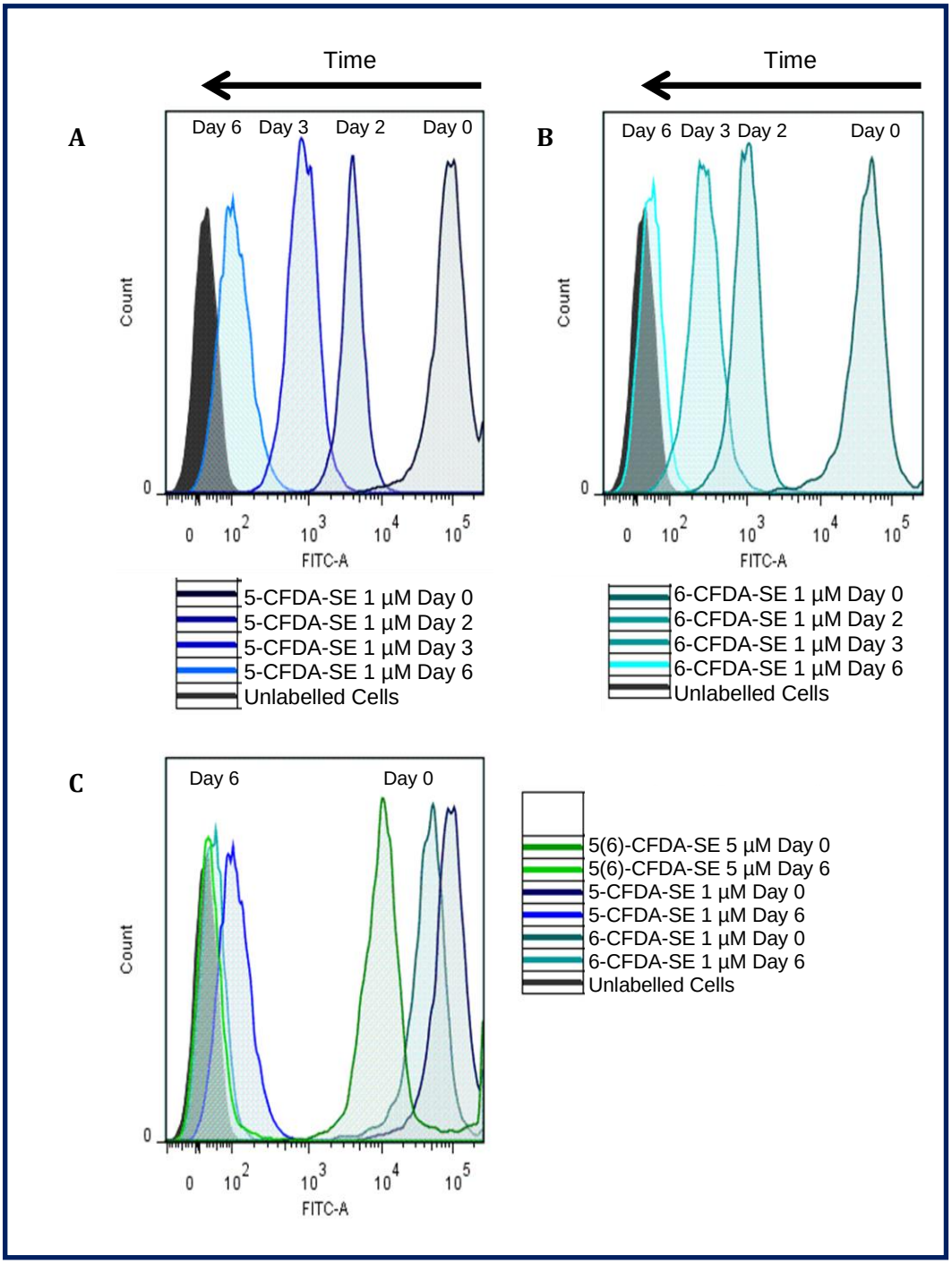

Figure 45: Fluorescence histograms of Jurkat cells labelled with **A.** 5-CFDA-SE (1 µM) over 6 days, **B.** 6-CFDA-SE (1 µM) over 6 days, **C.** 5(6)-CFDA-SE (5 µM), 5-CFDA-SE (1 µM) and 6-CFDA-SE (1 µM) at day 0 and day 6. FITC-A channel (λ_{ex} = 488 nm, λ_{em} = 515 – 545 nm). Data representative of duplicates experiments.

At t = 0, the fluorescence intensities of the cells incubated with 5-CFDA-SE-**53** and 6-CFDA-SE-**54** at a concentration of 5 µM were off scale, while fluorescence intensity of cells incubated at 1 µM was within the scale and is shown Figure 45A and Figure 45B. Decrease in fluorescence intensity over time was observed for population labelled with 5-CFDA-SE-**53** and 6-CFDA-SE-**54**, confirming division of the cells.

Fluorescence intensity was higher in cells labelled with 5-CFDA-SE-**53** than in cells labelled with 6-CFDA-SE-**54**, resulting in 5-CFDA-SE-**53** labelled population to be traced on the 6^{th} day unlike the 6-CFDA-SE-**54** labelled population (Figure 45C).

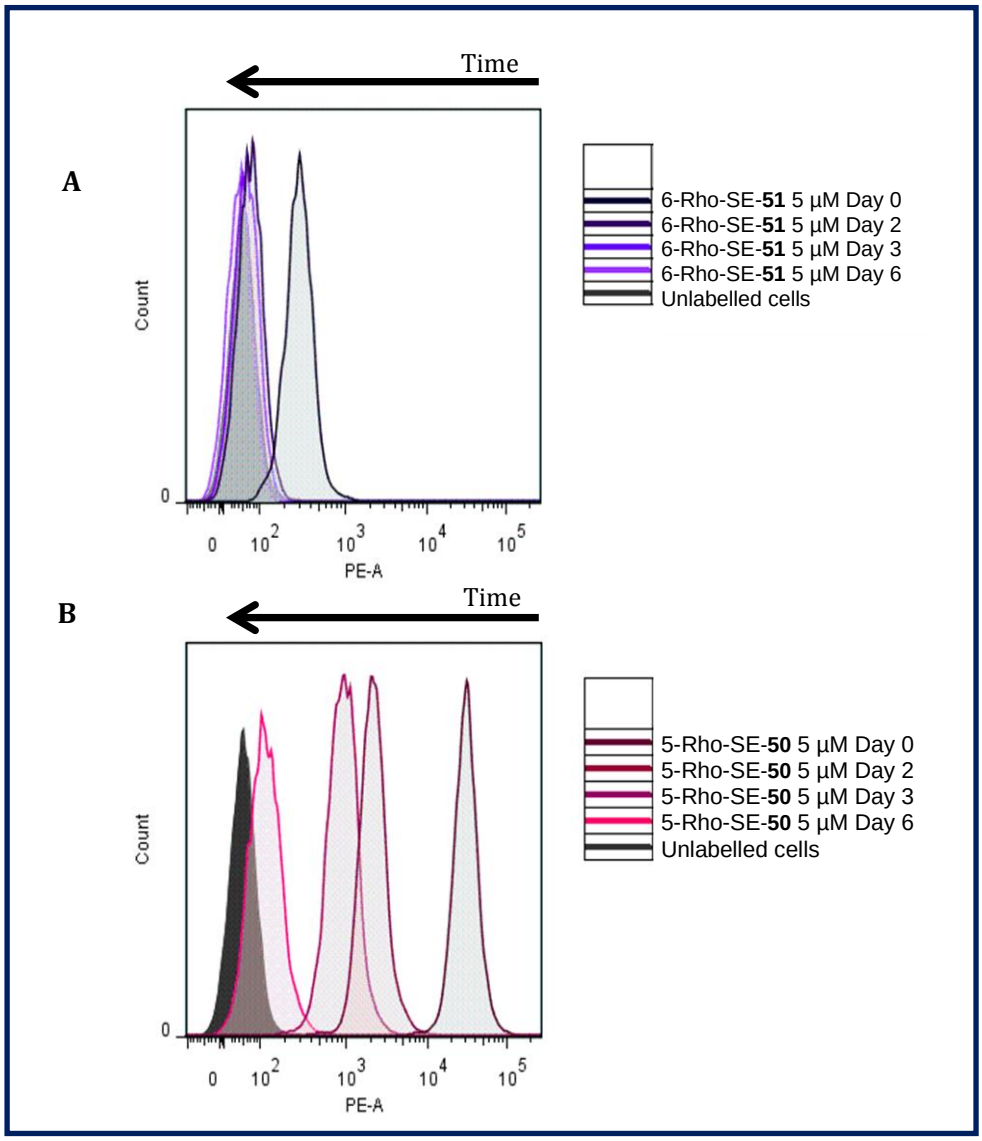

Figure 46: Fluorescence histograms of Jurkat cells labelled with **A.** 6-Rho-SE-**51** (5 µM), **B.** 5-Rho-SE-**50** (5 µM), and analysed over 6 days. PE-A channel (λ_{ex} = 488 nm, λ_{em} = 515 – 545 nm). Histograms representative of duplicate experiments.

Fluorescence intensity observed by flow cytometry in Jurkat cells incubated with 5-Rho-SE-**50** and 6-Rho-SE-**51** confirmed cellular labeling property of the probes. Decrease in fluorescence intensity over the 6 days was observed for both 6-Rho-SE-**51** labelled cells (Figure 46A) and 5-Rho-SE-**50** labelled cells (Figure 46B), indicating that the fluorophore was passed onto to daughter cell during cell division.

The fluorescence intensity of 5-Rho-SE-**50** labelled cells was higher than 6-Rho-SE-**51** labelled cells, allowing the 5-Rho-SE-**50** labelled population to be tracable over the 6 days.

3.3 Conclusions

5-CFDA-SE-**53** and 6-CFDA-SE-**54** were successfully synthesised and separated in a simple two step procedure. A method for generating the single isomers 5-Rho-SE-**50** and 6-Rho-SE-**51** has also been established. The cellular labelling properties of the four isomers were compared on primary T cells and on the Jurkat cell line. In both experiments the 5-CFDA-SE-**53** labelled cells showed stronger fluorescent intensities than 6-CFDA-SE-**54** labbelled cells.

5-Rho-SE-**50** and 6-Rho-SE-**51** labelled T cells and Jurkat cells, and were passed onto daughter cell in a similar fashion to CFDA-SE. For both cell types, 5-Rho-SE-**50** labelled population was more fluorescent than 6-Rho-SE-**51** labelled population.

These preliminary results suggest that 5-CFDA-SE-**53** is a better reagent for cell proliferation assays than 6-CFDA-SE-**54**, and that 5-Rho-SE-**50** can be used for cell division assays when a red dye is more convenient. Further investigations, will include the study of labelled T lymphocyte cultured *in vivo*, and the investigation of the labelling properties of the probes on different cell types.

Chapter 4:

Nuclear localisation dual-labelled dendron probes

4.1 Introduction

4.1.1 Delivery to the nucleus

The nucleus is a subcellular organelle found in eukaryotic cells. It contains genetic material and hosts DNA and RNA synthesis.[257] Bound by a double membrane, entry into and exit out of the nucleus is finely controlled.

Transport of specific cargos across the nuclear envelope is critical for cell division and all cellular processes.[258-260] Small molecules simply diffuse through nuclear pore complexes (NPCs)[261] which penetrate the double lipid bilayer,[262] while larger molecules such as proteins and DNA must be recognized by specific nuclear localisation sequences (NLSs) to be transported into the nucleus.[263, 264] The first NLS discovered was the seven-mer PKKKRKV found in the SV40 Large T-antigen.[265] The mechanism of action of nuclear uptake is illustrated Figure 47.

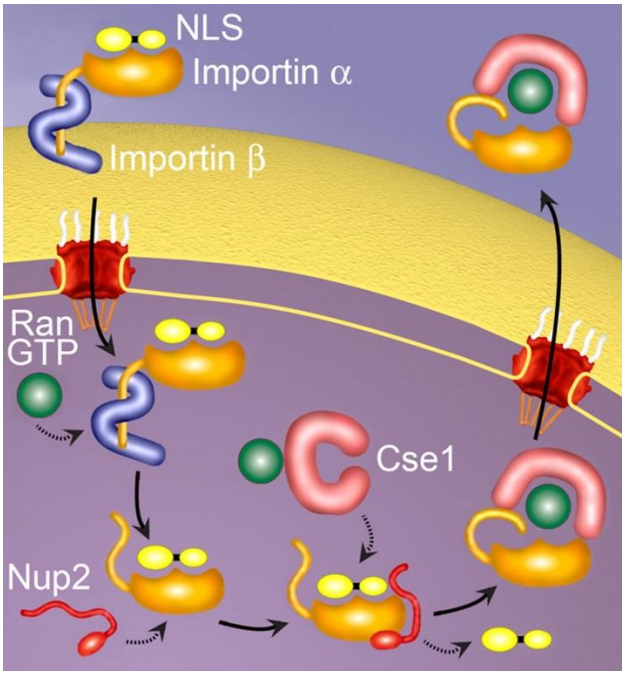

Figure 47: Classical nuclear import mechanism, where Ran GTP is a binding nuclear protein, Nup2 a nuclear pore complex protein and Cse1 an exportin protein. Reprinted with permission from Lange.[264] Copyright 2007 by the American Society for Biochemistry and Molecular Biology.

In the cytoplasm, the NLS attached to the desired cargo is recognised by the importin α-protein. Importin α recognizes the importin β protein which allows transport through the nuclear pore.[266] Once inside the nucleus, the nuclear protein RanGTP binds to the complex which causes a conformational change in importin β, resulting in the release of importin α. The dissociation of importin α from the cargo is then mediated by a nuclear pore complex protein (Nup2) and an exportin protein (Cse1).[267] Finally, importin α is recycled back to the cytoplasm by the exportin protein Cse1, in a trimeric complex with RanGTP.[264, 268]

4.1.2 Nuclear delivery applications

With the analysis of the human genome sequence, and detailed genetic analysis, many disorders have been shown to be the result of genetic mutations.[269] Gene therapy strategies are therefore being investigated for the permanent treatment of genetic disorders.[270] With more FDA approvals of gene therapy treatments such as fomivirsen and glybera, increased interest to the field is to be expected.[271, 272]

One approach to gene therapy is the delivery of DNA or cargo to the nucleus of the cells. Using modified viruses allows easy nuclear transport but has raised safety concerns.[273] Thus, non-viral delivery methods have been the subject of considerable research over the recent years,[274, 275] however, the nuclear transport of the DNA/vector complex remains a difficult step for non-viral gene transfer.[274]

4.1.3 Impact of fluorophores in nuclear transport

Puckett *et al.* (2009) have recently studied the impact of fluorescein on the nuclear delivery properties of their probes. Comparison of three peptide complexes of Ru(II): Ru-octaarginine (Ru-D-R8), Ruoctaarginine-fluorescein (Ru-D-R8-fluor), and Ru-fluorescein (Ru-fluor), showed that fluorescein re-directs the complex into the nucleus (Figure 48).

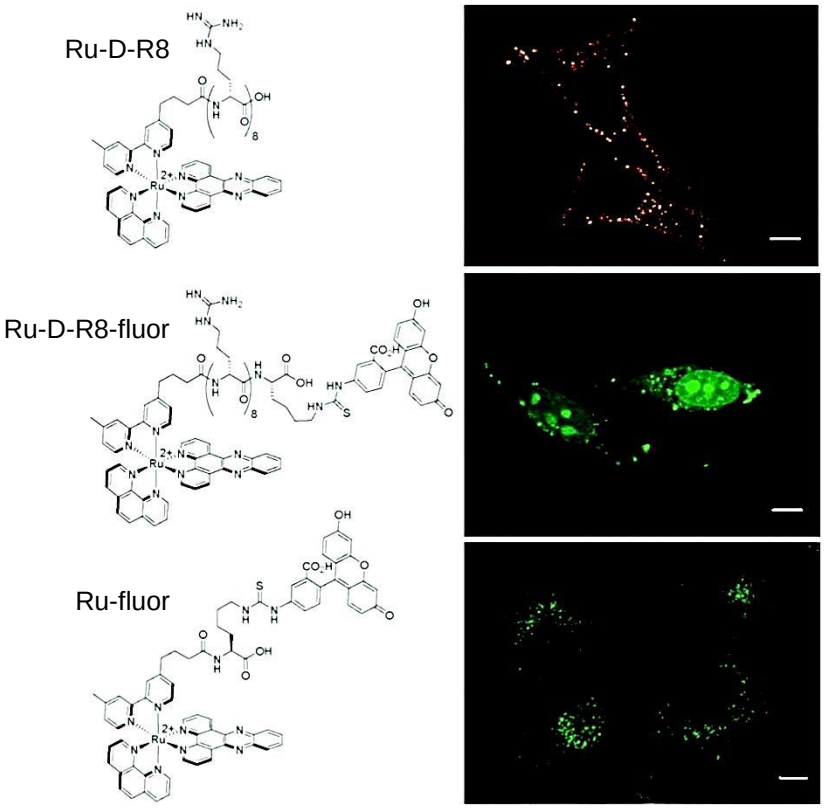

Figure 48: HeLa cells incubated with 5 μM Ru−D-R8 for 30 min (top), 5 μM Ru−D-R8−fluor for 30 min (middle), or 20 μM Ru−fluor for 41 h (bottom) at 37 °C in complete medium and then imaged by confocal microscopy. Structures of conjugates are shown on the left. Reprinted with permission from Puckett.[63] Copyright 2009 American Chemical Society.

HeLa cells incubated with Ru D-R8 showed punctate luminescence in the cytoplasm, with complete exclusion from the nucleus (Figure 48, top). When fluorescein was attached to the ruthenium complex in the presence of octaarginine, the nucleus was fluorescently labelled (Figure 48, middle). Finally, the ruthenium complex attached to fluorescein without octaarginine shows weak cytoplasmic staining. This ability of fluorescein to facilitate delivery to the nucleus was, according to Puckett, partly due to its high lipophilicity, increasing the interaction with cell membranes, promoting access to the cytosol and ultimately the nucleus.

4.1.4 Chapter aim

Recent studies have identified several proteins that contain more than one NLS, e.g. 5-lipoxygenase,[276] herpes simplex virus gene product ICP22,[277] HIV preintegration complex,[278] papillomavirus oncoprotein E6,[279] and BRCA2 tumour suppressor gene encoded protein.[280] Multiple NLSs could generate redundancy in proteins that require successful nuclear import, such as in cell cycle proteins or viral integration proteins.[276]

Based on this concept, the aim of this chapter was to synthesise dendron structures bearing three NLS sequences with either one or three fluorescein moieties (Figure 49) as well as the single NLS sequences fluorescently labelled as a comparison. *In vitro* assays would then be carried out to assess whether the structure could penetrate cellular and nuclear membranes.

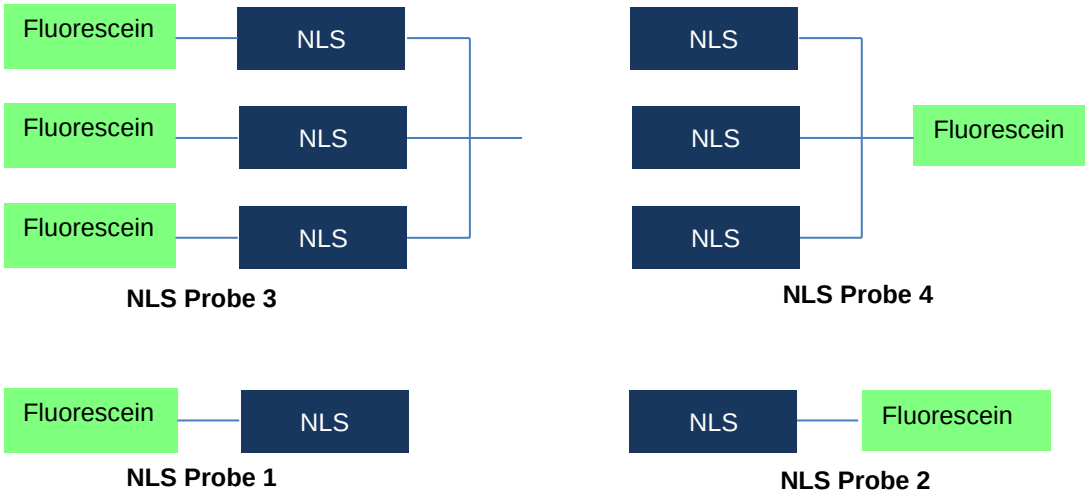

Figure 49: Generic structures of targeted probes.

4.2 Synthesis of dual labelled dendrons

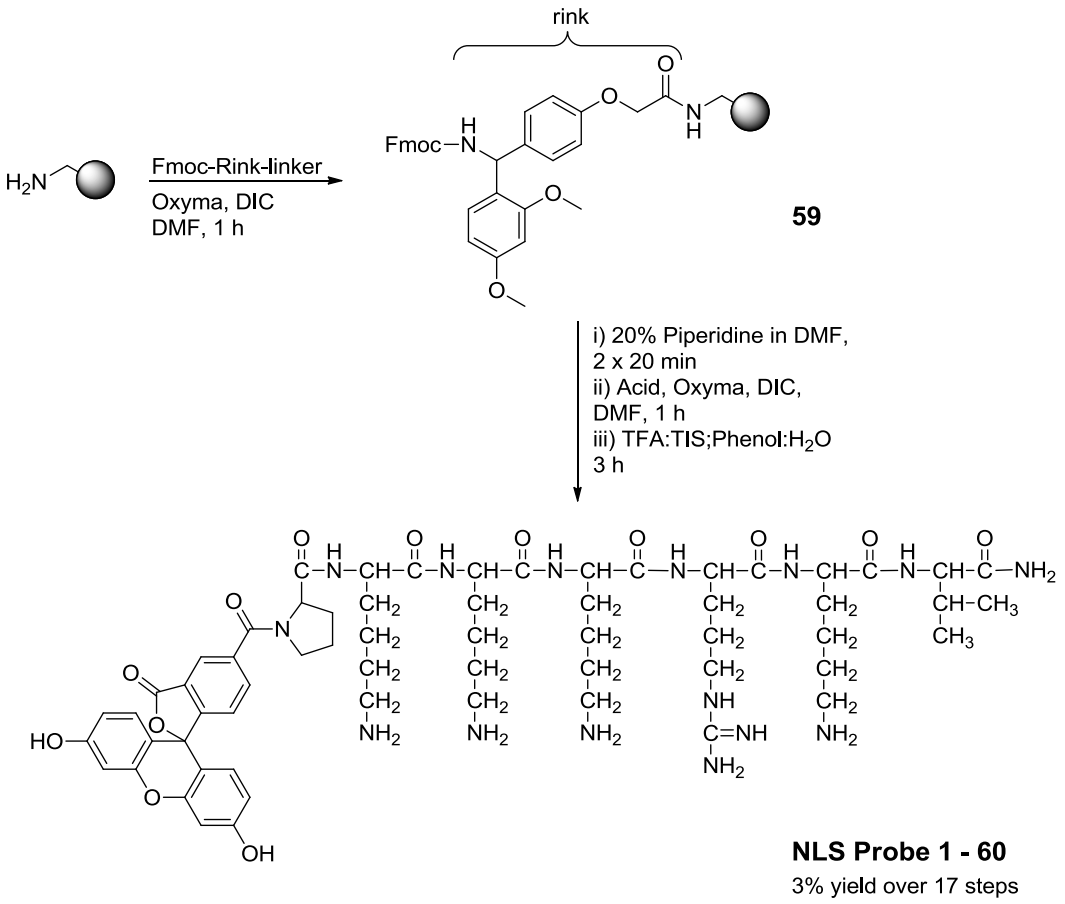

Scheme 27: Synthesis of NLS Probe 1-**60**.

The synthesis started with aminomethyl ChemMatrix resin, a PEG-based resin (loading value 1 mmol.g^{-1}, particle size 35-100 mesh). *N*-Fmoc-Rink linker acid was coupled onto the resin using Oxyma and DIC in DMF. The Fmoc group was removed using piperidine. The peptide was built using standard Fmoc chemistry; all Fmoc protected amino acids were coupled using Oxyma and DIC in DMF except Arginine which was coupled using HBTU and DIPEA. After each amino acid coupling, the Fmoc was removed using piperidine. 5-Carboxyfluorescein diacetate

N-succinimidyl ester was added in the presence of DIPEA, and the acetyl groups were removed using piperidine. All reactions were monitored using the qualitative Kaiser test.[150] The compound was cleaved from the resin using TFA and purified using semi-preparative HPLC (Scheme 27).

For the next target compound, the dye was attached to the *C*- terminus of the NLS peptide and for this purpose, synthesis started with 2-chlorotrityl linker on a ChemMatrix resin (Scheme 28).

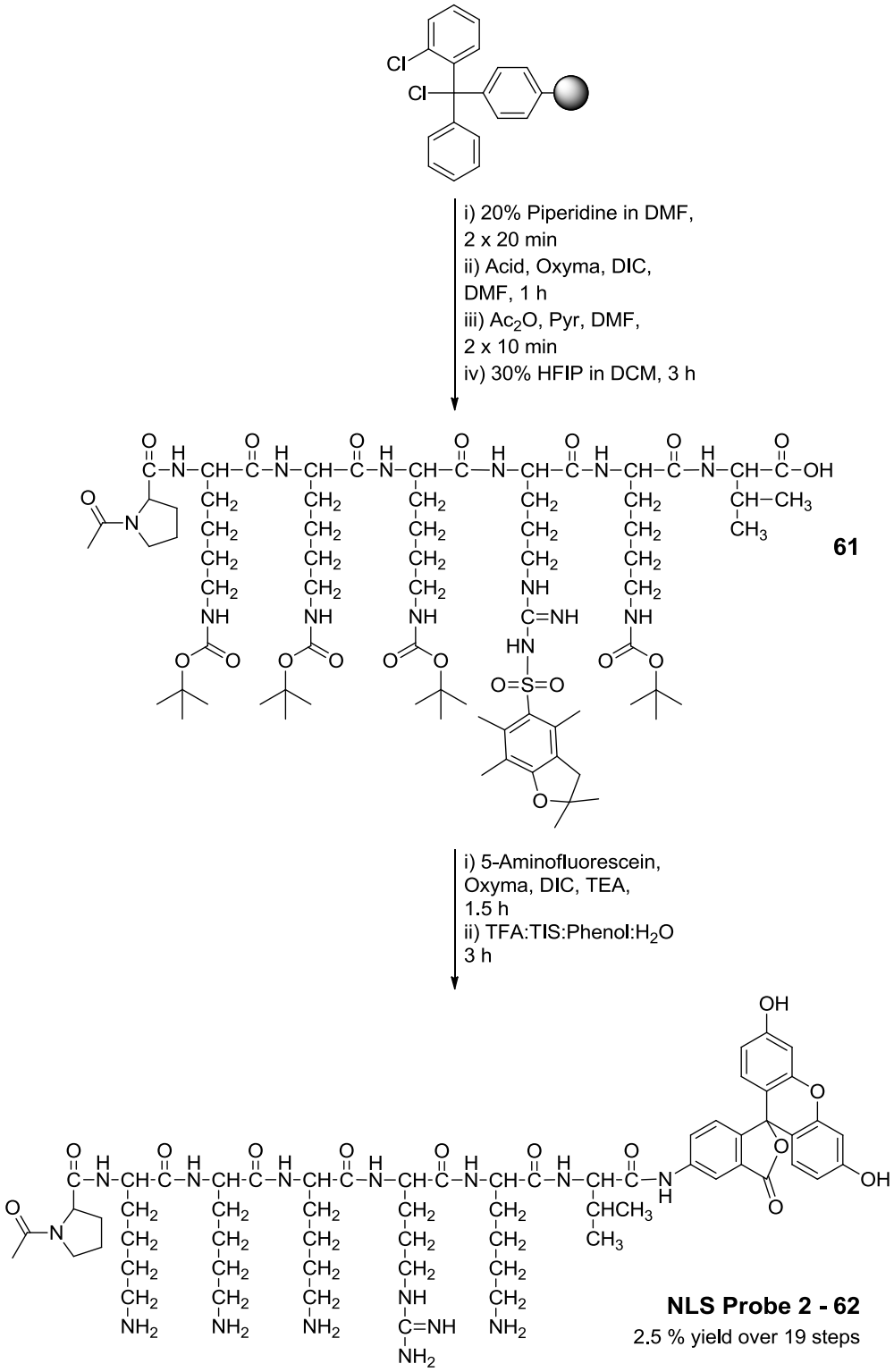

Scheme 28: Synthesis of NLS probe 2-**62**.

The 2-chlorotrityl ChemMatrix resin (loading value 0.65 mmol.g^{-1}, particle size 35-100 mesh) was pre-activated using thionyl chloride, and the peptide was built using standard Fmoc chemistry. After the final Fmoc removal the resulting amine moiety was acylated using acetic anhydride. The fully protected probe was cleaved from the resin using 30% HFIP in DCM. Volatile solvents were removed under reduced pressure in the presence of hexane to prevent concentration of HFIP. The acid moiety of the peptide was activated using Oxyma and DIC in DMF and coupled to 5-aminofluorescein in the presence TEA. All protecting groups were then removed using TFA and purified using semi-preparative HPLC.

The next targets were tri-branched probes. The first synthesised possessed three fluorescein moieties at the *N*- terminus of the peptide (Scheme 29).

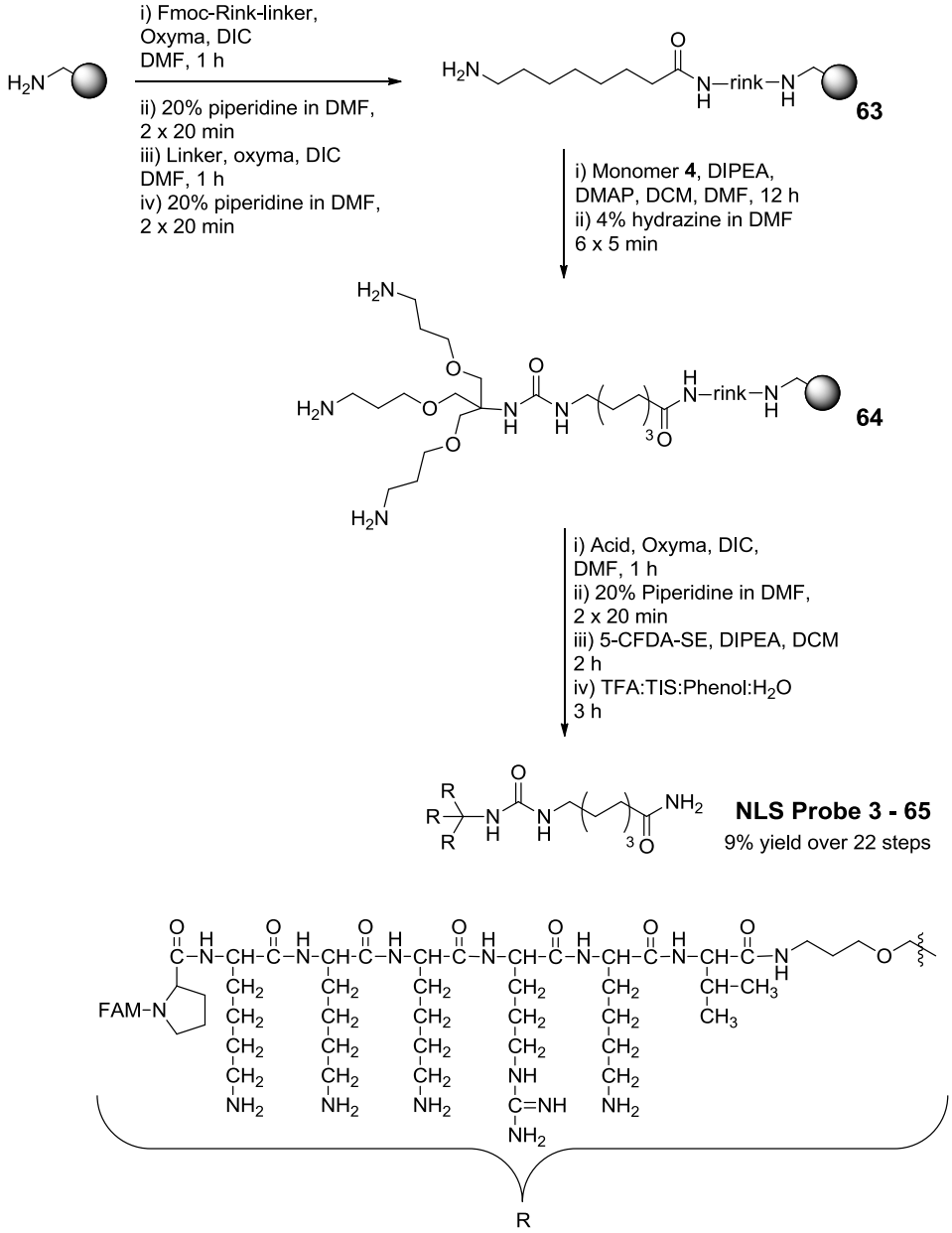

Scheme 29: Synthesis of NLS probe 3-**65**.

The synthesis started with aminomethyl ChemMatrix resin. *N*-Fmoc-Rink linker acid was coupled to the resin using Oxyma and DIC in DMF. Fmoc was removed using 20% piperidine in DMF. *N*-Fmoc-8-aminooctanoic acid was coupled to the resin using Oxyma and DIC in DMF. This additional spacer was chosen to allow fair

comparison with the **NLS probe 4-** (Scheme 30). The isocyanate dendron **4** was freshly synthesised as shown in chapter 2 and coupled using DMAP and DIPEA. Dde groups were removed using a solution of 4% hydrazine in DMF. The peptides were built using standard Fmoc chemistry. After final Fmoc removal, 5-carboxyfluorescein diacetate *N*-succinimidyl ester was added onto the resin in the presence of DIPEA. The desired compound was obtained using semi-preparative HPLC after TFA cleavage.

The next target compound was designed with only one fluorescein moiety at the dendron side of the molecule (Scheme 30).

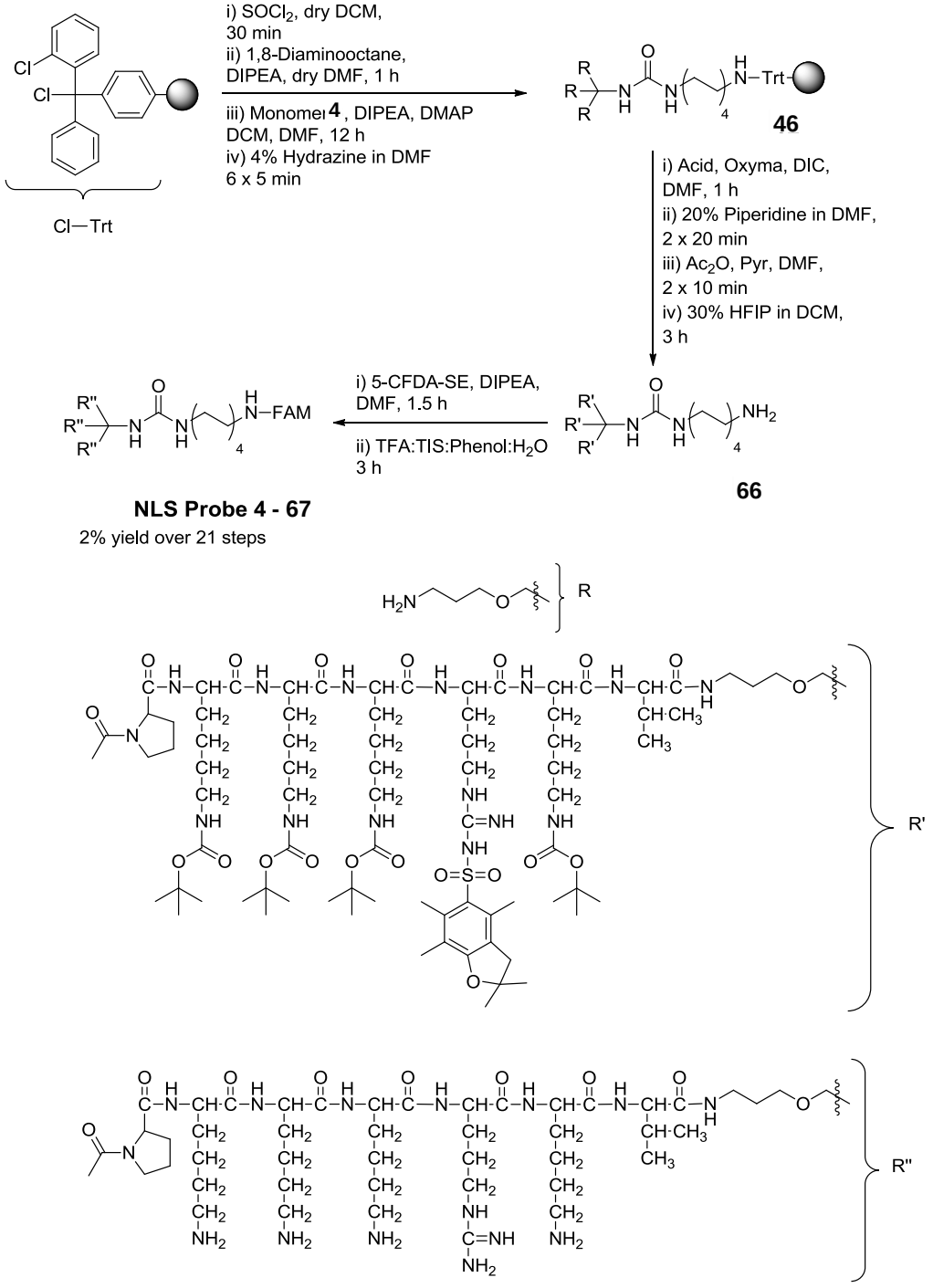

Scheme 30: Synthesis of NLS probe 4-**67**.

The synthesis started with the pre-activation of 2-chlorotrytil ChemMatrix resin using thionylchloride. Diaminooctane then was attached onto the resin in the presence of DIPEA. The use of this spacer will result in a primary amine after cleavage from the resin, a handle for the fluorescein attachment. The isocyanate dendron was freshly synthesised and coupled onto the resin using DMAP and DIPEA. Dde groups were removed using 4% hydrazine in DMF. The peptide was built using standard Fmoc chemistry. After the last Fmoc removal the resulting amine moiety was acylated using acetic anhydride. The fully protected tri-peptide compound was cleaved off the resin under mild conditions using HFIP. The resulting compound was coupled to 5-carboxyfluorescien diacetate *N*-succinimidyl ester in the presence of DIPEA. After TFA treatment and semi-preparative HPLC purification the NLS probe 4-**67** was obtained.

4.3 *In vitro* studies

To A549 cells fixed onto poly-D-lysine-coated multi-well chambers, a solution of 10 μM of the probe of interest in complete DMEM media was incubated at 37 °C for 1 h. For each probe, two separate experiments were carried out, with or without Syto 82 orange fluorescent nucleic acid stain (5 μM for 20 min). The media was then removed and replaced with fresh media, followed by imaging using confocal microscopy using excitation wavelengths of 488 nm (fluorescein) and 543 nm (Syto 82).

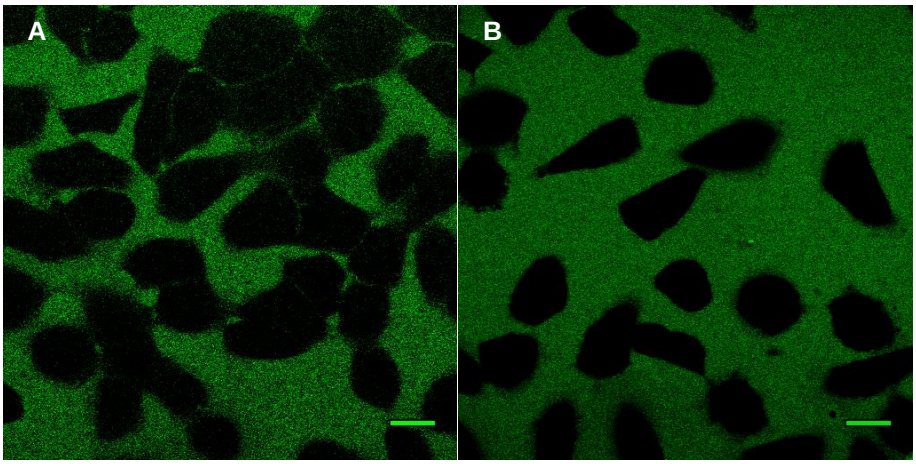

Figure 50 Confocal microscopy images: A549 fixed on poly-D-lysine-coated multi-well chamber, incubated with probe for 1.5 h. **A.** NLS probe 1-**60** (10 µM), B**.** NLS probe 2-**62** (10 µM), for 1 h. Fluorescein emission image (λ_{ex} = 488 nm, λ_{em} = 501 – 522 nm). Scale bars 20 µm. Images are representative of duplicates experiments carried out on different days.

In Figure 50 we see A549 cells incubated with fluorescein labelled single stranded NLSs. The fluorescence intensity is only observed outside the cells and therefore did not penetrate the cell membrane. NLS Probes 1-**60** and 2-**62** did not show any nuclear labelling, or cytoplasmic labelling. The NLS sequence combined with one fluorescein moiety did not penetrate the cell membrane of A549 cells, thus, the construct requires to be coupled to a cellular delivery structure to allow nuclear delivery.

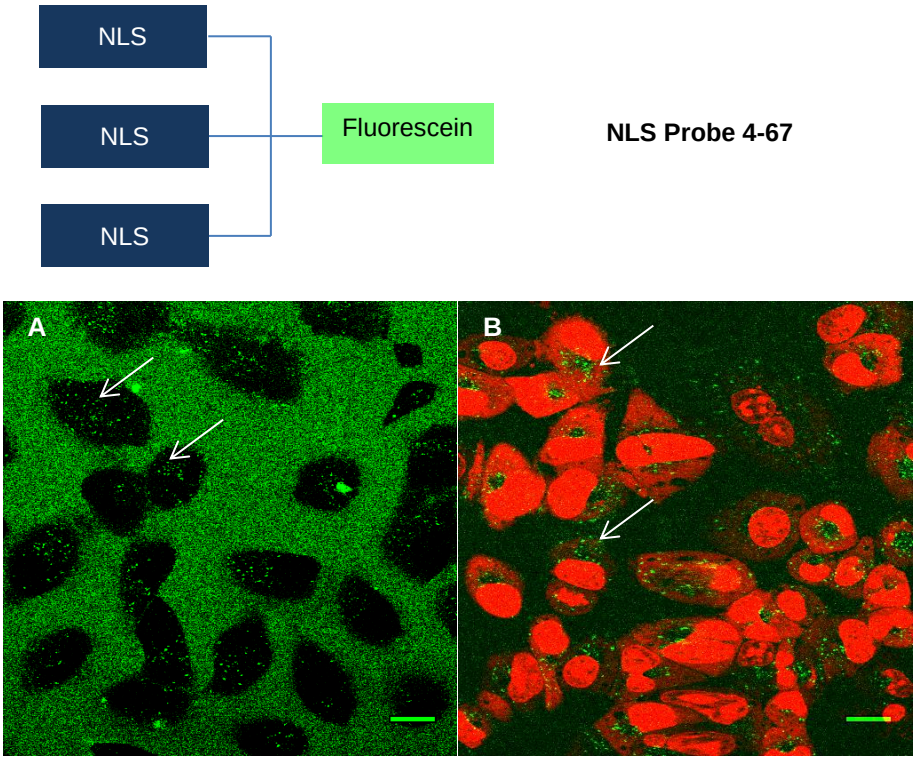

Figure 51 Confocal microscopy images: A549 fixed on poly-D-lysine-coated multi-well chamber, incubated with NLS probe 4-**67** (10 µM) (structure above images) for 1.5 h at 37 °C. **A.** Fluorescein emission image (λ_{ex} = 488 nm, λ_{em} = 512 – 565 nm), **B.** nuclei stained red with Syto 82, merge of fluorescein emission wavelength and stain emission wavelength (λ_{ex} = 543 nm, λ_{em} = 576 – 619 nm). Arrows highlight high fluorescence intensities. Scale bars 20 µm. Images are representative of duplicates experiments carried out on different days.

The fluorescein labelled tri branched NLS dendron **67**, incubated in A549 cells is shown in Figure 51. From figure A and B we can observe fluorescence within the cells. The fluorescence is punctually distributed throughout the cytoplasm which implies endocytosis and is consistent with previous work.[63, 281] In image 2, the nuclei are stained red and complete nuclear exclusion of the probe is clear. Entrapment in endosomes can explain the lack of nuclear entry.[63]

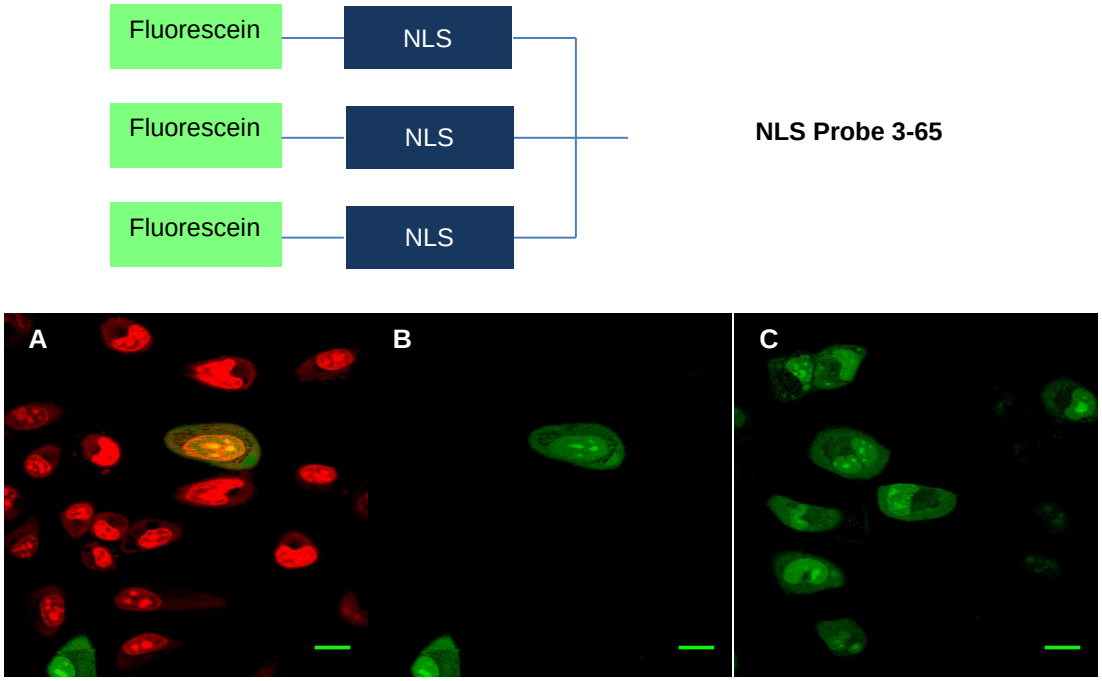

Figure 52 Confocal microscopy images: A549 fixed on poly-D-lysine-coated multi-well chamber, incubated with NLS probe 3-**65** (10 µM) (structure above images) for 1.5 h. **A.** Nuclei stained red with Syto 82, merge image of fluorescein emission image (λ_{ex} = 488 nm, λ_{em} = 512 – 565 nm) and stain emission image (λ_{ex} = 543 nm, λ_{em} = 576 – 619 nm), **B.** nuclei stained with Syto 82, fluorescein emission image, **C.** nuclei unstained, fluorescein emission image. Images are representative of duplicates experiments carried out on different days. Scale bars 20 µm.

Remarkably, the triple fluorescein labelled dendron NLS probe 3-**65** enters the nucleus under the same incubation conditions for which the NLS probe 4-**67** is excluded (Figure 51 and Figure 52). NLS probe 3-**65** shows diffuse cytoplasmic and nuclear fluorescence, strong nuclear staining, and some punctate cytoplasmic staining. To further confirm the presence of the probe within the nucleus further confocal microscopy experiments were carried out (Figure 53).

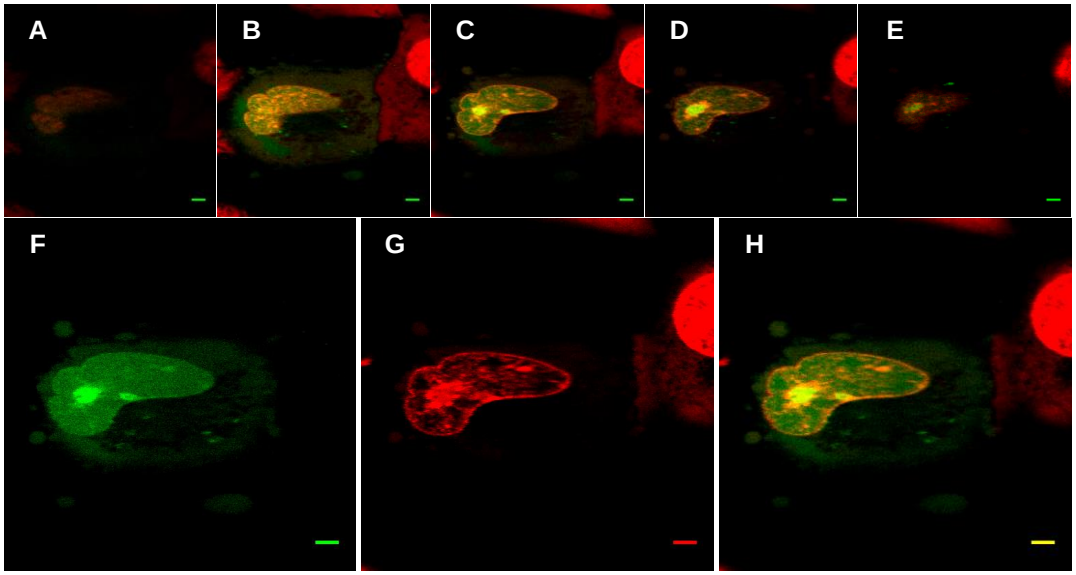

Figure 53: Confocal microscopy images: A549 fixed on poly-D-lysine-coated multi well chamber, incubated with NLS probe 3-**65** (10 µm) for 1.5 h. Nuclei stained red with Syto 82. **A-E.** Show the different planes of a neutrophil cell. **F, G and H.** Show slice 15/30, at different wavelengths. A**-E, H.** Merge of fluorescein emission images (λ_{ex} = 488 nm, λ_{em} = 512 – 565 nm), and stain emission images (λ_{ex} = 543 nm, λ_{em} = 576 – 619 nm), **F.** fluorescein emission image, **G.** stain emission images. Slice thickness: 0.37 µm. Scale bars: 5 µm. Images are representative of duplicates experiments carried out on different days.

Figure 53 displays a Z-staking experiment. The fluorescence within the nucleus in every plane confirms that the triple fluorescein labelled dendron NLS probe 3-**65** stains the nucleus. Bright fluorescent pocket observed within the nucleus suggesting fluorescent labelling of the nucleolus.

4.4 Conclusions

This chapter aimed to better understand the behaviour of dendron delivery vehicles in their ability to penetrate the nucleus. Successful synthesis of two fluorescein labelled NLS peptides **60** and **62** and two fluorescein labelled tri-branched NLS dendrons **65** and **67** were carried out, with findings associated to their endocytic and nuclear uptake discussed. A combination of cellular delivery structures with multiple NLS sequences is not sufficient for nuclear delivery, as it can remain entrapped in endosomes. The cellular delivery system must be carefully chosen to prevent the conjugate from being captured in endosomes, and ensure release into the cytoplasm. The increased number of fluorescein molecules on the probe has greatly improved the cellular delivery and allowed nuclear delivery, confirming that subtle structural differences have considerable consequences on internalisation mechanisms and cellular/nuclear localisation. Therefore, the development of this vector can be further investigated in varied cell lines or in conjugation to a cargo of interest.

Chapter 5:

Conclusion and Future Work

The aim of this thesis was to contribute to the field of fluorescent imaging by the development of imaging probes, as well as improving the synthesis and purity of well-known dyes such as fluorescein and rhodamine. Previously in the Bradley group self-quenched dendrons were developed. To broaden their applications and further understand their mode of action, the first aim of this thesis was to study the dendron core with respect to cell permeability and solubility and to then develop a synthesis for a "dual-colour" self-quenched dendron for the detection of human neutrophil elastase. The second aim of this thesis was to establish a single isomer synthesis of 5- and 6-carboxyfluoresceindiacetate *N*-succinimidyl ester (CFDA-SE) as well as 5- and 6-carboxytetraethylrhodamine *N*-succinimidyl ester, as the use of single isomer would allow the development of purer and more fluorescent probes. The final aim was to synthesise and investigate the nuclear labelling properties of the dendron structure when conjugated to nuclear localisation sequences (NLS).

In chapter 2, six non peptidic probes were synthesised for the investigation of the dendron core structure. After the synthesis was optimised, cell studies showed that the dendron core, labelled with fluorescein, diacetylated fluorescein or tetraethylrhodamine do not penetrate A549 cells or non-activated neutrophils. On neutrophil activation, the diacetylated fluorescein labelled dendron entered the cells.

A synthesis for a dual labelled dendron-based probe specific to neutrophil elastase was developed and its cleavage by the target enzyme was confirmed by enzyme kinetics studies. This peptidic probe was cleaved in the presence of activated neutrophils resulting in a fluorescence signal but was not cleaved in the presence of non-activated neutrophils, nor in the presence of activated neutrophils with elastase inhibitor, confirming probe specificity to elastase. This probe should be further investigated, carrying out *in vivo* experiments using an endoscopic fluorescence system for the detection of neutrophils in lungs. The concept should also be exploited using a different peptide sequence for the detection of other proteases such as cathepsin G or protease 3.

In chapter 3, 5-CFDA-SE-**53** and 6-CFDA-SE-**54** were successfully synthesised and separated in a simple two step procedure. A method for generating the single isomers 5-Rho-SE-**50** and 6-Rho-SE-**51** has also been established. The cellular labelling properties of the four isomers were compared using primary T cells and a Jurkat cell line. In both cell types the 5-CFDA-SE-**53** labelled cells showed better cellular labeling than 6-CFDA-SE-**54** labelled cells.

5-Rho-SE-**50** and 6-Rho-SE-**51** successfully labelled the cyplotasmic protein of T cells and Jurkat cells, and were passed onto daughter cells in a similar fashion to CFDA-SE. The studies suggest that 5-Rho-SE-**50** can be used for cell division if a higher wavelength is more convenient.

The development of this single isomer synthesis is obviously an advantage in terms of probe synthesis as its use would lead to purer reactions and simpler analyses. In

the future, fluorescein labelled probes should be developed using single isomers. For the use of the single isomer of CFDA-SE in proliferation assays, further studies should be carried out to completely confirm the superiority of 5-CFDA-SE-**53** over 6-CFDA-SE-**54**, such experiments should include the labelling of T cells grown *in vivo*, and proliferation assays on a library of cell types.

In chapter 4, successful synthesis of two fluorescein labelled NLS peptides and two fluorescein labelled tri-branched NLS dendrons were carried out. Studies on A549 cells showed that NLS sequences labelled with fluorescein did not enter the cell within 2 h. Tri-branched NLS dendrons labelled with one fluorescein moiety do enter the cell but remain entrapped in endosomes, however, tri-branched NLS dendrons labelled with three fluorescein moieties does enter the cell as well as the nucleus within 2 h. The dendron structures developed in chapter 2 offer two points of functionalisation, therefore, future experiments should functionalise this fluorescent nuclear penetrating dendron further, with the attachment of a cargo to investigate the nuclear delivery properties of this construct, in various cell types.

Chapter 6:

Experimental section

General information

Solvents and reagents were obtained from commercial suppliers and used as received. Reactions involving moisture sensitive reagents were performed under a positive pressure of dry nitrogen, and the glassware used was oven dried and cooled under dry nitrogen prior to the experiment. Reactions involving light sensitive compounds were kept under aluminium foil at all times.

Microwave assisted heating reactions were performed in sealed heavy-walled Pyrex tubes using a Biotage Initiatior Microwave. Microwave irradiation was conducted at 2.45 Hz for a fixed temperature and pressure followed by thin layer chromatography (TLC), and/or analytical reverse-phase high-performance liquid chromatography (RP-HPLC) and/or Electrospray ionization mass spectrometry (ESI-MS).

Removal of solvents was performed at reduced pressure, using a Büchi rotary evaporator.

TLC was carried out on aluminium sheets precoated with silica gel 60 F_{254} and were visualised at 254 nm and 344 nm and/or stained with ninhydrin (0.3% ninhydrin in *n*-butanol and 3% acetic acid).

Column chromatography was performed using glass columns and silica gel 60 (mesh 0.040-0.063).

Solid-phase synthesis was carried out in polypropylene syringes equipped with polyethylene frits (mesh) and Teflon stopcocks.

^{1}H and ^{13}C nuclear magnetic resonance spectra were recorded on automated Bruker instruments: ARX250 (250 and 63 MHz respectively), DPX360 (360 and 90 MHz respectively), AV400 (400 and 100 MHz respectively), AV500 (500 and 126 MHz respectively). Chemical shifts (δ_H and δ_C) are quoted in parts per million (ppm) relative to the residual solvent signal and all coupling constants (*J*) given in Hertz (Hz). Resonances were characterised as singlet (s), broad singlet (bs), doublet (d), doublet of doublet (dd), triplet (t), quartet (q), quintet (quint) or multiplet (m).

Analytical reverse-phase high-performance liquid chromatography (RP–HPLC) was conducted on an Agilent Technologies 1100 modular HPLC system coupled to a Polymer Lab 100 ES Evaprorative Scattering Detector (ELSD), with detection at 220, 254, 260, 282 and 495 nm. Column: Supelco Discovery® C18, 5 μm particle size, reverse-phase (5 cm × 4.6 mm) with a flow rate of 1 mL/min or Poroshell 120, SB-C18 4.6 × 50 mm. Solvents used were HPLC grade and supplemented with 0.1% formic acid.

Method 1: 5 min method starting from water/MeOH 95:5 gradient to 5:95 over 3 min, then 1 min isocratic, 1 min back to the original values.

Method 2: 5 min method starting from water/MeCN 95:5 gradient to 5:95 over 3 min, then 1 min isocratic, 1 min back to the original values.

Method 3: 15 min method starting from water/MeOH 95:5 gradient to 5:95 over 10 min, then 4 min isocratic, 1 min back to the original values.

Method 4: 15 min method starting from water/MeCN 95:5 gradient to 5:95 over 10 min, 4 min isocratic, 1 min back to the original values.

Method 5: 15 min method starting from water/MeCN 95:5 gradient to 5:95 over 10 min, 4 min isocratic, 1 min back to the original values.

Semi-preparative RP–HPLC was performed on an Agilent Technologies HP1100 Chemstation equipped with a Phenomenex Prodigy C18, 5 μm particle size, reverse-phase column (250 × 10 mm,) with a flow rate 2 mL/min and eluting following method 6 or 7.

Method 6: 50 min method starting from water/MeOH 95:5 gradient to 5:95 over 30 min, 10 min isocratic, then 1 min back to the original values.

Method 7: 50 min method starting from water/MeCN/FA 95:5 to 5:95 over 30 min, 10 min isocratic, 1 min back to the original values.

Electrospray ionization mass spectrometry (ESI–MS) analyses were acquired on a VG platform single quadrupole electrospray ionozation mass spectrometer.

High Resolution Mass Spectra (HRMS) were performed on a Finnigan MAT 900 XLP high resolution double-focussing mass spectrometer.

Matrix assisted laser desorption ionisation-time of flight (MALDI-TOF) mass spectrometry was carried out using an Applied Biosystems Voyager-DE™ STR and analysed with the Voyager Instrument Control Panel software. Sinapic acid was used as a matrix solution (10 mg/mL) in 50% MeCN in water with 0.1% TFA.

Fourier Transform Infrared Spectroscopy (FTIR) spectra were obtained using neat compounds on a Fourier transform IR Bruker Tensor 27 spectrophotometer with a golden gate accessory.

Melting points were determined using a Gallenkamp melting point apparatus.

Qualitative ninhydrin test:[150] 3 drops of reagent A and 1 drop of reagent B are added to a few beads of interest and allowed to sit at 110 °C for 3 min. Solution A (1.3 mg KCN in water (2 mL), phenol : EtOH (8 : 2: 50 mL), freshly distilled pyridine (100 mL)) and Solution B (2.5 g ninhydrin in EtOH (50 mL)).

Mono Dde protected diaminoctane **16** was synthesised and given by T. Jong.

General protocols

Solid phase:

Unless stated otherwise, all solid phase protocols were carried out on resin (100 mg) preswollen in DCM (3 mL) for 10 min. Peptide couplings, deprotections and capping reactions were stopped by collection of the resin by filtration and washing of the resin with DMF (3 × 10 mL), DCM (3 × 10 mL), and MeOH (3 × 10 mL).

All peptides were built using standard Fmoc strategy with attachment of the amino acid using Oxyma or HBTU followed by Fmoc deprotection.

Cleavage reactions were carried out using 2 mL of the cleavage solution and stopped by collection of the cleavage solution from the resin by filtration and removal of the volatiles under reduced pressure.

P1) Pre-activation of 2-chlorotrityl linker: to 2-chlorotrityl linker functionalised resin (300 mg), 1 mL of thionyl chloride in DCM (1:2) was added and

the reaction stirred for 30 min. The resin was then washed with dry DCM (2 × 5 mL).

P2) Diamine linker attachment to the 2-chlorotrityl linker:[157] The resin (100 mg) was preswollen in dry DCM (2 mL; 1 min), and a solution of diamine (10 eq, 5 M) with DIPEA (10 eq) in dry DMF was added and shaken for 1 h.

P3) Coupling of isocyanate 4 to amine functionalised resin: Isocyanate **4** (50 mg, 0.06 mmol), DIPEA (10 μL, 0.06 mmol) and 4-dimethylaminopyridine DMAP (2 mg, 0.02 mmol) were dissolved in DCM (2 mL) and DMF (2 mL) and added to the desired amine functionalised resin and the mixture shaken for 12 h.

P4) Hydrazine Dde Deprotection: The resin (100 mg) was stirred (6 × 5 min) with 4% hydrazine in DMF (v/v) (4 mL). Between each hydrazine treatment the resin was washed with DCM (5 mL).

P5) Oxyma coupling: Oxyma (3 eq) was added to a solution of Fmoc protected amino acid (3 eq) in DMF (0.1 M), and stirred for 10 min. DIC (4 eq) was then added and the mixture stirred for a further 3 min. The coupling solution was added to the corresponding resin (1 eq, 100 mg), and shaken for 1 h.

P6) HBTU coupling: *O*-Benzotriazole-*N*,*N*,*N*',*N*'-tetramethyl-uronium-hexafluoro-phosphate HBTU (5 eq) and DIPEA (10 eq) were added to the solution of Fmoc protected amino acid (5 eq) in DMF (0.1 M), and stirred for 3 min. The coupling solution was added to the corresponding resin (1 eq, 200 mg) and shaken for 1 h.

P7) Fmoc Deprotection: The resin (100 mg) was stirred (2 × 10 min) with 20% piperidine in DMF (v/v) (2 mL).

P8) Capping: The resin (100 mg) was treated with 2 mL of a solution of DMF, pyridine and Ac_2O (15:3:2) and stirred (2 × 10 min).

P9) Carboxyfluorescein diacetate *N*-succinimidyl ester solid phase coupling: To the resin (100 mg) was added a solution of carboxyfluorescein diacetate

N-succinimidyl ester (3 eq, 0.01 M), DIPEA (2 eq) in dry DCM. The reaction was shaken for 2 h. The resin was then washed with dry DCM (3 × 5 mL).

P10) TFA cleavage cocktail for organic compounds: The resin was treated with TFA/DCM/H_2O (95: 2.5: 2.5) and stirred for 3 h.

P11) TFE procedure for cleavage of protected molecules from a resin: The resin was treated with a solution of TFE/AcOH/DCM (1:1:3) and stirred for 1 h.

P12) HFIP procedure for cleavage of protected molecules from a resin: The resin was treated with 30% HFIP in DCM (v/v) and stirred for 3 h. Hexane (3 mL) added prior to the removal of volatiles.

P13) TFA cleavage cocktail for peptidic compounds: The resin was treated with 2 mL of TFA: Phenol: H_2O: Triisopropylsilane (88:5:5:2) for 3 h. Peptide precipitated by addition of cold diethyl ether.

Solution phase:

P14) Carboxyfluorescein diacetate *N*-succinimidyl ester solution phase coupling: The amine (1 eq) was dissolved in dry DMF/MeCN (9:1; 0.01 M) and DIPEA (2 eq) added. Carboxyfluorescein diacetate *N*-succinimidyl ester (or carboxytetraethylrhodamine *N*-succinimidyl ester) (1.2 eq) was dissolved in dry

DMF/MeCN (9:1; 0.02 M) and added to the solution of the amine. The reaction was stirred for 2 h.

P15) Acetyl group deprotection: The compound of interest (20 mg) was dissolved in 20% piperidine in DMF (v/v) (0.5 mL), and stirred for 30 min. DMF was removed under reduced pressure.

Chapter 2 compounds

3-[2-Amino-3-(2-cyano-ethoxy)-2-(2-cyano-ethoxymethyl)-propoxy]-propionitrile (6)[139]

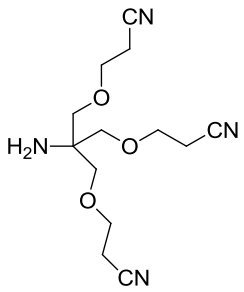

To a stirred solution of tris(hydroxymethyl)aminomethane (6.0 g, 49.6 mmol) in THF (100 mL), was added aqueous KOH (40%, 2 mL) followed by acrylonitrile (13 mL, 198.2 mmol) and distilled water (5 mL) and the resulting solution stirred for 24 h. After concentrating under reduced pressure, water (20 mL) was added, the aqueous layer was extracted with DCM (3 × 60 mL). Organic layers were combined and washed with brine (40 mL). After drying over Na_2SO_4 the solvents were evaporated under reduced pressure to yield amine **6** as a colourless oil (10.7 g, 77%).

HPLC: 0.82 min (method 1). Purity ≥ 99% by ELSD detection.

m/z (ES^+): $C_{13}H_{20}N_4O_3$ calculated 280.3, found 281.2 $[M+H]^+$ (100%).

^{1}H NMR (360 MHz, $CDCl_3$) δ_H 3.67 (t, *J* = 6.0 Hz, 6H, Alkyl-H), 3.43 (s, 6H, Alkyl-H), 2.62 (t, *J* = 6.0 Hz, 6H, Alkyl-H), 1.96 (s, 2H).

^{13}C NMR (90 MHz, $CDCl_3$) δ_C 117.7 (C), 71.9 (CH_2), 65.3 (CH_2), 55.7 (C), 18.4 (CH_2).

Data in agreement with the literature.[139]

[2-(2-Cyano-ethoxy)-1,1-*bis*-(2-cyano-ethoxymethyl)-ethyl]-carbamic acid *tert*-butyl ester (7)[282]

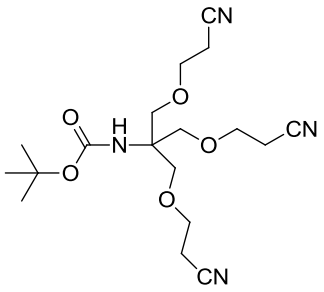

Amine **6** (4.5 g, 16.1 mmol) in THF (100 mL) was cooled to 0 ºC. A solution of Boc_2O (5.3 g, 24.1 mmol) and DIPEA (4.2 mL, 24.1 mmol) in THF (60 mL) was added. The solution was allowed to warm to room temperature and was stirred for 16 h before being concentrated under reduced pressure. EtOAc (100 mL) was added and the solution washed with aqueous $KHSO_4$ (1 M, 50 mL), saturated aqueous $NaHCO_3$ (2 × 80 mL) and brine (50 mL). Organic layers were dried over Na_2SO_4 and concentrated under reduced pressure to yield carbamate **7** as a colourless oil (6.0 g, 98%).

HPLC: 3.59 min (method 1). Purity ≥ 99% by ELSD detection.

m/z (ES^+): $C_{18}H_{28}N_4O_5Na_1^+$ calculated 403.4, found 403.0 $[M+Na]^+$ (100%).

^{1}H NMR (250 MHz, $CDCl_3$) δ_H 4.82 (s, 1H), 3.73 (s, 6H, Alkyl-H), 3.65 (t, *J* = 6.0 Hz, 6H, Alkyl-H), 2.58 (t, *J* = 6.0 Hz, 6H, Alkyl-H), 1.48 (s, 9H, Alkyl-H)

^{13}C NMR (62.5 MHz, $CDCl_3$) δ_C 155.7 (C), 117.7 (C), 79.1 (C), 68.9 (CH_2), 65.4 (CH_2), 58.1 (C), 27.9 (CH_3), 18.4 (CH_2).

Data in agreement with the literature.[282]

[2-(2-amino-ethoxy)-1,1-bis-(2-cyano-ethoxymethyl)-ethyl]-carbamic acid *tert*-butyl ester (25)

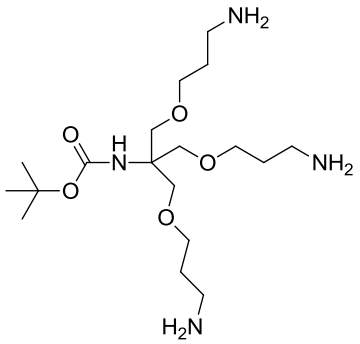

A solution of BH_3.THF (1 M, 47.5 mL, 48.15 mmol) was added slowly to a solution of *tris*-(nitrile)amine **7** (3.0 g, 8.03 mmol) in THF (20 mL) and the resulting solution was stirred at reflux for 5 h. After cooling, aqueous HCl (2 M) was added dropwise until pH 1-2 was reached. The solution was neutralised with aqueous NaOH (1 M) and solvents removed under reduced pressure. The crude product **25** was carried onto the next step without any further purification.[117]

[2-{3-[1-(4,4-Dimethyl-2,6-dioxo-cyclohexylidene)-ethylamino]-propoxy}-1,1-*bis*-{3-[1-(4,4-dimethyl-2,6-dioxo-cyclohexylidene)-ethylamino]-propoxymethyl}-ethyl] carbamic acid *tert*-butyl ester (8)[117, 282]

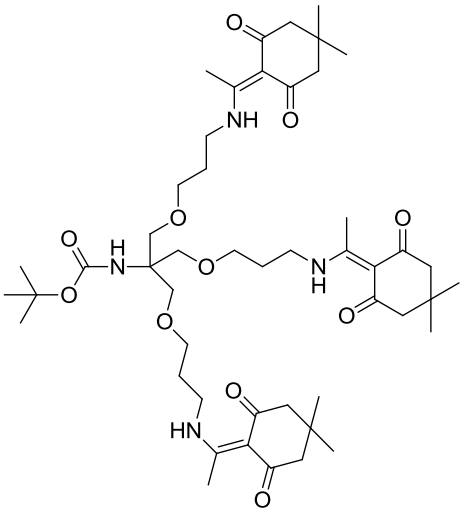

The crude product **25** was dissolved in MeOH (50 mL) and *N*,*N*-diisopropylethylamine (DIPEA) (1 mL, 5.74 mmol) was added. A solution of **DdeOH-10** (5.8 g, 32.1 mmol) in MeOH (10 mL) was added and the reaction mixture stirred for 16 h. The reaction mixture was poured into brine and extracted with DCM (2 × 250 mL). The combined organics were washed with water (2 × 200 mL), brine (200 mL), dried over Na_2SO_4 and concentrated under reduced pressure. Purification by column chromatography [eluting solvent: DCM:MeOH (1:0 to 19:1)] yielded

tris-enamine **8** as a brown oil (1.8 g, 22%).

HPLC: R_t 4.62 min (method 1). Purity ≥ 99% by ELSD detection.

m/z (ES^+): $C_{48}H_{76}N_4O_{11}$ calculated 884.6, found 885.2 $[M+H]^+$ (5%), 907.3 $[M+Na]^+$ (95%).

^{1}H NMR (360 MHz, $CDCl_3$) δ_H 3.60 (s, 6H, Alkyl-H), 3.47 (t, *J* = 6.0 Hz, 6H, Alkyl-H), 3.42 (t, *J* = 5.8 Hz, 6H, Alkyl-H), 2.50 (s, 9H, Alkyl-H), 2.29 (s, 12H, Alkyl-H), 1.86 (quint, *J* = 6.1 Hz, 6H, Alkyl-H), 1.34 (s, 9H), 0.96 (s, 18H, Alkyl-H).

^{13}C NMR (90 MHz, $CDCl_3$) δ_C 198.5 (C), 173.5 (C), 154.9 (C), 107.9 (C), 79.1 (C), 69.8 (CH_2), 68.3 (CH_2), 58.5 (C), 53.5 (CH_2), 40.6 (CH_2), 30.9 (C), 30.1 (CH_3), 29.3 (CH_2), 28.5 (CH_3), 17.8 (CH_3).

Data in agreement with the literature.[117, 282]

2-(1-Hydroxyethylidene)-5,5-dimethylcyclohexane-1,3-dione (DdeOH-10)[140]

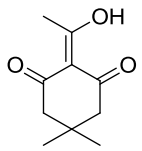

Dimedone **9** (10.0 g, 71 mmol), DMAP (11.64 g, 95 mmol) and 1-ethyl-3-(3-dimethylaminopropyl)carbodiimide hydrochloride EDCI.HCl (18.27 g, 95 mmol) were dissolved in DMF (160 mL). Acetic acid (5.45 mL, 95 mmol) was added and the resulting solution stirred for 16 h. The resulting yellow/orange solution was concentrated under reduced pressure. EtOAc (400 mL) was added and the organics washed with aqueous HCl (1 M, 150 mL), aqueous $KHSO_4$ (1 M, 150 mL), water (150 mL) and brine (150 mL). The organic layer was dried over Na_2SO_4 and concentrated under reduced pressure to give the crude as a yellow oil that solidified

on standing. Purification by column chromatography [eluting with hexane/EtOAc (6:4)] yielded **DdeOH-10** as a yellow solid (10.67 g, 65%).

HPLC: 4.28 min (method 1). Purity ≥ 99% by ELSD detection.

m/z (ES^+): $C_{10}H_{14}O_3$ calculated 182.2, found 183.1 $[M+H]^+$ (5%), 205.0 $[M+Na]^+$ (5%).

^{1}H NMR (400 MHz, $CDCl_3$) δ_H 2.56 (s, 3H, Alkyl-H), 2.48 (s, 2H, Alkyl-H), 2.31 (s, 2H, Alkyl-H), 1.03 (s, 6H, Alkyl-H).

^{13}C NMR (100 MHz, $CDCl_3$) δ_C 202.3 (C), 197.8 (C), 195.1 (C), 112.3 (C), 52.4 (CH_2), 46.8 (CH_2), 30.5 (CH_3), 28.4 (CH_3), 28.1 (CH_3).

m.p.: 36 – 37 ºC

Data in agreement with the literature.[140, 283]

[2-{3-[1-(4,4-Dimethyl-2,6-dioxo-cyclohexyliene)-ethylamino]-propoxy}-1,1-*bis*-{3-[1-(4,4-dimethyl-2,6-dioxo-cyclohexylidene)-ethylamino]-propoxymethyl}-ethyl]-amine (11)[282]

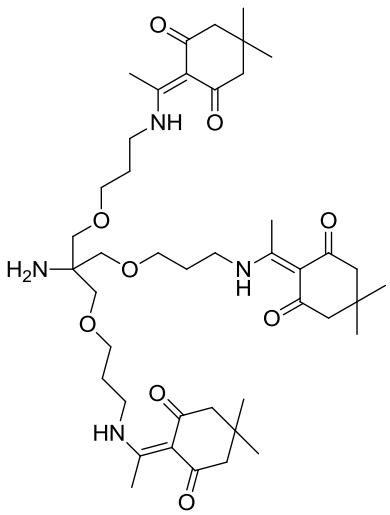

A solution of carbamate **8** (1.75 g, 1.98 mmol) in 20% TFA/DCM (30 mL) was stirred for 2 h. After concentration under reduced pressure, DCM (150 mL) was added and the solution neutralised with saturated aqueous sodium carbonate (250 mL). Extraction with DCM (3 × 150 mL) and the combined organic layers were washed with brine, dried over Na_2SO_4 and concentrated under reduced pressure to yield amine **11** as a colourless oil (1.32 g, 85%).

HPLC: 3.77 min (method 1). Purity ≥ 99% by ELSD detection.

m/z (ES^+): $C_{43}H_{68}N_4O_9$ calculated 784.5, foun, 785.2 $[M+H]^+$ (100%).

^{1}H NMR (250 MHz, $CDCl_3$) δ_H 3.50 – 3.44 (m, 12H, Alkyl-H), 3.32 (s, 6H, Alkyl-H) 2.53 (s, 9H, Alkyl-H), 2.32 (s, 12H, Alkyl-H), 1.93 – 1.86 (m, 6H, Alkyl-H), 0.99 (s, 18H, Alkyl-H).

^{13}C NMR (62.5 MHz, $CDCl_3$) δ_C 197.4 (C), 173.5 (C), 107.9 (C), 72.9 (CH_2), 68.6 (CH_2), 56.2 (C), 53.5 (CH_2), 40.8 (CH_2), 31.0 (C), 29.3 (CH_2), 28.3 (CH_3), 17.9 (CH_3).

Data in agreement with the literature.[282]

(4-Formyl-phenoxy)-acetic acid methyl ester (68)[284]

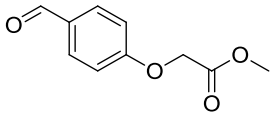

p-Hydroxybenzaldehyde (2 g, 16.4 mmol), K_2CO_3 (3.6 g, 18.0 mmol), KI (5 mg, 0.3 mmol) were stirred in CH_3CN (50 mL) for 15 min. Ethyl bromoacetate (3.01 g, 19.7 mmol) was added dropwise and the resultant mixture was refluxed for 16 h. After cooling, CH_3CN was removed under reduced pressure. EtOAc (30 mL) was added

and the organic layers washed with aqueous NaOH (1 M, 20 mL), water (20 mL) and brine (20 mL). The organic layer was dried over Na_2SO_4 and solvent evaporated under reduced pressure to yield aldehyde **68** as a pale yellow oil (2.5 g, 78%).

HPLC: 3.33 min (method 1). Purity ≥99% by ELSD detection.

m/z (ES^+): $C_{10}H_{10}O_4$ calculated 194.2, found 217.0 $[M+Na]^+$ (30%).

^{1}H NMR (400 MHz, $CDCl_3$) δ_H 9.65 (s, 1H), 7.61 (dd, *J* = 8.8, 2.0 Hz, Ar-H), 6.83 (dd, *J* = 8.8, 2.0 Hz, Ar-H), 4.53 (s, 2H, Alkyl-H), 3.57 (s, 3H, Alkyl-H)

^{13}C NMR (100 MHz, $CDCl_3$) δ_C 190.1 (CH), 167.9 (C), 161.9 (C), 131.2 (C), 130.0 (CH), 114.2 (CH), 64.3 (CH_2), 51.5(CH_3).

Data in agreement with the literature.[284]

(4-Hydroxymethyl-phenoxy)-acetic acid methyl ester (14)[285]

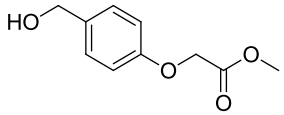

To a solution of aldehyde **68** (1.8 g, 9.2 mmol) in MeOH (55 mL), sodium borohydride (352 mg, 9.2 mmol) was added at 0 °C. The reaction was stirred for 2 h before concentrating under reduced pressure. EtOAc (20 mL) was added and organic layer washed with aqueous HCl (1 M, 20 mL), aqueous $KHSO_4$ (1 M, 20 mL), water (20 mL), and brine (20 mL), dried over $MgSO_4$ and concentrated under reduced pressure. Purification by column chromatography [eluting with hexane-EtOAc (1:0 to 6:4)] yielded alcohol **14** (0.9 g, 50%) as a white solid.

HPLC: 3.09 min (method 1). Purity ≥ 99% by ELSD detection.

m/z (ES^+): $C_{10}H_{12}O_4$ calculated 196.2, found 219.1 $[M+Na]^+$ (100%).

^{1}H NMR (400 MHz, $CDCl_3$) δ_H 7.29 (dt, 2H, *J* = 8.8, 2.0 Hz, 2H, Ar-H), 6.90 (dt, 2H, *J* = 8.8, 2.0 Hz, 2H, Ar-H), 4.64 (s, 2H, Alkyl-H), 4.61 (s, 2H, Alkyl-H), 3.81 (s, 3H, Alkyl-H).

^{13}C NMR (100 MHz, $CDCl_3$) δ_C 169.3 (C), 157.2 (C), 134.3 (C), 128.5 (CH), 114.6 (CH), 65.3 (CH_2), 64.6 (CH_2), 52.2 (CH_3).

Mp: 44 – 45 ºC

Data in agreement with the literature.[285]

[4-(4-Nitro-phenoxycarbonyloxymethyl)-phenoxy]-acetic acid methyl ester (15)

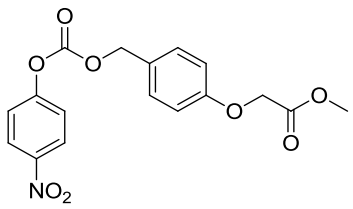

Benzylic alcohol **14** (1.20 g, 6.12 mmol) was dissolved in dry DCM (18 mL), dry pyridine was added (985 µL, 12.23 mmol) and the reaction cooled to 0 ºC. After 10 min stirring a solution of 4-nitrophenyl chloroformate (2.47 g, 12.23 mmol) in dry DCM (7 mL) was added dropwise and the reaction stirred for 2 h at 0 ºC. The resulting cloudy solution was filtered and the filtrate dried over Na_2SO_4. Purification by column chromatography [eluting solvent: Hexane:EtOAc (8:2)] yielded the nitro compound **15** as a white solid (1.48 g, 67%).

HPLC: 4.21 min (method 2). Purity ≥ 99% by ELSD detection.

m/z (ES^+): $C_{17}H_{15}NO_8$ calculated 361.3, found 384.0 $[M+Na]^+$ (100%).

m/z (HRMS, ES^+): $C_{17}H_{15}NO_8Na_1$ calculated $[M+Na]^+$ 384.06899, found 384.06860.

^{1}H NMR (400 MHz, $CDCl_3$) δ_H 8.24 (dt, *J* = 9.2, 2.7 Hz, 2H, Ar-H), 7.39 – 7.32 (m, 4H, Ar-H), 6.91 (dt, *J* = 8.7, 2.5 Hz, 2H, Ar-H), 5.21 (s, 2H, Alkyl-H), 4.64 (s, 2H, Alkyl-H), 3.79 (s, 3H, Alkyl-H).

^{13}C NMR (100 MHz, $CDCl_3$) δ_C 169.3 (C), 158.6 (C), 155.7 (C), 152.6 (C), 145.6 (C), 130.9 (CH), 127.7 (C), 125.5 (CH), 122.0 (CH), 115.0 (CH), 70.9 (CH_2), 65.4 (CH_2), 52.5 (CH_3).

Mp: 77 – 78 ºC.

IR (neat):, 1756 (s, $\nu_{C=O}$), 1529 (s, ν_{NO2}), 1348 (m, ν_{NO2}) cm^{-1}.

{4-{3-[1-(4,4-Dimethyl-2,6-dioxo-cyclohexylidene)-ethylamino]-hexyl-carbamoyloxy)-methyl}-phenoxy-acetic acid methyl ester (17)

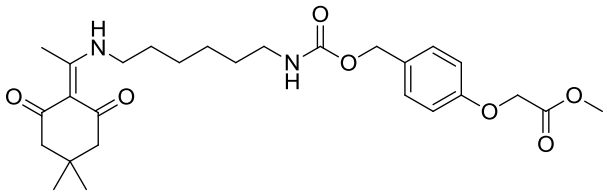

Carbonate **15** (755 mg, 2.09 mmol) was dissolved in dry DCM (20 mL), dry pyridine (1.4 mL, 20.91 mmol) and DMAP (2 mg, catalytic amount) were added and the solution cooled to 0 ºC. A solution of mono Dde protected diaminoctane **16** (687 mg, 1.74 mmol) in dry DCM (145 mL) was added slowly. The reaction was warmed to room temperature and stirred for 5 h. The reaction was monitored by TLC using ninhydrin staining. The reaction mixture was washed with water (20 mL), 1 M $KHSO_4$ (2 × 20 mL), and brine (20 mL). Purification by column chromatography

[eluting solvent: Hexane:EtOAc (7:3 to 3:7)] yielded **17** as a colourless oil (473 mg, 40%).

HPLC: 4.17 min (method 1). Purity ≥ 99% by ELSD detection.

m/z (ES^+): $C_{27}H_{38}N_2O_7$ calculated 502.6, found 503.3 $[M+H]^+$ (85%), 525.3 $[M+Na]^+$ (100%).

m/z (HRMS, ES^+): $C_{27}H_{38}N_2O_7Na_1$ calculated $[M+Na]^+$ 525.25712, found 525.25810.

^{1}H NMR (400 MHz, $CDCl_3$) δ_H 13.39 (s, 1H), 7.26 (d, *J* = 8.6 Hz, 2H, Ar-H), 6.84 (dt, *J* = 8.7, 2.4 Hz, 2H, Ar-H), 4.98 (s, 2H, Alkyl-H), 4.83 (bs, 1H), 4.59 (s, 2H, Alkyl-H), 3.76 (s, 3H, Alkyl-H), 3.36 (dt, *J* = 6.6, 5.6 Hz, 2H, Alkyl-H), 3.14 (dt, *J* = 6.6, 6.4 Hz, 2H, Alkyl-H), 2.51 (s, 3H, Alkyl-H), 2.32 (s, 4H, Alkyl-H, 1.67 – 1.60 (m, 2H, Alkyl-H), 1.52 – 1.45 (m, 2H, Alkyl-H), 1.42 – 1.30 (m, 4H, Alkyl-H), 0.99 (s, 6H, Alkyl-H).

^{13}C NMR (100 MHz, $CDCl_3$) δ_C 198.1 (C), 173.6 (C), 169.4 (C), 157.8 (C), 156.6 (C), 130.2 (CH), 114.8 (CH), 108.0 (C), 66.3 (CH_2), 65.5 (CH_2), 53.0 (CH_2), 52.4 (CH_3), 43.5 (CH_2), 41.0 (CH_2), 30.3 (C), 29.9 (CH_2), 29.0 (CH_2), 28.4 (CH_3), 26.6 (CH_2), 26.4 (CH_2), 18.1 (CH_3).

IR (neat):, 1714 (m, $\nu_{C=O}$), 1633 (m, $\nu_{C=C}$), 1569 (s, ν_{N-H}) cm^{-1}.

{4-{3-[1-(4,4-Dimethyl-2,6-dioxo-cyclohexylidene)-ethylamino]-hexyl-carbamoyloxy)-methyl}-phenoxy-acetic acid (12)

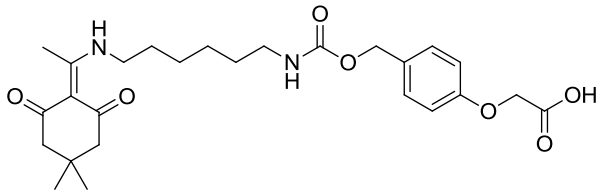

To a solution of ester **17** (355 mg, 0.71 mmol, 0.1 M) in MeOH (3.5 mL) was added dropwise a 2 M Cs_2CO_3 aqueous solution (3.5 mL) and the reaction stirred for 2 h. MeOH was removed under reduced pressure and the residue was dissolved in water (15 mL). 1 M $KHSO_4$ was added (pH 5-6) and the solution washed with EtOAc (15 mL). The aqueous solution was extracted three times with DCM (3 × 10 mL). Organic layers were combined, dried over Na_2SO_4 and concentrated under reduced pressure to give the desired compound **12** as a yellow solid (345 mg, 99%).

HPLC: 4.15 min (method 1). Purity ≥ 99% by ELSD detection.

m/z (ES^+): $C_{26}H_{36}N_2O_7$ calculated 488.57, found 489.3 $[M+H]^+$ (35%), 511.3 $[M+Na]^+$ (10%).

m/z (HRMS, ES^+): $C_{26}H_{36}N_2O_7Na_1$ calculated $[M+Na]^+$ 511.24147, found 511.24040.

^{1}H NMR (400 MHz, $CDCl_3$) δ_H 13.29 (bs, 1H), 7.26 (d, *J* = 8.5 Hz, 2H, Ar-H), 6.86 (d, *J* = 8.6 Hz, 2H, Ar-H), 4.99 (s, 2H, Alkyl-H), 4.88 (bs, 1H), 4.61 (s, 2H, Alkyl-H), 3.40 – 3.27 (m, 2H, Alkyl-H), 3.20 – 3.08 (m, 2H, Alkyl-H), 2.51 (s, 3H, Alkyl-H), 2.35 (s, 4H, Alkyl-H), 1.68 – 1.57 (m, 2H, Alkyl-H), 1.50 – 1.43 (m, 2H, Alkyl-H), 1.39 – 1.25 (m, 4H, Alkyl-H), 1.00 (s, 6H, Alkyl-H).

^{13}C NMR (100 MHz, $CDCl_3$) δ_C 198.5 (C), 174.2 (C), 171.3 (C), 157.9 (C), 156.8 (C), 130.2 (CH), 114.8 (CH), 108.0 (C), 66.4 (CH_2), 65.3 (CH_2), 52.6 (CH_2), 43.7 (CH_2), 40.9 (CH_2), 30.4 (C), 29.9 (CH_2) 29.0 (CH_2), 28.4 (CH_3), 26.6 (CH_2), 26.3 (CH_2), 18.4 (CH_3).

IR (neat): 1684 (m, $\nu_{C=O}$), 1573 (m, ν_{N-H}), 1429 (m, ν_{O-H}), 1243 (m, ν_{C-OH}) cm^{-1}.

Mp: 80 – 82 ºC.

Attachment of the Linker to the aminomethyl TentaGel resin and Dde deprotection (69)

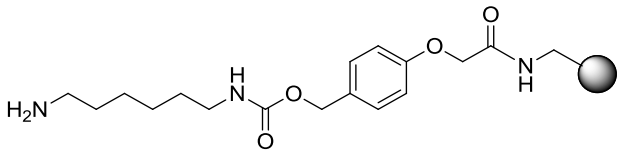

Linker **12** was attached to aminomethyl TentaGel resin (loading value: 0.45 $mmol.g^{-1}$, particle size: 150-200 µm) using the Oxyma coupling protocols P5 followed by Dde group removal according to protocol P4.

[2-{3-[1-(4,4-Dimethyl-2,6-dioxo-cyclohexylidene)-ethylamino]-propoxy}-1,1-*bis*-{3-[1-(4,4-dimethyl-2,6-dioxo-cyclohexylidene)-ethylamino]-propoxymethyl}-ethyl]-isocyanate (4)[117]

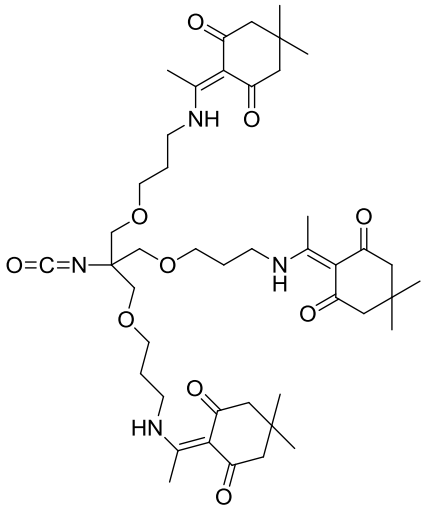

A solution of Boc_2O (19.5 mg, 0.09 mmol) in anhydrous DCM (1 mL) was added dropwise to a solution of monomer **11** (50 mg, 0.06 mmol) and DMAP (8.6 mg, 0.01 mmol) in anhydrous DCM (1 mL). The resulting solution was stirred for 1 h, the solvent was removed under reduced pressure and used immediately.

IR (neat): 2245 (m, $\nu_{N=C=O}$) , 1638 (m, $\nu_{C=C}$), 1571(s, ν_{N-H}) cm^{-1}.

m/z (ES^+): $C_{44}H_{66}N_4O_{10}$ calculated 811.0, found 811.3 $[M]^+$ (40%), 812.2 $[M+H]^+$ (20%), 834.4 $[M+Na]^+$ (5%).

Data in agreement with the literature.[117]

1-(6-aminohexyl)-3-(1,3-bis(3-((3',6'-dihydroxy-3-oxo-3*H*-spiro[isobenzofuran-1,9'-xanthen]-5-yl)amino)propoxy)-2-((3-((3',6'-dihydroxy-3-oxo-3*H*-spiro[isobenzofuran-1,9'-xanthen]-5-yl)amino)propoxy)methyl)propan-2-yl)urea (20)

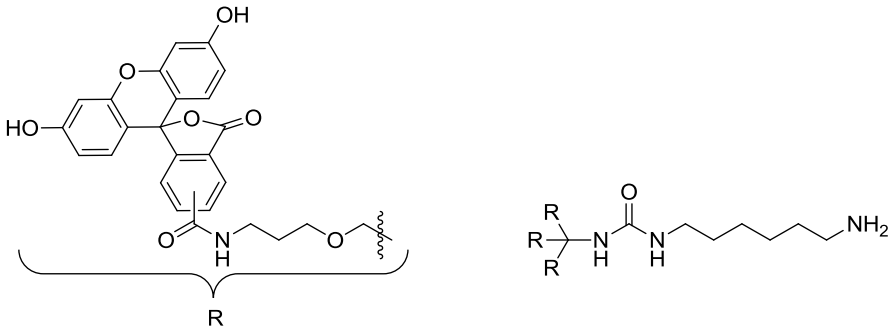

The isocyanate **4** was attached to resin **69** (50 mg, 0.3 mmol.g^{-1}) and Dde groups removed following protocol P4. 5(6)-Carboxyfluorescein was attached using Oxyma protocol P5. Compound **20** was cleaved from the linker using TFA protocol P10 (22 mg, 16%).

m/z (ES$^+$): $C_{83}H_{76}N_6O_{22}$ calculated 1509.5, found 1509.3 $[M+H]^+$ (10%).

HPLC: 3.72 min (method 1). Purity ≥ 99% by ELSD detection.

N,N'-(((2-((3-acetamidopropoxy)methyl)-2-(3-(2-aminoethyl)ureido)propane-1,3-diyl)bis(oxy))bis(propane-3,1-diyl))diacetamide (31)

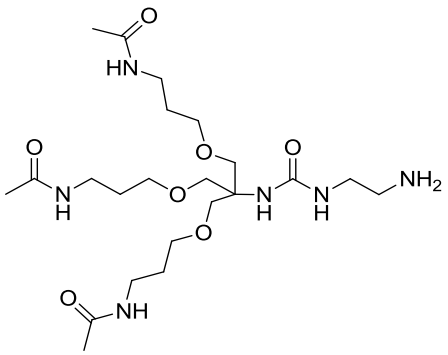

1,2-Diaminoethane was attached to the activated 2-chlorotrityl linker polystyrene resin (30 mg, 1.4 mmol.g^{-1}, particle size 100-200 mesh) (protocols P1 and P2). The isocyanate **4** was then attached and the Dde groups removed (protocols P3 and P4). The resulting amine moiety was acylated and the compound was cleaved from the linker using TFA (protocols P8 and P10) (21 mg, 64%).

HPLC: 0.88 min using method 1. Purity ≥ 99% by ELSD detection.

m/z (ES$^+$): $C_{22}H_{44}N_6O_7$ calculated 504.6, found 505.4 $[M+H]^+$ (100%), 527.3 $[M+Na]^+$ (30%).

^{1}H NMR (500 MHz, CD_3OD) δ_H 3.66 (s, 6H, Alkyl-H), 3.47 (t, *J* = 6.0 Hz, 6H, Alkyl-H), 3.34 – 3.32 (m, 2H, Alkyl-H), 3.26 (dd, *J* = 8.3, 5.6 Hz, 6H, Alkyl-H), 3.02 – 2.98 (m, 2H, Alkyl-H), 1.94 (s, 9H, Alkyl-H), 1.74 (quint, *J* = 6.5, 6H, Alkyl-H).

N,N'-(((2-((3-acetamidopropoxy)methyl)-2-(3-(8-aminooctyl)ureido)propane-1,3-diyl)bis(oxy))bis(propane-3,1-diyl))diacetamide (32)

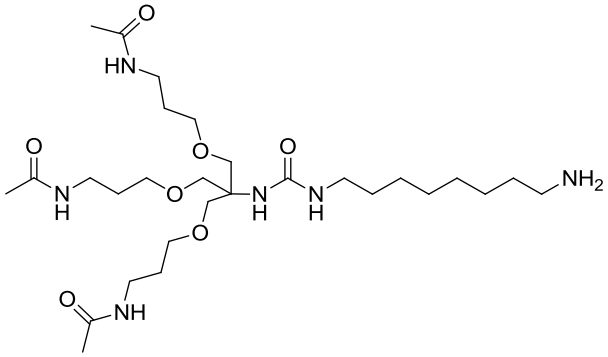

1,8-Diaminooctane was attached to the activated 2-chlorotrityl linker polystyrene resin (30 mg, 1.4 mmol.g^{-1}) (protocols P1 and P2). The isocyanate **4** was then attached and the Dde groups removed (protocols P3 and P4). The resulting amine moiety was acylated and the compound was cleaved from the linker using TFA (protocols P8 and P10) (25 mg, 67%).

HPLC: 0.90 min using method 1. Purity ≥ 99% by ELSD detection.

m/z (ES$^+$): $C_{28}H_{56}N_6O_7$ calculated 588.4, found 589.5 $[M+H]^+$ (100%).

^{1}H NMR (500 MHz, CD_3OD) δ_H 3.65 (s, 6H, Alkyl-H), 3.47 (t, *J* = 6.0 Hz, 6H, Alkyl-H), 3.26 (t, *J* = 6.8 Hz, 6H, Alkyl-H), 3.06 (t, *J* = 6.9 Hz, 2H, Alkyl-H), 2.91 (t, *J* = 7.6 Hz, 2H, Alkyl-H), 1.94 (s, 9H, Alkyl-H), 1.73 (quint, *J* = 6.4 Hz, 6H, Alkyl-H), 1.66 – 1.62 (m, 2H, Alkyl-H), 1.47 – 1.43 (m, 2H, Alkyl-H), 1.40 – 1.34 (m, 8H, Alkyl-H).

Compound 33

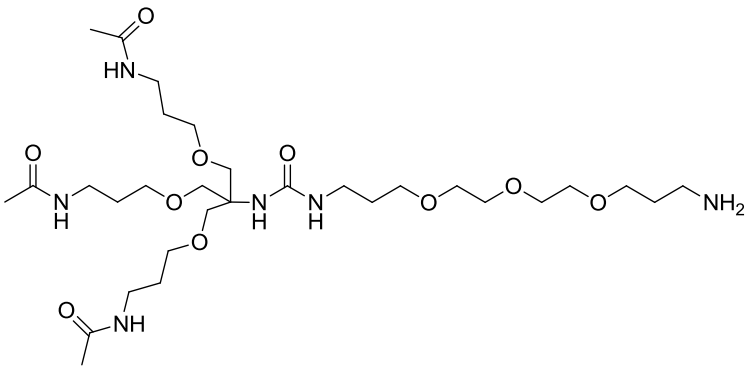

4,7,10-trioxa-1,13-tridecanyldiamine was attached to the activated 2-chlorotrityl linker polystyrene resin (30 mg, 1.4 mmol.g^{-1}) (protocols P1 and P2). The isocyanate **4** was then attached and the Dde groups removed (protocols P3 and P4). The resulting amine moiety was acylated and the compound was cleaved from the linker using TFA (protocols P8 and P10) (28 mg, 68%).

HPLC: 0.86 min using method 1. Purity ≥ 99% by ELSD detection.

m/z (ES$^+$): $C_{30}H_{60}N_6O_{10}$ calculated 664.4, found 665.5 $[M+H]^+$ (80%).

^{1}H NMR (500 MHz, CD_3OD) δ_H 3.69 – 3.62 (m, 18H, Alkyl-H), 3.60 – 3.58 (m, 2H, Alkyl-H), 3.51 (t, *J* = 6.1 Hz, 2H, Alkyl-H), 3.47 (t, *J* = 6.0 Hz, 6H, Alkyl-H), 3.25 (t, *J* = 6.9 Hz, 6H, Alkyl-H), 3.16 – 3.09 (m, 4H, Alkyl-H), 1.94 (s, 9H, Alkyl-H), 1.76 – 1.69 (m, 8H, Alkyl-H).

Compound 35

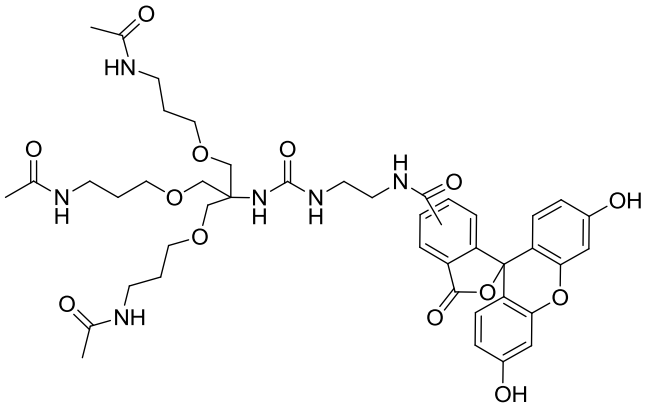

Compound **31** (15 mg, 0.030 mmol) was dissolved in DMF (500 µL) and coupled to 5(6)-carboxyfluorescein using protocol P5. Crude was purified *via* semi-preparative HPLC (method 7) (1.6 mg, 6.3%).

HPLC: 4.78 min (method 4). Purity ≥ 99% by ELSD detection.

MALDI-TOF: $C_{43}H_{55}N_6O_{13}$ calculated $[M+H]^+$ 863.3822; found = 863.4364.

Compound 28

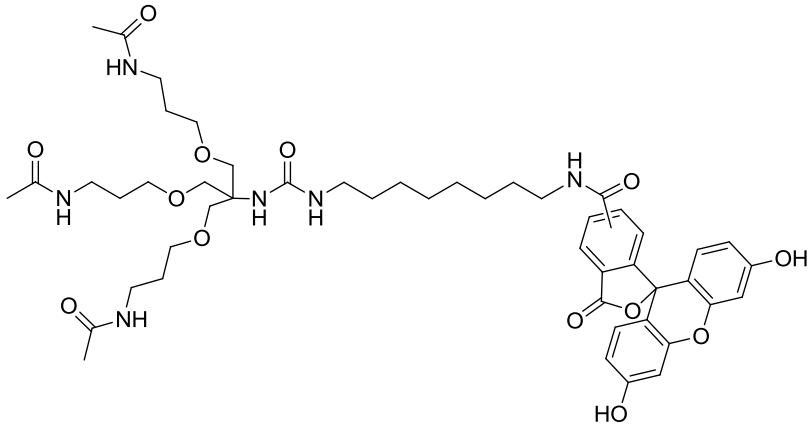

Compound **32** (15 mg, 0.025 mmol) was dissolved in DMF (500 µL) and coupled to 5(6)-carboxyfluorescein using protocol P5. Crude was purified *via* semi-preparative HPLC (method 7) (1.1 mg, 4.5%).

HPLC: 4.09 min (method 5). Purity ≥ 99% by ELSD detection.

MALDI-TOF: $C_{49}H_{67}N_6O_{13}$ calculated $[M+H]^+$ 947.4761; found = 947.6069.

Compound 36

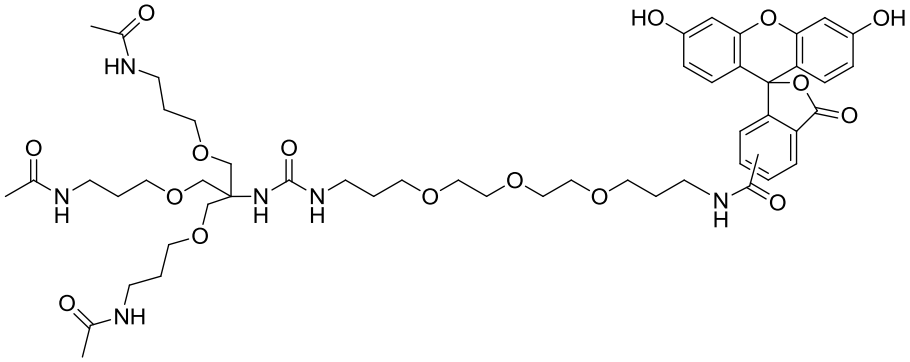

Compound **33** (20 mg, 0.030 mmol) was dissolved in DMF (500 µL) and coupled to 5(6)-carboxyfluorescein using protocol P5. Crude was purified *via* semi-preparative HPLC (method 7) (0.8 mg, 2.7%).

HPLC: 5.00 min (method 4). Purity ≥ 99% by ELSD detection.

MALDI-TOF: $C_{51}H_{71}N_6NaO_{16}$ calculated $[M+Na]^+$ 1045.4741; found = 1045.2856.

Compound 37

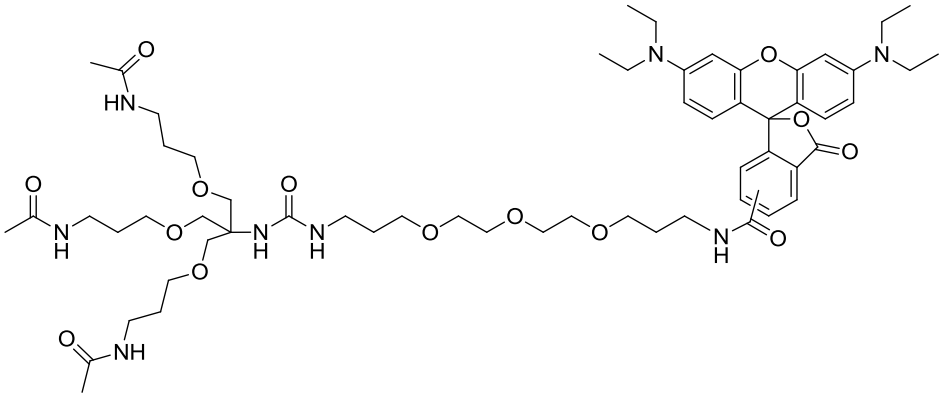

Compound **33** (20 mg, 0.030 mmol) was dissolved in DMF (500 µL) and coupled to 5(6)-carboxyfluorescein using protocol P5. Crude was purified *via* semi-preparative HPLC (method 7) (2.7 mg, 8%).

HPLC: 4.38 min (method 5). Purity ≥ 99% by ELSD detection.

MALDI-TOF: $C_{59}H_{88}N_8NaO_{14}$ calculated $[M+Na]^+$ 1155.6312; found = 1155.5582.

6-((6,6-bis((3-acetamidopropoxy)methyl)-4,13-dioxo-8-oxa-3,5,12-triazatetradecyl)amino)-3-oxo-3H-spiro[isobenzofuran-1,9'-xanthene]-3',6'-diyl diacetate (C_2CFDA-39)

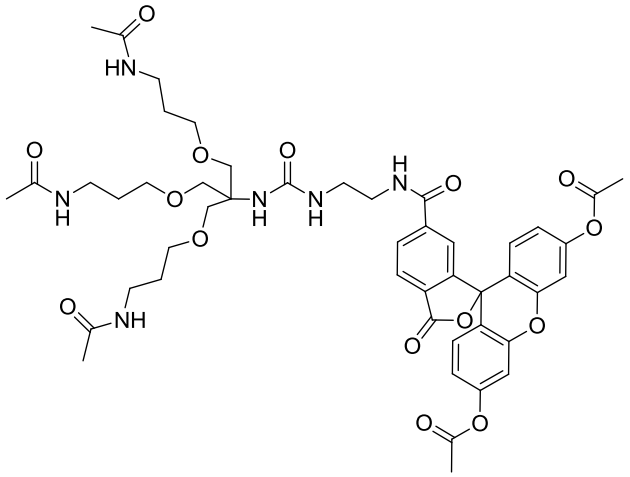

1,2-Diaminoethane was attached to the activated 2-chlorotrityl linker polystyrene resin (30 mg, 1.4 mmol.g^{-1}) (protocols P1 and P2). The isocyanate **4** was then attached and the Dde groups removed (protocols P3 and P4). The resulting amine moiety was acylated and the compound was cleaved from the linker using TFA (protocols P8 and P10). The crude mixture was coupled to 6-carboxyfluorescein *N*-succinimidyl ester (protocol P14) and purified *via* semi-preparative HPLC (method 7) (3.5 mg, 8% over 7 steps).

HPLC: 8.42 min (method 4). Purity ≥ 99% by ELSD detection.

m/z (ES$^+$): $C_{47}H_{58}N_6O_{15}$ calculated 946.4, found 947.5 $[M+H]^+$ (20%), 969.3 $[M+Na]^+$ (100%).

^{1}H NMR (500 MHz, CD_3CN) δ_H 8.31 (bs, 1H), 8.18 (dd, *J* = 8.1, 1.3 Hz, 1H, Ar-H), 8.09 (d, *J* = 8.0 Hz, 1H, Ar-H), 7.69 (bs, 1H, Ar-H), 7.16 (d, *J* = 2.2 Hz, 2H, Ar-H), 6.92 (d, *J* = 8.7 Hz, 2H, Ar-H), 6.88 (dd, *J* = 8.7, 2.2 Hz, 2H, Ar-H), 6.51 (t, *J* = 4.8

Hz, 3H), 6.19 (t, *J* = 5.5 Hz, 1H), 5.63 (s, 1H), 3.46 (s, 6H, Alkyl-H), 3.32 – 3.29 (m, 8H, Alkyl-H), 3.24 – 3.22 (m, 2H, Alkyl-H), 3.16 – 3.12 (m, 6H, Alkyl-H), 2.27 (s, 6H, Alkyl-H), 1.78 (s, 9H, Alkyl-H), 1.60 – 1.55 (m, 6H, Alkyl-H).

^{13}C NMR (126 MHz, CD_3CN) δ_C 171.1 (C), 170.3 (C), 166.0 (C), 160.2 (C), 153.7 (C), 152.7 (C), 152.5 (C), 142.9 (C), 130.7 (C), 130.4 (CH), 129.2 (CH), 126.3 (CH), 123.4 (C), 119.5 (CH), 117.2 (CH), 111.7 (CH), 71.3 (CH_2), 69.4 (CH_2), 59.7 (C), 43.4 (CH_2), 39.7 (CH_2), 37.1 (CH_2), 30.3 (CH_2), 23.3 (CH_3), 21.4 (CH_3).

5-((9,9-bis((3-acetamidopropoxy)methyl)-2,11-dioxo-7-oxa-3,10,12-triazaicosan-20-yl)amino)-3-oxo-3H-spiro[isobenzofuran-1,9'-xanthene]-3',6'-diyl diacetate (C_8CFDA-38)

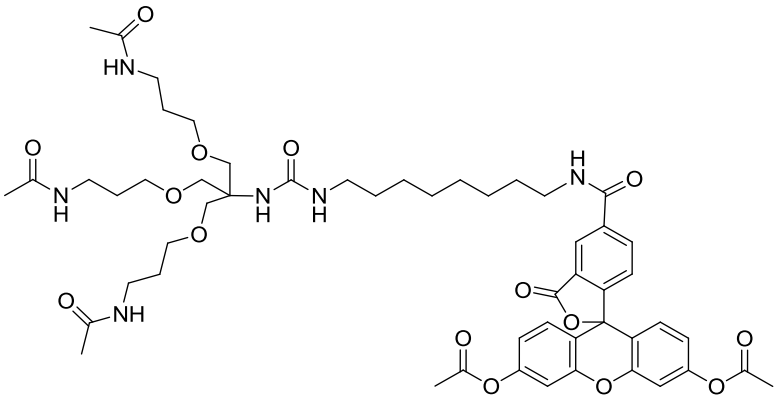

1,8-Diaminooctane was attached to the activated 2-chlorotrityl linker polystyrene resin (30 mg, 1.4 mmol.g^{-1}) (protocols P1 and P2). The isocyanate **4** was then attached and the Dde groups removed (protocols P3 and P4). The resulting amine moiety was acylated and the compound was cleaved from the linker using TFA (protocols P8 and P10). The crude mixture was coupled to 5-carboxyfluorescein *N*-succinimidyl ester (protocol P14) and purified *via* semi-preparative HPLC (method 7) (4.5 mg, 9% over 7 steps).

HPLC: 8.83 min (method 4). Purity ≥ 99 % by ELSD detection.

m/z (ES^+): $C_{53}H_{70}N_6O_{15}$ calculated 1030.5, found 1031.6 $[M+H]^+$ (20%), 1053.4 $[M+Na]^+$ (100%).

m/z (HRMS, ES^+): $C_{53}H_{70}O_{15}N_6Na_1$ calculated $[M+Na]^+$ 1053.47914, found 1053.47920.

^{1}H NMR (500 MHz, CD_3CN) δ_H 8.42 (d, *J* = 0.6 Hz, 1H, Ar-H), 8.20 (dd, *J* = 8.1, 1.5 Hz, 1H, Ar-H), 7.53 (t, *J* = 5.4 Hz, 1H), 7.34 (d, *J* = 8.1 Hz, 1H, Ar-H), 7.14 (d, *J* = 2.1 Hz, 2H, Ar-H), 6.91 (d, *J* = 8.7 Hz, 2H, Ar-H), 6.87 (dd, *J* = 8.7, 2.2 Hz, 2H, Ar-H), 6.66 (bs, 3H), 5.89 (t, *J* = 5.0 Hz, 1H), 5.59 (s, 1H), 3.60 (s, 6H, Alkyl-H), 3.42 – 3.36 (m, 8H, Alkyl-H), 3.24 – 3.20 (m, 6H, Alkyl-H), 3.05 – 3.01 (m, 2H, Alkyl-H), 2.26 (s, 6H, Alkyl-H), 1.86 (s, 9H, Alkyl-H), 1.65 – 1.57 (m, 8H, Alkyl-H), 1.41 – 1.27 (m, 10H, Alkyl-H).

^{13}C NMR (126 MHz, CD_3CN) δ_C 171.1 (C), 170.2 (C), 169.3 (C), 166.2 (C), 159.3 (C), 155.8 (C), 153.7 (C), 152.5 (C), 138.5 (C), 135.8 (CH), 130.2 (CH), 127.5 (C), 125.2 (CH), 124.7 (CH), 119.5 (CH), 117.2 (C), 111.6 (CH), 71.7 (CH_2), 69.5 (CH_2), 59.6 (C), 40.8 (CH_2), 40.3 (CH_2), 37.1 (CH_2), 31.1 (CH_2), 30.3 (CH_2), 30.1 (CH_2), 30.0 (CH_2), 27.6 (CH_2), 27.6 (CH_2), 23.3 (CH_3), 21.3 (CH_3).

***N*,*N*'-(((2-((3-acetamidopropoxy)methyl)-2-(3-(8-((3',6'-dihydroxy-3-oxo-3*H*-spiro[isobenzofuran-1,9'-xanthen]-5-yl)amino)octyl)ureido)propane-1,3-diyl)bis(oxy))bis(propane-3,1-diyl))diacetamide (C_8FAM-42)**

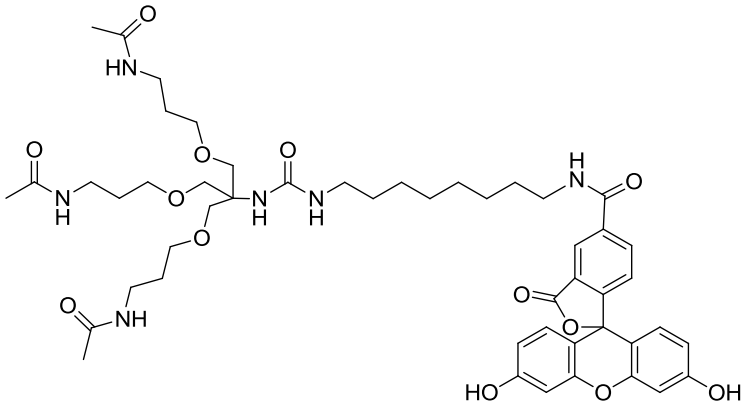

1,8-Diaminooctane was attached to the activated 2-chlorotrityl linker polystyrene resin (30 mg, 1.4 mmol.g^{-1}) (protocols P1 and P2). The isocyanate **4** was then attached and the Dde groups removed (protocols P3 and P4). The resulting amine moiety was acylated and the compound was cleaved from the linker using TFA (protocols P8 and P10). The crude mixture was coupled to 5-carboxyfluorescein *N*-succinimidyl ester, the acetyl groups removed (protocols P14 and P15) and purified *via* semi-preparative HPLC (method 6) (4.5 mg 11% over 7 steps).

HPLC: 8.13 min (method 4). Purity ≥ 99% by ELSD detection.

m/z (ES$^+$): $C_{49}H_{66}N_6O_{13}$ calculated 946.5, found 947.5 $[M+H]^+$ (30%), 969.5 $[M+Na]^+$ (20%).

m/z (HRMS, ES$^+$): $C_{49}H_{66}O_{13}N_6Na_1$ calculated $[M+Na]^+$ 969.45801, found 969.45330.

^{1}H NMR (500 MHz, CD_3OD) δ_H 8.52 (s, 2H), 8.43 (bs, 1H, Ar-H), 8.15 (dd, *J* = 8.0, 1.4 Hz, 1H, Ar-H), 7.31 (d, *J* = 8.0 Hz, 1H, Ar-H), 6.72 (d, *J* = 8.9 Hz, 2H, Ar-H),

6.69 (d, *J* = 2.2 Hz, 2H, Ar-H), 6.77 (dd, *J* = 8.8, 2.3 Hz, 2H, Ar-H), 3.65 (s, 6H, Alkyl-H), 3.49 – 3.40 (m, 8H, Alkyl-H), 3.25 (t, *J* = 6.8 Hz, 6H, Alkyl-H), 3.07 (t, *J* = 6.8 Hz, 2H, Alkyl-H), 1.93 (s, 9H, Alkyl-H), 1.73 (quint, *J* = 6.5 Hz, 6H, Alkyl-H), 1.66 (quint, *J* = 7.1 Hz 2H, Alkyl-H), 1.50 – 1.33 (m, 10H, Alkyl-H).

^{13}C NMR (126 MHz, CD_3OD) δ_C 173.3 (C), 168.7 (C), 165.3 (C), 160.8 (C), 156.6 (C), 155.4 (C), 141.0 (C), 138.0 (C), 135.4 (C), 130.9 (CH), 128.0 (CH), 126.4 (CH), 120.8 (CH), 118.0 (CH), 112.3 (C), 103.9 (CH), 71.7 (CH_2), 70.0 (CH_2), 61.2 (C), 41.4 (CH_2), 40.8 (CH_2), 37.9 (CH_2), 30.5 (CH_2), 30.5 (CH_2), 28.2 (CH_2), 28.1 (CH_2), 22.8 (CH_3).

PegCFDA-40

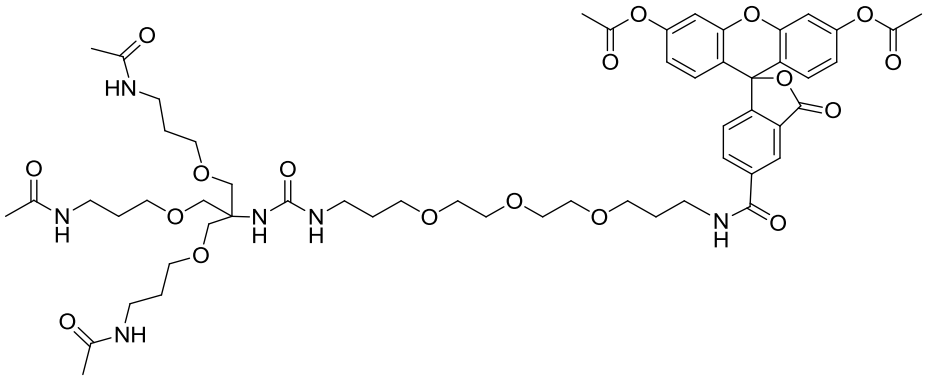

4,7,10-trioxa-1,13-tridecanyldiamine was attached to the activated 2-chlorotrityl linker polystyrene resin (30 mg, 1.4 mmol.g^{-1}) (protocols P1 and P2). The isocyanate **40** was then attached and the Dde groups removed (protocols P3 and P4). The resulting amine moiety was acylated and the compound was cleaved from the linker using TFA (protocols P8 and P10). The crude mixture was coupled to 5-carboxyfluorescein *N*-succinimidyl ester (protocol P15) and purified *via* semi-preparative HPLC (method 7). (7.9 mg, 17% over 7 steps).

HPLC: 7.75 min (method 4). Purity ≥ 99% by ELSD detection.

m/z (ES^+): $C_{55}H_{74}N_6O_{18}$ calculated 1107.2, found 1107.4 $[M]^+$ (25%), 1130.5 $[M+Na]^+$ (100%).

m/z (HRMS, ES^+): $C_{55}H_{74}O_{18}N_6Na_1$ calculated $[M+Na]^+$ 1129.49518, found 1129.49420.

^{1}H NMR (500 MHz, CD_3CN) δ_H 8.41 (bs, 1H, Ar-H), 8.20 (dd, *J* = 8.0, 1.5 Hz, 1H, Ar-H), 7.71 (t, *J* = 5.3 Hz, 1H), 7.35 (d, *J* = 8.0 Hz, 1H, Ar-H), 7.15 (d, *J* = 1.9 Hz, 2H, Ar-H), 6.91 (d, *J* = 8.6 Hz, 2H, Ar-H), 6.87 (dd, *J* = 8.7, 2.1 Hz, 2H, Ar-H), 6.63 (bs, 3H), 5.89 (t, *J* = 5.4 Hz, 1H), 5.58 (s, 1H), 3.58 (s, 6H, Alkyl-H), 3.57 – 3.55 (m, 4H, Alkyl-H), 3.55 – 3.45 (m, 6H, Alkyl-H), 3.42 – 3.36 (m, 8H, Alkyl-H), 3.23 – 3.18 (m, 6H, Alkyl-H), 3.07 (q, *J* = 6.3 Hz, 2H, Alkyl-H), 2.27 (s, 6H, Alkyl-H), 2.10 – 2.05 (m, 2H, Alkyl-H), 1.89 – 1.86 (m, 2H, Alkyl-H), 1.85 (s, 9H, Alkyl-H), 1.66 – 1.55 (m, 8H, Alkyl-H).

^{13}C NMR (126 MHz, CD_3CN) δ_C 171.06 (C), 170.17 (C), 169.24 (C), 166.24 (C), 159.24 (C), 155.79 (C), 153.70 (C), 152.49 (C), 138.49 (C), 135.80 (CH), 130.23 (CH), 127.51 (C), 125.25 (CH), 124.79 (CH), 119.49 (CH), 117.18 (C), 111.60 (CH), 71.6 (CH_2), 71.2 (CH_2), 71.1 (CH_2), 71.0 (CH_2), 70.9 (CH_2), 70.1 (CH_2), 69.6 (CH_2), 69.5 (CH_2), 59.6 (C), 38.8 (CH_2), 37.6 (CH_2), 37.1 (CH_2), 31.3 (CH_2), 30.3 (CH_2), 30.2 (CH_2), 23.3 (CH_3), 21.3 (CH_3).

PegFAM-43

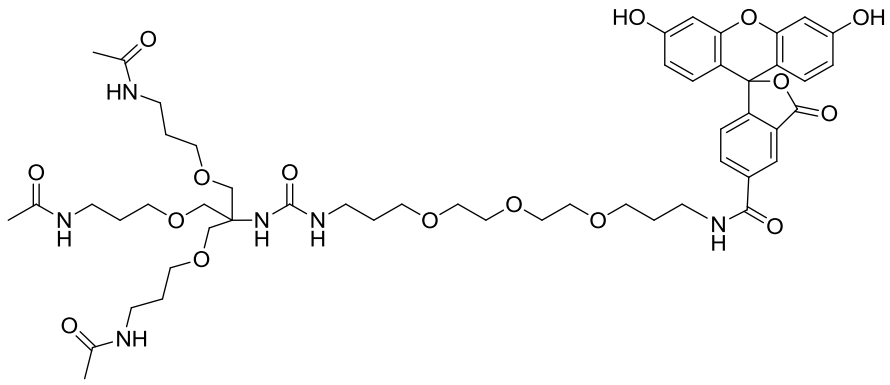

4,7,10-trioxa-1,13-tridecanyldiamine was attached to the activated 2-chlorotrityl linker polystyrene resin (30 mg, 1.4 mmol.g^{-1}) (protocols P1 and P2). The isocyanate **4** was then attached and the Dde groups removed (protocols P3 and P4). The resulting amine moiety was acylated and the compound was cleaved from the linker using TFA (protocols P8 and P10). The crude mixture was coupled to 5-carboxyfluorescein *N*-succinimidyl ester, the acetyl groups removed (protocols P4 and P15) and purified *via* semi-preparative HPLC (method 6) (10 mg, 23% over 7 steps).

HPLC: 7.73 min (method 3). Purity ≥ 99% by ELSD detection.

m/z (HRMS, ES$^+$): $C_{51}H_{71}O_{16}N_6$ calculated $[M+H]^+$ 1023.49211, found 1023.49190.

^{1}H NMR (500 MHz, CD_3OD) δ_H 8.46 (s, 1H, Ar-H), 8.14 (d, *J* = 7.9 Hz, 1H, Ar-H), 7.33 (d, *J* = 8.0 Hz, 1H, Ar-H), 6.79 (d, *J* = 8.5 Hz, 2H, Ar-H), 6.69 (d, *J* = 2.0 Hz, 2H, Ar-H), 6.58 (dd, *J* = 8.9, 2.1 Hz, 2H, Ar-H), 3.69 – 3.60 (m, 14H, Alkyl-H), 3.56 – 3.54 (m, 4H, Alkyl-H), 3.44 – 3.49 (m, 8H, Alkyl-H), 3.24 (t, *J* = 6.8 Hz, 6H, Alkyl-H), 3.13 (t, *J* = 6.7 Hz, 2H, Alkyl-H), 1.94 – 1.92 (m, 2H, Alkyl-H), 1.92 (s, 9H, Alkyl-H), 1.74 – 1.65 (m, 8H, Alkyl-H).

^{13}C NMR (126 MHz, CD_3OD) δ_C 174.4 (C), 173.3 (C), 168.8 (C), 160.7 (C), 155.9 (C), 152.7 (C), 143.4 (C), 137.8 (C), 136.3 (C), 131.3 (CH), 128.2 (CH), 124.7 (CH), 122.2 (CH), 117.7 (CH), 111.3 (C), 104.0 (CH), 71.7 (CH_2), 71.6 (CH_2), 71.5 (CH_2), 71.4 (CH_2), 70.4 (CH_2), 70.0 (CH_2), 60.2 (C), 40.6 (CH_2), 39.1 (CH_2), 38.0 (CH_2), 37.9 (CH_2), 30.5 (CH_2), 22.8 (CH_3).

PegRho-41

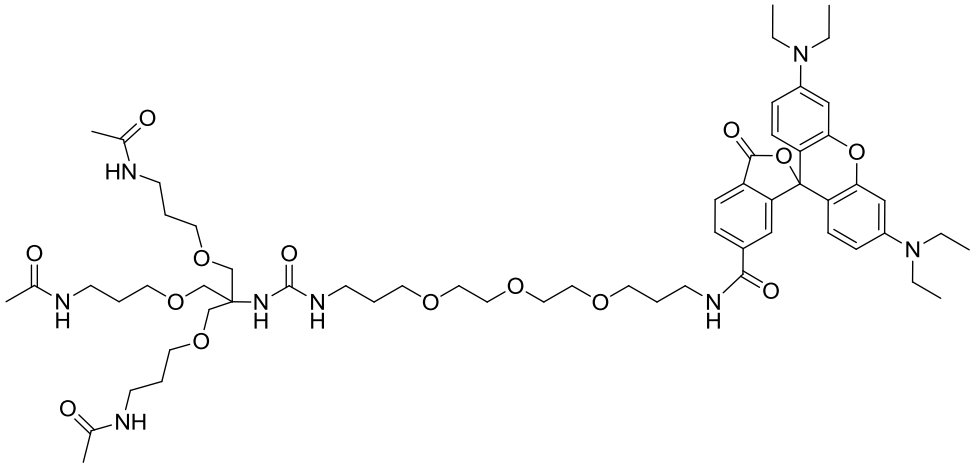

4,7,10-trioxa-1,13-tridecanyldiamine was attached to the activated 2-chlorotrityl linker polystyrene resin (30 mg, 1.4 mmol.g^{-1}) (protocols P1 and P2). The isocyanate **4** was then attached and the Dde groups removed (protocols P3 and P4). The resulting amine moiety was acylated and the compound was cleaved from the linker using TFA (protocols P and P10). The crude mixture was coupled to 6-carboxytetraethylrhodamine *N*-succinimidyl ester (protocol P14) and purified *via* semi-preparative HPLC (method 6) (10 mg, 21% over 7 steps).

HPLC: 6.24 min (method 4). Purity ≥ 99% by ELSD detection.

m/z (ES^+): $C_{59}H_{88}N_8O_{14}$ calculated 1133.4, found 1033.7 $[M]^+$ (100%), 1155.5 $[M+Na]^+$ (45%).

m/z (HRMS, ES^+): $C_{59}H_{89}O_{14}N_8$ calculated $[M+H]^+$ 1133.64928, found 1133.65130.

^{1}H NMR (500 MHz, CD_3OD) δ_H 8.54 (s, 3H), 8.15 (d, *J* = 8.1 Hz, 1H, Ar-H), 8.08 (dd, *J* = 8.1, 1.7 Hz, 1H, Ar-H), 7.71 (d, *J* = 1.6 Hz, 1H, Ar-H), 7.26 (d, *J* = 9.5 Hz, 2H, Ar-H), 7.01 (dd, *J* = 9.5, 2.4 Hz, 2H, Ar-H), 6.94 (dd, *J* = 2.3 Hz, 2H, Ar-H), 3.67 (q, *J* = 7.1 Hz, 8H, Alkyl-H), 3.63 (s, 6H, Alkyl-H), 3.58 – 3.56 (m, 8H, Alkyl-H), 3.50 – 3.43 (m, 12H, Alkyl-H), 3.23 (t, *J* = 6.8 Hz, 6H, Alkyl-H), 3.12 (t, *J* = 6.7 Hz, 2H, Alkyl-H), 1.92 (s, 9H, Alkyl-H), 1.89 – 1.86 (m, 2H, Alkyl-H), 1.75 – 1.63 (m, 8H, Alkyl-H), 1.30 (t, *J* = 7.1 Hz, 12H, Alkyl-H).

^{13}C NMR (126 MHz, CD_3OD) δ_C 179.7 (C), 173.3 (C), 168.7 (C), 160.7 (C), 159.6 (C), 157.1 (C), 146.7 (C), 144.8 (C), 136.6 (C), 133.2 (CH), 131.3 (CH), 129.7 (CH), 129.5 (CH), 115.2 (C), 115.1 (CH), 97.2 (CH), 71.6 (CH_2), 71.3 (CH_2), 70.4 (CH_2), 70.0 (CH_2), 60.2 (C), 46.9 (CH_2), 39.1 (CH_2), 38.0 (CH_2), 37.9 (CH_2), 31.5 (CH_2), 30.5 (CH_2), 30.5 (CH_2), 22.8 (CH_3), 12.8 (CH_3).

Protected HNE Peptide (45)

Fmoc-Ala-Pro-Glu(^{t}Bu)-Glu(^{t}Bu)-Ile-Met-Arg(Pbf)-Arg(Pbf)-Gln−OH

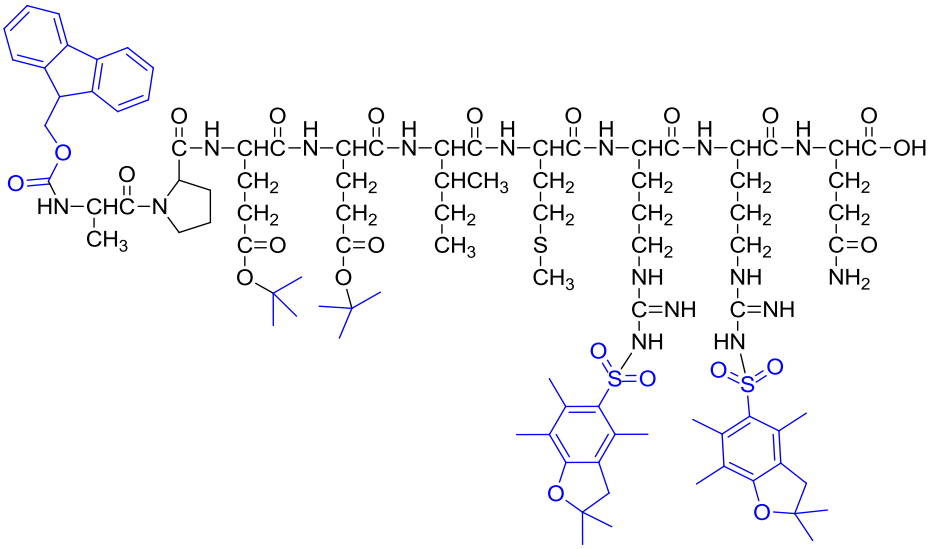

The fully protected peptide was synthesised using an automated peptide synthesiser Liberty Automatic Microwave Peptide Synthesizer on a L-Glutamine-2-chlorotrityl polystyrene resin (100 mg, 0.6 mmol.g^{-1}, particle size 100-200 mesh) and the cleavage from the linker was carried out using TFE (protocol P11) to give an orange oil (18 mg, 15% over 15 steps).

HPLC: 7.87 min (method 3). Purity ≥ 99% by ELSD detection.

MALDI-TOF: $C_{95}H_{138}N_{16}O_{23}S_3Na_1$ calculated $[M+Na]^+$ 1989.9175; found 1989.2461.

AB429-49

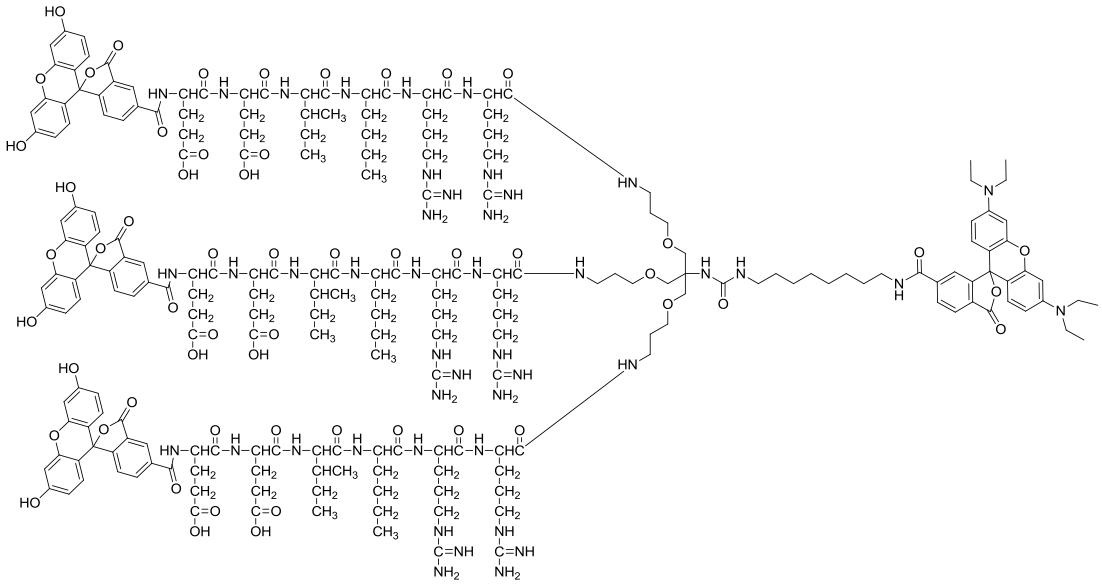

1,8-Diaminooctane was attached to the activated 2-chlorotrityl linker ChemMatrix resin (50 mg, 0.65 mmol.g^{-1}, particle size 35-100 mesh) (protocols P1 and P2). The isocyanate **4** was then attached and the Dde groups removed (protocols P3 and P4). Amino acid coupled using Oxyma except the Arginines which were coupled using HBTU (protocols P5, P6 and P7). 5-Carboxyfluorescein diacetate *N*-succinimidyl ester was coupled and the compound cleaved from the linker using the HFIP (protocols P9 and P12). The resulting compound was coupled to 6-carboxytetraethylrhodamine

N-succinimidyl ester and protecting groups removed using TFA cleavage procedure for peptidic compound (protocols P14 and P13). The compound was purified *via* semi-preparative HPLC (method 6). (11 mg, 8% over 20 steps).

HPLC: 8.67 min (method 3); or 5.25 min (method 4). Purity ≥ 99% by ELSD detection.

MALDI-TOF: $C_{216}H_{289}N_{44}O_{56}$ calculated $[M+H]^+$ 4395.1114; Found 4395.0959.

Chapter 3 compounds

5(6)-Carboxyfluorescein Diacetate (52)[286, 287]

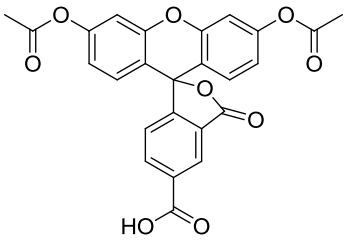

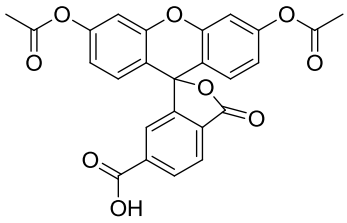

To a solution of 5(6)-carboxyfluorescein (1.00 g, 2.66 mmol) in Ac_2O (12 mL) was added pyridine (1.2 mL, 14.9 mmol) and the reaction stirred for 30 min at 110ºC. The clear solution was concentrated under reduced pressure. The crude mixture was dissolved in EtOAc (20 mL) and washed with aqueous $KHSO_4$ (1 M, 2 × 20 mL) and brine (20 mL). The organic layer was dried over Na_2SO_4, filtered and concentrated under reduced pressure to give the desired compound as a light yellow solid (1.18 g, 97%).

m/z (ES^+): $C_{25}H_{16}O_9$ calculated 460.39, found 461.0 $[M+H]^+$ (100%).

m/z (HRMS, ES^+): $C_{25}H_{16}O_9Na_1$ calculated $[M+Na]^+$ 483.06865, found 483.06850.

HPLC: 7.50 and 7.61 min (method 4). Purity ≥ 99% by ELSD detection.

^{1}H NMR (500 MHz, CD_3CN) δ_H 8.55 (dd, *J* = 1.5, 0.8 Hz, 0.5H, Ar-H), 8.34 (dd, *J* = 8.1, 1.5 Hz, 0.5H, Ar-H), 8.29 (dd, *J* = 8.0, 1.4 Hz, 0.5H, Ar-H), 8.1 (dd, *J* = 8.0, 0.8 Hz, 0.5H, Ar-H), 7.85 (dd, *J* = 1.3, 0.8 Hz, 0.5H, Ar-H), 7.38 (dd, *J* = 8.0, 0.6 Hz, 0.5H, Ar-H), 7.14 (t, *J* = 2.3 Hz, 2H, Ar-H), 6.92 – 6.85 (m, 4H, Ar-H), 2.26 (s, 6H, Alkyl-H).

^{13}C NMR (500 MHz, CD_3CN) δ_C 170.2 (C), 168.9 (C), 168.9 (C), 166.4 (C), 166.4 (C), 157.3 (C), 153.9 (C), 153.7 (C), 153.7 (C), 152.6 (C),152.5 (C), 138.2 (C), 137.7 (CH), 133.7 (C), 132.5 (CH), 130.7 (C), 130.3 (CH), 130.2 (CH) 127.8 (C), 127.5 (CH), 126.4 (CH), 126.2 (CH), 125.5 (CH), 119.5 (CH), 119.4 (CH), 117.1 (C) 116.9 (C), 111.6 (CH), 111.6 (CH), 21.3 (CH_3).

Mp: 167 – 169 ºC.[286]

IR (neat):, 1757 (s, $\nu_{C=O}$), 1420 (m, $\nu_{C=C}$), 1268 (m, ν_{C-OH}) cm^{-1}.

5- and 6- Carboxyfluorescein diacetate *N*-succinimidyl ester (5-CFDA-SE-53)[286]

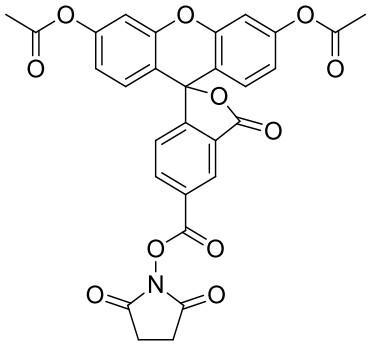

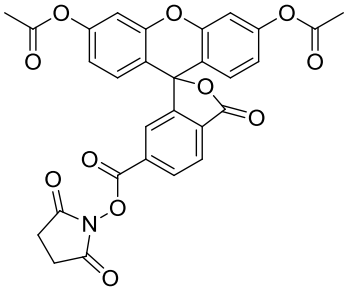

5(6)-Carboxyfluorescein diacetate (1.00 g, 2.17 mmol) was dissolved in DCM (15 mL), HOSu (300 mg, 2.61 mmol) was added and stirred until fully dissolved. DIC (410 µl, 2.61 mmol) was added and the reaction stirred at room temperature for 30 min. The organic layer was washed with water (2 × 10 mL), with brine (10 mL), dried over Na_2SO_4 and filtered. The crude mixture was re-dissolved in toluene (10 mL), loaded onto an equilibrated column (4.5 × 15 cm bed of silica) and eluted with 20% EtOAc in toluene to afford the pure individual isomers as white solids 5-isomer (495 mg, 41%) and 6-isomer (505 mg, 42%).

*5-Carboxyfluorescein diacetate N-succinimidyl ester (5-CFDA-SE-**53**) :*

Rf 0.37 in 50:50 EtOAc:Toluene.

HPLC : 8.56 min (method 4). Purity ≥ 99% 6-isomer <1% by ELSD detection.

m/z (ES^+): $C_{29}H_{19}N_1O_{11}$ calculated 557.46, found 558.1 $[M+H]^+$ (95%).

m/z (HRMS, ES^+): $C_{29}H_{19}N_1O_{11}Na_1$ calculated $[M+Na]^+$ 580.08503, found 580.08550.

^{1}H NMR (500 MHz, $CDCl_3$) δ_H 8.77 (dd, *J* = 1.5, 0.7 Hz, 1H, Ar-H), 8.38 (dd, *J* = 8.1, 1.6 Hz, 1H, Ar-H), 7.33 (dd, *J* = 8.1, 0.7 Hz, 1H, Ar-H), 7.09 (d, *J* = 2.2 Hz, 2H, Ar-H), 6.82 (dd, *J* = 8.7, 2.2 Hz, 2H, Ar-H), 6.78 (d, *J* = 8.7 Hz, 2H, Ar-H), 2.88 (s, 4H, Alkyl-H), 2.27 (s, 6H, Alkyl-H).

^{13}C NMR (126 MHz, $CDCl_3$) δ_C 169.1 (C), 168.9 (C), 167.4 (C), 160.6 (C), 158.2 (C), 152.5 (C), 151.5 (C), 137.0 (CH), 129.0 (CH), 128.1 (C), 127.7 (CH), 127.2 (C), 125.2 (CH), 118.2 (CH), 115.3 (C), 110.8 (CH), 25.8 (CH_2), 21.2 (CH_3).

Mp: > 250 ºC.[286]

IR (neat):, 1770 (s, $\nu_{C=O}$), 1738 (s, $\nu_{C=O}$), 1422 (m, $\nu_{C=C}$), 1187 (s, ν_{C-N}), 1154 (s, ν_{C-O}) cm^{-1}.

*6-Carboxyfluorescein diacetate N-succinimidyl ester (6-CFDA-SE-**54**) :*

Rf 0.53 in 50:50 EtOAc:Toluene

HPLC: 7.78 min (method 4). Purity ≥ 99% 5-isomer <1% by ELSD detection.

m/z (ES^+): $C_{29}H_{19}N_1O_{11}$ calculated 557.46, found 558.2 $[M+H]^+$ (100%), 580.2 $[M+Na]^+$ (70%).

m/z (HRMS, ES^+): $C_{29}H_{19}N_1O_{11}Na_1$ calculated $[M+Na]^+$ 580.08503, found 580.08620.

^{1}H NMR (500 MHz, $CDCl_3$) δ_H 8.38 (dd, *J* = 8.0, 1.3 Hz, 1H, Ar-H), 8.16 (d, *J* = 8.0 Hz, 1H, Ar-H), 7.91 (s, 1H, Ar-H), 7.12 (d, *J* = 2.2 Hz, 2H, Ar-H), 6.84 (dd, *J* = 8.7, 2.3 Hz, 2H, Ar-H), 6.77 (d, *J* = 8.7 Hz, 2H, Ar-H), 2.87 (s, 4H, Alkyl-H), 2.30 (s, 6H, Alkyl-H).

^{13}C NMR (126 MHz, $CDCl_3$) δ_C 168.9 (C), 168.9 (C), 167.6 (C), 160.7 (C), 153.2 (C), 152.6 (C), 151.8 (C), 132.3 (CH), 131.8 (C), 131.5 (C), 129.1 (CH), 126.5 (CH), 126.1 (CH), 118.3 (CH), 115.4 (C), 110.9 (CH), 25.8 (CH_2), 21.3 (CH_3).

IR (neat):, 1764 (s, $\nu_{C=O}$), 1738 (s, $\nu_{C=O}$), 1421 (m, $\nu_{C=C}$), 1197 (s, ν_{C-N}), 1153 (s, ν_{C-O}) cm^{-1}.

Mp: > 250 ºC.[286]

3',6'-Bis(diethylamino)-3-oxo-3*H*-spiro[isobenzofuran-1,9'-xanthene]-5- and 6-carboxylic acid (57 and 58)[242]

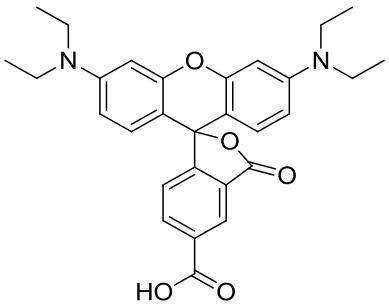

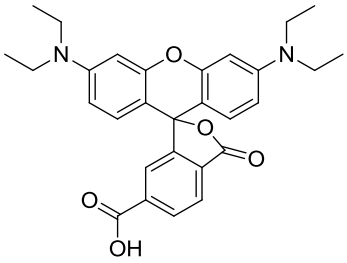

5(6)-Carboxytetraethyl rhodamine (2.00 g, 4.11 mmol) was purified by column chromatography [eluting solvent: TEA:DCM:MeOH (5:95:0 to 5:75:20)]. The two separated isomers were obtained as their TEA salts. The 5-isomer salt was redissolved in EtOAc (80 mL) and washed with 1 M $KHSO_4$ (3 × 50 mL), with brine (50 mL), dried over Na_2SO_4 and filtered, to afford pure

5- carboxytetraethylrhodamine **57** (833 mg, 42%) and 6- carboxytetraethylrhodamine **58** (670 mg, 33%) as dark pink solids.

*5- carboxytetraethylrhodamine **57**:*

Rf: 0.11 in 10:89.5:0.5 MeOH:DCM:TEA

HPLC: 7.54 min (method 4). Purity ≥ 99% by ELSD detection.

m/z (ES^+): $C_{29}H_{30}N_2O_5$ calculated 486.56, found 487.2 $[M+H]^+$ (100%).

m/z (HRMS, ES^+): $C_{26}H_{31}N_2O_5$ calculated $[M+H]^+$ 487.22275, found 487.22270.

^{1}H NMR (500 MHz, $CDCl_3$) δ_H 8.86 (d, *J* = 1.0 Hz, 1H, Ar-H), 8.27 (dd, *J* = 8.0, 1.4 Hz, 1H, Ar-H), 7.28 (d, *J* = 8.0 Hz, 1H, Ar-H), 6.91 (d, *J* = 9 Hz, 2H, Ar-H), 6.60 – 6.57 (m, 4H, Ar-H), 3.46 (q, *J* = 7.2 Hz, 8H, Alkyl-H), 1.23 (t, *J* = 7.1 Hz, 12H, Alkyl-H).

^{13}C NMR (126 MHz, $CDCl_3$) δ_C 172.7 (C), 169.2 (C), 168.4 (C), 161.3 (C), 1556.0 (C), 153.1 (CH), 133.5 (C), 131.0 (CH), 130.9 (CH), 127.7 (CH), 126.7 (C), 111.6 (CH), 109.7 (C), 96.9 (CH), 45.5 (CH_2), 12.8 (CH_3).

IR (neat) 1738 (m, $\nu_{C=O}$), 1335 (m, ν_{Ar-N}), 1178 (m, ν_{C-O}) cm^{-1}.

*6- carboxytetraethylrhodamine **58**:*

Rf: 0.22 in 10:89.5:0.5 MeOH:DCM:TEA

HPLC: 6.99 min (method 4). Purity ≥ 99% by ELSD detection.

m/z (ES^+): $C_{29}H_{30}N_2O_5$ calculated 486.56, found 487.2 $[M+H]^+$ (80%).

m/z (HRMS, ES^+): $C_{26}H_{31}N_2O_5$ calculated $[M+H]^+$ 487.22275, found 487.22260.

^{1}H NMR (500 MHz, MeOD) δ_H 8.41 (d, *J* = 8.2 Hz, 1H, Ar-H), 8.38 (dd, *J* = 8.2, 1.3 Hz, 1H, Ar-H), 7.98 (d, *J* = 1.1 Hz, 1H, Ar-H), 7.14 (d, *J* = 9.5 Hz, 2H, Ar-H), 7.04

(dd, *J* = 9.5, 2.4 Hz, 2H, Ar-H), 6.99 (d, *J* = 2.3 Hz, 2H, Ar-H), 3.69 (q, *J* = 7.1 Hz, 8H, Alkyl-H), 1.31 (t, *J* = 7.1 Hz, 12 H, Alkyl-H).

^{13}C NMR (126 MHz, MeOD) δ_C 168.0 (C), 167.8 (C), 159.9 (C), 159.5 (C), 157.3 (C), 136.6 (C), 136.1 (C), 135.5 (CH), 132.9 (CH), 132.4 (CH), 115.7 (CH), 114.9 (C), 97.4 (CH), 12.9 (CH_2), 7.8 (CH_3).

IR (neat) 1745 (m, $\nu_{C=O}$), 1337 (m, ν_{Ar-N}), 1179 (m, $\nu_{C=O}$) cm^{-1}.

2,5-Dioxopyrrolidin-1-yl 3',6'-bis(diethylamino)-3-oxo-3*H*-spiro[isobenzofuran-1,9'-xanthene]-5- and 6- carboxylate (5-Rho-SE-50) and (6-Rho-SE-51)[242]

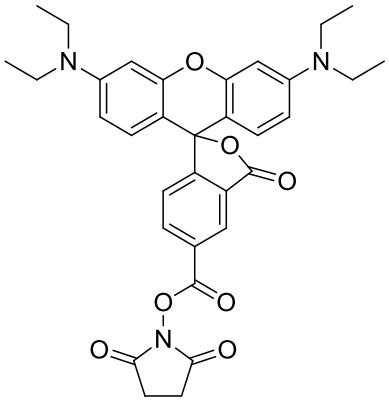

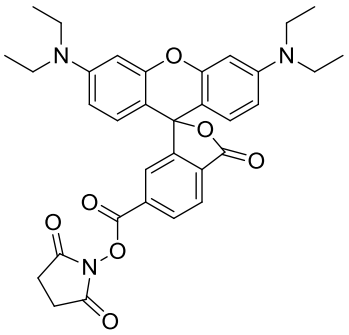

5-Carboxytetraethylrhodamine **57** (195 mg, 0.40 mmol), DMAP (244 mg, 2.0 mmol) and TEA (278.2 µL, 2.0 mmol) were dissolved in dry DCM (20 mL). DSC (205 mg, 0.80 mmol) was added and the reaction stirred at room temperature for 1 h. Reaction completion was confirmed by TLC. The reaction was quenched using AcOH (229 µL, 4.0 mmol) and without concentrating the solution was loaded onto an equilibrated column and eluted with 1% AcOH in acetone to afford pure the pure 5-Rho-SE-**50** (198 mg, 85%) or 6-Rho-SE-**51** (89 mg, 87%) as dark pink solids.

*5-Rho-SE-**50**:*

Rf: 0.27 in 89.9:2 DCM:MeOH:AcOH

HPLC: 6.44 min (method 4). Purity ≥ 99% by ELSD detection.

m/z (HRMS, ES^+): $C_{33}H_{34}N_3O_7$ calculated $[M+H]^+$ 584.23913, found 584.23840.

^{1}H NMR (500 MHz, $CDCl_3$) δ_H 8.85 (d, *J* = 1.1 Hz, 1H, Ar-H), 8.29 (dd, *J* = 8.0, 1.7 Hz, 1H, Ar-H), 7.29 (dd, *J* = 8.0, 0.5 Hz, 1H, Ar-H), 6.87 – 6.80 (m, 2H, Ar-H), 6.56 – 6.53 (m, 4H, Ar-H), 3.44 (q, *J* = 7.1 Hz, 8H, Alkyl-H), 2.94 (s, 4H, Alkyl-H), 1.22 (t, *J* = 7.1 Hz, 12H, Alkyl-H).

^{13}C NMR (126 MHz, $CDCl_3$) δ_C 172.7 (C), 169.2 (C), 168.4 (C), 161.3 (C), 156.0 (C), 153.1 (C), 135.2 (CH), 133.5 (C), 130.9 (CH), 130.9 (CH), 127.8 (CH), 126.7 (C), 111.6 (CH), 109.7 (C), 96.9 (CH), 45.5 (CH_2), 25.9 (CH_2), 12.8 (CH_3).

*6-Rho-SE-**51**:*

Rf: 0.31 in 89.9:2 DCM:MeOH:AcOH

HPLC: 6.45 min (method 4). Purity ≥ 99% by ELSD detection.

m/z (HRMS, ES^+): $C_{33}H_{34}N_3O_7$ calculated $[M+H]^+$ 584.23913, found 584.23910.

^{1}H NMR (500 MHz, $CDCl_3$) δ_H 8.32 (m, 2H, Ar-H), 7.86 (t, *J* = 1.1 Hz, 1H, Ar-H), 6.99 (d, *J* = 9.3 Hz, 2H, Ar-H), 6.66 (dd, *J* = 9.3, 2.4 Hz, 2H, Ar-H), 6.61 (d, *J* = 2.4 Hz, 2H, Ar-H), 3.49 (q, *J* = 7.3 Hz, 8H, Alkyl-H), 2.87 (s, 4H, Alkyl-H), 1.25 (t, *J* = 7.1 Hz, 12H, Alkyl-H).

^{13}C NMR (126 MHz, $CDCl_3$) δ_C 172.7 (C), 169.2 (C), 168.5 (C), 161.3 (C), 156.7 (C), 153.9 (C), 141.7 (C), 131.8 (CH), 131.5 (CH), 130.1 (CH), 129.7 (CH), 127.5 (C), 112.5 (CH), 111.4 (C), 96.6 (CH), 45.7 (CH_2), 25.6 (CH_2), 12.8 (CH_3).

Chapter 4 compounds

NLS Probe 1 - 60

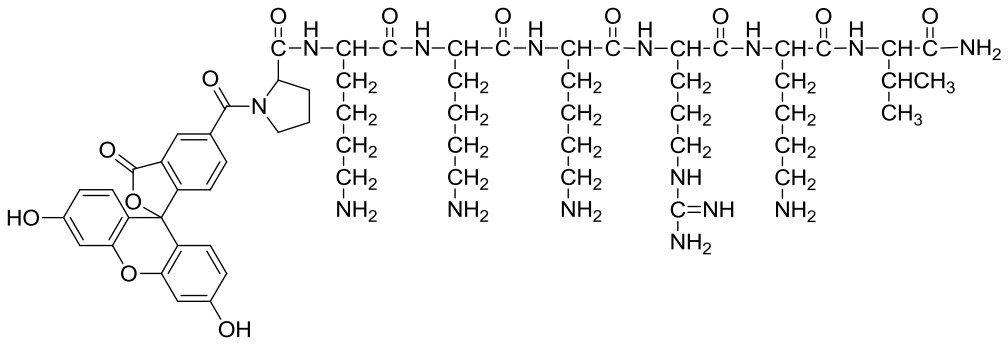

To aminomethyl ChemMatrix resin (40 mg, 1.0 mmol.g^{-1}) was attached Fmoc rink linker and amino acids using Oxyma (protocol P5). After final Fmoc removal (protocols P7), 5-carboxyfluorescein diacetate *N*-succinimidyl ester was attached and the compound cleaved from the linker using TFA (protocols P9 and P13) and purified *via* semi-preparative HPLC (method 6) (2.1 mg, 3% yield over 17 steps).

HPLC: 2.43 min (method 4). Purity ≥ 99% by ELSD detection.

MALDI-TOF: $C_{61}H_{90}N_{15}O_{13}$ calculated $[M+H]^+$ 1240.6837; Found = 1241.0300.

NLS Probe 2 - 62

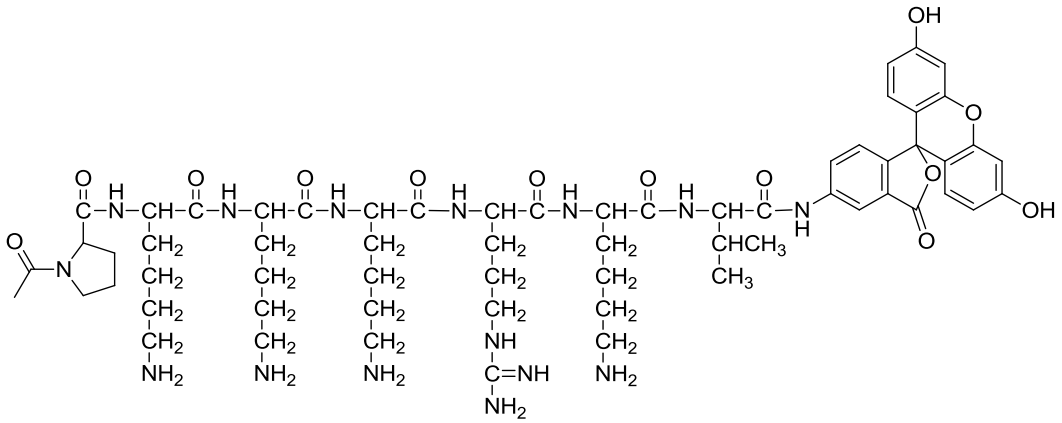

To aminomethyl ChemMatrix resin (50 mg, 1.0 mmol.g^{-1}, particle size 35-100 mesh) was attached Fmoc rink linker and amino acids using Oxyma (protocols P5 and P7). After final Fmoc removal (protocols P7), the amine was acylated and the compound was cleaved from the linker using the HFIP (protocols P8 and P12). To the resulting compound (5 mg, 1 eq) was added a solution of Oxyma in DMF (44 µL, 0.07 M, 1 eq) and left stirring for 10 min. DIC (0.49 µL, 1 eq) was added to the solution and left stirring for a further 5 min. 5-Aminofluorescein (1.32 mg, 1.2 eq) and TEA (0.5 µL, 1 eq) were added to the solution and the reaction left stirring for 1.5 h. All protecting groups were then removed using TFA (protocol P13). The compound was purified using semi-preparative HPLC (method 6). The desired product was obtained (1.1 mg) in 28% yield for the last step (2% yield over 19 steps).

HPLC: 10.81 min (method 4). Purity ≥ 99% by ELSD detection.

MALDI-TOF: $C_{62}H_{92}N_{15}O_{13}$ calculated $[M+H]^+$ 1254.6994; Found = 1254.7582.

NLS Probe 3 - 65

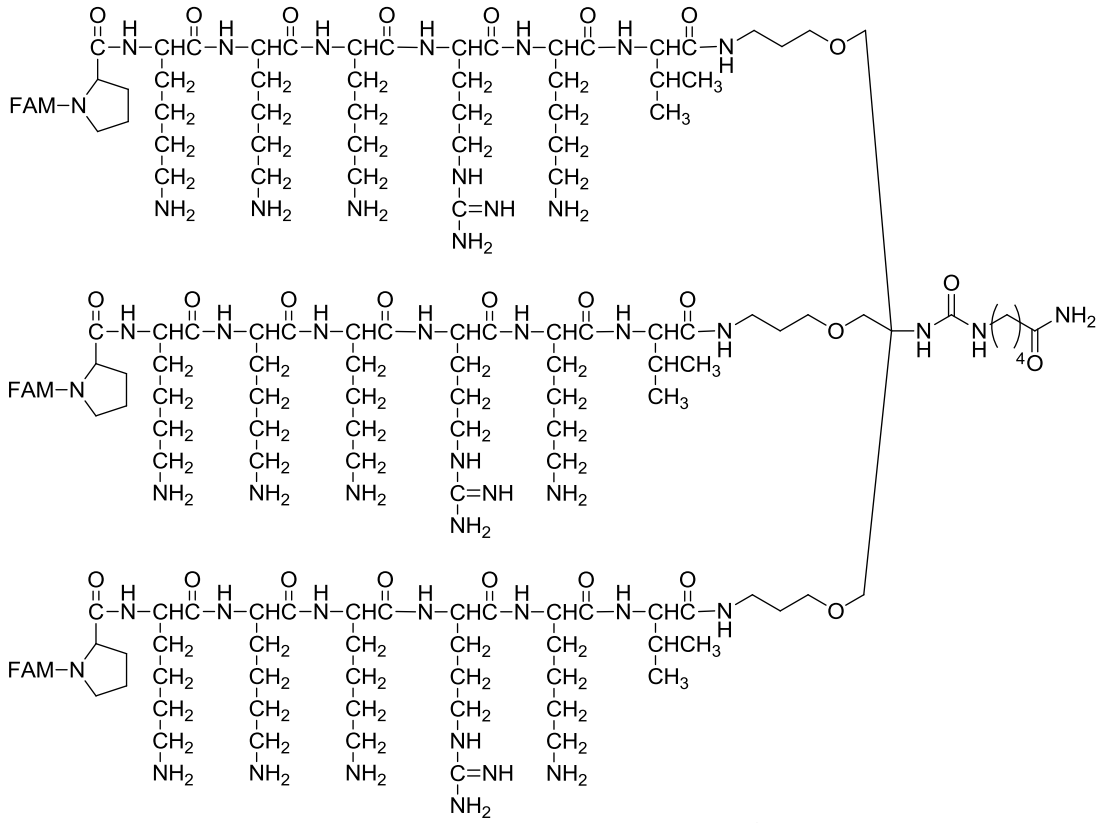

To aminomethyl ChemMatrix resin (40 mg, 1.0 mmol.g^{-1}) was attached Fmoc rink linker and *N*-Fmoc-8-aminooctanoic using Oxyma (protocols P5 and P7). After Fmoc removal, the isocyanate **4** was attached and Dde groups removed (protocols P5, P7, P3 and P4). Amino acids were coupled using Oxyma and after final Fmoc removal, 5-carboxyfluorescein diacetate *N*-succinimidyl ester was attached (protocols P7, P7 and P9). The compound was cleaved from the linker using TFA (protocol P13) and purified *via* semi-preparative HPLC (method 6) (14.0 mg, 9 % yield over 22 steps).

HPLC: 3.33 min (method 4). Purity ≥ 99% by ELSD detection.

MALDI-TOF: $C_{205}H_{306}N_{48}O_{44}$ calculated $[M+H]^+$ 4146.9133; found = 4147.4131.

NLS Probe 4 - 67

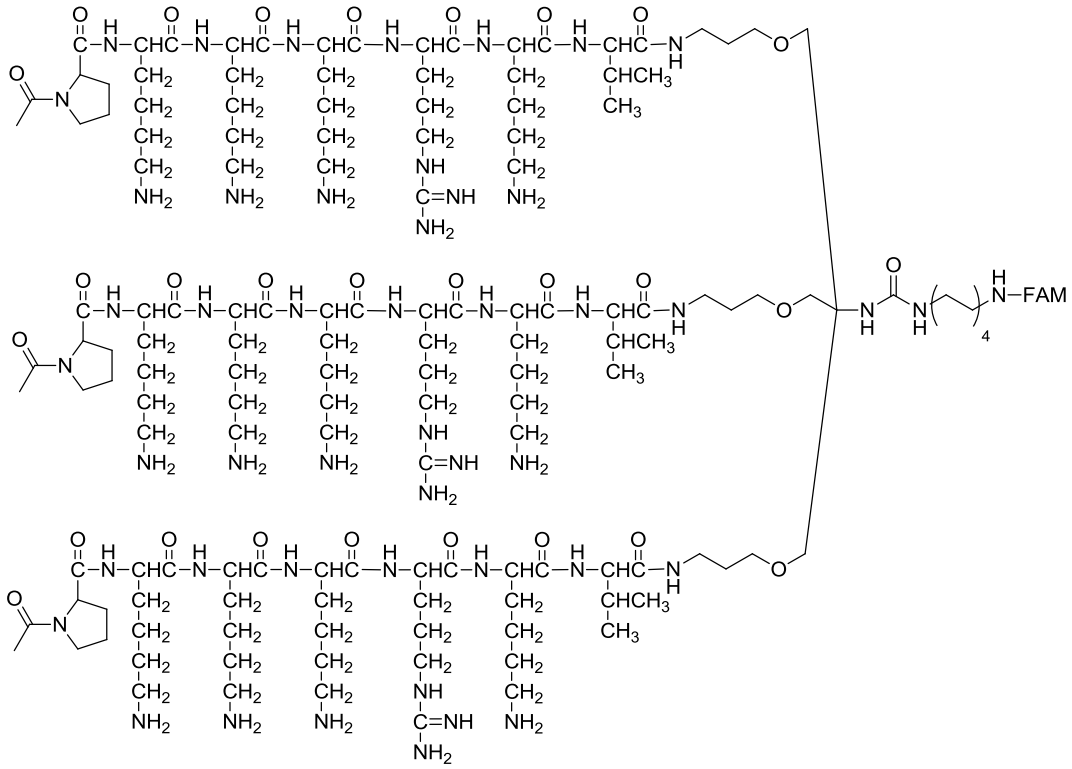

1,8-Diaminooctane was attached to the activated 2-chlorotrityl linker ChemMatrix resin (50 mg, 0.65 mmol.g^{-1}) (protocols P1 and P2). The isocyanate **4** was then attached and the Dde groups removed (protocols P3 and P4). Amino acids were coupled using Oxyma and after final Fmoc removal the amine was acylated (protocols P5, P7 and P8). The compound was cleaved from the linker using HFIP, and the resulting compound coupled to 5-carboxyfluorescein diacetate *N*-succinimidyl ester (protocols P12 and P14). Protecting groups were removed using TFA (protocol P13) and purified *via* semi-preparative HPLC (method 6) (2.0 mg, yield 2% over 21 steps).

HPLC: 2.68 min (method 4). Purity ≥ 99 % by ELSD detection.

MALDI-TOF: $C_{169}H_{295}N_{48}O_{34}$ calculated $[M+H]^+$ 3541.2752; Found = 3541.2616.

In vitro/*ex vivo* studies

Flow cytometry analyses were carried out on a Becton Dickinson (BD) FACS Canto II using the FlowJo Version 7.6.3 software for data analysis.

Microscopy studies were performed on Leica fluorescence microscope under bright light, 488 nm (fluorescein) and 543 nm (rhodamine).

Confocal microscopy was performed on a Leica SP5 Confocal using the Zeiss 510 Meta for digital acquisition and ImageJ for image analysis.

Ninety-six well plates were analysed on a **microplate reader** Synergy H1 Reader using the Gen 5 (1.11).

Jurkat cell culture: Jurkat cells were cultured in complete Roswell Park Memorial Institute (RPMI) media (RPMI 1640 (Gibco/Invitrogen), supplemented with 10% fetal bovine serum, 1% L-glutamine, 100 units/mL penicillin, 100 µg/mL streptomycin, complete RPMI) at 37 °C and 5% CO_2. Cells were cultured in T-75 flasks (Nunc) until 80% confluency before being prepared by centrifugation at 350 ḡ for 5 min for further analysis. Cellular experiments were carried out with cells passaged between 4- and 20-times.

T cells plating:

To purified $CD4^+$ T cells, six aliquots of 8 $x10^5$ cells per mouse sample were taken and re-suspended in 500 µL of PBS. One probe per aliquot was incubated for 10 min at 37 °C at a concentration of 5 µM made from a 5 mM DMSO stock solution. One aliquot per mouse was left probe-free. The reaction was stopped by adding cold complete RPMI media. Cells were washed twice to ensure complete excess probe

removal. Each cell experiment was re-suspended in complete RPMI media, halved in two and plated onto a 96-well plate pre-coated with anti CD3/28. The plate was incubated at 37 °C and 5% CO_2 and analysed using flow cytometry (BD FACS-Canto II using FlowJo Version 7.6.3 software for data analysis) after 48 h and 72 h as well as imaged under a Leica DM IRB fluorescence microscopy.

Flow cytometry on T cells:

T cells were labelled with two fluorescent antibodies: CD4-PE (clone GK 1.5) and CD3-APC (17A2) for fluorescein based studies and CD4-APC (clone GK 1.5) and CD3-FITC (17A2) for rhodamine based studies. The cells were also treated with FC block (clone 2.4G2). Controls for flow cytometry included: (1) Non-stained control, (2) CD4-PE and CD3-APC markers, (3) CD4-APC and CD3-FITC markers.

Jurkat cells experiment

Jurkat cells were divided into aliquots of 6 $x10^5$ cells in PBS. The cells were incubated with the probes at two concentrations 5 μM and 1 μM for 10 min at 37 °C and 5% CO_2. The reactions were quenched with cold complete RPMI media, and washed twice with complete media. The cells were grown at 37 °C and 5% CO_2 for 6 days with the media being replaced with fresh media every two days. Aliquots of each experiment were analysed at day 0, 2, 3 and 6 using Flow cytometry (BD FACS-Canto II using FlowJo Version 7.6.3 software for data analysis). Unlabelled cells were used as control and each experiment was carried out in duplicate.

Human neutrophil blood-preparation protocol: Sodium citrate tribasic dehydrate (4 mL of 3.8% in water) was added to human blood (40 mL) and

centrifuge at 350 ḡ for 20 min. The top layer was discarded and to the remaining layer, 6 mL of dextran [6g Dextran 500 in 100 mL of 0.9% NaCl] was added and made up to 50 mL with sodium chloride (0.9% in water). The resulting solution was then mixed and allowed to sit for 20 min. The top layer was taken, made up to 50 mL with sodium chloride (0.9% in water) and centrifuged down (350 ḡ for 6 min). The supernatant was removed, and the cell pellet was re-suspended in 3 mL of the 55% Percoll^{TM}. In a 15 mL falcon tube, was layered 3 mL of 68% Percoll^{TM} on top of 3 mL of 81% Percoll^{TM}. The 55% Percoll^{TM} cell suspension was then layered on top of the 68% Percoll^{TM} layer. The resulting three layers were centrifuged at 720 ḡ for 20 min. The first layer containing monocyte and the excess liquid of the second layer were discarded. The neutrophil layer at the interface of the second and third layer, was isolated and washed twice using 50 mL of PBS and centrifuged down at 350 ḡ for 6 min. Neutrophils were re-suspended at 10×10^6 cells/mL in complete IMDM media (phenol red free IMDM media, 1% L-glutamine, 25 mM hepes).

Confocal experiment on human neutrophils:

Neutrophils fixation: cover slips were immersed in fibronectin for 10 min. Fibronectin was removed and the coverslips washed twice with 2 mL of PBS. To the resulting coated fibronectin coverslips were added 2 mL of IMDM media and 100 µL of neutrophils using a wide mouth pipette tip. The neutrophils were allowed to sit for 15 min at 37 °C and 5% CO_2. Media was removed and replaced with the following options:

For non activated neutrophil studies: 1 mL of a 10 µM solution of probe in IMDM (stock solution of each probes were made at 1 mM using 10% DMSO in

PBS, and aliquots diluted with IMDM media to obtain a final probe concentration of 10 µM).

For activated neutrophil studies: 750 µL of a 10 µM solution of probe in IMDM, and then 250 µL of a solution of 10 µM of ionophore A23/87 to activate the neutrophils.

For activated neutrophils with elastase inhibitor studies: 750 µL of a 10 µM solution of probe in IMDM with 1 µL of inhibitor Sevelestat, and then 250 µL of a solution of 10 µM of ionophore A23/87 to activate the neutrophils.

Live cells were imaged using confocal microscopy performed on a Zeiss lsm 510 meta confocal microscope under bright light, 488 nm (fluorescein) and 543 nm (rhodamine), Zeiss 510 Meta software was used for digital acquisition and ImageJ for data analysis.

Kinetic studies:

In a 96 well plate were prepared solutions of the probe in acetate buffer at ten different concentrations in triplicates: 50 µM, 25 µM, 12.5 µM, 6.25 µM, 3.13 µM, 1.56 µM, 0.78 µM, 0.39 µM, 0.20 µM, 0.10 µM. Human sputum elastase (EC 3.4.21.37, No. SE563 obtained from Elastin products company, inc) was prepared in acetate buffer and used at a final concentration of 17 nM. The fluorescence increase was measured using an excitation wavelength of 485 nm and emission wavelength of 528 nm, every 17 sec at 37 °C for 30 min. The experiments were carried out on a microplate reader Synergy H1 Reader Serial Number: 253179.

A standard curve of 5(6)-carboxyfluorescein was carried out using concentrations ranging from 25 µM to $2.4.10^{-05}$ µM (See appendices section). The equation of the straight line obtained from plotting the concentration against the fluorescence allowed us to convert the fluorescence of the kinetic experiments into concentrations. Using GraphPad prism software the slope of the initial linear phase of each curve was accurately calculated allowing us to generate the Michaelis Menten data.

NLS Confocal experiment on A549:

To fixed A549 cells in 8 well chambers were added a solution of 10 µM of the probe of interest in complete DMEM media (phenol red free DMEM media, 10% fetal bovine serum, 1% L-glutamine, 100 units/mL penicillin, 100 µg/mL streptomycin) and incubated at 37 °C and 5% CO_2 for 1 h. Syto 82 orange fluorescent nucleic acid stain was then added to the cells at a concentration of 5 µM and incubated at 37 °C and 5% CO_2 for 20 min. The media was then remove and replace with fresh media containing 10 µM of the probe, and imaged using confocal microscopy performed on a Zeiss lsm 510 meta confocal microscope under bright light, 488 nm (fluorescein) and 543 nm (rhodamine), Zeiss 510 Meta software was used for digital acquisition and ImageJ for data analysis.

Confocal experiment on A549:

To fixed A549 cells in 8 well chambers, were added a solution of 10 µM of the probe of interest in complete DMEM media (phenol red free DMEM media, 10% fetal bovine serum, 1% L-glutamine, 100 units/mL penicillin, 100 µg/mL streptomycin) and incubated at 37 °C and 5% CO_2 for 15 h. The wells were imaged using confocal

microscopy performed on a Zeiss lsm 510 meta confocal microscope under bright light, 488 nm (fluorescein) and 543 nm (rhodamine), Zeiss 510 Meta software was used for digital acquisition and ImageJ for data analysis.

Appendices

Copyright permissions: All published material used in this thesis was used with permissions to reprint on paper and electronically. A summary of all the acquired permissions is listed below.

Chapter 1:

Figure 1, copyright mediaTUM - TU München, Photographer: Institute for Biological and Medical Imaging / Technische Universitaet Muenchen. Image can be found at: http://mediatum.ub.tum.de/node?id=1084090

Figure 3, copyright 2001 Macmillan Publishers Ltd, licence number 3262530634638, published in Nakajima, K.; Sena, G.; Nawy, T.; Benfey, P. N. *Nature* **2001,** *413*, 307. Doi: 10.1038/35095061

Figure 4, copyright 2011 Macmillan Publishers Ltd, licence number 3262570937049, published in Yusop, R. M.; Unciti-Broceta, A.; Johansson, E. M. V.; Sánchez-Martín, R. M.; Bradley, M. *Nature Chemistry* **2011,** *3*, 239. Doi: 10.1038/nchem.981

Figure 5, copyright 2009 Macmillan Publishers Ltd, licence number 3263140126512, published in Maetzel, D.; Denzel, S.; Mack, B.; Canis, M.; Went, P.; Benk, M.; Kieu, C.; Papior, P.; Baeuerle, P. A.; Munz, M.; Gires, O. *Nature Cell Biology* **2009,** *11*, 162. Doi: 10.1038/ncb1824

Figure 6, copyright 2007 American Chemical Society, published in Miller, E.; Bian, S.; Chang, C. *Journal of the American Chemical Society* **2007,** *129*, 3458. Doi: 10.1021/ja0668973

Figure 7, Copyright 2006 American Chemical Society, published in Ueno, T.; Urano, Y.; Setsukinai, K.; Takakusa, H.; Kojima, H.; Kikuchi, K.; Ohkubo, K.; Fukuzumi, S.; Nagano, T. *Journal of the American Chemical Society* **2004,** *126*, 14079. Doi: 10.1021/ja048241k

Chapter 2:

Figure 9, copyright 2008 Elsevier Masson SAS, published in Korkmaz, B.; Moreau, T.; Gauthier, F. *Biochimie* **2008,** *90*, 227. Doi: 10.1016/j.biochi.2007.10.009

Figure 10, copyright 2002 American Chemical Society, published in Hedstrom, L. *Chemical Reviews* **2002,** *102*, 4501. Doi: 10.1021/cr000033x

Figure 11, copyright 2002 Elsevier, licence number 3277120114490, published in Kawabata, K.; Hagio, T.; Matsuoka, S. *European Journal of Pharmacology* **2002,** *451*, 1. Doi: 10.1016/S0014-2999(02)02182-9

Table 1, copyright 2013 American Thoracic Society, published in Korkmaz, B.; Attucci, S.; Moreau, T.; Godat, E.; Juliano, L.; Gauthier, F. *American Journal of Respiratory Cell and Molecular Biology* **2004,** *30*, 801. Doi: 10.1165/rcmb.2003-0139OC

Chapter 3:

Figure 35, copyright 2002 American Chemical Society, published in Kvach, M. V.; Tsybulsky, D. A.; Ustinov, A. V.; Stepanova, I. A.; Bondarev, S. L.; Gontarev, S. V.; Korshun, V. A.; Shmanai, V. V. *Bioconjugate Chemistry* **2007,** *18*, 1691. Doi: 10.1021/bc7001874

Chapter 4:

Figure 46, copyright 2007 The American Society for Biochemistry and Molecular Biology, published in Lange, A.; Mills, R. E.; Lange, C. J.; Stewart, M.; Devine, S. E.; Corbett, A. H. *Journal of Biological Chemistry* **2007,** *282*, 5101. Doi: 10.1074/jbc.R600026200

Figure 47, copyright 2009 American Chemical Society, published in Puckett, C. A.; Barton, J. K. *Journal of the American Chemical Society* **2009,** *131*, 8738. Doi: 10.1021/ja9025165

Standard curve of 5(6)-carboxyfluorescein to convert arbitrary unit of fluorescent RFU to concentration for enzymatic studies.

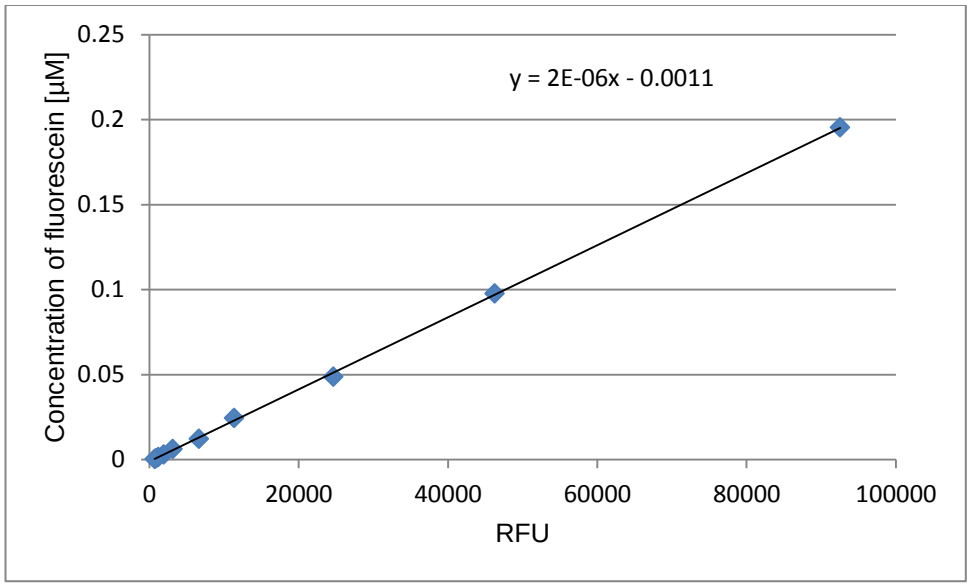

Single isomer 5-carboxyfluorescein diacetate *N*-succinimidyl ester Data

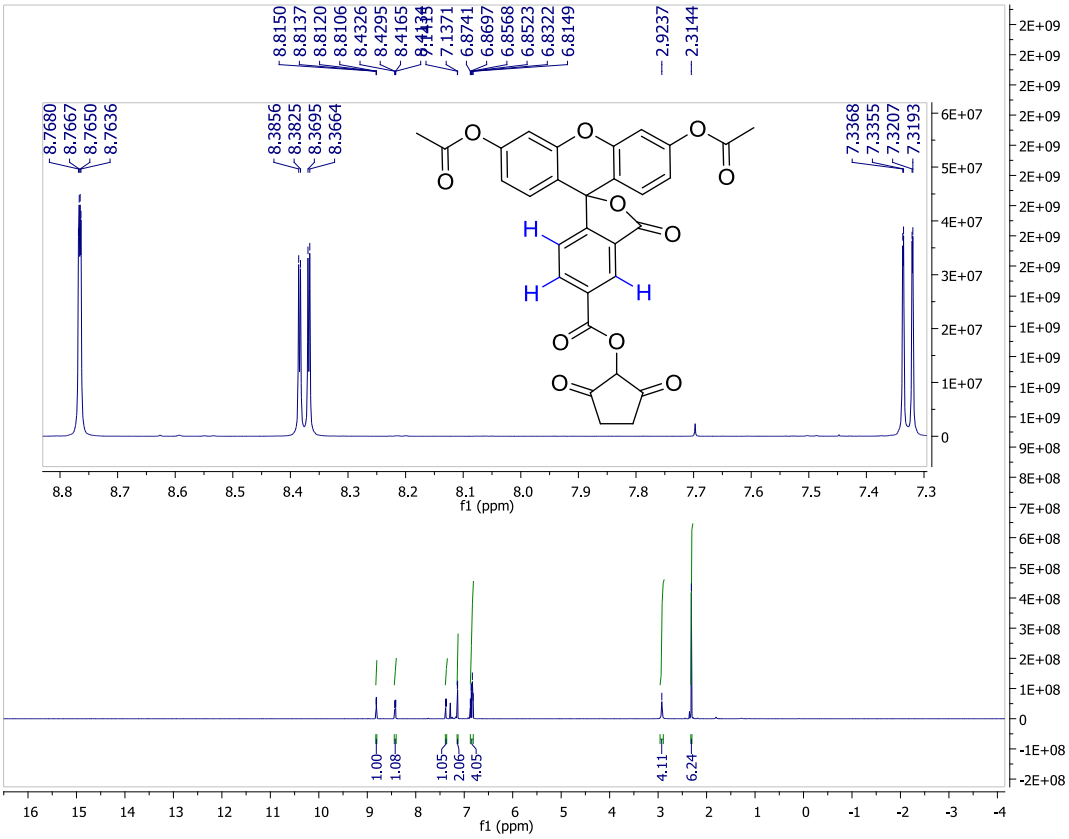

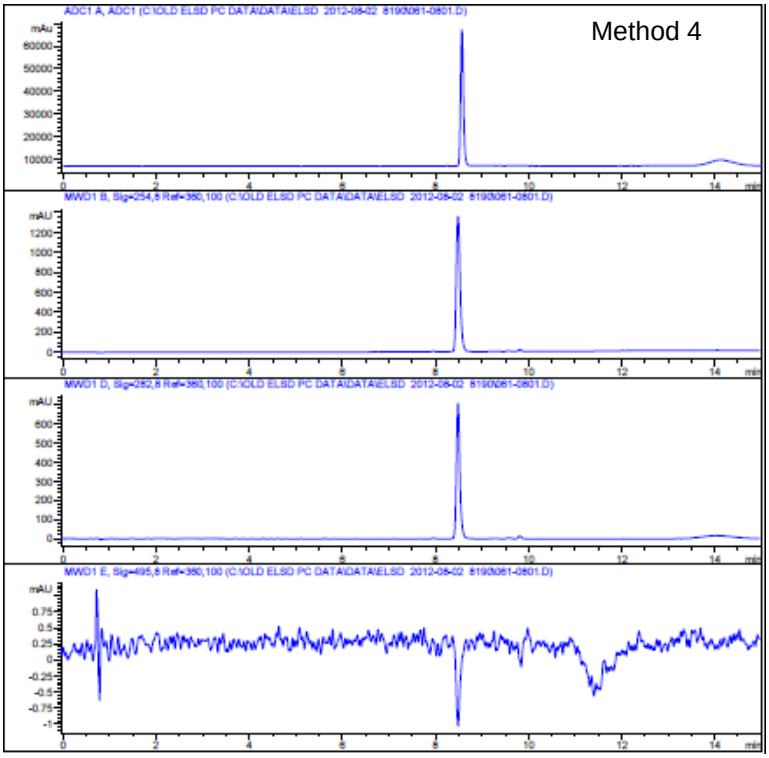

Single isomer 6-carboxyfluorescein diacetate *N*-succinimidyl ester data

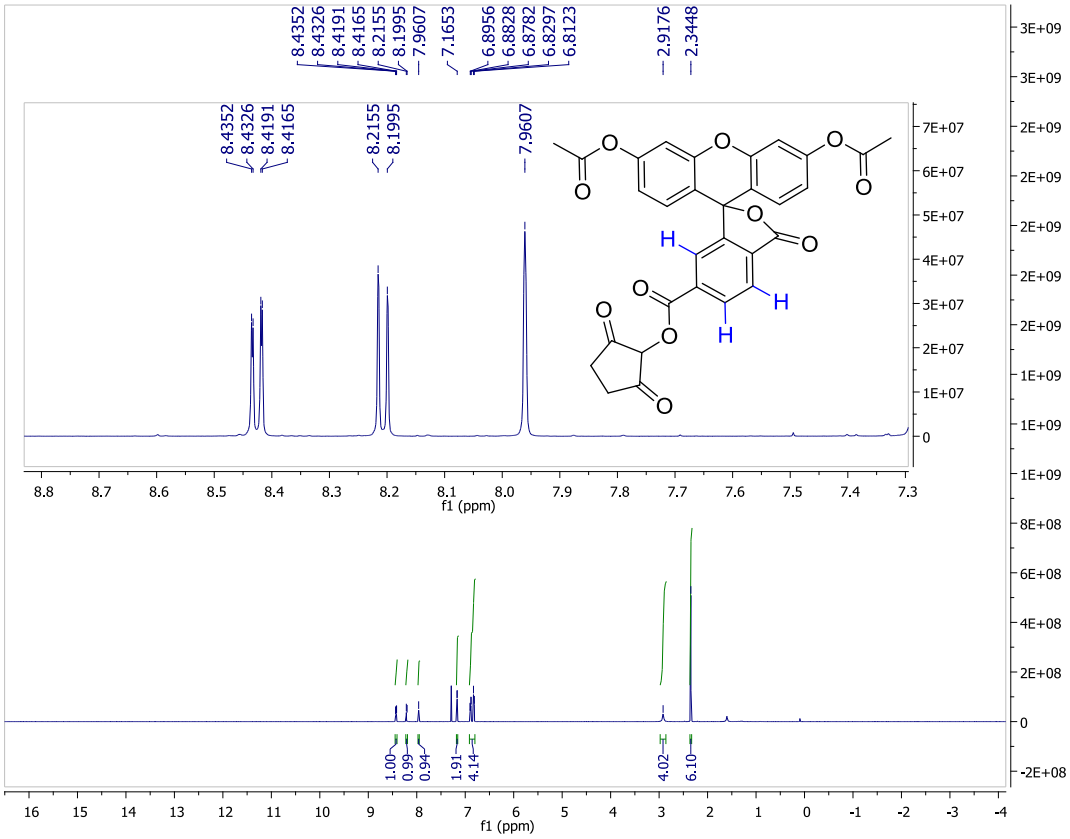

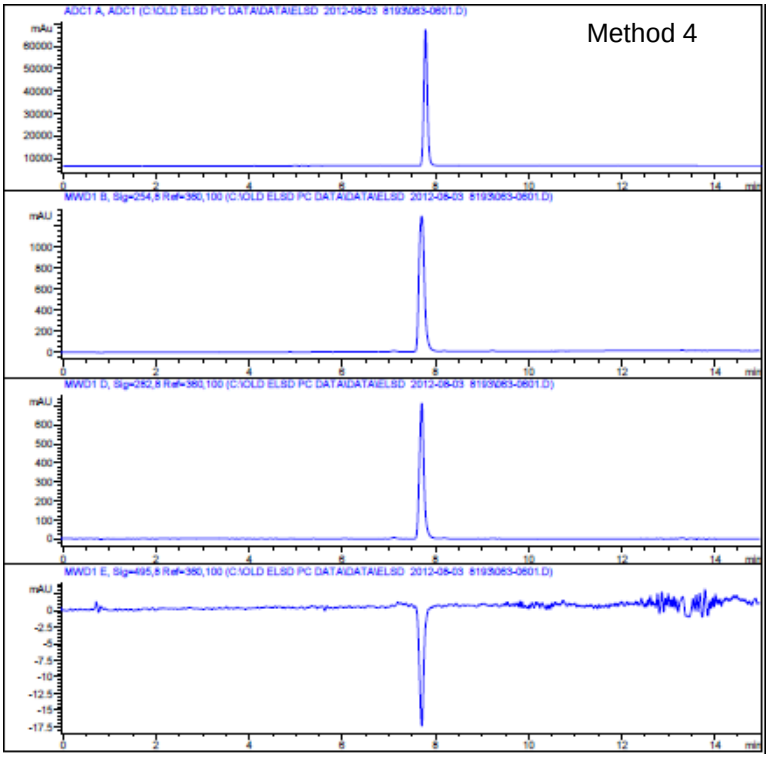

ELSEVIER

Bioorganic & Medicinal Chemistry Letters
journal homepage: www.elsevier.com

Separating the isomers – Efficient synthesis of the *N*-hydroxysuccinimide esters of 5 and 6-carboxyfluorescein diacetate and 5 and 6-carboxyrhodamine B

Aurélie Brunet, Tashfeen Aslam and Mark Bradley*

School of Chemistry, EaStChem, University of Edinburgh, West Mains Road, Edinburgh, EH9 3JJ, UK

ARTICLE INFO

Article history:
Received
Revised
Accepted
Available online

Keywords:
Carboxyfluorescein diacetate
Rhodamine B
N-hydroxysuccinimide ester
5(6)-Carboxyfluorescein

ABSTRACT

Diacetate protection of 5 and 6-carboxyfluorescein followed by synthesis of the *N*-hydroxysuccinimide esters allowed ready separation of the two isomers on a multi-gram scale. The 5 and 6-carboxyrhodamine B *N*-hydroxysuccinimide esters were also readily synthesised and separated.

* Corresponding author. Tel.: + 44-131-650-4820; e-mail: mark.bradley@ed.ac.uk

Fluorescein and its derivatives represent one of the most popular families of fluorescent labelling agents for various biomolecules,[1] including labelling of actin,[2] myosin,[3,4] hemoglobin,[5] histones,[6] DNA,[7] RNA,[8] and antibodies.[1,9] Peptides are also routinely tagged with carboxyfluorescein, as demonstrated by Nguyen who reported a carboxyfluorescein conjugated peptide that labels nerves in human tissues, with potential to aid surgery and prevent accidental transection.[10] The monitoring of enzymatic activities using fluorescein-based probes is wide spread. For example, Tanaka designed a quenched fluorescein phosphate-polymer that in the presence of alkaline phosphatase liberated fluorescein, while Bradley has developed a quenched multi-branched scaffold liberating fluorescein in the presence of human neutrophil elastase.[11,12] Furthermore, fluorescein has been incorporated into numerous chemical sensors that have been used to detect reactive oxygen species,[13] hydrogen peroxide,[13] nitric oxide,[13] or measure pH (*e.g.* pH sensing in living cells).[14,15]

Widely used derivatives of fluorescein are the *N*-hydroxysuccinimide esters of 5 and 6-carboxyfluorescein diacetate (often referred as CFSE), which have been extensively used to monitor cellular division,[16,17] with over 226 reports in 2013 alone.[18] Here the two acetate groups render the molecule membrane permeant, while once inside cells, the active ester labels intracellular proteins, while esterases remove the acetate groups restoring the fluorescein's fluorescence.[19]

Fluorescein is commonly used as a mixture, namely 5(6)-carboxyfluorescein, and the synthesis of fluorescein-labelled probes results in a mixture of isomers. This complicates their purification and analysis of the resulting fluorescein-tagged probes since labelling will result in two probes with slightly differing properties. Kvach studied the properties of 5 and 6-carboxyfluorescein conjugated to an oligonucleotide and demonstrated that, although they had similar absorbance and fluorescence quantum yields, the emission band from the 6-carboxyfluorescein–oligonucleotide was substantially sharper than that of the 5-carboxyfluorescein analogue, making it the optimal isomer for multiplex detection.[20] When proteins are labelled at multiple sites the situation is even more complex.

The separation of the 5 and 6-isomers of carboxyfluorescein by chromatography[21,22] or crystallisation[23,24] has been reported but the latter method, in our hands, was inconsistent and not easily reproduced. A recent review supports the view that a more efficient method of separation of the isomers is necessary.[25] Another fluorophore that is also used as a mixture is (5)6-carboxyrhodamine B. Rhodamine dyes are highly fluorescent and have good photostability,[26] and therefore have broad applications, such as a fluorescence standard for quantum yield determinations,[27] detection of reactive oxygen species,[13] ion sensors in living cells,[28] DNA and protein labelling[29,30] to name but a few. The efficient synthesis of 5 or 6-carboxytetraethylrhodamine *N*-hydroxysuccinimide ester is not well established.

Herein, a simple two-step process for the synthesis and subsequent separation of the two isomers of the *N*-hydroxysuccinimide esters of 5 and 6-carboxyfluorescein diacetate and 5 and 6-carboxytetraethylrhodamine is reported. The proposed routes have multiple advantages over existing methods in terms of scale, speed and ease of separation of the two isomers.

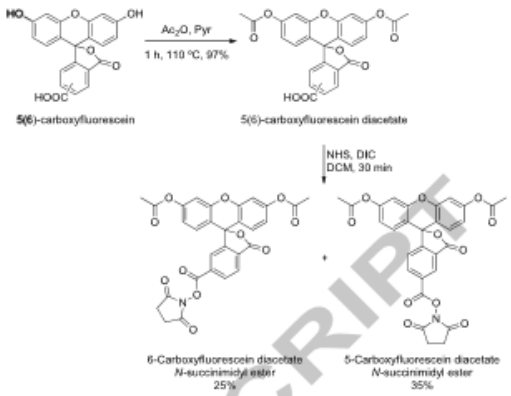

Scheme 1. *N*-hydroxysuccinimide ester formation and isomer separation of carboxyfluorescein diacetate.

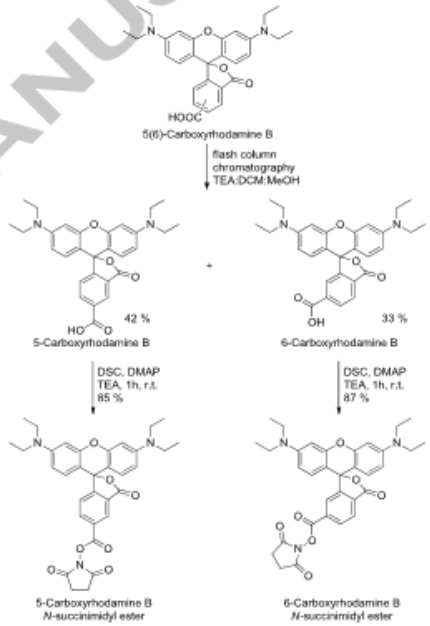

Scheme 2. Isomer separation and active ester formation of rhodamine B.

Synthesis began with acetylation of the phenol moieties of fluorescein, modifying the procedure reported by Tour[31] using acetic anhydride and pyridine (>15g scale, >95% yield), with a mild acid wash being the only work-up necessary (Scheme 1).[32] Carboxylic acid activation used *N,N*-diisopropylcarbodiimide (DIC) and *N*-hydroxysuccinimide (NHS) in dichloromethane. The two carboxyfluorescein diacetate *N*-hydroxysuccinimide esters were readily purified on a plug of silica gel (7 × 15 cm) using an optimised solvent system of EtOAc:Toluene (20:80) to give a 35% yield of 5-isomer and 25% yield of 6-isomer.[33]

Fung reported the synthesis of 5 and 6-carboxytetraethylrhodamine *N*-hydroxysuccinimide esters using *N,N'*-disuccinimidyl carbonate (DSC) and DMAP,[34] but in our hands, this gave a mixture of starting material and the di-ester product (Figure 1).

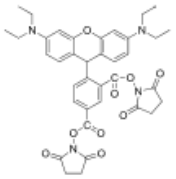

Figure 1. Di-ester obtained when treating carboxytetraethylrhodamine with DSC and DMAP.

To achieve 5 or 6-carboxylic acid regioselectivity over the 3-carboxylic acid, rhodamine must react in its closed lactone form; however, unlike fluorescein, rhodamine B is in the lactone form under basic conditions, and in the open form under acidic conditions.[35] Therefore it was reasoned that the active ester of 5 and 6-carboxytetraethylrhodamine would be generated using a combination of DMAP and DSC with 5 equivalents of triethylamine to give the desired regioselectivity (Scheme 2).[36] Larger quantities of base interfered with the efficiency of the reaction. The separation of the isomers of 5 and 6-carboxytetraethylrhodamine by column chromatography was straightforward using a gradient of TEA:DCM:MeOH (5:95:0 to 5:75:20).[37]

In conclusion, methods have been developed for the formation and separation of the active esters of 5 and 6-isomers of carboxyfluorescein and carboxyrhodamine B. These methods are robust and reliable, and make single isomers of these two widely used fluorophores readily available.

Acknowledgments

Financial support from the MRC and University of Edinburgh is gratefully acknowledged. Dr Annamaria Lilienkampf is acknowledged for help with the manuscript preparation.

References and Notes

1. Hermanson, G. T. *Bioconjugate Techniques*; New York: Academic Press, 2008.
2. Konno, K.; Morales, M. F. *Proceedings of the National Academy of Sciences* **1985,** *82*, 7904.
3. Ando, T. *Biochemistry* **1984,** *23*, 375.
4. Aguirre, R.; Gonsoulin, F.; Cheung, H. C. *Biochemistry* **1986,** *25*, 6827.
5. Hirsch, R. E.; Zukin, R. S.; Nagel, R. L. *Biochemical and Biophysical Research Communications* **1986,** *138*, 489.
6. Cocco, L.; Martelli, A. M.; Billi, A. M.; Matteucci, A.; Vitale, M.; Neri, L. M.; Manzoli, F. A. *Experimental Cell Research* **1986,** *166*, 465.
7. Kumke, M. U.; Li, G.; McGown, L. B.; Walker, G. T.; Linn, C. P. *Analytical Chemistry* **1995,** *67*, 3945.
8. Pagano, J. M.; Farley, B. M.; McCoig, L. M.; Ryder, S. P. *Journal of Biological Chemistry* **2007,** *282*, 8883.
9. Talian, J. C.; Olmsted, J. B.; Goldman, R. D. *The Journal of Cell Biology* **1983,** *97*, 1277.
10. Whitney, M. A.; Crisp, J. L.; Nguyen, L. T.; Friedman, B.; Gross, L. A.; Steinbach, P.; Tsien, R. Y.; Nguyen, Q. T. *Nature Biotechnology* **2011,** *29*, 352.
11. Tanaka, K.; Kitamura, N.; Chujo, Y. *Macromolecules* **2010,** *43*, 6180.
12. Avlonitis, N.; Debunne, M.; Aslam, T.; McDonald, N.; Haslett, C.; Dhaliwal, K.; Bradley, M. *Organic & Biomolecular Chemistry* **2013,** *11*, 4414.
13. Yang, Y.; Zhao, Q.; Feng, W.; Li, F. *Chemical Reviews* **2013,** *113*, 192.
14. Unciti-Broceta, A.; Yusop, R. M.; Richardson, P. R.; Walton, J.; Bradley, M. *Tetrahedron Letters* **2009,** *50*, 3713.
15. Bradley, M.; Alexander, L.; Duncan, K.; Chennaoui, M.; Jones, A. C.; Sánchez-Martín, R. M. *Bioorganic & Medicinal Chemistry Letters* **2008,** *18*, 313.
16. Quah, B. J. C.; Warren, H. S.; Parish, C. R. *Nature Protocols* **2007,** *2*, 2049.
17. Thaunat, O.; Granja, A. G.; Barral, P.; Filby, A.; Montaner, B.; Collinson, L.; Martinez-Martin, N.; Harwood, N. E.; Bruckbauer, A.; Batista, F. D. *Science* **2012,** *335*, 475.
18. Web of Knowledge, Search Topic "CFSE" for year 2013; 227 hits; Accessed on the 14th February 2014.
19. Parish, C. R. *Immunology and Cell Biology* **1999,** *77*, 499.
20. Kvach, M. V.; Tsybulsky, D. A.; Ustinov, A. V.; Stepanova, I. A.; Bondarev, S. L.; Gontarev, S. V.; Korshun, V. A.; Shmanai, V. V. *Bioconjugate Chemistry* **2007,** *18*, 1691.
21. Adamczyk, M.; Fishpaugh, J. R.; Heuser, K. J. *Bioconjugate Chemistry* **1997,** *8*, 253.
22. Adamczyk, M.; Chan, C. M.; Fino, J. R.; Mattingly, P. G. *The Journal of Organic Chemistry* **2000,** *65*, 596.
23. Ueno, Y.; Jiao, G.-S.; Burgess, K. *Synthesis* **2004**, 2591.
24. Rossi, F. M.; Kao, J. P. Y. *Bioconjugate Chemistry* **1997,** *8*, 495.
25. Duan, Y.; Liu, M.; Sun, W.; Wang, M.; Liu, S.; Li, Q. X. *Mini-Reviews in Organic Chemistry* **2009,** *6*, 35.
26. Demchenko, A. P.; Goncalves, T.; Callis, P. R.; Sameiro, M. In *Advanced Fluorescence Reporters in Chemistry and Biology I: Fundamentals and Molecular Design*; Springer, 2010, pp. 49.
27. Crosby, G. A.; Demas, J. N. *The Journal of Physical Chemistry* **1971,** *75*, 991.
28. Chen, X.; Pradhan, T.; Wang, F.; Kim, J. S.; Yoon, J. *Chemical Reviews* **2011,** *112*, 1910.
29. Li, J.; Brunner, A. M.; Meilan, R.; Strauss, S. H. *Tree Physiology* **2009,** *29*, 299.
30. Mayasari, D. S.; Emoto, N.; Yagi, K.; Vignon-Zellweger, N.; Nakayama, K.; Miyoshi, T.; Miyata, O.; Hirata, K. *Kobe Journal of Medical Sciences* **2013,** *59*, E54.
31. Tour, O.; Adams, S. R.; Kerr, R. A.; Meijer, R. M.; Sejnowski, T. J.; Tsien, R. W.; Tsien, R. Y. *Nature Chemical Biology* **2007,** *3*, 423.
32. **5(6)-Carboxyfluorescein diacetate**: To a solution of 5(6)-carboxyfluorescein (15.0 g, 39.9 mmol) in Ac_2O (180 mL) was added pyridine (18 mL, 22.3 mmol) and the reaction was stirred for 30 min at 110 °C. The clear solution was concentrated in vacuo. The crude mixture was dissolved in EtOAc (300 mL) and washed with aqueous $KHSO_4$ (1M, 2 x 300 mL) and brine (300 mL). The organic layer was dried over Na_2SO_4, filtered and concentrated under reduced pressure to give the desired

compound as a light yellow solid (18.1 g, 98%). HPLC t_R 7.5 min and 7.6 min.

Analytical HPLC was performed by using a diode array detector and Supelco Discovery® C18 column (4.6 mm x 50 mm), eluting from 5% ACN–H_2O to 95% ACN–H2O (with 0.1% formic acid) over 10 min, followed by 4 min isocratic (flow rate 1 min/mL). The summed absorbance between 220 nm and 495 nm was used for purity and homogeneity assessment.

33. **5 and 6-Carboxyfluorescein diacetate *N*-hydroxysuccinimide ester**: 5(6)-carboxyfluorescein diacetate (15.0 g, 32.6 mmol) was dissolved in DCM (225 mL) and HOSu (4.5 g, 39.1 mmol) was added and stirred until dissolved. DIC (6.06 mL, 39.1 mmol) was added and the reaction was stirred for 30 min. The organic layer was washed with water (2 x 50 mL), brine (50 mL), and dried over Na_2SO_4. The crude mixture was dissolved in toluene (50 mL), loaded onto an equilibrated column (7 x 15 cm bed of silica) and eluted with 20 % EtOAc in toluene to afford the pure individual isomers (5-isomer 4.5 g, 25% – 6-isomer 6.4 g, 35%). 5-Carboxyfluorescein diacetate *N*-hydroxysuccinimide ester: R_f 0.37 (50:50 EtOAc:Toluene), HPLC t_R 8.6 min (<1% of 6-isomer). 6-Carboxyfluorescein diacetate *N*-hydroxysuccinimide ester: R_f 0.53 (50:50 EtOAc:Toluene), HPLC t_R 7.8 min (<1% of 5-isomer).
34. Fung, S.; Menchen, S. M. EP0272007 A2; **1988**.
35. Adamczyk, M.; Grote, J. *Bioorganic & Medicinal Chemistry Letters* **2003,** *13*, 2327.
36. **5-Carboxyrhodamine B *N*-hydroxysuccinimide ester**: 5-Carboxytetraethylrhodamine (195 mg, 0.40 mmol), DMAP (244 mg, 2.0 mmol) and TEA (278 µL, 2.0 mmol) were dissolved in dry DCM (20 mL). DSC (205 mg, 0.80 mmol) was added and the reaction stirred for 1 h. The reaction was quenched with AcOH (229 µL, 4.0 mmol) and the solution was directly loaded onto an equilibrated flash chromatography column and eluted with 1 % AcOH in acetone to afford the pure compound (198 mg, 85%). R_f 0.27 (9:89:2 MeOH:DCM:AcOH), HPLC t_R 6.4 min. 6-Carboxyrhodamine B *N*-hydroxysuccinimide ester was prepared as described above (87% yield). R_f 0.31 (9:89:2 MeOH:DCM:AcOH), HPLC t_R 6.5 min.
37. **5 and 6-Carboxyrhodamine B:** 5(6)-carboxytetraethylrhodamine (2.0 g, 4.11 mmol) was purified by flash column chromatography (gradient of TEA:DCM:MeOH from 5:95:0 to 5:75:20). The two separated isomers were obtained as a TEA salt. Solvents were removed under reduced pressure. The individual isomers (as their salts) were dissolved in EtOAc (80 mL) and washed with 1M $KHSO_4$ (3 x 50 mL), brine (50 mL), dried over Na_2SO_4 and filtered, to afford the pure individual isomers 5-carboxytetraethylrhodamine (833 mg, 42%) and 6-carboxytetraethylrhodamine (670 mg, 33%) as a dark pink solids. 5-Carboxyrhodamine B: R_f 0.11 (10:89.5:0.5 MeOH:DCM:TEA), HPLC t_R 7.5 min. 6-Carboxyrhodamine B: R_f 0.22 (10:89.5:0.5 MeOH:DCM:TEA), HPLC t_R 7.0 min.

References

1. Parish, C. R. *Immunology and Cell Biology* **1999,** *77*, 499.
2. Hedstrom, L. *Chemical Reviews* **2002,** *102*, 4501.
3. Korkmaz, B.; Moreau, T.; Gauthier, F. *Biochimie* **2008,** *90*, 227.
4. Ueno, T.; Urano, Y.; Kojima, H.; Nagano, T. *Journal of the American Chemical Society* **2006,** *128*, 10640.
5. Korkmaz, B.; Attucci, S.; Moreau, T.; Godat, E.; Juliano, L.; Gauthier, F. *American Journal of Respiratory Cell and Molecular Biology* **2004,** *30*, 801.
6. Pinkel, D.; Landegent, J.; Collins, C.; Fuscoe, J.; Segraves, R.; Lucas, J.; Gray, J. *Proceedings of the National Academy of Sciences* **1988,** *85*, 9138.
7. George, T. C.; Fanning, S. L.; Fitzgeral-Bocarsly, P.; Medeiros, R. B.; Highfill, S.; Shimizu, Y.; Hall, B. E.; Frost, K.; Basiji, D.; Ortyn, W. E.; Morrissey, P. J.; Lynch, D. H. *Journal of Immunological Methods* **2006,** *311*, 117.
8. Tsien, R. Y.; Pozzan, T.; Rink, T. J. *The Journal of Cell Biology* **1982,** *94*, 325.
9. Caswell, A. H.; Hutchison, J. D. *Biochemical and Biophysical Research Communications* **1971,** *42*, 43.
10. Bonner, W. A.; Hulett, H. R.; Sweet, R. G.; Herzenberg, L. A. *Review of Scientific Instruments* **1972,** *43*, 404.
11. Suzuki, T.; Fujikura, K.; Higashiyama, T.; Takata, K. *Journal of Histochemistry & Cytochemistry* **1997,** *45*, 49.
12. Koltermann, A.; Kettling, U.; Bieschke, J.; Winkler, T.; Eigen, M. *Proceedings of the National Academy of Sciences* **1998,** *95*, 1421.
13. Miller, E.; Bian, S.; Chang, C. *Journal of the American Chemical Society* **2007,** *129*, 3458.
14. Schäferling, M. *Angewandte Chemie International Edition* **2012,** *51*, 3532.
15. Seo, S.; Lee, H. Y.; Park, M.; Lim, J. M.; Kang, D.; Yoon, J.; Jung, J. H. *European Journal of Inorganic Chemistry* **2010**, 843.
16. Unciti-Broceta, A.; Yusop, R. M.; Richardson, P. R.; Walton, J.; Bradley, M. *Tetrahedron Letters* **2009,** *50*, 3713.
17. Van Dam, G. M.; Themelis, G.; Crane, L. M.; Harlaar, N. J.; Pleijhuis, R. G.; Kelder, W.; Sarantopoulos, A.; de Jong, J. S.; Arts, H. J.; van der Zee, A. G.; Bart, J.; Low, P. S.; Ntziachristos, V. *Nature Medicine* **2011,** *17*, 1315.
18. Lakowicz, J. R. *Principles of Fluorescence Spectroscopy*; New York: Springer, 2007.
19. Jablonski, A. *Nature* **1933,** *131*, 839.
20. Lavis, L. D.; Raines, R. T. *American Chemical Society Chemical Biology* **2008,** *3*, 142.
21. Seidel, C. A.; Schulz, A.; Sauer, M. H. *The Journal of Physical Chemistry* **1996,** *100*, 5541.
22. Zelent, B.; Kuśba, J.; Gryczynski, I.; Johnson, M. L.; Lakowicz, J. R. *Biophysical Chemistry* **1998,** *73*, 53.

23. de Silva, A. P.; Gunaratne, H. N.; Gunnlaugsson, T.; Huxley, A. J.; McCoy, C. P.; Rademacher, J. T.; Rice, T. E. *Chemical Reviews* **1997,** *97*, 1515.
24. Heinrichs, A. *Nature Cell Biology* **2009,** *11*, S7.
25. Stokes, G. G. *Philosophical Transactions of the Royal Society of London* **1852,** *142*, 463.
26. Von Bayer, A. *Berichte der Deutschen Chemischen Gesellschaft* **1871,** *4*, 555.
27. Heimstädt, O. *Zeitschrift fur Wissenschaftliche Mikroskopie und Mikroskopische Technik* **1911,** *28*, 330.
28. Rost, F. W. D. *Quantitative Fluorescence Microscopy*: Cambridge University Press, 1991.
29. Ellinger, P.; Hirt, A. *Archiv fur Experimentelle Pathologie und Pharmacologie* **1929,** *147*, 67.
30. Ploem, J. S. *Zeitschrift fur Wissenschaftliche Mikroskopie und Mikroskopische Technik* **1967,** *68*, 129.
31. Minsky, M. US3013467 A; **1961**.
32. Coons, A. H.; Creech, H. J.; Jones, R. N. *Proceedings of the Society for Experimental Biology and Medicine* **1941,** *47*, 200.
33. Coons, A. H.; Kaplan, M. H. *The Journal of Experimental Medicine* **1950,** *91*, 1.
34. Coons, A. H. *The Journal of Immunology* **1961,** *87*, 499.
35. Buchwalow, I.; Böcker, W. *Immunohistochemistry: Basics and Methods*: Springer Berlin Heidelberg, 2010.
36. Tsien, R. Y.; Rink, T. J.; Poenie, M. *Cell Calcium* **1985,** *6*, 145.
37. Amos, W. B.; White, J. G. *Biology of the Cell* **2003,** *95*, 335.
38. O'Rourke, N.; Fraser, S. *Neuron* **1990,** *5*, 159.
39. Lee, S.; Wisniewski, J. C.; Dentler, W. L.; Asai, D. J. *Molecular Biology of the Cell* **1999,** *10*, 771.
40. Fujiu, K.; Numata, O. *Cell Structure and Function* **1999,** *24*, 401.
41. Fujiu, K.; Numata, O. *Cell Motility and the Cytoskeleton* **2000,** *46*, 17.
42. Gaertig, J. *Journal of Eukaryotic Microbiology* **2000,** *47*, 185.
43. Kiersnowska, M.; Kaczanowski, A.; Morga, J. *Journal of Eukaryotic Microbiology* **2000,** *47*, 139.
44. Stuart, K. R.; Cole, E. S. *Methods in Cell Biology*: Academic Press, 1999.
45. Marsh, T. C.; Cole, E. S.; Romero, D. P. *Genetics* **2001,** *157*, 1591.
46. Ward, J. G.; Blomberg, P.; Hoffman, N.; Yao, M. C. *Chromosoma* **1997,** *106*, 233.
47. Foyouzi-Youssefi, R.; Arnaudeau, S.; Borner, C.; Kelley, W. L.; Tschopp, J.; Lew, D. P.; Demaurex, N.; Krause, K. H. *Proceedings of the National Academy of Sciences* **2000,** *97*, 5723.
48. Hajnóczky, G.; Robb-Gaspers, L. D.; Seitz, M. B.; Thomas, A. P. *Cell* **1995,** *82*, 415.
49. Rutter, G. A.; Burnett, P.; Rizzuto, R.; Brini, M.; Murgia, M.; Pozzan, T.; Tavaré, J. M.; Denton, R. M. *Proceedings of the National Academy of Sciences* **1996,** *93*, 5489.
50. Rizzuto, R.; Bastianutto, C.; Brini, M.; Murgia, M.; Pozzan, T. *The Journal of Cell Biology* **1994,** *126*, 1183.

51. Stehno-Bittel, L.; Perez-Terzic, C.; Clapham, D. E. *Science* **1995,** *270*, 1835.
52. Terai, T.; Urano, Y.; Izumi, S.; Kojima, H.; Nagano, T. *Chemical Communications* **2012,** *48*, 2840.
53. Nakajima, K.; Sena, G.; Nawy, T.; Benfey, P. N. *Nature* **2001,** *413*, 307.
54. Yusop, R. M.; Unciti-Broceta, A.; Johansson, E. M.; Sánchez-Martín, R. M.; Bradley, M. *Nature Chemistry* **2011,** *3*, 239.
55. Dell, E. J. *Genetic Engineering and Biotechnology News* **2012,** *32*.
56. Ntziachristos, V. *Annual Review of Biomedical Engineering* **2006,** *8*, 1.
57. Janssen, Y. M.; Van Houten, B.; Borm, P. J.; Mossman, B. T. *Laboratory Investigation* **1993,** *69*, 261.
58. Schaeffter, T. *Imaging in Drug Discovery and Early Clinical Trials*: Birkhäuser Basel, 2005.
59. Ntziachristos, V.; Ripoll, J.; Weissleder, R. *Optics Letters* **2002,** *27*, 333.
60. Ntziachristos, V.; Bremer, C.; Weissleder, R. *European Radiology* **2003,** *13*, 195.
61. Kobayashi, H.; Ogawa, M.; Alford, R.; Choyke, P. L.; Urano, Y. *Chemical Reviews* **2009,** *110*, 2620.
62. Lin, Y.; Weissleder, R.; Tung, C. H. *Bioconjugate Chemistry* **2002,** *13*, 605.
63. Puckett, C. A.; Barton, J. K. *Journal of the American Chemical Society* **2009,** *131*, 8738.
64. Ogawa, M.; Regino, C. A.; Choyke, P. L.; Kobayashi, H. *Molecular Cancer Therapeutics* **2009,** *8*, 232.
65. Kobayashi, H.; Hama, Y.; Koyama, Y.; Barrett, T.; Regino, C. A.; Urano, Y.; Choyke, P. L. *Nano Letters* **2007,** *7*, 1711.
66. Hama, Y.; Koyama, Y.; Choyke, P. L.; Kobayashi, H. *Journal of Biomedical Optics* **2007,** *12*, 034016.
67. Ogawa, M.; Kosaka, N.; Choyke, P. L.; Kobayashi, H. *Cancer Research* **2009,** *69*, 1268.
68. Longmire, M.; Kosaka, N.; Ogawa, M.; Choyke, P. L.; Kobayashi, H. *Cancer Science* **2009,** *100*, 1099.
69. Kosaka, N.; Ogawa, M.; Longmire, M. R.; Choyke, P. L.; Kobayashi, H. *Journal of Biomedical Optics* **2009,** *14*, 014023.
70. Nguyen, Q. T.; Tsien, R. Y. *Nature Review Cancer* **2013,** *13*, 653.
71. Buchwalow, I. B.; Böcker, W. *Immunohistochemistry: Basics and Methods*: Springer, 2010.
72. Murphy, D. B. *Fundamentals of Light Microscopy and Electronic Imaging*: Wiley, 2002.
73. Lecoeur, H. *Experimental Cell Research* **2002,** *277*, 1.
74. Neri, D.; Carnemolla, B.; Nissim, A.; Leprini, A.; Querze, G.; Balza, E.; Pini, A.; Tarli, L.; Halin, C.; Neri, P.; Zardi, L.; Winter, G. *Nature Biotechnology* **1997,** *15*, 1271.
75. Folli, S.; Westermann, P.; Braichotte, D.; Pèlegrin, A.; Wagnières, G.; van den Bergh, H.; Mach, J. *Cancer Research* **1994,** *54*, 2643.
76. Ramjiawan, B.; Maiti, P.; Aftanas, A.; Kaplan, H.; Fast, D.; Mantsch, H. H.; Jackson, M. *Cancer* **2000,** *89*, 1134.

77. Achilefu, S.; Bloch, S.; Markiewicz, M. A.; Zhong, T.; Ye, Y.; Dorshow, R. B.; Chance, B.; Liang, K. *Proceedings of the National Academy of Sciences* **2005,** *102*, 7976.
78. Licha, K.; Hessenius, C.; Becker, A.; Henklein, P.; Bauer, M.; Wisniewski, S.; Wiedenmann, B.; Semmler, W. *Bioconjugate Chemistry* **2001,** *12*, 44.
79. Chen, X.; Conti, P. S.; Moats, R. A. *Cancer Research* **2004,** *64*, 8009.
80. Ke, S.; Wen, X.; Gurfinkel, M.; Charnsangavej, C.; Wallace, S.; Sevick-Muraca, E. M.; Li, C. *Cancer Research* **2003,** *63*, 7870.
81. Llopis, J.; McCaffery, J. M.; Miyawaki, A.; Farquhar, M. G.; Tsien, R. Y. *Proceedings of the National Academy of Sciences* **1998,** *95*, 6803.
82. Spivak, G.; Guo, J.; Hanawalt, P. *Protocol Exchange* **2013**, 1.
83. Maetzel, D.; Denzel, S.; Mack, B.; Canis, M.; Went, P.; Benk, M.; Kieu, C.; Papior, P.; Baeuerle, P. A.; Munz, M.; Gires, O. *Nature Cell Biology* **2009,** *11*, 162.
84. Floyd, D. N.; Ashall, F.; Djamgoz, M. B. *Neurochemistry International* **1992,** *21*, 527.
85. Rotman, B.; Papermaster, B. W. *Proceedings of the National Academy of Sciences* **1966,** *55*, 134.
86. Crow, J. P. *Nitric Oxide* **1997,** *1*, 145.
87. Domaille, D. W.; Que, E. L.; Chang, C. J. *Nature Chemical Biology* **2008,** *4*, 168.
88. Tanaka, K.; Miura, T.; Umezawa, N.; Urano, Y.; Kikuchi, K.; Higuchi, T.; Nagano, T. *Journal of the American Chemical Society* **2001,** *123*, 2530.
89. Miura, T.; Urano, Y.; Tanaka, K.; Nagano, T.; Ohkubo, K.; Fukuzumi, S. *Journal of the American Chemical Society* **2003,** *125*, 8666.
90. Umezawa, N.; Tanaka, K.; Urano, Y.; Kikuchi, K.; Higuchi, T.; Nagano, T. *Angewandte Chemie International Edition* **1999,** *38*, 2899.
91. Gabe, Y.; Urano, Y.; Kikuchi, K.; Kojima, H.; Nagano, T. *Journal of the American Chemical Society* **2004,** *126*, 3357.
92. Sasaki, E.; Kojima, H.; Nishimatsu, H.; Urano, Y.; Kikuchi, K.; Hirata, Y.; Nagano, T. *Journal of the American Chemical Society* **2005,** *127*, 3684.
93. Setsukinai, K. I.; Urano, Y.; Kakinuma, K.; Majima, H. J.; Nagano, T. *Journal of Biological Chemistry* **2003,** *278*, 3170.
94. Koide, Y.; Urano, Y.; Kenmoku, S.; Kojima, H.; Nagano, T. *Journal of the American Chemical Society* **2007,** *129*, 10324.
95. Izumi, S.; Urano, Y.; Hanaoka, K.; Terai, T.; Nagano, T. *Journal of the American Chemical Society* **2009,** *131*, 10189.
96. Fujikawa, Y.; Urano, Y.; Komatsu, T.; Hanaoka, K.; Kojima, H.; Terai, T.; Inoue, H.; Nagano, T. *Journal of the American Chemical Society* **2008,** *130*, 14533.
97. Yang, J.; Chen, H.; Vlahov, I. R.; Cheng, J. X.; Low, P. S. *Proceedings of the National Academy of Sciences* **2006,** *103*, 13872.
98. Carmona, A. K.; Juliano, M. A.; Juliano, L. *Anais da Academia Brasileira de Ciencias* **2009,** *81*, 381.
99. Sato, M.; Ozawa, T.; Inukai, K.; Asano, T.; Umezawa, Y. *Nature Biotechnology* **2002,** *20*, 287.
100. Azpiazu, I.; Gautam, N. *Journal of Biological Chemistry* **2004,** *279*, 27709.

101. Valdes-Aguilera, O.; Neckers, D. C. *Accounts of Chemical Research* **1989,** *22*, 171.
102. Ogawa, M.; Kosaka, N.; Choyke, P. L.; Kobayashi, H. *American Chemical Society Chemical Biology* **2009,** *4*, 535.
103. Kemnitz, K.; Yoshihara, K. *The Journal of Physical Chemistry* **1991,** *95*, 6095.
104. López Arbeloa, I.; Ruiz Ojeda, P. *Chemical Physics Letters* **1982,** *87*, 556.
105. Weissleder, R.; Tung, C. H.; Mahmood, U.; Bogdanov, A. *Nature Biotechnology* **1999,** *17*, 375.
106. Grahn, S.; Ullmann, D.; Jakubke, H. D. *Analytical Biochemistry* **1998,** *265*, 225.
107. Torchilin, V. P. *European Journal of Pharmaceutical Sciences* **2000,** *11, Supplement 2*, S81.
108. Jaffer, F. A.; Kim, D. E.; Quinti, L.; Tung, C. H.; Aikawa, E.; Pande, A. N.; Kohler, R. H.; Shi, G. P.; Libby, P.; Weissleder, R. *Circulation* **2007,** *115*, 2292.
109. Bremer, C.; Tung, C. H.; Bogdanov, A.; Weissleder, R. *Radiology* **2002,** *222*, 814.
110. Tung, C. H.; Bredow, S.; Mahmood, U.; Weissleder, R. *Bioconjugate Chemistry* **1999,** *10*, 892.
111. Del Nery, E.; Alves, L.; Melo, R.; Cesari, M.; Juliano, L.; Juliano, M. *Journal of Protein Chemistry* **2000,** *19*, 33.
112. Jezierska, A.; Motyl, T. *Medical Science Monitor* **2009,** *15*, 32.
113. Koutroulis, I.; Zarros, A.; Theocharis, S. *Expert Opinion on Therapeutic Targets* **2008,** *12*, 1577.
114. Bremer, C.; Bredow, S.; Mahmood, U.; Weissleder, R.; Tung, C. H. *Radiology* **2001,** *221*, 523.
115. Bremer, C.; Tung, C. H.; Weissleder, R. *Nature Medecine* **2001,** *7*, 743.
116. Ellard, J. M.; Zollitsch, T.; Cummins, W. J.; Hamilton, A. L.; Bradley, M. *Angewandte Chemie International Edition* **2002,** *41*, 3233.
117. Avlonitis, N.; Debunne, M.; Aslam, T.; McDonald, N.; Haslett, C.; Dhaliwal, K.; Bradley, M. *Organic & Biomolecular Chemistry* **2013,** *11*, 4414.
118. Hama, Y.; Urano, Y.; Koyama, Y.; Kamiya, M.; Bernardo, M.; Paik, R. S.; Shin, I. S.; Paik, C. H.; Choyke, P. L.; Kobayashi, H. *Cancer Research* **2007,** *67*, 2791.
119. Kricka, L. J. *Optical Methods: A Guide to the "-escences"*; USA: American Association for Clinical Chemistry Press, 2003.
120. Farber, S. A.; Pack, M.; Ho, S. Y.; Johnson, I. D.; Wagner, D. S.; Dosch, R.; Mullins, M. C.; Hendrickson, H. S.; Hendrickson, E. K.; Halpern, M. E. *Science* **2001,** *292*, 1385.
121. Bullok, K.; Piwnica-Worms, D. *Journal of Medicinal Chemistry* **2005,** *48*, 5404.
122. Blum, G.; von Degenfeld, G.; Merchant, M. J.; Blau, H. M.; Bogyo, M. *Nature Chemical Biology* **2007,** *3*, 668.
123. Ogawa, M.; Kosaka, N.; Longmire, M. R.; Urano, Y.; Choyke, P. L.; Kobayashi, H. *Molecular Pharmaceutics* **2009,** *6*, 386.
124. Ogawa, M.; Kosaka, N.; Choyke, P. L.; Kobayashi, H. *Bioconjugate Chemistry* **2008,** *20*, 147.
125. Sharon, J. *Basic immunology*; Baltimore ; London: Williams & Wilkins, 1998.
126. Male, D. *Immunology*; Philadelphia: Mosby Elsevier, 2006.

127. Young, B. *Wheater's functional histology : a text and colour atlas*; Edinburgh: Churchill Livingstone/Elsevier, 2006.
128. Hellewell, P.; Williams, T. *Immunopharmacology of neutrophils*; London: Academic Press, 1994.
129. Nathan, C. *Nature Reviews Immunology* **2006,** *6*, 173.
130. Lacy, P. *Allergy, Asthma & Clinical Immunology* **2006,** *2*, 98
131. Hampton, M. B.; Kettle, A. J.; Winterbourn, C. C. *Blood* **1998,** *92*, 3007.
132. Faurschou, M.; Borregaard, N. *Microbes and Infection* **2003,** *5*, 1317.
133. Liou, T. G.; Campbell, E. J. *Biochemistry* **1995,** *34*, 16171.
134. Pham, C. T. *Nature Review Immunology* **2006,** *6*, 541.
135. Doring, G. *American Journal of Respiratory Critical Care Medicine* **1994,** *150*, S114.
136. Kawabata, K.; Hagio, T.; Matsuoka, S. *European Journal of Pharmacology* **2002,** *451*, 1.
137. Campbell, E. J.; Senior, R. M.; McDonald, J. A.; Cox, D. L.; Greco, J. M.; Landis, J. A. *The Journal of Clinical Investigation* **1982,** *70*, 845.
138. Chen, H.; Lin, H.; Liu, C.; Hwang, T.; Wang, C.; Huang, T.; Lin, C.; Kuo, H. *Journal of Biomedical Science* **2004,** *11*, 49.
139. Trouche, N.; Wieckowski, S.; Sun, W.; Chaloin, O.; Hoebeke, J.; Fournel, S.; Guichard, G. *Journal of the American Chemical Society* **2007,** *129*, 13480.
140. Demmer, O.; Dijkgraaf, I.; Schottelius, M.; Wester, H. J.; Kessler, H. *Organic Letters* **2008,** *10*, 2015.
141. Lebreton, S.; How, S.-E.; Buchholz, M.; Yingyongnarongkul, B.-E.; Bradley, M. *Tetrahedron* **2003,** *59*, 3945.
142. Brown, H. C.; Choi, Y. M.; Narasimhan, S. *The Journal of Organic Chemistry* **1982,** *47*, 3153.
143. Chan, W. C.; White, P. D. *Fmoc solid phase peptide synthesis: a practical approach*; New York: Oxford University Press, 2000.
144. Yang, L. *Tetrahedron Letters* **2000,** *41*, 6981.
145. Wells, N. J.; Basso, A.; Bradley, M. *Biopolymers* **1998,** *47*, 381.
146. Tam, J. P.; Kaumaya, P. T. *Peptides Frontiers of Peptide Science*; New York: Springer, 1999.
147. Augustyns, K.; Kraas, W.; Jung, G. *The Journal of Peptide Research* **1998,** *51*, 127.
148. Bialy, L.; Díaz-Mochón, J. J.; Specker, E.; Keinicke, L.; Bradley, M. *Tetrahedron* **2005,** *61*, 8295.
149. Breipohl, G.; Knolle, J.; Langner, D.; O'Malley, G.; Uhlmann, E. *Bioorganic & Medicinal Chemistry Letters* **1996,** *6*, 665.
150. Kaiser, E.; Colescott, R. L.; Bossinger, C. D.; Cook, P. I. *Analytical Biochemistry* **1970,** *34*, 595.
151. Valeur, E.; Bradley, M. *Chemical Society Reviews* **2009,** *38*, 606.
152. Subirós-Funosas, R.; Prohens, R.; Barbas, R.; El-Faham, A.; Albericio, F. *Chemistry – A European Journal* **2009,** *15*, 9394.
153. Fischer, R.; Mader, O.; Jung, G.; Brock, R. *Bioconjugate Chemistry* **2003,** *14*, 653.

154. Liu, W.; Greytak, A. B.; Lee, J.; Wong, C. R.; Park, J.; Marshall, L. F.; Jiang, W.; Curtin, P. N.; Ting, A. Y.; Nocera, D. G.; Fukumura, D.; Jain, R. K.; Bawendi, M. G. *Journal of the American Chemical Society* **2010,** *132*, 472.
155. Mukai, T.; Suwada, J.; Sano, K.; Okada, M.; Yamamoto, F.; Maeda, M. *Bioorganic & Medicinal Chemistry* **2009,** *17*, 4285.
156. Hermanson, G. T. *Bioconjugate Techniques*: Elsevier Science, 2013.
157. Swali, V.; Wells, N. J.; Langley, G. J.; Bradley, M. *The Journal of Organic Chemistry* **1997,** *62*, 4902.
158. Leadbeater, N. E.; Torenius, H. M. *The Journal of Organic Chemistry* **2002,** *67*, 3145.
159. Tour, O.; Adams, S. R.; Kerr, R. A.; Meijer, R. M.; Sejnowski, T. J.; Tsien, R. W.; Tsien, R. Y. *Nature Chemical Biology* **2007,** *3*, 423.
160. Barlos, K.; Gatos, D.; Kallitsis, J.; Papaphotiu, G.; Sotiriu, P.; Wenqing, Y.; Schäfer, W. *Tetrahedron Letters* **1989,** *30*, 3943.
161. Albericio, F.; Giralt, E.; Lloyd-Williams, P. *Chemical Approaches to the Synthesis of Peptides and Proteins - New directions in organic & biological chemistry series*; Boca Ranton: CRC Press, 1997.
162. Bollhagen, R.; Schmiedberger, M.; Barlosb, K.; Grell, E. *Journal of the Chemical Society, Chemical Communications* **1994,** *22*, 2559
163. Buckley, S.; Kim, K.; Ehrhardt, C.; Smyth, H. D.; Hickey, A. J. *In vitro cell culture models*; New York: Springer, 2011.
164. Lieberman, M.; Marks, A. D.; Smith, C. M.; Marks, D. B. *Marks' Essential Medical Biochemistry*; Baltimore: Lippincott Williams & Wilkins, 2006.
165. Fischer, K. G. *Hemodialysis International* **2007,** *11*, 178.
166. Nauseef, W. M.; Quinn, M. T.; DeLeo, F. R.; Bokoch, G. M. In *Neutrophil Methods and Protocols*; Humana Press, 2007, pp. 15.
167. Pertoft, H.; Laurent, T. C.; Låås, T.; Kågedal, L. *Analytical Biochemistry* **1978,** *88*, 271.
168. Kawabata, K.; Suzuki, M.; Sugitani, M.; Imaki, K.; Toda, M.; Miyamoto, T. *Biochemical and Biophysical Research Communications* **1991,** *177*, 814.
169. Mayasari, D. S.; Emoto, N.; Yagi, K.; Vignon-Zellweger, N.; Nakayama, K.; Miyoshi, T.; Miyata, O.; Hirata, K. *Kobe Journal of Medical Sciences* **2013,** *59*, E54.
170. Baeyer, A. *Berichte der Deutschen Chemischen Gesellschaft* **1871,** *4*, 555.
171. Porrès, L.; Holland, A.; Palsson, L. O.; Monkman, A. P.; Kemp, C.; Beeby, A. *Journal of Fluorescence* **2006,** *16*, 267.
172. Hermanson, G. T. *Bioconjugate Techniques*, 2010.
173. Gonçalves, M. S. T. *Chemical Reviews* **2008,** *109*, 190.
174. Konno, K.; Morales, M. F. *Proceedings of the National Academy of Sciences* **1985,** *82*, 7904.
175. Ando, T. *Biochemistry* **1984,** *23*, 375.
176. Plank, L.; Ware, B. R. *Biophysical Journal* **1987,** *51*, 985.
177. Aguirre, R.; Gonsoulin, F.; Cheung, H. C. *Biochemistry* **1986,** *25*, 6827.
178. Greene, L. E. *Journal of Biological Chemistry* **1986,** *261*, 1279.

179. Hirsch, R. E.; Zukin, R. S.; Nagel, R. L. *Biochemical and Biophysical Research Communications* **1986,** *138*, 489.
180. Cocco, L.; Martelli, A. M.; Billi, A. M.; Matteucci, A.; Vitale, M.; Neri, L. M.; Manzoli, F. A. *Experimental Cell Research* **1986,** *166*, 465.
181. Fujita, H.; Hirao, T.; Takahashi, M. *Skin Research and Technology* **2007,** *13*, 84.
182. Chaudhuri, A. R.; de Waal, E. M.; Pierce, A.; Van Remmen, H.; Ward, W. F.; Richardson, A. *Mechanisms of Ageing and Development* **2006,** *127*, 849.
183. Gorman, J. J.; Corino, G. L.; Mitchell, S. J. *European Journal of Biochemistry* **1987,** *168*, 169.
184. Scherson, T.; Kreis, T. E.; Schlessinger, J.; Littauer, U. Z.; Borisy, G. G.; Geiger, B. *The Journal of Cell Biology* **1984,** *99*, 425.
185. Ahn, B.; Rhee, S. G.; Stadtman, E. R. *Analytical Biochemistry* **1987,** *161*, 245.
186. Lee, J. A.; Fortes, P. A. G. *Biochemistry* **1985,** *24*, 322.
187. Draper, D. E.; Gold, L. *Biochemistry* **1980,** *19*, 1774.
188. Ferguson, B. Q.; Yang, D. C. H. *Biochemistry* **1986,** *25*, 5298.
189. Friedrich, K.; Woolley, P.; Steinhauser, K. G. *European Journal of Biochemistry* **1988,** *173*, 233.
190. Pagano, J. M.; Farley, B. M.; McCoig, L. M.; Ryder, S. P. *Journal of Biological Chemistry* **2007,** *282*, 8883.
191. Odom, O. W.; Robbins, D. J.; Lynch, J.; Dottavio-Martin, D.; Kramer, G.; Hardesty, B. *Biochemistry* **1980,** *19*, 5947.
192. Odom, O. W.; Dabbs, E. R.; Dionne, C.; Muller, M.; Hardesty, B. *European Journal of Biochemistry* **1984,** *142*, 261.
193. Clausen, J. *Laboratory Techniques in Biochemistry and Molecular Biology*; New York: Elsevier Science, 1988.
194. Beutner, E. H. *Annals of the New York Academy of Sciences* **1971,** *177*, 506.
195. Duijndam, W. A. L.; Wiegant, J.; Van Duijn, P.; Haaijman, J. J. *Journal of Immunological Methods* **1988,** *109*, 289.
196. Hebert, G. A.; Pittman, B.; Cherry, W. B. *Journal of Immunology* **1967,** *98*, 1204.
197. Sun, M. M.; Beam, K. S.; Cerveny, C. G.; Hamblett, K. J.; Blackmore, R. S.; Torgov, M. Y.; Handley, F. G.; Ihle, N. C.; Senter, P. D.; Alley, S. C. *Bioconjugate Chemistry* **2005,** *16*, 1282.
198. Dodd, C. H.; Hsu, H. C.; Chu, W. J.; Yang, P.; Zhang, H. G.; Mountz, J. D.; Zinn, K.; Forder, J.; Josephson, L.; Weissleder, R.; Mountz, J. M.; Mountz, J. D. *Journal of Immunological Methods* **2001,** *256*, 89.
199. França, L. T.; Carrilho, E.; Kist, T. B. *Quarterly Reviews of Biophysics* **2002,** *35*, 169.
200. White, L. D. *Next Generation Sequencing*; New York: Springer, 2013.
201. Sims, P. A.; Greenleaf, W. J.; Duan, H.; Xie, X. S. *Nature Methods* **2011,** *8*, 575.
202. Sintchenko, V. *Infectious Disease Informatics*: Springer New York, 2010.
203. Tanaka, K.; Kitamura, N.; Chujo, Y. *Macromolecules* **2010,** *43*, 6180.
204. Duan, Y.; Liu, M.; Sun, W.; Wang, M.; Liu, S.; Li, Q. X. *Mini-Reviews in Organic Chemistry* **2009,** *6*, 35.

205. Kvach, M. V.; Tsybulsky, D. A.; Ustinov, A. V.; Stepanova, I. A.; Bondarev, S. L.; Gontarev, S. V.; Korshun, V. A.; Shmanai, V. V. *Bioconjugate Chemistry* **2007,** *18*, 1691.
206. Li, Y.; Zhao, L. D.; Tong, L. S.; Qian, S. N.; Ren, Y.; Zhang, L.; Ding, X.; Chen, Y.; Wang, Y. X.; Zhang, W.; Zeng, X. F.; Zhang, F. C.; Tang, F. L.; Zhang, X.; Ba, D. N.; He, W.; Cao, X. T.; Lipsky, P. *Arthritis Research & Therapy* **2012,** *14*, R123.
207. Quah, B. J. C.; Warren, H. S.; Parish, C. R. *Nature Protocols* **2007,** *2*, 2049.
208. Walenda, T.; Bokermann, G.; Ventura Ferreira, M. S.; Piroth, D. M.; Hieronymus, T.; Neuss, S.; Zenke, M.; Ho, A. D.; Müller, A. M.; Wagner, W. *Experimental Hematology* **2011,** *39*, 617.
209. Chen, Q.; Ross, A. C. *Proceedings of the National Academy of Sciences of the United States of America* **2005,** *102*, 14142.
210. Thaunat, O.; Granja, A. G.; Barral, P.; Filby, A.; Montaner, B.; Collinson, L.; Martinez-Martin, N.; Harwood, N. E.; Bruckbauer, A.; Batista, F. D. *Science* **2012,** *335*, 475.
211. Noelting, E.; Dziewoński, K. *Berichte der Deutschen Chemischen Gesellschaft* **1905,** *38*, 3516.
212. Velapoldi, R. A.; Tønnesen, H. H. *Journal of Fluorescence* **2004,** *14*, 465.
213. Boyarskiy, V. P.; Belov, V. N.; Medda, R.; Hein, B.; Bossi, M.; Hell, S. W. *Chemistry – A European Journal* **2008,** *14*, 1784.
214. Crosby, G. A.; Demas, J. N. *The Journal of Physical Chemistry* **1971,** *75*, 991.
215. Zhou, Z.; Yu, M.; Yang, H.; Huang, K.; Li, F.; Yi, T.; Huang, C. *Chemical Communications* **2008**, 3387.
216. Mao, J.; Wang, L.; Dou, W.; Tang, X.; Yan, Y.; Liu, W. *Organic Letters* **2007,** *9*, 4567.
217. Lee, M. H.; Kim, H. J.; Yoon, S.; Park, N.; Kim, J. S. *Organic Letters* **2007,** *10*, 213.
218. Zhang, X.; Shiraishi, Y.; Hirai, T. *Organic Letters* **2007,** *9*, 5039.
219. Xiang, Y.; Tong, A.; Jin, P.; Ju, Y. *Organic Letters* **2006,** *8*, 2863.
220. Yang, H.; Zhou, Z.; Huang, K.; Yu, M.; Li, F.; Yi, T.; Huang, C. *Organic Letters* **2007,** *9*, 4729.
221. Wu, J. S.; Hwang, I. C.; Kim, K. S.; Kim, J. S. *Organic Letters* **2007,** *9*, 907.
222. Wu, D.; Huang, W.; Duan, C.; Lin, Z.; Meng, Q. *Inorganic Chemistry* **2007,** *46*, 1538.
223. Lee, M. H.; Wu, J. S.; Lee, J. W.; Jung, J. H.; Kim, J. S. *Organic Letters* **2007,** *9*, 2501.
224. Yang, Y. K.; Yook, K. J.; Tae, J. *Journal of the American Chemical Society* **2005,** *127*, 16760.
225. Xiang, Y.; Tong, A. *Organic Letters* **2006,** *8*, 1549.
226. Yang, Y.; Zhao, Q.; Feng, W.; Li, F. *Chemical Reviews* **2013,** *113*, 192.
227. Chen, X.; Pradhan, T.; Wang, F.; Kim, J. S.; Yoon, J. *Chemical Reviews* **2011,** *112*, 1910.
228. Kim, H. N.; Lee, M. H.; Kim, H. J.; Kim, J. S.; Yoon, J. *Chemical Society Reviews* **2008,** *37*, 1465.
229. Quang, D. T.; Kim, J. S. *Chemical Reviews* **2010,** *110*, 6280.
230. Bossi, M.; Belov, V.; Polyakova, S.; Hell, S. W. *Angewandte Chemie International Edition* **2006,** *45*, 7462.

231. Shiraishi, Y.; Miyamoto, R.; Zhang, X.; Hirai, T. *Organic Letters* **2007,** *9*, 3921.
232. Shiraishi, Y.; Miyamoto, R.; Hirai, T. *Journal of Photochemistry and Photobiology A: Chemistry* **2008,** *200*, 432.
233. Miura, Y.; Thoburn, C. J.; Bright, E. C.; Hess, A. D. *Biology of Blood and Marrow Transplantation* **2004,** *10*, 156.
234. Li, J.; Brunner, A. M.; Meilan, R.; Strauss, S. H. *Tree Physiology* **2009,** *29*, 299.
235. Cano, M.; Fijalkowski, N.; Kondo, N.; Dike, S.; Handa, J. *The American Journal of Pathology* **2011,** *179*, 850.
236. Hummel, S.; Lynn, E. G.; Osanger, A.; Hirayama, S.; Nimpf, J.; Schneider, W. J. *Journal of Lipid Research* **2003,** *44*, 1633.
237. Hofer, G.; Steyrer, E.; Kostner, G. M.; Hermetter, A. *Journal of Lipid Research* **1997,** *38*, 2411.
238. Gordiyenko, N.; Campos, M.; Lee, J. W.; Fariss, R. N.; Sztein, J.; Rodriguez, I. R. *Investigative Ophthalmology & Visual Science* **2004,** *45*, 2822.
239. Huang, H.; Martasek, P.; Roman, L. J.; Silverman, R. B. *Journal of Medicinal Chemistry* **2000,** *43*, 2938.
240. Adamczyk, M.; Grote, J. *Bioorganic & Medicinal Chemistry Letters* **2003,** *13*, 2327.
241. Wei, Y.; Laurent, R.; Majoral, J. P.; Caminade, A. M. *Archive for Organic Chemistry* **2010**, 318.
242. Fung, S.; Menchen, S. M. EP0272007 A2; **1988**.
243. Mak, T. W.; Saunders, M. E. *The Immune Response*; Burlington: Academic Press, 2006.
244. Miller, J. *Principles of Medical Biology*: Elsevier, 1996.
245. Sprent, J.; Zhang, X.; Sun, S.; Tough, D. *Philosophical Transactions of the Royal Society of London. Series B: Biological Sciences* **2000,** *355*, 317.
246. Mak, T. W.; Saunders, M. E. In *The Immune Response*; Academic Press: Burlington, 2006, pp. 17.
247. Mosmann, T. R.; Coffman, R. L. *Annual Review of Immunology* **1989,** *7*, 145.
248. Weston, S. A.; Parish, C. R. *Journal of Immunological Methods* **1990,** *133*, 87.
249. Quah, B. J.; Parish, C. R. *Journal of Immunological Methods* **2012,** *379*, 1.
250. Padureanu, L.; Cozmei, C.; Sorete–Arbore, A.; Gramada, D.; Arama, S.; Mihaescu, T.; Carasevici, E. *The Journal of Preventive Medicine* **2003,** *11*, 67.
251. Even, M. S.; Sandusky, C. B.; Barnard, N. D. *Trends in Biotechnology* **2006,** *24*, 105.
252. Levine, B. L.; Bernstein, W. B.; Connors, M.; Craighead, N.; Lindsten, T.; Thompson, C. B.; June, C. H. *The Journal of Immunology* **1997,** *159*, 5921.
253. Johnson, I. Lifetechnologies, Ed.; Invitrogen Corporation.
254. Gillis, S.; Watson, J. *The Journal of Experimental Medicine* **1980,** *152*, 1709.
255. Abraham, R. T.; Weiss, A. *Nature Reviews Immunology* **2004,** *4*, 301.
256. Gillis, S.; Smith, K. A.; Watson, J. *The Journal of Immunology* **1980,** *124*, 1954.
257. Goodman, S. R. *Medical Cell Biology*: Elsevier Science, 2007.
258. Hiscox, J. A. *Nature Review Microbiology* **2007,** *5*, 119.
259. Henry, T.; Gorvel, J. P.; Méresse, S. *Cellular Microbiology* **2006,** *8*, 23.

260. Weller, S. K. *PLOS Pathogens* **2010,** *6*, e1001105.
261. Feldherr, C. M.; Kallenbach, E.; Schultz, N. *The Journal of Cell Biology* **1984,** *99*, 2216.
262. Panté, N.; Aebi, U. *International Review of Cytology*: Academic Press, 1996.
263. Terry, L. J.; Shows, E. B.; Wente, S. R. *Science* **2007,** *318*, 1412.
264. Lange, A.; Mills, R. E.; Lange, C. J.; Stewart, M.; Devine, S. E.; Corbett, A. H. *Journal of Biological Chemistry* **2007,** *282*, 5101.
265. Kalderon, D.; Roberts, B. L.; Richardson, W. D.; Smith, A. E. *Cell* **1984,** *39*, 499.
266. Lee, S. J.; Matsuura, Y.; Liu, S. M.; Stewart, M. *Nature* **2005,** *435*, 693.
267. Gilchrist, D.; Mykytka, B.; Rexach, M. *Journal of Biological Chemistry* **2002,** *277*, 18161.
268. Matsuura, Y.; Stewart, M. *Nature* **2004,** *432*, 872.
269. Hamosh, A.; Scott, A. F.; Amberger, J. S.; Bocchini, C. A.; McKusick, V. A. *Nucleic Acids Research* **2005,** *33*, D514.
270. Rogers, M. L.; Rush, R. A. *Journal of Controlled Release* **2012,** *157*, 183.
271. Golan, D. E. *Principles of Pharmacology: The Pathophysiologic Basis of Drug Therapy*: Lippincott Williams & Wilkins, 2008.
272. Flemming, A. *Nature Review Drug Discovery* **2012,** *11*, 664.
273. Robbins, P. D.; Ghivizzani, S. C. *Pharmacology & Therapeutics* **1998,** *80*, 35.
274. Pouton, C. W.; Wagstaff, K. M.; Roth, D. M.; Moseley, G. W.; Jans, D. A. *Advanced Drug Delivery Reviews* **2007,** *59*, 698.
275. Pouton, C. W. *Advanced Drug Delivery Reviews* **1998,** *34*, 51.
276. Luo, M.; Pang, C. M.; Gerken, A. E.; Brock, T. G. *Traffic* **2004,** *5*, 847.
277. Stelz, G.; Rücker, E.; Rosorius, O.; Meyer, G.; Stauber, R. H.; Spatz, M.; Eibl, M. M.; Hauber, J. *Virology* **2002,** *295*, 360.
278. Haffar, O. K.; Popov, S.; Dubrovsky, L.; Agostini, I.; Tang, H.; Pushkarsky, T.; Nadler, S. G.; Bukrinsky, M. *Journal of Molecular Biology* **2000,** *299*, 359.
279. Tao, M.; Kruhlak, M.; Xia, S.; Androphy, E.; Zheng, Z. M. *Journal of Virology* **2003,** *77*, 13232.
280. Yano, K. I.; Morotomi, K.; Saito, H.; Kato, M.; Matsuo, F.; Miki, Y. *Biochemical and Biophysical Research Communications* **2000,** *270*, 171.
281. Nakase, I.; Takeuchi, T.; Tanaka, G.; Futaki, S. *Advanced Drug Delivery Reviews* **2008,** *60*, 598.
282. Lebreton, S.; How, S. E.; Buchholz, M.; Yingyongnarongkul, B. E.; Bradley, M. *Tetrahedron* **2003,** *59*, 3945.
283. Portal, C.; Launay, D.; Merritt, A.; Bradley, M. *Journal of Combinatorial Chemistry* **2005,** *7*, 554.
284. Folkes, A.; Roe, M. B.; Sohal, S.; Golec, J.; Faint, R.; Brooks, T.; Charlton, P. *Bioorganic & Medicinal Chemistry Letters* **2001,** *11*, 2589.
285. Naganawa, A.; Matsui, T.; Ima, M.; Saito, T.; Murota, M.; Aratani, Y.; Kijima, H.; Yamamoto, H.; Maruyama, T.; Ohuchida, S.; Nakai, H.; Toda, M. *Bioorganic & Medicinal Chemistry* **2006,** *14*, 7121.

286. Sabnis, R. W. *Handbook of Acid-Base Indicators*: Taylor & Francis, 2007.
287. Chen, C. S.; Poenie, M. *Journal of Biological Chemistry* **1993,** *268*, 15812.